

FLORIDA DEPARTMENT OF TRANSPORTATION

Task 9 Deliverable: Final Report

Title: Evaluation of Silica-Based Materials for Use in Portland Cement Concrete

FDOT Contract Number: BDV31-977-76

University of Florida, Department of Civil & Coastal Engineering

April 2021

Submitted to:

Research Center

The Florida Department of Transportation
605 Suwannee Street, MS 30 Tallahassee, FL 32399

Dr. Harvey DeFord, Ph.D.
Structures Materials Research Specialist
State Materials Office

Submitted by:

Christopher C. Ferraro, Ph.D., P.E. (ferraro@ce.ufl.edu) (Principal Investigator)

Jerry M. Paris Ph.D., P.E.

Kyle A. Riding Ph.D., P.E

Timothy G. Townsend Ph.D., P.E

Eduard Tora Bueno M.E

Engineering School of Sustainable Infrastructure and Environment

University of Florida
Gainesville, Florida 32611

DISCLAIMER

The opinions, findings, and conclusions expressed in this publication are those of the authors and not necessarily those of the State of Florida Department of Transportation.

The Florida Department of Transportation does not concur with the findings and conclusions of this research.

Prepared in cooperation with the State of Florida Department of Transportation and the U.S. Department of Transportation.

SI (MODERN METRIC) CONVERSION FACTORS (FROM FHWA)

Symbol	When You Know	Multiply By	To Find	Symbol
Length				
in	inches	25.4	millimeters	mm
ft	feet	0.305	meters	m
yd	yards	0.914	meters	m
mi	miles	1.61	kilometers	km
Area				
in²	square inches	645.2	square millimeters	mm ²
ft²	square feet	0.093	square meters	m ²
yd²	square yard	0.836	square meters	m ²
mi²	square miles	2.59	square kilometers	km ²
Volume				
fl oz	fluid ounces	29.57	milliliters	mL
gal	gallons	3.785	liters	L
ft³	cubic feet	0.028	cubic meters	m ³
yd³	cubic yards	0.765	cubic meters	m ³
NOTE: volumes greater than 1000 L shall be shown in m³				
Mass				
oz	ounces	28.35	grams	g
lb	pounds	0.454	kilograms	kg
Temperature (exact degrees)				
°F	Fahrenheit	5 (F-32)/9 or (F-32)/1.8	Celsius	°C
Illumination				
fc	foot-candles	10.76	lux	lx
fl	foot-Lamberts	3.426	candela/m ²	cd/m ²
Force and Pressure or Stress				
lbf	pound-force	4.45	newtons	N
lbf/in²	pound-force per square inch	6.89	kilopascals	kPa

Technical Report Documentation Page

1. Report No.	2. Government Accession No.	3. Recipient's Catalog No.	
4. <i>Evaluation of Silica-Based Materials for Use in Portland Cement Concrete</i>		5. Report Date: January 2021	
6. Performing Organization Code			
7. Author(s) Christopher C. Ferraro, Jerry M. Paris, Kyle A. Riding, Timothy G. Townsend, Eduard Tora Bueno		8. Performing Organization Report No.	
9. Performing Organization Name and Address: University of Florida Engineering School of Sustainable Infrastructure and Environment. 365 Weil Hall – P.O. Box 116580 Gainesville, FL 32611-6580		10. Work Unit No.	
11. Contract or Grant No. BDK31-977-76			
12. Sponsoring Agency Name and Address Florida Department of Transportation 605 Suwannee Street, MS 30 Tallahassee, FL 32399		13. Type of Report and Period Covered 6/1/2017 to 2/1/2021	
14. Sponsoring Agency Code			
15. Supplementary Notes			
16. Abstract: The purpose of this research was to evaluate the mechanical performance and long-term durability of concrete containing alternative supplementary cementitious materials (ASCM) available in the state of Florida that were identified in a previous research project (FDOT BDV-31-977-06) as warranting further investigation. The ASCM chosen were two types of Florida sugarcane bagasse ash, ground sand, ground recycled container glass, and ground volcanic rock, all of which were identified as potential substitutes to class F fly ash for future use in concrete. Both Type I/II and Type IL cements were included in the investigation to account for the increasing use of IL cements in industry. Mixes containing Class F fly ash, Class C fly ash, and silica fume were used for comparison and Class C fly ash was used for all ternary mixes. Raw material testing included elemental and mineralogical compositions determined by x-ray fluorescence (XRF) and x-ray diffraction (XRD), chloride content, particle size distribution employing laser particle size analysis, apparent specific gravity determined with a helium pycnometer, specific heat capacity using a differential scanning calorimeter (DSC), and quantity and rate of heat generation of the cementitious materials found by isothermal calorimetry. Fresh properties of mortars and concretes examined included mortar flow, time of set, slump, temperature, density, and air content. Hardened mechanical properties measured included compressive strength, splitting tensile strength, flexural strength, modulus of elasticity, and coefficient of thermal expansion. Durability testing included surface and bulk resistivity, resistance to alkali-silica reaction and resistance to sulfate attack. Ground glass produced the most promising results of all the ASCM that were evaluated. Sugarcane bagasse ash performed well in some regards but has a variety of barriers towards implementation. Volcanic rock and ground sand produced results indicating that both are likely filler materials with little pozzolanic reactivity.			
17. Keywords. Concrete; Supplementary Cementitious Materials; Pozzolans; Portland Cement; Fly Ash; Sugarcane Bagasse Ash; Ground Glass; Volcanic Rock; Alkali Silica Reaction; Class IL Cement		18. Distribution Statement No restrictions.	
19. Security Classif. Unclassified.	20. Security Classif. (of this page) Unclassified.	21. Pages: 299	22. Price

ACKNOWLEDGEMENTS

The Florida Department of Transportation (FDOT) is acknowledged for their funding and other contributions to this study. Special acknowledgement is given to the Project manager, Dr. H.D. DeFord for his guidance and assistance throughout this project. Additionally, the authors would like to thank Timothy Ruelke, Patrick Upshaw, Jose Armenteros, Richard DeLorenzo, David Hudson and Brandon Sawyer for their guidance and assistance.

The authors would like to thank the donors of material used throughout this research: Argos USA, Titan America, Lehigh Hanson, Inc., Urban Mining, Boral Materials, Cemex, Caribe, Edgar Minerals, Jobe Materials, and the donor of sugarcane bagasse ash.

The following students and faculty are acknowledged for their imperative contributions for conducting laboratory research: Dr. Taylor Rawlinson, Dr. Caitlin Tibbetts, Taylor Humbarger, Maitland Melnyk, Cailin Chacon, Ethan Huber, Cassandra Trahey, Jamison Rushnell, Maya Lowe, Celeste Sambrano, Brian Ortiz, Madeleine Murphree, Jeanine Marrou, Ashley Joseph, Rolando Te, Amogh Shinde, Bradley Williams, Oscar Wong, Suraj Raje, and Michael Orense.

Executive Summary

BACKGROUND

With recent changes in the generation of power in the United States, including Florida, there has been a significant reduction in the number of coal-burning utilities. The availability of Class F fly ash has steadily decreased, and local shortages have occurred. It is likely that regional shortages will be common in the near future. It is imperative to find alternatives to coal fly ash that are abundant and suitable for use in concrete in Florida.

The purpose of this proposed research is to make significant advancements with respect to the use of alternative pozzolans available in the state of Florida. Recently, the research project (FDOT BDV-31-977-06) made recommendations with respect to usage of alternative sources of coal fly ash and identified local sources of supplementary cementitious materials (SCM), including sugarcane bagasse ash and ground glass. The research herein served as an extension to the findings made in BDV-31-977-06 with the purpose of investigating the long-term durability of two types of sugarcane bagasse ash and ground glass along with the evaluation of other locally available materials, such as ground volcanic rock. Recently, the Florida Department of Transportation has begun to allow the use of cements which incorporate 15% limestone (Type IL). This project incorporated the use of Type IL cements into the research program to evaluate the use of high limestone cements and their compatibility with available pozzolans in concrete.

The long-term durability characteristics of these alternative supplementary cementitious materials were investigated in addition to compatibility testing to ensure that these materials could be combined with Type IL limestone cements. Durability testing included three alkali-silica reactivity testing methods, sulfate resistance, and dimensional stability. Compatibility testing incorporated plastic properties testing such as mortar flow, isothermal conduction calorimetry, and concrete slump, as well as physical testing such as compressive strength, flexural strength, modulus of elasticity, and splitting tensile strength of concrete.

RESEARCH OBJECTIVES

The primary objectives of this research were:

- Investigate state and federal DOTs specifications and material suppliers to identify any potential sources of material not currently being investigated for partial replacement of cement.
- Confirm compatibility of alternative SCM with Type IL portland cement.
- Investigate the long-term durability of mortars and concretes with alternatives with respect to:
 - Resistance to alkali silica reactivity
 - Resistance to sulfate attack
 - Long-term dimensional stability

- Identify any limiting factors for material use, range of addition, or appropriate testing method to provide guidance to the Florida DOT with regards to implementation.

MAIN FINDINGS

The main findings from this study are summarized as follows:

- Of the state and federal DOTs and road agencies surveyed, there were no materials being investigated that were not already known to the FDOT.
- When contacting the source of the sugarcane bagasse ash producer for sample material, the researchers were informed that they had completed the upgrades to their emissions controls and provided samples from two different facilities which had differing chemical compositions.
 - The newer emission controls result in a material that is burned more completely, which results in a cleaner but more crystalline material.
 - This newer material (termed SCBA-B throughout) has lower reactivity due to the increased crystallinity.
 - The emission controls also concentrate chlorides in the ash, with the resulting ash having approximately 0.6% chloride content; therefore, limitations on the inclusion rate, depending on application, would need to be strictly monitored for adherence to FDOT concrete chloride limits.
 - The SCBA-B has a lower loss on ignition, and therefore, does not experience the same issues with respect to workability compared to the original SCBA (SCBA-A). Regardless, workability at high replacements requires the use of admixtures to attain workability regardless of SCBA type.
- Ground sand was investigated as a potential SCM as the material is abundant in Florida, however, after evaluating in isothermal calorimetry, it was determined that the material had negligible effect on hydration and was acting primarily as a filler and is not suitable for use as a pozzolan.
- Ground volcanic rock was investigated as a pozzolan, when combined to a portland cement system, it acts as a non-reactive filler (similar to ground sand); this material was generally neither beneficial, nor detrimental beyond dilution of cement.
- Ground glass was obtained for testing to investigate more rigorously compared to previous research. The incorporation of ground glass to a portland cement system that does not have potentially reactive aggregates does not increase the potential for ASR in the system.
- The short-term accelerated mortar bar experiments are not valid for ground glass mixtures due to the alkali content of the glass; when tested at full scale in the long-term ASTM C1293 test and in long-term outdoor exposure of durability blocks, the ground glass mitigated but did not prevent ASR when it was used in concrete with alkali-silica reactive aggregate.
- In general, the Type IL cement performed similarly to the Type I/II cements without compatibility issues with alternative SCM

- The specific Type IL cement used had significantly lower resistance to sulfate attack than the Type I/II cement used.

RECOMMENDATIONS

Based upon the findings from this study, the following recommendations are suggested:

- Revise the FDOT Standard Specification for Road and Bridge Construction Section 929 to allow the use of Class N fly ash that does not meet ASTM C618 with respect to loss on ignition only. This will allow the use of Sugarcane Bagasse Ash as a pozzolan in FDOT concrete.
- Revise the FDOT Standard Specification for Road and Bridge Construction Section 929 to allow the use of ASTM C618 Class C fly ash in ternary concrete mixes in aggressive environments and in binary concrete mixes placed in non-aggressive environments.
- Revise the FDOT Standard Specification for Road and Bridge Construction Section 929 to allow the use of ground glass in concrete for all exposures except when an aggregate is used that has been shown to have potential for being alkali-silica reactive. In this case, ground glass should be used in a ternary cementitious material blend that has passed ASTM C1293 testing with the specific alkali-silica-reactive aggregate.

MATERIAL-SPECIFIC RECOMMENDATIONS

Based upon the findings from this study, the following recommendations are suggested if any of the following materials are accepted as a qualified material:

Sugarcane Bagasse Ash

- Sugarcane bagasse ash may be used as a pozzolan in concrete provided that the chloride limits are not exceeded per the FDOT specification.
- Electrical test methods, such as surface resistivity, bulk resistivity, or chloride ion migration should not be performed on mixes incorporating sugarcane bagasse ash; conductive carbon within the material will give false measurements.
- Sugarcane bagasse ash should not be used in a binary mix when resistance to sulfate attack or alkali-silica reactivity is required.
- Sugarcane bagasse ash from facility A can be used in a ternary mix to suppress expansion caused by ASR. Sugarcane bagasse ash from facility B should not be used in ternary mixes when suppression of expansion caused by ASR is required.

Ground Glass

- The use of accelerated ASR testing methods should not be used with ground glass with an alkali content above 4.0%; this will produce unconservatively low results.
- Inclusions rates for binary mixtures should be limited to no more than 30% to ensure proper strength development.

Type II Cement

- Type II cement should not be used in areas where exposure to external sulfates will be anticipated without performance testing mixes incorporating SCM to show that sulfate degradation is not likely.

RECOMMENDATIONS FOR FUTURE STUDY

- The research conducted in this study indicates that alternative pozzolans, including sugarcane bagasse ash, ground glass, and Class C fly ash should be investigated further on a pilot scale for initial validation of use, application, and durability in service.
- Sugarcane bagasse ash and ground glass should be investigated further to determine threshold values for replacement level, particle size, optimum processing (bagasse ash), and long-term chloride durability (with electrical and physical testing).
- Investigate correction factors for sugarcane bagasse ashes of varying carbon contents to correct electric test methods such as surface resistivity, bulk resistivity, and chloride ion penetrability.

Table of Contents

Technical Report Documentation Page	iv
ACKNOWLEDGEMENTS	v
Executive Summary	vi
Background	vi
Research Objectives	vi
Main Findings	vii
Recommendations	viii
Material-Specific Recommendations	viii
Recommendations for Future Study	ix
List of Figures	xiii
List of Tables	xxii
1. Introduction	1
1.1 Background	1
1.1.1 Cement Manufacture	2
1.1.2 Cement Chemistry	2
1.1.3 Cement Hydration	3
1.1.4 Types of Cement	6
1.1.5 Supplementary Cementitious Materials (SCM)	8
1.2 Materials Review	9
1.2.1 Conventional SCM	10
1.2.2 Sugar Cane Bagasse Ash (SCBA)	11
1.2.3 Ground Glass (GG)	13
1.2.4 Ground Sand (GS)	15
1.2.5 Ground Volcanic Rock (VR)	16
1.3 Alkali-Silica Reaction (ASR)	17
1.3.1 Mechanisms and Symptoms	17
1.3.2 Test Methods	18
1.3.3 Mitigation	19
1.3.4 Effects of SCM	19
1.4 External Sulfate Attack	20
1.4.1 Mechanisms and Symptoms	21
1.4.2 Test Methods	22
1.4.3 Mitigation	22
1.5 Effect of Supplementary Cementitious Materials	22
1.6 Supplementary Cementitious Material Summary	23
1.7 Material Availability	24
1.7.1 Sugarcane Bagasse Ash (SCBA)	24
1.7.2 Ground Glass	25
1.7.3 Ground Volcanic Rock	25
1.7.4 Fly Ash	26
1.8 Survey of Select US Transportation Agencies	27
1.8.1 Alabama Department of Transportation (ALDOT)	28
1.8.2 Arkansas State Highway and Transportation Department (AHTD)	28
1.8.3 California Department of Transportation (Caltrans)	29
1.8.4 Florida Department of Transportation (FDOT)	30

1.8.5	Georgia Department of Transportation (GDOT)	31
1.8.6	Illinois Department of Transportation (IDOT)	32
1.8.7	Louisiana Department of Transportation and Development (LaDOTD).....	32
1.8.8	Mississippi Department of Transportation (MDOT)	33
1.8.9	North Carolina Department of Transportation (NCDOT)	34
1.8.10	Oklahoma Department of Transportation (ODOT)	35
1.8.11	South Carolina Department of Transportation (SCDOT).....	35
1.8.12	Tennessee Department of Transportation (TDOT).....	36
1.8.13	Texas Department of Transportation (TxDOT).....	37
1.8.14	Virginia Department of Transportation (VDOT).....	37
1.8.15	Unified Facilities Criteria (UFC)	38
1.8.16	Summary	39
2.	Material Acquisition and Characterization	41
2.1	Elemental Composition.....	43
2.2	Mineral Composition	45
2.3	Particle Size Distribution	47
2.4	Specific Heat Capacity.....	50
2.5	Apparent Specific Gravity	54
2.6	Concrete Aggregate Properties	54
2.7	Isothermal Conduction Calorimetry	55
2.7.1	Portland Cement.....	57
2.7.2	Class F Fly Ash.....	58
2.7.1	Class C Fly Ash	59
2.7.1	Silica Fume	62
2.7.2	Sugarcane Bagasse Ash	64
2.7.3	Ground Glass	68
2.7.4	Volcanic Rock.....	70
2.7.5	Ground Sand – R ³ Method.....	74
2.8	Chloride Concentration.....	76
3.	Mortar Testing.....	78
3.1	Mixture Design and Composition.....	78
3.2	Testing Results.....	80
3.2.1	Mortar Flow – ASTM C1437	80
3.2.2	Time of Set – ASTM C403.....	82
3.2.3	Compressive Strength – ASTM C109	93
3.2.4	Length Change – ASTM C157	104
3.2.5	Alkali-Silica Reaction – ASTM C1567	115
3.2.6	Sulfate Resistance – ASTM C1012	135
4.	Concrete Testing	154
4.1	Mixture Design and Composition.....	154
4.2	Concrete Mix Proportions.....	155
4.3	Testing Results.....	158
4.3.1	Slump – ASTM C143	158
4.3.1	Temperature – ASTM C1064	162
4.3.2	Density (Unit Weight) – ASTM C138.....	164
4.3.3	Air Content – ASTM C231.....	166

4.4	Mechanical Properties.....	169
4.4.1	Compressive Strength – ASTM C39	170
4.4.2	Splitting Tensile Strength – ASTM C496.....	188
4.4.3	Flexural Strength – ASTM C78.....	194
4.4.4	Modulus of Elasticity – ASTM C469.....	197
4.4.5	Coefficient of Thermal Expansion – AASHTO T 336.....	200
4.5	Long-Term Durability Testing.....	202
4.5.1	Alkali-Silica Reaction – ASTM C1293	202
4.5.2	Durability Blocks.....	211
4.5.3	Comparison of ASTM C1293 and Concrete Durability Blocks.....	226
4.5.4	Surface and Bulk Resistivity – AASHTO T 358 [182] and AASHTO TP 119.....	227
5.	Summary and Recommendations.....	251
	Recommendations.....	252
	Material-Specific Recommendations.....	253
	Recommendations for Future Study	253
	References.....	254
	Appendix A – X-Ray Diffractograms.....	271

List of Figures

Figure 1-1. Typical hydration of tricalcium silicate adapted from [1].	4
Figure 1-2. Rate of heat of evolution adapted from [1].	5
Figure 1-3: Coal fly ash production and consumption over time. [108].	26
Figure 1-4: State Departments of Transportation included in this survey.	28
Figure 2-1. Left: SCBA A. Right: SCBA B.	41
Figure 2-2. Alkali-silica reactive fine aggregate from the Jobe mine in El Paso, Texas.	43
Figure 2-3. Classic photon emission during x-ray fluorescence. A – X-Ray emitted onto an inner-shell electron. B – Inner-shell electron. C – Characteristic X-Ray being emitted from atom.	44
Figure 2-4. Particle size distribution for SCBA-A.	48
Figure 2-5. Particle size distribution for SCBA-B.	48
Figure 2-6. Particle size distribution for Class F fly ash.	49
Figure 2-7. Particle size distribution for Class C fly ash.	49
Figure 2-8. Particle size distribution for Ground Glass.	49
Figure 2-9. Particle size distribution for Volcanic Rock.	49
Figure 2-10. Particle size distribution for Silica Fume.	50
Figure 2-11: Particle size distribution for Ground Sand.	50
Figure 2-12: Specific heat capacity graph for Type I/II portland cement.	51
Figure 2-13: Specific heat capacity graph for high alkali Type I/II portland cement.	51
Figure 2-14: Specific heat capacity graph for Type IL limestone cement.	51
Figure 2-15: Specific heat capacity graph for Class C fly ash.	51
Figure 2-16: Specific heat capacity graph for Class F fly ash.	52
Figure 2-17: Specific heat capacity graph for silica fume.	52
Figure 2-18: Specific heat capacity graph for volcanic rock.	52
Figure 2-19: Specific heat capacity graph for ground glass.	52
Figure 2-20: Specific heat capacity graph for SCBA-A.	53
Figure 2-21: Specific heat capacity graph for SCBA-B.	53
Figure 2-22: Internal mixing ampoule.	56
Figure 2-23. Instantaneous heat curve of Type I/II and Type IL cement pastes.	57
Figure 2-24. Cumulative heat curve of Type I/II and Type IL cement pastes.	57
Figure 2-25. Instantaneous heat curve of cement paste with a 20% replacement of Class F Fly ash compared to a Type I/II cement paste.	58
Figure 2-26. Instantaneous heat curve of cement paste with a 20% replacement of Class F Fly ash compared to a Type IL cement paste.	58
Figure 2-27. Cumulative heat curve of cement paste with a 20% replacement of Class F Fly ash compared to a Type I/II cement paste.	59
Figure 2-28. Cumulative heat curve of cement paste with a 20% replacement of Class F Fly ash compared to a Type IL cement paste.	59
Figure 2-29. Instantaneous heat curve of cement paste with 20 and 30% replacements of Class C Fly ash compared to a Type I/II cement paste.	60
Figure 2-30. Instantaneous heat curve of cement paste with 20 and 30% replacements of Class C Fly ash compared to a Type IL cement paste.	60
Figure 2-31. Cumulative heat curve of cement paste with 20 and 30% replacements of Class C Fly ash compared to a Type I/II cement paste.	61

Figure 2-32. Cumulative heat curve of cement paste with 20 and 30% replacements of Class C Fly ash compared to a Type IL cement paste.	61
Figure 2-33. Instantaneous heat curve of cement paste with a 4% replacement of Silica Fume compared to a Type I/II cement paste.	62
Figure 2-34. Instantaneous heat curve of cement paste with a 4% replacement of Silica Fume compared to a Type IL cement paste.	62
Figure 2-35. Cumulative heat curve of cement paste with a 4% replacement of Silica Fume compared to a Type I/II cement paste.	63
Figure 2-36. Cumulative heat curve of cement paste with a 4% replacement of Silica Fume compared to a Type IL cement paste.	63
Figure 2-37. Instantaneous heat curve of cement paste with 10% – 30% replacements of SCBA-A compared to a Type I/II cement paste.	64
Figure 2-38. Instantaneous heat curve of cement paste with 10% – 30% replacements of SCBA-B compared to a Type I/II cement paste.	65
Figure 2-39. Instantaneous heat curve of cement paste with 10% – 30% replacements of SCBA-A compared to a Type IL cement paste.	65
Figure 2-40. Instantaneous heat curve of cement paste with 10% – 30% replacements of SCBA-B compared to a Type IL cement paste.	66
Figure 2-41. Cumulative heat curve of cement paste with 10% – 30% replacements of SCBA-A compared to a Type I/II cement paste.	66
Figure 2-42. Cumulative heat curve of cement paste with 10% – 30% replacements of SCBA-B compared to a Type I/II cement paste.	67
Figure 2-43. Cumulative heat curve of cement paste with 10% – 30% replacements of SCBA-A compared to a Type IL cement paste.	67
Figure 2-44. Cumulative heat curve of cement paste with 10% – 30% replacements of SCBA-B compared to a Type IL cement paste.	68
Figure 2-45. Instantaneous heat curve of cement paste with 20% – 40% replacements of GG compared to a Type I/II cement paste.	69
Figure 2-46. Instantaneous heat curve of cement paste with 20% – 40% replacements of GG compared to a Type IL cement paste.	69
Figure 2-47. Cumulative heat curve of cement paste with 20% – 40% replacements of GG compared to a Type I/II cement paste.	70
Figure 2-48. Cumulative heat curve of cement paste with 20% – 40% replacements of GG compared to a Type IL cement paste.	70
Figure 2-49. Instantaneous heat curve of cement paste with a 20% replacement of VR compared to a Type I/II cement paste.	71
Figure 2-50. Instantaneous heat curve of cement paste with a 20% replacement of VR compared to a Type IL cement paste.	71
Figure 2-51. Cumulative heat curve of cement paste with a 20% replacement of VR compared to a Type I/II cement paste.	72
Figure 2-52. Cumulative heat curve of cement paste with a 20% replacement of VR compared to a Type IL cement paste.	72
Figure 2-53: Instantaneous heat (A) and cumulative heat output (B) results from the R ³ method comparing 30% slag and 30% GS replacements to control.	75
Figure 2-54: Reactivity curve comparing 30% slag cement and 30% ground sand mixtures.	76
Figure 2-55: Chloride content limits for concrete construction (Table 346-5 from [107])	77

Figure 3-1: Scanning electron microscopy (SEM) image of SCBA-A.....	81
Figure 3-2: Time of set of mortar containing SCBA replacement of Type I/II cement.	83
Figure 3-3: Time of set of mortar containing GG, SF, or VR replacement of Type I/II cement..	84
Figure 3-4: Time of set of mortar containing C ash or F ash replacement of Type I/II cement. ..	85
Figure 3-5: Time of set of mortar containing a ternary blend of C ash and SCBA replacement of Type I/II cement.....	86
Figure 3-6: Time of set of mortar containing a ternary blend of C ash and GG, VR, or SF replacement of Type I/II cement.	86
Figure 3-7: Time of set of mortar containing a ternary blend of C ash and F ash replacement of Type I/II cement.....	87
Figure 3-8: Time of set of mortar containing SCBA replacement of Type IL cement.....	89
Figure 3-9: Time of set of mortar containing GG, SF, or VR replacement of Type IL cement. ..	90
Figure 3-10: Time of set of mortar containing C ash or F ash replacement of Type IL cement. .	90
Figure 3-11: Time of set of mortar containing a ternary blend of C ash and SCBA replacement of Type IL cement.	91
Figure 3-12: Time of set of mortar containing a ternary blend of C ash and GG, VR, or SF replacement of Type IL cement.	92
Figure 3-13: Time of set of mortar containing a ternary blend of C ash and F ash replacement of Type IL cement.	92
Figure 3-14: Compressive strength of mortar containing SCBA replacement of Type I/II cement.	94
Figure 3-15: Compressive strength of mortar containing GG, SF, or VR replacement of Type I/II cement.	95
Figure 3-16: Compressive strength of mortar containing C ash or F ash replacement of Type I/II cement.	96
Figure 3-17: Compressive strength of mortar containing a ternary blend of C ash and SCBA replacement of Type I/II cement.....	97
Figure 3-18: Compressive strength of mortar containing a ternary blend of C ash and GG, VR, or SF replacement of Type I/II cement.	97
Figure 3-19: Compressive strength of mortar containing a ternary blend of C ash and F ash replacement of Type I/II cement.....	98
Figure 3-20: Compressive strength of mortar containing C ash or F ash replacement of Type IL cement.	100
Figure 3-21: Compressive strength of mortar containing SCBA replacement of Type IL cement.	101
Figure 3-22: Compressive strength of mortar containing GG, SF, or VR replacement of Type IL cement.	101
Figure 3-23: Compressive strength of mortar containing a ternary blend of C ash and SCBA replacement of Type IL cement.	102
Figure 3-24: Compressive strength of mortar containing a ternary blend of C ash and GG, VR, or SF replacement of Type IL cement.....	103
Figure 3-25: Compressive strength of mortar containing a ternary blend of C ash and F ash replacement of Type IL cement.	103
Figure 3-26: Length change of mortar containing SCBA-A replacement of Type I/II cement..	105
Figure 3-27: Length change of mortar containing SCBA-B replacement of Type I/II cement..	105
Figure 3-28: Length change of mortar containing SCBA-A replacement of Type IL cement. ..	106

Figure 3-29: Length change of mortar containing SCBA-B replacement of Type IL cement ...	106
Figure 3-30: Length change of mortar containing a ternary blend of C ash and SCBA-A replacement of Type I/II cement.....	107
Figure 3-31: Length change of mortar containing a ternary blend of C ash and SCBA-B replacement of Type I/II cement.....	107
Figure 3-32: Length change of mortar containing a ternary blend of C ash and SCBA-A replacement of Type IL cement.....	108
Figure 3-33: Length change of mortar containing a ternary blend of C ash and SCBA-B replacement of Type IL cement.....	108
Figure 3-34: Length change of mortar containing GG replacement of Type I/II cement.....	109
Figure 3-35: Length change of mortar containing GG replacement of Type IL cement.....	109
Figure 3-36: Length change of mortar containing a ternary blend of C ash and GG replacement of Type I/II cement.....	110
Figure 3-37: Length change of mortar containing a ternary blend of C ash and GG replacement of Type IL cement.....	110
Figure 3-38: Length change of mortar containing SF or VR replacement of Type I/II cement.	111
Figure 3-39: Length change of mortar containing SF or VR replacement of Type IL cement. .	111
Figure 3-40: Length change of mortar containing a ternary blend of C ash and VR or SF replacement of Type I/II cement.....	112
Figure 3-41: Length change of mortar containing a ternary blend of C ash and VR or SF replacement of Type IL cement.....	112
Figure 3-42: Length change of mortar containing C ash or F ash replacement of Type I/II cement.....	113
Figure 3-43: Length change of mortar containing C ash or F ash replacement of Type IL cement.....	114
Figure 3-44: Length change of mortar containing a ternary blend of C ash and F ash replacement of Type I/II cement.....	114
Figure 3-45: Length change of mortar containing a ternary blend of C ash and F ash replacement of Type IL cement.....	115
Figure 3-46: Accelerated ASR results using Florida sand and Type I/II and Type IL cements.	117
Figure 3-47: Accelerated ASR results using Florida sand and F ash with Type I/II cement.	118
Figure 3-48: Accelerated ASR results using Florida sand and F ash with Type IL cement.....	118
Figure 3-49: Accelerated ASR results using Florida sand and C ash with Type I/II cement.	119
Figure 3-50: Accelerated ASR results using Florida sand and C ash with Type IL cement.	119
Figure 3-51: Accelerated ASR results using Florida sand and SF with Type I/II cement.....	120
Figure 3-52: Accelerated ASR results using Florida sand and SF with Type IL cement.....	120
Figure 3-53: Accelerated ASR results using Florida sand and SCBA-A with Type I/II cement.....	121
Figure 3-54: Accelerated ASR results using Florida sand and SCBA-B with Type I/II cement.	122
Figure 3-55: Accelerated ASR results using Florida sand and SCBA-A with Type IL cement.	122
Figure 3-56: Accelerated ASR results using Florida sand and SCBA-B with Type IL cement.	123
Figure 3-57: Accelerated ASR results using Florida sand and GG with Type I/II cement.	124
Figure 3-58: Accelerated ASR results using Florida sand and GG with Type IL cement.....	124
Figure 3-59: Accelerated ASR results using Florida sand and VR with Type I/II cement.	125
Figure 3-60: Accelerated ASR results using Florida sand and VR with Type IL cement.....	125

Figure 3-61: Accelerated ASR results using Florida sand for ternary mixes incorporating SCBA with Type I/II cement.....	126
Figure 3-62: Accelerated ASR results using Florida sand for ternary mixes incorporating SCBA with Type IL cement.....	126
Figure 3-63: Accelerated ASR results using Florida sand for ternary mixes incorporating GG, F ash, VR, and SF with Type IL cement.....	127
Figure 3-64: Accelerated ASR results using Jobe sand with Type I/II or Type IL cement.....	130
Figure 3-65: Accelerated ASR results using Jobe sand and SCBA-A with Type I/II cement....	131
Figure 3-66: Accelerated ASR results using Jobe sand and SCBA-A with Type IL cement.....	131
Figure 3-67: Accelerated ASR results using Jobe sand and SCBA-B with Type I/II cement....	132
Figure 3-68: Accelerated ASR results using Jobe sand and SCBA-B with Type IL cement.....	132
Figure 3-69: Accelerated ASR results using Jobe sand and GG with Type I/II cement.....	133
Figure 3-70: Accelerated ASR results using Jobe sand and GG with Type IL cement.....	133
Figure 3-71: Accelerated ASR results using Jobe sand and VR with Type I/II cement.....	134
Figure 3-72: Accelerated ASR results using Jobe sand and VR with Type IL cement.....	134
Figure 3-73: X-ray diffractogram showing the scans of cement powders using Type I/II and Type IL cements along with the reference scans for ettringite and thaumasite.....	138
Figure 3-75: Sulfate attack induced expansion results comparing Type I/II with Type IL cement mixtures.....	139
Figure 3-76: Sulfate attack induced expansion results comparing C ash and F ash mixtures in Type I/II systems to control.....	140
Figure 3-77: Sulfate attack induced expansion results comparing C ash and F ash mixtures in Type IL systems to control.....	141
Figure 3-78: Sulfate attack induced expansion results comparing the SF mixture in a Type I/II system to control.....	142
Figure 3-79: Sulfate attack induced expansion results comparing the SF mixture in a Type IL system to control.....	142
Figure 3-80: Sulfate attack induced expansion results comparing SCBA-A mixtures in Type I/II systems to control.....	143
Figure 3-81: Sulfate attack induced expansion results comparing SCBA-B mixtures in Type I/II systems to control.....	144
Figure 3-82: Sulfate attack induced expansion results comparing SCBA-A mixtures in Type IL systems to control.....	144
Figure 3-83: Sulfate attack induced expansion results comparing SCBA-B mixtures in Type IL systems to control.....	145
Figure 3-84: Sulfate attack induced expansion results comparing GG mixtures in Type I/II systems to control.....	146
Figure 3-85: Sulfate attack induced expansion results comparing GG mixtures in Type IL systems to control.....	146
Figure 3-86: Sulfate attack induced expansion results comparing VR mixtures in Type I/II systems to control.....	147
Figure 3-87: Sulfate attack induced expansion results comparing VR mixtures in Type IL systems to control.....	147
Figure 3-88: Sulfate attack induced expansion results comparing ternary SCBA mixtures Type I/II systems to control.....	148

Figure 3-89: Sulfate attack induced expansion results comparing ternary SCBA mixtures Type IL systems to control.	148
Figure 3-90: Sulfate attack induced expansion results comparing ternary mixtures with GG or F ash with C ash in Type I/II systems to control.....	149
Figure 3-91: Sulfate attack induced expansion results comparing ternary mixtures with GG or F ash with C ash in Type IL systems to control.....	149
Figure 3-92: Sulfate attack induced expansion results comparing ternary mixtures with VR or SF with C ash in Type I/II systems to control.....	150
Figure 3-93: Sulfate attack induced expansion results comparing ternary mixtures with VR or SF with C ash in Type IL systems to control.	150
Figure 4-1: Compressive strength of Type IL Class I concrete, Type IL Class IV concrete, and Type I/II Class IV concrete mixes.	170
Figure 4-2: Compressive strength of concrete with 10% – 30% SCBA-A or SCBA-B as Type I/II cement replacements.	172
Figure 4-3: Compressive strength of concrete with 10% – 30% SCBA as Type IL cement replacements.	172
Figure 4-4: Compressive strength of concrete with 20% – 40% GG or 20% VR as I/II cement replacements.	173
Figure 4-5: Compressive strength of concrete with 20% – 40% GG or 20% VR as IL cement replacements.	174
Figure 4-6: Compressive strength of concrete with 20 – 30% F or C ash, or 4% SF as I/II cement replacements.	175
Figure 4-7: Compressive strength of concrete with 20 – 30% F or C ash, or 4% SF as IL cement replacements.	175
Figure 4-8: Compressive strength of mixes containing 30% C fly ash and 5% – 10% SCBA as Type I/II replacements.	177
Figure 4-9: Compressive strength of mixes containing 30% C ash with 5% – 10% SCBA as Type IL replacements.....	177
Figure 4-10: Compressive strength of ternary mixes containing 20% or 30% C ash with 5-10% GG, 10% F ash, 10% VR, or 4% SF as I/II cement replacements.....	178
Figure 4-11: Compressive strength of ternary mixes containing 20% C ash and 5% or 10% GG or 30% C ash with 5% – 10% F ash, 10% VR, or 4% SF as IL cement replacements.	178
Figure 4-12: Compressive strength of concrete with 10% – 30% SCBA-A or SCBA-B as Type IL cement replacements.	183
Figure 4-13: Compressive strength of concrete with 20% – 40% GG and 20% VR as IL cement replacements.	184
Figure 4-14: Compressive strength of concrete with 20 – 30% F or C ash, or 4% SF as IL cement replacements.	185
Figure 4-15: Compressive strength of Class I ternary mixes containing 30% C ash with 5% – 10% SCBA-A and SCBA-B as IL cement replacements.....	186
Figure 4-16: Compressive strength of Class I ternary mixes containing 20% C ash and 5% or 10% GG or 30% C ash with 5% – 10% F ash, 10% VR, or 4% SF as IL cement replacements.	186
Figure 4-17: Concrete prism test results for mixtures incorporating SCBA-A.	205
Figure 4-18: Concrete prism test results for mixtures incorporating SCBA-B.	206
Figure 4-19: Concrete prism test results for mixtures incorporating ground glass.....	206

Figure 4-20: Concrete prism test results for mixtures incorporating C ash and F ash.....	207
Figure 4-21: Concrete prism test results for mixtures incorporating VR and SF.	208
Figure 4-22: Concrete prism test results for ternary mixtures incorporating SCBA.	209
Figure 4-23: Concrete prism test results for ternary mixtures incorporating GG and F ash.	209
Figure 4-24: Concrete prism test results for ternary mixtures incorporating SF and VR.	210
Figure 4-25: Comparison of test results for binary systems utilizing Type I/II and Type IL cements replaced with alternative SCM	210
Figure 4-26: Gauge point created by drilling into threaded rod before embedding into concrete.	212
Figure 4-27: Measurement of "top" face of block using mechanical strain gauge with digital indicator of 0.0001" precision.....	213
Figure 4-28: Reference bar used to calibrate the comparator before each measurement.	213
Figure 4-29: Measurement of "right" face of block with applied pressure in the direction of the red arrows.....	214
Figure 4-30: Durability block internal temperature measurement with embedded thermocouple.	215
Figure 4-31: Example block and measurement orientation.	215
Figure 4-32: Concrete exposure site at Powell Laboratory, University of Florida.....	216
Figure 4-33: Expansion of durability blocks containing high alkali cement, reactive aggregate, and 10% - 30% SCBA-A.	217
Figure 4-34: Expansion of durability blocks containing high alkali cement, reactive aggregate, and 10% - 30% SCBA-B.	218
Figure 4-35: Expansion of durability blocks containing high alkali cement, reactive aggregate, and 20% - 40 % ground glass.	219
Figure 4-36: Expansion of durability blocks containing high alkali cement, reactive aggregate, and 20% Class F fly ash.....	220
Figure 4-37: Expansion of durability blocks containing high alkali cement, reactive aggregate, and 20% - 30% Class C fly ash.....	221
Figure 4-38: Expansion of durability blocks containing high alkali cement, reactive aggregate, and 20% volcanic rock.....	222
Figure 4-39: Expansion of durability blocks containing high alkali cement, reactive aggregate, and 4% silica fume.....	222
Figure 4-40: Expansion of durability blocks containing high alkali cement, reactive aggregate, and 30% Class C fly ash and 5% or 10% of SCBA-A or SCBA-B.....	223
Figure 4-41: Expansion of durability blocks containing high alkali cement, reactive aggregate, and 20% Class C fly ash and 5% or 10% ground glass.	224
Figure 4-42: Expansion of durability blocks containing high alkali cement, reactive aggregate, and 30% Class C fly ash and 5% or 10% Class F fly ash.	225
Figure 4-43: Expansion of durability blocks containing high alkali cement, reactive aggregate, and 30% Class C fly ash with 10% volcanic rock or 4% silica fume.....	225
Figure 4-44: Comparison of ASTM C1293 and durability block expansion.....	227
Figure 4-45: Surface resistivity of Class IV concrete with Type I/II cement and SCBA.....	229
Figure 4-46: Surface resistivity of Class IV concrete with Type IL cement and SCBA.	229
Figure 4-47: Surface resistivity of Class I concrete with Type IL cement and SCBA.....	230
Figure 4-48: Bulk resistivity of Class IV concrete with Type I/II cement and SCBA.	231
Figure 4-49: Bulk resistivity of Class IV concrete with Type IL cement and SCBA.	231

Figure 4-50: Bulk resistivity of Class I concrete with Type IL cement and SCBA.	232
Figure 4-51: Class IV concrete with Type I/II cement and Class C fly ash, Class F fly ash, or ground glass replacement surface resistivity measurements.	233
Figure 4-52: Class IV, Type IL cement with Class C fly ash, Class F fly ash, or ground glass replacement surface resistivity measurements.....	234
Figure 4-53: Class I, Type IL cement with Class C fly ash, Class F fly ash, or ground glass replacement surface resistivity measurements.....	234
Figure 4-54: Class IV, Type I/II cement with Class C fly ash, Class F fly ash, or ground glass replacement bulk resistivity measurements.	235
Figure 4-55: Class IV, Type IL cement with Class C fly ash, Class F fly ash, or ground glass replacement bulk resistivity measurements.	235
Figure 4-56: Class I, Type IL cement with Class C fly ash, Class F fly ash, or ground glass replacement bulk resistivity measurements.	236
Figure 4-57: Class IV, Type I/II cement with volcanic rock or silica fume replacement surface resistivity measurements.	237
Figure 4-58: Class IV, Type IL cement with volcanic rock or silica fume replacement surface resistivity measurements.	237
Figure 4-59: Class I, Type IL cement with volcanic rock or silica fume replacement surface resistivity measurements.	238
Figure 4-60: Class IV, Type I/II cement with volcanic rock or silica fume replacement bulk resistivity measurements.	238
Figure 4-61: Class IV, Type IL cement with volcanic rock or silica fume replacement bulk resistivity measurements.	239
Figure 4-62: Class I, Type IL cement with volcanic rock or silica fume replacement bulk resistivity measurements.	239
Figure 4-63: Class IV, Type I/II ternary blends with Class C fly ash and SCBA-A, SCBA-B, or ground glass surface resistivity measurements.	240
Figure 4-64: Class IV, Type IL ternary blends with Class C fly ash and SCBA-A, SCBA-B, or ground glass surface resistivity measurements.	240
Figure 4-65: Class I, Type IL ternary blends with Class C fly ash and SCBA-A, SCBA-B, or ground glass surface resistivity measurements.	241
Figure 4-66: Class IV, Type I/II ternary blends with Class C fly ash and SCBA-A, SCBA-B, or ground glass bulk resistivity measurements.	242
Figure 4-67: Class IV, Type IL ternary blends with Class C fly ash and SCBA-A, SCBA-B, or ground glass bulk resistivity measurements.	242
Figure 4-68: Class I, Type IL ternary blends with Class C fly ash and SCBA-A, SCBA-B, or ground glass bulk resistivity measurements.	243
Figure 4-69: Class IV, Type I/II ternary blends with Class C fly ash and Class F fly ash, volcanic rock, or silica fume surface resistivity measurements.	244
Figure 4-70: Class IV, Type IL ternary blends with Class C fly ash and Class F fly ash, volcanic rock, or silica fume surface resistivity measurements.	245
Figure 4-71: Class I, Type IL ternary blends with Class C fly ash and Class F fly ash, volcanic rock, or silica fume surface resistivity measurements.	245
Figure 4-72: Class IV, Type I/II ternary blends with Class C fly ash and Class F fly ash, volcanic rock, or silica fume bulk resistivity measurements.....	246

Figure 4-73: Class IV, Type IL ternary blends with Class C fly ash and Class F fly ash, volcanic rock, or silica fume bulk resistivity measurements.....	246
Figure 4-74: Class I, Type IL ternary blends with Class C fly ash and Class F fly ash, volcanic rock, or silica fume bulk resistivity measurements.....	247
Figure A-1. X-ray diffractogram for Type I/II cement.	271
Figure A-2. X-ray diffractogram for Type IL cement.	271
Figure A-3. X-ray diffractogram for high alkali Type I/II portland cement.....	272
Figure A-4. X-ray diffractogram for Class F fly ash.	272
Figure A-5. X-ray diffractogram for Class C fly ash.....	273
Figure A-6. X-ray diffractogram for SCBA-A.	273
Figure A-7. X-ray diffractogram for SCBA-B.	274
Figure A-8. X-ray diffractogram for VR.	274

List of Tables

Table 1-1. Cement chemistry notation for common oxides.....	2
Table 1-2. Typical chemical composition (mass %) of portland cement	3
Table 1-3. Properties of the four main cement compounds [1]	3
Table 1-4. Chemical reactants and products of cement hydration [1].	6
Table 1-5. General SCM limits for blended cements per ASTM C595 [20].....	7
Table 1-6. Typical chemical compositional ranges (mass %) for PLC.	8
Table 1-7. Effects due to the PLC.....	8
Table 1-8. Typical chemical compositional ranges (mass %) for conventional SCM [3].....	11
Table 1-9. Effects due to the addition conventional SCM to PCC [3].	11
Table 1-10. Typical chemical compositional ranges (mass %) for sugarcane bagasse ash.....	12
Table 1-11. Effects due to the addition of SCBA to PCC.	13
Table 1-12. Typical chemical compositional ranges (mass %) for ground glass [8].....	14
Table 1-13. Effects due to the addition of GG to PCC.	15
Table 1-14. Typical chemical compositional ranges (mass %) for ground sand.	15
Table 1-15. Typical chemical compositional ranges (mass %) for ground volcanic rock.....	16
Table 1-16. ASTM mortar test method for ASR.	19
Table 1-17. Supplementary cementitious materials and limits as per ALDOT [111].	28
Table 1-18. Supplementary cementitious materials and limits as per AHTD [112].....	29
Table 1-19. Supplementary cementitious materials and limits as per Caltrans [113].	30
Table 1-20. Supplementary cementitious materials and limits as per FDOT [21].	31
Table 1-21. Supplementary cementitious materials and limits as per GDOT [114].....	32
Table 1-22. Supplementary cementitious materials and limits as per IDOT [115].	32
Table 1-23. Supplementary cementitious materials and limits as per LaDOTD [116].	33
Table 1-24. Supplementary cementitious materials and limits as per MDOT [117].	34
Table 1-25. Supplementary cementitious materials and limits as per NCDOT [118].	34
Table 1-26. Supplementary cementitious materials and limits as per ODOT [119].....	35
Table 1-27. Supplementary cementitious material replacement of blended cements as per [119].	35
Table 1-28. Supplementary cementitious materials and limits as per SCDOT [120].....	36
Table 1-29. Supplementary cementitious materials and limits as per TDOT [121].	36
Table 1-30. Supplementary cementitious materials and limits as per TxDOT [122].	37
Table 1-31. Supplementary cementitious materials and limits as per VDOT [123].....	38
Table 1-32. Minimum level of replacement by supplementary cementitious materials as per [123].	38
Table 1-33. Supplementary cementitious materials and limits as per UFC [124].	39
Table 2-1. Materials acquired for this research.	42
Table 2-2. Elemental oxide composition of materials by x-ray fluorescence.....	45
Table 2-3. Mineral composition of materials by x-ray powder diffraction.	46
Table 2-4. Summary of particle size distribution of materials.....	48
Table 2-5. Specific heat capacity of materials used for this evaluation.....	53
Table 2-6. Summary of measured specific gravities of materials.....	54
Table 2-7. Measured aggregate proprieties.....	55
Table 2-8: Summary table of isothermal data for Type I/II cement with SCM replacements.....	73
Table 2-9: Summary table of isothermal data for Type IL cement with SCM replacements.....	74
Table 2-10. Summary of acid soluble chlorides present in each material.	77

Table 3-1: Mortar mix proportions (lb/yd ³) with Type I/II cement and Florida sand for ASTMs C109, C157, C403, C1437, and C1567.	79
Table 3-2: Mortar mix proportions (lb/yd ³) with Type IL cement and Florida sand for ASTMs C109, C157, C403, C1437, and C1567.	80
Table 3-3: Summary of flow of mortars using Type I/II or Type IL cement with SCM.....	82
Table 3-4: Summary of time of set of mortars using a Type I/II cement with SCM.....	88
Table 3-5: Summary of time of set of mortars using a Type IL cement with SCM.	93
Table 3-6: Summary of compressive strength of mortars using Type I/II cement and SCM.	99
Table 3-7: Summary of compressive strength of mortars using Type IL cement and SCM.	104
Table 3-8: ASTM C1567 14-day expansions of mortars with Florida sand using Type I/II or Type IL cement and SCM.....	128
Table 3-9: Mortar mix proportions (in lb/yd ³) with Type I/II cement and Jobe sand for ASTM C1567.....	129
Table 3-10: Mortar mix proportions (in lb/yd ³) with Type IL cement and Jobe sand for ASTM C1567.....	129
Table 3-11: ASTM C1567 14-day expansions of mortars with Jobe sand using Type I/II or Type IL cement and SCM.....	135
Table 3-12: Mortar mix proportions (in lb/yd ³) for sulfate testing with I/II cement	136
Table 3-13: Mortar mix proportions (in lb/yd ³) for sulfate testing with IL cement.....	137
Table 3-14: Summary of sulfate expansion values at 12 months and 18 months for Type I/II cementitious mixtures.	151
Table 3-15: Summary of sulfate expansion values at 12 months and 18 months for Type IL cementitious mixtures.	152
Table 3-16: Summary of damaged mortar bars.	153
Table 4-1. Minimum cement content and maximum w/cm as per FDOT [21]	155
Table 4-2: Class IV concrete proportions (lb/yd ³) using Type I/II cement	156
Table 4-3: Class IV concrete proportions (lb/yd ³) using Type IL cement.....	157
Table 4-4: Class I concrete proportions (lb/yd ³) using Type IL cement.....	158
Table 4-5: Slump of Class IV concrete mixes using Type I/II concrete.....	160
Table 4-6: Slump of Class IV concrete mixes using Type IL concrete	161
Table 4-7: Slump of Class I concrete mixes using Type IL concrete.....	162
Table 4-8: Fresh temperature of Class IV concrete using Type I/II or Type IL cement with SCM	163
Table 4-9: Fresh temperature of Class I concrete using Type IL cement with SCM	164
Table 4-10: Unit weight of Class IV concrete using Type I/II or Type IL cement with SCM... ..	165
Table 4-11: Unit weight of Class I concrete using Type IL cement with SCM	166
Table 4-12: Air content of Class IV concrete mixes using Type I/II or Type IL cement with SCM	168
Table 4-13: Air content of Class I concrete mixes using Type IL cement with SCM.....	169
Table 4-14: Summary table of compressive strength results for Class IV concrete mixes utilizing Type I/II cement.....	179
Table 4-15: Summary chart of normalized compressive strengths for Class IV concrete mixes utilizing Type I/II cement.	180
Table 4-16: Summary chart of compressive strength results for Class IV concrete mixes utilizing Type IL cement.	181

Table 4-17: Summary chart of normalized compressive strengths for concrete mixes utilizing Type II cement.	182
Table 4-18: Summary chart of compressive strength results for Class I concrete mixes utilizing Type II cement.	187
Table 4-19: Summary chart of normalized compressive strengths for Class I concrete mixes utilizing Type II cement.	188
Table 4-20: Splitting tensile strength results for Class IV concrete utilizing Type I/II cement.	189
Table 4-21: Comparison of splitting tensile strength results normalized to control for Class IV concrete utilizing Type I/II cement.	190
Table 4-22: Splitting tensile strength results for Class IV concrete utilizing Type II cement.	191
Table 4-23: Comparison of splitting tensile strength results normalized to control for Class IV concrete utilizing Type II cement.	192
Table 4-24: Splitting tensile strength results for Class I concrete utilizing Type II cement.	193
Table 4-25: Comparison of splitting tensile strength results normalized to control for Class I concrete utilizing Type II cement.	194
Table 4-26: Summary of flexural strength results for Class I concrete utilizing Type II cement.	195
Table 4-27: Summary of normalized flexural strength results for Class I concrete utilizing Type II cement.	196
Table 4-28: Summary of MOE values for Class IV concrete utilizing Type I/II cement.	198
Table 4-29: Summary of MOE values for Class IV concrete utilizing Type II cement.	199
Table 4-30: Summary of MOE values for Class I concrete utilizing Type II cement.	200
Table 4-31: Summary of the CTE results (reported in microstrain/°C) for each class of concrete with each type of cement.	201
Table 4-32: ASTM C1293 concrete binder proportions (in lb/yd ³) using high-alkali Type I/II cement.	204
Table 4-33: Summary of ASTM C1293 expansion of concrete with SCM.	211
Table 4-34: Chloride ion penetrability classification values for surface and bulk resistivity. Adapted from [202,206].	228
Table 4-35: Surface and bulk resistivity results for Class IV concrete using Type I/II cement.	248
Table 4-36: Surface and bulk resistivity results for Class IV concrete using Type II cement.	249
Table 4-37: Surface and bulk resistivity results for Class I concrete using Type II cement.	250

1. Introduction

1.1 BACKGROUND

The Romans and Greeks primarily used lime mortar and hydraulic lime to build their roads, aqueducts, and temples [1]. Today, portland cement concrete (PCC) is the preferred material for construction throughout the world. Several benefits for the selection and use of PCC include its ease of implementation, accessibility of raw materials, versatility as a construction material, low cost, and it does not require highly skilled or specialized workmanship to install. Even with these favorable characteristics, concrete has vulnerabilities, some of which can lead to complete deterioration. Vulnerabilities related to durability can be mitigated using supplementary cementitious materials (SCM). The use of SCM such as Class F coal fly ash, ground granulated blast furnace slag (GGBFS), silica fume, and metakaolin are common throughout North America.

The recent reduction in the production of Class F fly ash (F-FA) in North America [2] due to closures of coal-powered energy production facilities has caused the need for alternative SCM that are suitable for partial replacement in the PCC system. Recently, researchers have proposed solutions to this shortage [3–7]. The use of alternative SCM is a viable solution that can provide better, or similar, properties compared to conventional SCM. For example, Ferraro et al. [8], in previous Florida Department of Transportation (FDOT) research project BDV31-977-06, identified potential candidates for replacement of F-FA. The SCM identified include sugarcane bagasse ash (SCBA), ground glass (GG), and rice husk ash (RHA).

The focus of project BDV31-977-06 was the identification of materials that have comparable plastic, mechanical, and durability properties in PCC to F-FA. To ensure the materials are appropriate for inclusion in the FDOT Standard Specification for Road and Bridge Construction, a more in-depth durability study was required that would serve as a complement to the previous study to validate the viability of the SCM candidates. This durability study assessed the long-term effects of sulfate exposure, alkali-silica reactivity (ASR), and chloride exposure on PCC and limestone cement concrete systems when used in combination with alternative SCM.

1.1.1 Cement Manufacture

The manufacture of cement begins with combining limestone, clay, and other raw materials that contain the following minerals: lime (CaO), silica (SiO₂), alumina (Al₂O₃), and iron (Fe₂O₃) [9]. The raw materials are then heated to 1400°C to 1600°C in a kiln. During this process, chemical reactions (partial fusion) and phase changes occur between the minerals to form clinker [10]. Lastly, the clinker is mixed and inter-ground with gypsum (calcium sulfate) to produce the commercial portland cement.

1.1.2 Cement Chemistry

Short-hand notation for cement chemistry is used throughout this report and is presented in Table 1-1. Table 1-2 presents typical chemical compositional ranges of PC.

Table 1-3 presents the four main mineralogical compounds of cement; namely tricalcium silicate (alite), dicalcium silicate (belite), tricalcium aluminate (aluminat), and tetracalcium aluminoferrite (ferrite), with some of their properties, respectively.

Table 1-1. Cement chemistry notation for common oxides

Notation	Chemical Formula	Chemical Name (Common Name)
<i>C</i>	CaO	Calcium Oxide (Lime)
<i>S</i>	SiO ₂	Silicon Dioxide (Silica)
<i>A</i>	Al ₂ O ₃	Aluminum Oxide (Alumina)
<i>H</i>	H ₂ O	Water
<i>F</i>	Fe ₂ O ₃	Iron Oxide
<i>T</i>	TiO ₂	Titanium Dioxide (Titania)
<i>M</i>	MgO	Magnesium Oxide (Periclase)
<i>K</i>	K ₂ O	Potassium Oxide
<i>N</i>	Na ₂ O	Sodium Oxide
<i>S̄</i>	SO ₃	Sulfate
<i>C̄</i>	CO ₂	Carbon Dioxide

Table 1-2. Typical chemical composition (mass %) of portland cement

Chemical Component	Portland Cement [11]
SiO ₂	18 – 23
Al ₂ O ₃	2.2 – 7.3
Fe ₂ O ₃	0.2 – 5.9
CaO	61 – 69
MgO	0.3 – 4.5
K ₂ O	0.3 – 1.2
SO ₃	1.7 – 4.9
TiO ₂	–
Na ₂ O	0.1 – 1.2
Other	~1
LOI	0 – 3

Table 1-3. Properties of the four main cement compounds [1]

Compound	Approximate percentage in Type I/II portland cement	Characteristics
C ₃ S	35 – 70%	<ul style="list-style-type: none"> Hydrates and hardens rapidly Responsible for initial set and early strength
C ₂ S	5 – 30%	<ul style="list-style-type: none"> Hydrates and hardens slowly Contributes to later age strength
C ₃ A	2 – 15%	<ul style="list-style-type: none"> Liberates large amount of heat Contribute slightly to early strength Low C₃A contents are more sulfate resistant
C ₄ AF	5 – 15%	<ul style="list-style-type: none"> Reduces temperature in clinker formation Hydrates rapidly Little contribution to strength Provide the grey color in cement

1.1.3 Cement Hydration

There are many proposed mechanisms that attempt to describe the early-age hydration behaviors of portland cement [12–15]. One description of the hydration process is that it can be divided into five basic stages: dissolution, dormant period, acceleration, deceleration, and steady state [1]. The hydration process of PC is a combination of the hydration of the four main compounds and a few additional minor chemical reactions [1]. The heat of hydration of C₃S and C₃A are the primary contributors to the hydration of cement as a whole. The heat of hydration of C₂S is similar to the hydration of C₃S but is slower and less intense. The least abundant major

component of cement is C_4AF and the heat of hydration associated with this phase also contributes the least amount of exothermic activity during hydration.

The shape of the heat of hydration curves for each phase of cement is similar, but the timing and intensity vary; the heat of hydration curve for C_3S is shown in Figure 1-1. The resulting compound heat of hydration of portland cement is a combination of the hydration curves of the individual components (with some variance due to interrelated reactions and minor component reactions). Initially, C_3A reacts exothermically with gypsum and water during the first stage to form ettringite, a hydration product that controls initial set time and stiffening [9]. This formation of ettringite forms a diffusion layer that slows the continued hydration of C_3A in Stage 2 of cement hydration. Following stage 2, the diffusion barrier is broken and the C_3A is allowed to react again during the conversion of ettringite to monosulfate. The duration of stage 2 for C_3A depends on the amount of sulfate in the system, with larger amounts of sulfate leading to extended times. Frequently, the C_3A hydration occurs after the peak of stage 3 (the initiation of stage 4) for the calcium silicates, leading to a stepped heat of hydration curve as shown in Figure 1-2 [1].

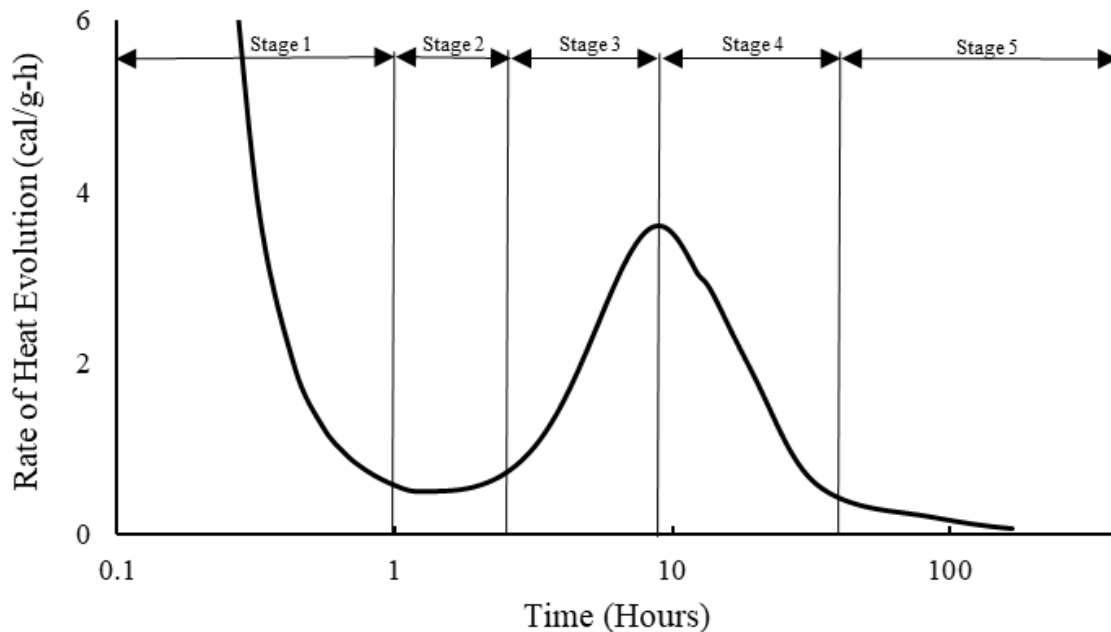


Figure 1-1. Typical hydration of tricalcium silicate adapted from [1].

The hydration reactions of the C_3S and C_2S are also exothermic and the rate of hydration is proportional to the rate of heat evolution [1,11]. The C-S-H product formed from the calcium silicates will fill in the spaces previously occupied by water that has reacted or evaporated and by cement that has been consumed by hydration [9]. This process continues until the available water is consumed by the cement particles and forms a solid matrix (cement paste) in the concrete [16].

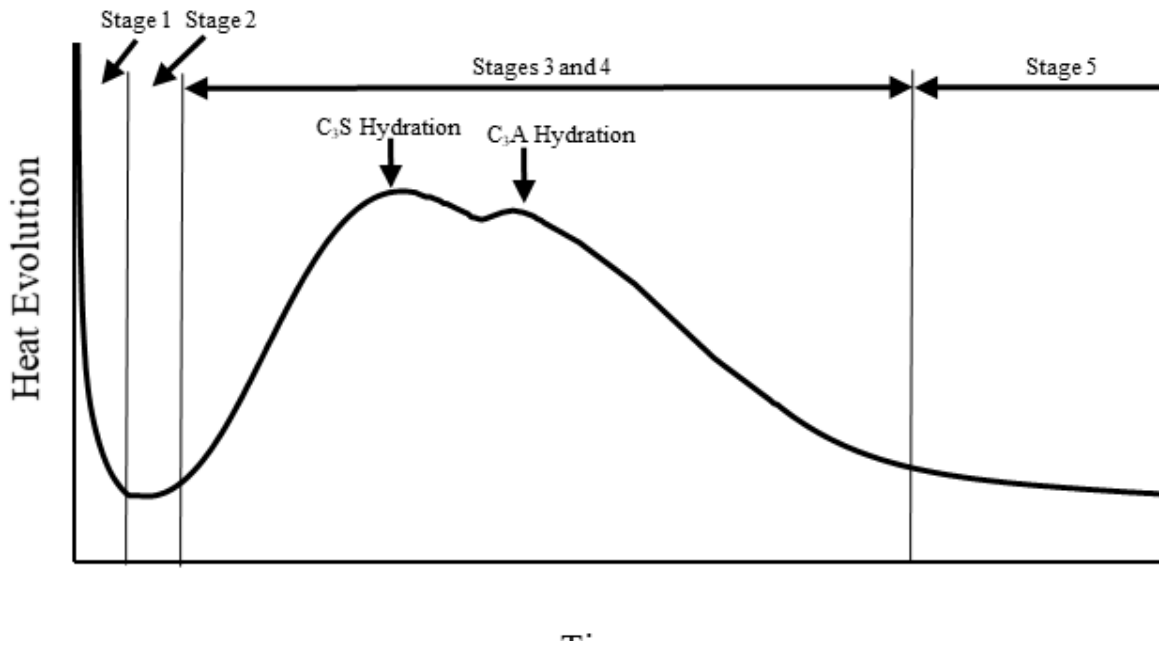


Figure 1-2. Rate of heat of evolution adapted from [1].

Following stage 4, the reactions are largely complete and release little heat. Slower reactions such as pozzolanic reactions take place during stage 5. Table 1-4 shows some of the products from hydration are presented in Table 1-4. the cement hydration process with their respective reactants. The first two reactions involve calcium silicates (alite and belite), that are important in the hydration process, as they produce approximately 75% of the mass of the cement paste volume [1].

Table 1-4. Chemical reactants and products of cement hydration [1].

Reactants	Products
$2C_3S + 6H$	$C_3S_2H_8 + 3CH$
$2C_2S + 9H$	$C_3S_2H_8 + CH$
$2C_3A + 26H + 3C\bar{S}H_2$	$C_6A\bar{S}_3H_{32}$
$2C_3A + 22H + C_6A\bar{S}_3H_{32}$	$3C_4A\bar{S}H_{18}$
$3C_3A + 21H$	$C_4AH_{13} + C_2AH_8$
$C_4A\bar{S}H_{12} + 2C\bar{S}H_2 + 16H$	$C_6A\bar{S}_3H_{32}$
$C_4A\bar{S}H_{12} + C_3A + CH + 12H$	$2C_3A(C\bar{S},CH)H_{12}$
$C_4AH_{13} + C_2AH_8$	$2C_3AH_6 + 9H$
$C_4AF + 3C\bar{S}H_2 + 3H$	$C_6(A,F)\bar{S}_3H_{32} + (F,A)H_3 + CH$
$C_4AF + C_6(A,F)\bar{S}_3H_{32} + 23H + 2CH$	$3C_4(A,F)\bar{S}H_{18} + (F,A)H_3$

1.1.4 Types of Cement

Portland cement for general concrete construction is classified by ASTM C150 [17], and contains minimum requirements for chemical components such as alite and belite, and physical properties such as fineness. This standard defines ten types of cements; however, five main types, namely Type I, Type II, Type III, Type IV, and Type V. The other five types of cement are modifications of the five main types by adding other properties such as air entrainment and moderate heat of hydration, represented by the suffix A and MH, respectively. Type I is a general cement, Type II and Type V are moderate and high sulfate resistance cement, respectively. The most commonly used cement is a Type I/II as it meets the requirements for both grades. Type III is a high-early-strength cement typically used in prestressed concrete construction industry [18]. Type IV provides lowered heat of hydration, but is no longer produced in the US with the exception of special projects. Recent changes to the AASHTO and ASTM Specifications for portland cement have resulted in little differences between the chemistries of Type I, II and III cements [19]. Type IV and V cements are not produced, nor are they available in the state of Florida.

Blended hydraulic cements combine one or more constituents with ordinary portland cement for an improvement of specific properties. Examples of these constituent materials include slag, fly ash, silica fume, and calcined clay. The requirements for the following cement types: IS, IP, IL, and IT are specified ASTM C595 [20]; a general summary of the acceptable cement replacement levels is presented in Table 1-5. For blended cements, the blend type will include the composition of blended material in the classification. For instance, a Type IS(30) is a

slag cement blend with 30% slag cement; a Type IT(S20)(L10) is a ternary blended cement with 20% slag cement, and 10% limestone.

Table 1-5. General SCM limits for blended cements per ASTM C595 [20].

Blended Cement Type	Included SCM	Composition Limits
Type IS	Slag cement	<ul style="list-style-type: none"> Up to 95% slag; when 70% or more, hydrated lime may be used as an alkali activator.
Type IP	Any pozzolan that meets specific requirements outlined in ASTM C595 - Table 4.	<ul style="list-style-type: none"> Up to 40% pozzolan
Type IL	Limestone	<ul style="list-style-type: none"> 5 – 15% limestone
Type IT	Any two listed above (not two “pozzolans”)	<ul style="list-style-type: none"> Type IT(S\geq70): include 15% L max Type IT(S<70): 70% SCM content max. Up to 40% Pozzolan Up to 15% Limestone

The FDOT has allows the use of Type IL cement, which has been incorporated into the “Standard Specifications For Road and Bridge Construction” [21]. Portland-limestone cement (PLC) or Type IL cement is ordinary portland cement with 5% to 15% of limestone and a loss of ignition (LOI) of 10% or less. The addition of the limestone to the cement is be inter-ground with the clinker during the production of the cement or blended with the cement subsequent to grinding [20]. The use of PLC has gained popularity due to its benefits with regards to environmental concerns of carbon dioxide emission in the ordinary portland cement production, as well as cost reduction. The cements used for this research will be a Type I/II and a Type IL. Typical chemical composition of portland-limestone cement is presented in Table 1-6.

Table 1-6. Typical chemical compositional ranges (mass %) for PLC.

Chemical Component	Portland Cement [11]	Portland-Limestone Cement [22–27] Portland limestone cement [22–27]
SiO ₂	18 – 23	16 – 22
Al ₂ O ₃	2.2 – 7.3	3.4 – 5.1
Fe ₂ O ₃	0.2 – 5.9	2.0 – 3.6
CaO	61 – 69	56 – 67
MgO	0.3 – 4.5	0.9 – 2.6
K ₂ O	0.3 – 1.2	0.3 – 1.1
SO ₃	1.7 – 4.9	0.5 – 4.3
TiO ₂	–	~0.2
Na ₂ O	0.1 – 1.2	0.1 – 0.2
Other	~1	–
LOI	0 – 3	4.2 – 5.7

Table 1-7 shows the summary of the effects on PCC due to the PLC. The symbols provided indicate an increase (↑), or decrease (↓), or (↔) no significant effect for that material property with the replacement percentages shown in parentheses.

Table 1-7. Effects due to the PLC.

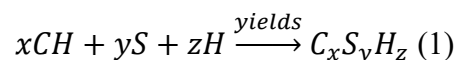
Effect Due to Addition of SCM:	Portland-Limestone Cement [26–31] Limestone Cement [26–31]
Compressive Strength	↓ (10 – 15%)
Tensile Strength	↓ (5 – 15%)
Flexural Strength	↔ (10%)
Permeability	↑ (10 – 15%)
Workability	↔; dependent on particle size distribution
Heat of Hydration	↓ (5 – 15%)
Resistance to ASR	–
Freeze/Thaw Resistance	↓ (10 – 15%)
Sulfate/Chloride Resistance	↓ (5 – 15%); dependent on w/c
Resistance to Corrosion	↑ (10 – 15%)
Setting Time	↓ (15%)
Bleeding and Segregation	↓

1.1.5 Supplementary Cementitious Materials (SCM)

Supplementary Cementitious Materials (SCM) can be classified as self-cementing materials or pozzolans. The difference between them is that self-cementing materials will hydrate in the presence of water and pozzolans will not; self-cementing materials can provide

pozzolanic activity, but they hydrate in the presence of water without the need for additional materials [3]. Self-cementing materials include ground granulated blast furnace slag (GGBFS) and Class C fly ash (C-FA), while pozzolanic materials include Class F fly ash (F-FA), silica fume (SF), ground glass (GG), rice hush ash, and sugarcane bagasse ash (SCBA), amongst others. Some benefits of SCM include: increased strength at ages beyond 28 days, improved durability properties, decreased environmental impact, reduced permeability, and improved workability [32–34]. Supplementary Cementitious Materials (SCM) can be classified as self-cementing materials or pozzolans. The difference between them is that self-cementing materials will hydrate in the presence of water and pozzolans will not; self-cementing materials can provide pozzolanic activity, but they hydrate in the presence of water without the need for additional materials [3]. Self-cementing materials include granulated blast furnace slag and Class C fly ash (C-FA), while pozzolanic materials include Class F fly ash (F-FA), silica fume (SF), ground glass (GG), rice hush ash, and sugarcane bagasse ash (SCBA), amongst others. Some benefits of SCM include: increased strength at ages beyond 28 days, improved durability properties, decreased environmental impact, reduced permeability, and improved workability [32–34].

A pozzolanic reaction is defined as the reaction between the silica (S) supplied by an SCM and calcium hydroxide (CH) produced during hydration of cement. This pozzolanic reaction can be represented by the equation 1 (M. Thomas, 2013):



[32]. The CH is a chemical product formed by the reactions of C_3S and C_2S with water during the hydration process of cement. The SCM of interest for this study are materials with high silica content to promote pozzolanic reactivity with the excess calcium hydroxide and their effects on the durability properties of the PCC will be assessed.

1.2 MATERIALS REVIEW

Some of the SCM selected for this investigation were explored in previous work done by Ferraro et al. [8]. The research performed during that project included a rigorous and thorough evaluation of the structural adequacy, workability, and accelerated durability testing of these

SCM. Chemical and physical properties were also evaluated. In this section, a summary of these materials' properties and their effects on PCC are presented.

1.2.1 Conventional SCM

Fly ash, slag cement, and silica fume are conventional SCM. They are widely accepted and have been used extensively in North America since the 1970s [11]. The widespread use of these materials in concrete is due to the alleviated cost of production by reducing the cement content of concrete mixes, SCM reduce environmental impact associated with disposal of these waste materials, and improve some of the concrete properties [16]. For these reasons, numerous studies have been carried out to understand the effects of SCM in the PCC system [32,34,35].

Fly ash is a byproduct of the coal burning process to generate electricity. The difference between Class C and F fly ash is that F-FA is low calcium ash obtained from burning anthracite or bituminous coal, while C-FA is from burning sub-bituminous or lignite coal [11]. In order to classify as fly ash based on ASTM C618, the sum of silica, alumina, and iron oxide needs to be greater than 70% and 50% for Class F and Class C, respectively [36].

Fly ash is composed of fine particles typically between the range of 1 to 150 μm [34,37]. The glassy structure and silica content of the F-FA enhances or improves nearly every aspect of PCC, but it can reduce the compressive strength in replacements between 10 and 40%, especially at early ages [3,38]. With respect to durability, additions of F-FA with CaO and Na₂O_e contents higher than 20% and 5%, respectively, are not effective against alkali silica reaction (ASR) with replacement below 25% of PC [39].

Silica fume, SF, is a non-crystalline ultra-fine product obtained from siliceous metals and ferro-siliceous alloys in electric arc furnaces [40]. The specification that governs the requirements of SF is ASTM C1240 [41]. SF can be obtained commercially in three forms: as-produced, slurry, or densified [11]. The densified version is the most used due to the ease in handling. The particle size of SF is very fine, typically about 0.1 micron, and possesses a specific gravity ranging from 2.20 and 2.50 [11]. Some drawbacks of using SF as an SCM are the decrease in workability and the increase of plastic shrinkage [11]. Also, an increase in water and air demand are expected, but in a concrete mixture with 5 to 10% of SF, this can help with bleeding, segregation, and cohesiveness of the concrete [11].

The typical chemical compositions of Class C and Class F fly ash, as well as silica fume are presented Table 1-8. Their effects on concrete properties are presented in

Table 1-9. The symbols provided indicate an increase (↑) or decrease (↓) or (-) no significant effect on the property of interest. The replacement percentages are shown in parentheses.

Table 1-8. Typical chemical compositional ranges (mass %) for conventional SCM [3].

Chemical Component	Class C Fly Ash	Class F Fly Ash	Silica Fume
SiO ₂	23 – 51	45 – 65	85 – 97
Al ₂ O ₃	13 – 22	19 – 31	0.2 – 0.9
Fe ₂ O ₃	3.7 – 23	3.8 – 24	0.4 – 2.0
CaO	11 – 29	0.7 – 7.5	0.3 – 0.5
MgO	1.5 – 7.5	0.7 – 2.8	0.0 – 1.0
K ₂ O	0.4 – 1.9	0.7 – 4.1	0.5 – 1.3
SO ₃	0.0 – 3.0	0.0 – 0.5	0.0 – 0.4
TiO ₂	–	0.9 – 1.2	–
Na ₂ O	1.0 – 2.1	0.2 – 0.5	0.1 – 0.4
Other	0.2 – 1.1	0.1 – 5.5	0.0 – 1.4
LOI	0.3 – 3.5	0.2 – 7.2	0.0 – 2.8

Table 1-9. Effects due to the addition conventional SCM to PCC [3].

Concrete Property	Class C Fly Ash	Class F Fly Ash	Silica Fume
Compressive Strength	↑ (10% – 50%)	↑ (10% – 50%; sand replacement)	↑ (28 days) (5–20%)
Tensile Strength	↑ (10% – 50%)	↑ (10% – 50%)	↑ (5% – 30%)
Flexural Strength	↑ (40% – 75%)	↑ (40% – 75%)	↑ (5% – 25%)
Permeability	↑ (10% – 100%)	↓ (10% – 100%)	↓ (>5%)
Workability	↑ (10% – 40%)	↓	↓ (10%)
Heat of Hydration	↓	↑ (20% – 40%)	↑ (4% – 20%)
Resistance to ASR	↑ (20% – 40%)	↑ (40% – 60%)	↑ (10% – 20%)
Freeze/Thaw Resistance	↑ (40% – 60%)	↑ (<50%)	↑ (5% – 15%)
Sulfate/Chloride Resistance	–	↑ (10% – 30%)	↑ (<20% SF)
Resistance to Corrosion	↑ (10% – 30%)	↑	↑ (5% – 20%)
Setting Time	↑ or ↓	↓ (10% – 40%)	–
Bleeding and Segregation	↓ (10% – 40%)	–	–

1.2.2 Sugar Cane Bagasse Ash (SCBA)

Sugar Cane Bagasse Ash (SCBA) is a pozzolan obtained as a byproduct from the sugar industry. The production of sugar begins by crushing the sugarcane and then extracting the juice.

The woody residue, called bagasse, can be used as fuel for generation of electricity, or production of papers, etc. [3,42]. Finally, the SCBA is generated from the burning of the bagasse for power generation.

When collected, SCBA may contain a high amount of unburnt fibrous particles from the burning process [43], which have negative effects on workability and may [43]. These unburnt particles hinder the pozzolanic reaction with the cement and may lead to negative effect in workability [44]. In order to improve the reactivity of the SCBA, post-processing techniques are suggested for optimum usage as an SCM [45]. The main chemical composition of the SCBA is silica; although, the remaining chemical components vary. The typical chemical composition of sugarcane bagasse ash and PC are presented in Table 1-10.

Table 1-10. Typical chemical compositional ranges (mass %) for sugarcane bagasse ash

Chemical Component	Portland Cement [11]	SCBA [8,43,46,47]
SiO ₂	18 – 23	58 – 79
Al ₂ O ₃	2.2 – 7.3	1.7 – 15
Fe ₂ O ₃	0.2 – 5.9	2.3 – 11
CaO	61 – 69	2.1 – 21
MgO	0.3 – 4.5	0.0 – 4.1
K ₂ O	0.3 – 1.2	1.9 – 9.6
SO ₃	1.7 – 4.9	0.3 – 3.0
TiO ₂	–	0.1 – 2.7
Na ₂ O	0.1 – 1.2	0.0 – 0.5
Other	~1	1.2 – 3.0
LOI	0 – 3	0.4 – 9.0

SCBA in addition rates of 5 – 20% have been shown to have properties that are comparable or better than the control at ages from 7 to 91 days for compressive strength, tensile strength, and flexural strength [8,48,49]. However, some research reports reductions in mechanical strength at replacement levels of 25% [50]; this discrepancy may be a point of diminishing returns or may be due to the difference in SCBA mineralogy and morphology.

In terms of plastic properties, Ferraro et al (2017). found that SCBA replacements between 10% to 30% reduced the workability and the use of admixture was needed [3]. Similarly, replacements of 10% to 40% of SCBA increased the time of initial set by 2.5 times, and the final set by 45% [51]. The increase of time of set may be attributed to a slower reaction of the SCBA and absorption of water due to a larger surface area of the particles of SCBA during

hydration process [52]. In terms of plastic properties, Paris et al. indicated that SCBA replacements between 10% to 30% reduced the workability and the use of admixture was needed [3]. Similarly, replacements of 10% to 40% of SCBA increased the time of initial set by 2.5 times, and the final set by 45% [51]. The increase of time of set may be attributed to a slower reaction of the SCBA and absorption of water due to a larger surface area of the particles of SCBA during hydration process [52].

A summary of the effects of SCBA in PCC is presented in Table 1-11 where the arrows indicate an increase (↑) or decrease (↓) or (-) no significant effect on the property of interest. The replacement percentages are shown in parentheses.

Table 1-11. Effects due to the addition of SCBA to PCC.

Effect Due to Addition of SCM:	SCBA [3,48–50,52]
Compressive Strength	↑ (10% – 30%)
Tensile Strength	↑ (5% – 15%)
Flexural Strength	↓ (5% – 25%); ↑ (2 – 20%) (Discrepancy)
Permeability	↓ (10% – 30%)
Workability	↓ (10% – 30%)
Heat of Hydration	↓ (10% – 30%)
Resistance to ASR	–
Freeze/Thaw Resistance	–
Sulfate/Chloride Resistance	↑ (5% – 30%)
Resistance to Corrosion	↑ (20%)
Setting Time	↑ (10% – 40%)
Bleeding and Segregation	–

1.2.3 Ground Glass (GG)

Ground glass (GG) is typically obtained from the grinding of recycled waste glass that is not viable for recycling into new glass [53]. Most recycled glass is clear glass and not the colored glasses because of the difficulty of recycling process [54]. Recycled waste glass can be used as an aggregate (coarse or fine) or cement replacement based on the size of the glass particles [55,56]. The content ranges, in mass percent, of typical ground glass components are shown in Table 1-12. Ground glass (GG) is obtained from the grinding of recycled waste glass when it is not viable for recycling into new glass [53]. Most recycled glass is clear glass and not the colored glasses because of the difficulty of recycling process [54]. Recycled waste glass can be used as an aggregate (coarse or fine) or cement replacement based on the size of the glass particles [55,56]. The content ranges, in mass percent, of typical ground glass components are shown in Table

1-12. The main chemical constituents of GG are silicon dioxide (50 to 80%), calcium oxide (5 to 15%), and sodium oxide (12.0 to 13.5%).

Table 1-12. Typical chemical compositional ranges (mass %) for ground glass [8].

Chemical Component	Portland Cement [11]	GG [8]
SiO ₂	18 – 23	50 – 80
Al ₂ O ₃	2.2 – 7.3	1.0 – 10
Fe ₂ O ₃	0.2 – 5.9	0.0 – 0.5
CaO	61 – 69	5.0 – 15
MgO	0.3 – 4.5	0.6 – 4.0
K ₂ O	0.3 – 1.2	<1.0
SO ₃	1.7 – 4.9	<1.0
TiO ₂	–	<1.0
Na ₂ O	0.1 – 1.2	1.0 – 15
Other	~1	<5.0
LOI	0 – 3	<1.0 – 2.5

Mechanical properties such compressive, tensile, and flexural strength are typically reduced with the addition of 10% to 30% of GG compared with the PCC control [3]. Although there have been reports of adverse effects on the mechanical properties amended with GG, research has shown benefits on the durability properties such as permeability (with 15% to 60% replacement), freeze/thaw resistance (increase of 6% with 20% replacement), and reduction of chloride penetration (50% with 30% replacement) due to the improvement in the microstructure and reduction of pore size and connectivity [57–59]. In terms of plastic properties, the use of GG can lower the heat of hydration and contribute to pozzolanic reactivity [60,61]. Mechanical properties such compressive, tensile, and flexural strength are affected negatively with the addition of 10% to 30% of GG compared with the PCC control [3]. Contrary to the negative effect on the mechanical properties, a positive effect has been noticed on durability properties such as permeability (with 15% to 60% replacement), freeze/thaw resistance (increase of 6% with 20% replacement), and reduction of chloride penetration (50% with 30% replacement) due to the improvement in the microstructure and reduction of pore size and connectivity [57–59]. In terms of plastic properties, the use of GG can lower the heat of hydration and contribute to pozzolanic reactivity [60,61].

In Table 1-13, a summary of the effects of GG in PCC is presented. The arrows indicate an increase (↑) or decrease (↓) or (-) no significant effect on the property of interest. The replacement percentages are shown in parentheses.

Table 1-13. Effects due to the addition of GG to PCC.

Effect Due to Addition of SCM:	GG [3,57,59,60,62,63]
Compressive Strength	↓ (10% – 30%)
Tensile Strength	↓ (10% – 20%)
Flexural Strength	↓ (10% – 30%)
Permeability	↓ (15% – 60%)
Workability	↓ (20% – 30%)
Heat of Hydration	↓ (5% – 20%)
Resistance to ASR	↑ (5% – 20%)
Freeze/Thaw Resistance	↑ (20%)
Sulfate/Chloride Resistance	↑ (20% – 30%)
Resistance to Corrosion	↑ (20% – 30%)
Setting Time	↑ (20%)
Bleeding and Segregation	–

1.2.4 Ground Sand (GS)

Sand is a natural mineral aggregate obtained from the environment or from grinding coarse aggregate. Historically, it has been used as a filler in the production of PCC. However, when the sand is ground fine enough, it can show a pozzolanic effect if it is siliceous [64]. A typical chemical composition of GS is presented in Table 1-14.

Table 1-14. Typical chemical compositional ranges (mass %) for ground sand.

Chemical Component	Portland Cement [11]	Ground Sand [64–67]
SiO ₂	18 – 23	88 – 97
Al ₂ O ₃	2.2 – 7.3	0.7 – 5.0
Fe ₂ O ₃	0.2 – 5.9	0.3 – 1.5
CaO	61 – 69	0.0 – 0.6
MgO	0.3 – 4.5	0.2 – 0.5
K ₂ O	0.3 – 1.2	0.0 – 0.3
SO ₃	1.7 – 4.9	–
TiO ₂	–	–
Na ₂ O	0.1 – 1.2	0.0 – 0.4
Other	~1	–
LOI	0 – 3	0.0 – 0.7

In terms of compressive strength, Sata et al. performed compressive tests on PC mortar with GS (median particle size of 11.5 μm) with 10% to 40% replacement of PC and with water-

to-cementitious material ratios (w/cm) of 0.50, 0.575, 0.65 [67]. The results obtained showed a decrease of the compressive strength of PC mortar with each level of replacement ranging from approximately 10% to 50%. In another study performed by Chindapasirt & Rukzon, the compressive strength was reduced by approximately 10% and 40% of the control with replacement of 20% and 40%, respectively [65].

1.2.5 Ground Volcanic Rock (VR)

Ground Volcanic Rock (VR) is a ground natural pozzolan produced from volcanic rocks found in natural deposits. VR is rich in silica content, but the chemical composition depends on the mineralogy. One of the major contributions to reactivity is the glassy phase content. During formation, if the molten rock cooled quickly, a high percentage of the rock will be in a glassy state. Slow cooling allows minerals to crystallize from the melt, resulting in a lower glassy phase content where the glassy phase is more reactive than the crystalline phase [68]. The typical chemical composition of ground volcanic rock is presented in Table 1-15. Few researchers have done studies on ground volcanic rock as a pozzolan due to its scarcity, the remoteness of the sources, and thus limited availability of the material. Therefore, the knowledgebase regarding its use as a pozzolan is not comprehensive.

Table 1-15. Typical chemical compositional ranges (mass %) for ground volcanic rock.

Chemical Component	Portland Cement [11]	VR; [69,70]
SiO ₂	18 – 23	65 – 77
Al ₂ O ₃	2.2 – 7.3	9.3 – 15
Fe ₂ O ₃	0.2 – 5.9	1.0 – 3.9
CaO	61 – 69	0.3 – 2.7
MgO	0.3 – 4.5	0.0 – 2.3
K ₂ O	0.3 – 1.2	1.9 – 5.6
SO ₃	1.7 – 4.9	–
TiO ₂	–	–
Na ₂ O	0.1 – 1.2	0.0 – 3.9
Other	~1	–
LOI	0 – 3	1.7 – 3.6

Volcanic rock has been researched by Yu et al. (2015) where characterized eight specimens of volcanic rock that were collected from the south of the Xunwu–Longnan–Quannan–Dinnan volcanic belt in the Jiangxi Province, China. The research included Yu et al.

(2015) also performed compressive and flexural testing on mortars with various VR inclusion levels [69]. The results showed that two particular specimens amended with VR were (denoted as NQ and CZ in the original article) performed comparable to the control in compression and flexure, for 28 and 90 days with replacement level of 10% and 20%. Other specimens indicated a decrease in strength with increase in the replacement level. Some of the specimens that performed worse than the control were similar in mineralogy and morphology to the specimens that performed comparably. Therefore, there may be other variables, such as particle size and glassy (amorphous) phase content also, that dictate performance but are not fully understood.

1.3 ALKALI-SILICA REACTION (ASR)

Alkali-silica reaction (ASR) is the most common type of alkali-aggregate reaction (AAR) that occurs in portland cement concrete (ACI 201, 2016).[71]. Alkali-carbonate reaction (ACR) is the next most common, which is a reaction between alkalis (sodium and potassium) and some carbonate rocks (calcareous dolomite and dolomitic limestone) [72]. Alkali silica reaction is the reaction between alkalis and certain siliceous rocks or minerals such as opaline chert, strained quartz, and acidic volcanic glass that are present in some aggregates [72]. The focus of this review is on ASR because it has affected concrete structures around the world [71], and its occurrence is not isolated to a few locations as is the case with ACR.

Since discovery of ASR in the late 1930s [71], research has been performed to better understand ASR, methods to quantify or measure ASR, and mitigation measures to prevent or repair the affected structure after ASR has occurred. Alkali-silica reaction can cause damage in concrete by expansion of an alkali-silica gel between the cement paste and the aggregates, or it can take place after the concrete has cracked or been damaged. In rare circumstances, ASR can occur in voids in the concrete, resulting in no damage to the concrete.

1.3.1 Mechanisms and Symptoms

For ASR to occur, three essential components must be present and interact between each other: alkalis, reactive silica, and water. In most cases the alkalis are present in the PC as sodium and potassium, but also can be present in other sources such as contaminated mixing water, contaminated aggregate, or environmental sources such as soil or sea water. The reactive silica is chemically unstable in high alkaline environments such as hydrating cement. The most common reactive aggregates are ash chert, chalcedony, and rhyolites [11]. The reactivity of the silica

depends on the mineralogy of the aggregate, crystallinity, and water solubility [71]. Lastly, water is necessary to form the gel-like structure in between the aggregates and the cement pastes, commonly in the form of. Common sources of water are ground water, sea water, and precipitation.

Alkali-silica reaction is a complex process that starts with the dissolution of sodium oxide (Na) and potassium oxide (K) during hydration of cement. Reactive aggregate in contact with pore solution will be attacked by hydroxyl (OH^+) ions first, then followed by sodium (Na^+) and potassium (K^+) ions [72]. A chemical reaction occurs between the siliceous aggregates and the ions to form an alkali-silica gel around the available surface area of reactive silica [72,73]. Finally, when this gel absorbs water from the cement paste, it will start to expand and cause cracking.

Cracking of the cement paste exposes more surfaces for alkali and water ingress, the new exposed surface can then form more alkali-silica gel, thus more expansion [9]. Symptoms caused by the deleterious effects of ASR include cracking, misalignment between adjacent elements, and expansion [74]. ASR commonly produces a randomly oriented cracking called map cracking in unrestrained concrete [72,75].

1.3.2 Test Methods

Three groups of test methods are available that serve to identify the potential for ASR, and the tests can be classified into three categories based on the material to be investigated: aggregate, mortar, or concrete. For testing aggregates, a microscopic analysis testing is typically performed on the aggregates and described in ASTM C295 [76]. For mortar testing, four test methods used for determination of ASR in mortar are available and are described in Table 1-16. ASTM C1293 [77] is used to evaluate the potential of deleterious concrete expansion due to ASR of an aggregate or a combination of an aggregate with an SCM. This test method measures the expansion of concrete prisms over a period of one year for aggregates and two years when an SCM is used, and is compared to the limit specified in the standard. Additionally, ASTM C1778 is a performance-based guide used to identify and mitigate ASR in concrete [78].

Table 1-16. ASTM mortar test method for ASR.

Standard	Description
ASTM C227 [79]	Measure the susceptibility for ASR of a particular combination of cement and aggregate
ASTM C441 [80]	Test the effectiveness of pozzolan or slag for potential of ASR
ASTM C1260 [81]	Used for testing the potential of ASR of aggregates
ASTM C1567 [82]	Used for testing the potential of ASR for combinations of cementitious materials and aggregate

1.3.3 Mitigation

Alkali-silica reaction (ASR) is mitigated by using one or more of the following preventive measures. Using non-reactive aggregate will likely prevent ASR by removing reactive silica from the system [72]. Using concrete mix designs that have low permeability mitigate the reaction by reducing water absorption and alkali ingress [74,83]. Lastly, concrete mixes with lower alkali content (sodium equivalent below 0.6%) can also reduce the potential for ASR [74].

1.3.4 Effects of SCM

One of the benefits from SCM additions include the reduction in concrete permeability, which decreases the mobility of chemical agents involved in ASR [16]. Also, the incorporation of SCM with high silica content can help to reduce the expansion by increasing the silica/alkali ratio to prevent the formation of expansive alkali-silica gel [9].

Ground glass (GG) typically possesses a relatively high amount of alkali, which is a concern if the aggregate used is reactive [62,84], and ASTM C1567 [82] recommends the use of ASTM C1293 [77] to test the ASR potential when the alkali content exceeds four percent because accelerated testing used in ASTM C1567 can underestimate the expansion. Much of the research involving testing of GG as a pozzolan has been performed incorrectly under ASTM C1567; most times citing the use of ASTM C1260 (which is incorrectly noted, as the use of an SCM is not permitted in that method). The researchers intend to evaluate the use of GG using the ASTM C1293 method, which is more accurate when compared to field performance [85].

Ground glass (GG) can possess a relatively high amount of alkali, which is a concern if the aggregate used is reactive [62,84], and ASTM C1567 [82] recommends the use of ASTM C1293 [77] to test the ASR potential when the alkali content exceeds four percent because accelerated testing used in ASTM C1567 can underestimate the expansion. The majority of research involving testing of GG as a pozzolan has been performed incorrectly under ASTM C1567; most

times citing the use of ASTM C1260 (which is incorrectly noted, as the use of an SCM is not permitted in that method). The researchers intend to evaluate the use of GG using the ASTM C1293 method, which is more accurate when compared to field performance [85].

1.4 EXTERNAL SULFATE ATTACK

Sulfate attack is caused by sulfate salt ions, acids, or a combination of both that are present in coastal areas, groundwater, and soil. The source of sulfate attack can be internal or external [86]. Also, sulfate attack can be grouped into chemical or physical reaction. In general, chemical attack refers to a chemical reaction between two or more reactants to form a product. While physical attack refers to a change in the phase of the compound; in this case, an evaporating sulfate ion-rich pore solution that forms sulfate salt crystals. This precipitation of sulfate crystals causes internal pressures to increase, leading to cracking [87].

Internal sulfate attack, also known as delayed ettringite formation (DEF), can cause internal damage (microcracks) due to the formation of ettringite at later ages of the hardened concrete due to curing at 70°C or higher [71]. Ettringite is a hydration product formed from reaction of C₃A and sulfate; however, when the temperature is above 70°C, ettringite becomes unstable and decomposes, leading to absorption of sulfate the C-S-H [9]. Later, when exposed to water, sulfate ions are released from the C-S-H and begin to form ettringite crystals which form with needle-like crystals, the aspect ratio. This causes internal pressures within an increase in volume of the C-S-H structure, resulting in cracking. The study of DEF is out of the scope of this project; therefore, subsequent sections cover only external sulfate attack.

The chemicals responsible for external sulfate attack in concrete can be categorized in terms of the aggressiveness of attack from. From most aggressive to least aggressive with their respective reaction products: magnesium sulfate forms brucite, sodium sulfate converts monosulfate into ettringite and converts calcium hydroxide into gypsum, calcium sulfate forms ettringite, and potassium sulfate reacts similarly to sodium sulfate (both alkali sulfates) but to a lesser extent. These sulfate compounds can interact with calcium hydroxide, C-S-H, and monosulfate resulting in a loss of structural capacity [86].

1.4.1 Mechanisms and Symptoms

The mechanisms of chemical external sulfate attack are not dependent on sulfate species, but environmental conditions; typically involving the leaching of calcium from C-S-H when sulfate ions react with unhydrated cement minerals, such as C_3A , C_4AF , and hydration products including CH to form gypsum or ettringite ($C_6A\bar{S}_3H_{32}$) that lead to cracking and spalling of concrete [88]. This removal of calcium from C-S-H leaves behind a silicate hydrate gel that when in combination with alkalis (a source of which may be sodium sulfate or potassium sulfate) can form an alkali-silica reactive reaction further damaging the microstructure [75]. Both the formation of ettringite and gypsum causes an overall voluminous increase in the concrete; thereby weakening the material. Magnesium sulfate tends to form surface layers of gypsum and brucite (magnesium hydroxide) [75]. Thaumasite formation is another indicator of sulfate exposure; however, thaumasite has rarely been determined to be the main contributor to concrete degradation. The formation of thaumasite requires a very specific set of environmental conditions that make it unlikely to develop in most climates; these include: constant high relative humidity, temperature between 5 – 10°C, sulfate and carbonate ions, and reactive alumina [75,86]. Additionally, there are many complex and inter-connected chemical reactions that have varying effects on the ionic composition of the pore water.

For concrete experiencing physical sulfate attack, the sulfate in solution gets absorbed into the concrete structure, then upon dehydration, sulfate salts precipitate out and crystallize to create internal pore stresses in the concrete matrix known resulting in scaling [71]. The repeated cycling of crystallization formation and dissolution cycle causes escalating damage in concrete. For instance, thenardite, an anhydrous sodium sulfate salt, can react with water to form mirabilite (the hydrated salt) which results in a volume increase of nearly 320% [86]; it is this crystallization volume increase to forms inside pores that causes internal stresses in the microstructure to propagate. This particular form of sulfate attack tends to happen with concrete structures near bodies of water (tidal zones) where thenardite is present at temperatures above 32°C and the hydration of the salt takes place at a lower temperature. Another mechanism is thaumasite formation, a reaction of sulfate and the C-S-H structure that forms a silica-based compound ($CaO \cdot SiO_2 \cdot CaSO_4 \cdot CaCO_3 \cdot H_2O$ or $CaSiO_3 \cdot CaCO_3 \cdot CaSO_4 \cdot 15H_2O$) [71]. The symptom of thaumasite attack is the disintegration of the hardened cement paste matrix, hence, a loss of cohesion in the binding properties of the concrete is manifested [71].

1.4.2 Test Methods

A common standardized test method to determine an equivalent sulfate resistance is ASTM C1012, which measures the length change in mortar bars over time using a 5% sodium sulfate solution exposure [89]. Per ACI 201 [71], expansion equal to or less than 0.10% at 6 months indicates a moderate sulfate resistance, while an expansion equal or less than 0.10% at 12 months indicates high sulfate resistance; these limits have longer durations when SCM are present due to the lowered permeability of the specimens.

1.4.3 Mitigation

Some strategies to prevent sulfate attack are the use of sulfate-resistant cement (low C_3A content) such as Type II or Type V cements, lower water-cement (w/c) ratio, and the addition of SCM. The use of a low w/c ratio produces a less permeable concrete, which improves the resistance against external sulfate attack [86]. The use of SCM in PCCPC helps to reduce the permeability and the quantity of sulfate inclusion from cement [11].

1.5 EFFECT OF SUPPLEMENTARY CEMENTITIOUS MATERIALS

Portland-limestone cement systems are often compromised by sulfate attack due to high levels of tricalcium aluminate content, typically over 10%, which reacts with sulfate to form ettringite [90–94]. Tosun-Felekoğlu [90] reported that limestone cements, regardless of C_3A content, show decreased sulfate resistance as limestone content increases from 5% – 40%; however, specimens stored at colder temperatures performed markedly worse due to dissolution of calcium and carbonate ions leading to thaumasite formation. Some studies suggest alternatives to improve durability of PLC, such as incorporation of higher percentages of SCM and/or ternary blended cements [95]. Sulfate attack has been shown to be mitigated with 25% fly ash and 5% silica fume [96]. Other studies indicate that PLC in combination with 50% of slag contributes to sulfate and thaumasite resistance [97].

Recent studies have indicated that the inclusion of SCBA can increase sulfate resistance with replacements below 25%, but replacement of 30% was vulnerable to sulfate attack [98]. Carsana et al. [58] found that 30% replacement with GG delayed expansion of mortar, but ultimately failed approximately 15 months after exposure.

1.6 SUPPLEMENTARY CEMENTITIOUS MATERIAL SUMMARY

This report presents a review of the current state of research on the effects of SCM-blended PCC and PLC. The materials reviewed are sugarcane bagasse ash, ground glass, ground sand, ground volcanic rock, Class C fly ash, Class F fly ash, slag cement, and silica fume. Also, two relevant aspects of common durability problems such as sulfate attack and ASR are presented.

The following are observations based on publications (reports, books, and papers) reviewed on concrete and mortar:

1. Use of supplementary cementitious materials for partial replacement of PC can improve plastic, mechanical, and durability properties of concrete; however, long-term exposure testing has not been performed on alternative supplementary cementitious materials. Most of the durability-related research performed using SCM has been based on accelerated testing methods that may not be representative of field performance.
2. With the continuously increasing use of concrete, more evaluations of non-conventional pozzolanic materials are needed for a sustainable long-term supply of SCM that provide better or comparable performance to existing conventional SCM and meet the standards for the construction industry.
3. In addition to ASR and sulfate attack, other properties affected by the use of alternative supplemental cementitious materials, such as resistances to freeze-thaw, bleeding, and segregation, have not been widely evaluated.
4. Most of the literature reviewed focused on ASR testing of mortars (ASTM C1567), with a lack of research evident for concrete prisms (ASTM C1293). Therefore, the use of the ASTM C1293 with concrete prisms for this research program will help alleviate a current deficiency in the research with respect to ASR and pozzolans.
5. GG has great potential as a silica-rich pozzolanic material; however, there is a concern about the potential of ASR since it contains a relatively high amount of alkali (Ferraro et al., 2017). Durability testing with concrete prisms is needed to validate results for ASR obtained in mortar tests.

6. Sugarcane bagasse ash and ground glass are materials locally available in Florida. Based on the information collected from the literature and previous research performed, these materials show promise for further exposure testing to strengthen the argument for implementation into the FDOT Standard Specifications for Road and Bridge Construction.
7. There was a lack of literature on the hardened properties and long-term durability of concrete incorporating materials of interest in this investigation, particularly for ground sand and ground volcanic rock.
8. The use of PLC presents a sustainable solution for the global cement consumption and shows plastic and mechanical performance compared to OPC; however, durability concerns, particularly the effect on sulfate resistance due the addition of limestone in PC, needs to be assessed in combination with alternative SCM.

This research is aimed at filling the gaps observed for the following aspects:

- Viability of binary and ternary blends of non-conventional SCM;
- Effects on mechanical, plastic, and durability properties due to different replacement levels of non-traditional SCM;
- Comparison between the recently FDOT-approved portland-limestone cement concrete and portland cement; and
- Effects of the environment on field-placed durability blocks.

1.7 MATERIAL AVAILABILITY

1.7.1 Sugarcane Bagasse Ash (SCBA)

Two types of sugarcane bagasse ash were used for this research, the difference between them being the incineration methods. Sugarcane bagasse ash is a seasonal byproduct of sugar production. Therefore, a consistent supply is not produced throughout the year; however, excess material is impounded and may be recovered at a later time. Sugarcane bagasse ash was supplied by two farms in the Southern part of Florida Osceola farms (SCBA-A) and Okeelanta farms (SCBA-B), both local to Florida. The SCBA-A facility burns about 35-46 tons of bagasse per hour per boiler at 575-600°F, depending on the boiler. The SCBA-B facility burns about 50.9

tons of bagasse at 975°F. According to the suppliers, the SCBA-A facility produces approximately 39,000 tons of ash per year and the SCBA-B facility produces about 17,000 tons of ash per year. The SCBA-B facility does not stockpile material while the SCBA-A facility accumulates ash from annual cleaning of its settling pond. The SCBA-B facility mixes the bagasse ash with water and stores it in impoundments for periods that can be in excess of a year. Subsequent to storage, the resulting material is a compost with the appearance of soil and can be used to partially substitute peat in seeding production systems. [99]

1.7.2 Ground Glass

According to the Florida Department of Environmental Protection (FDEP), approximately 30% of waste glass in Florida is recycled [100]. This is partly due to a lack of monetary incentive for recycling [101]. However, there is interest in establishing a reliable market in Florida if ground glass becomes an approved construction material in the Florida Department of Transportation Standard Specifications for Road and Bridge Construction [21]. Determining how much waste glass is produced and recycled in Florida can be used to estimate the potential for glass as a fly ash replacement. The historical data from the Florida Department of Environmental Protection reports the tons of Municipal Solid Waste (MSW), specifically waste glass, and how much of that waste was recycled for each county in Florida. The available data from the last eight years indicates an increasing trend in the total volume of collected waste glass from approximately 730,000 tons in 2010 to over 1,000,000 tons in 2017 [100]. The amount of waste glass that was recycled has remained consistent at $29 \pm 3\%$ of the total waste glass collected except for 2010 and 2011 in which the percentages were 18% and 15% respectively. Using 2017 data as the benchmark, accounting for recycled waste glass, 750,000 tons of waste glass would be available for reuse [100]. However, in the interest of being conservative, averaging the difference from the past six years yields about 615,000 tons per year. As expected, there is a larger production of waste glass in counties with higher populations.

1.7.3 Ground Volcanic Rock

Ground volcanic rock was supplied by Carib Sand & Stone Ltd. The supplier provided an estimate of approximately 500,000 metric tons of annual production allotted for North America, where Florida would be a primary target market [102].

1.7.4 Fly Ash

Class F fly ash is a common cement replacement in the production of concrete [103], [104], [105], [106]. The consumption of fly ash can be used as a baseline for comparison with respect to potential replacements. Figure 1-3 shows the decline in coal fly ash production and the corresponding increase in consumption [107]. Class F fly ash is a common cement replacement in the production of concrete [103], [104], [105], [106]. The consumption of fly ash can be used as a baseline for comparison with respect to potential replacements. Figure 1-3 shows the decline in coal fly ash production and the corresponding increase in consumption [107].

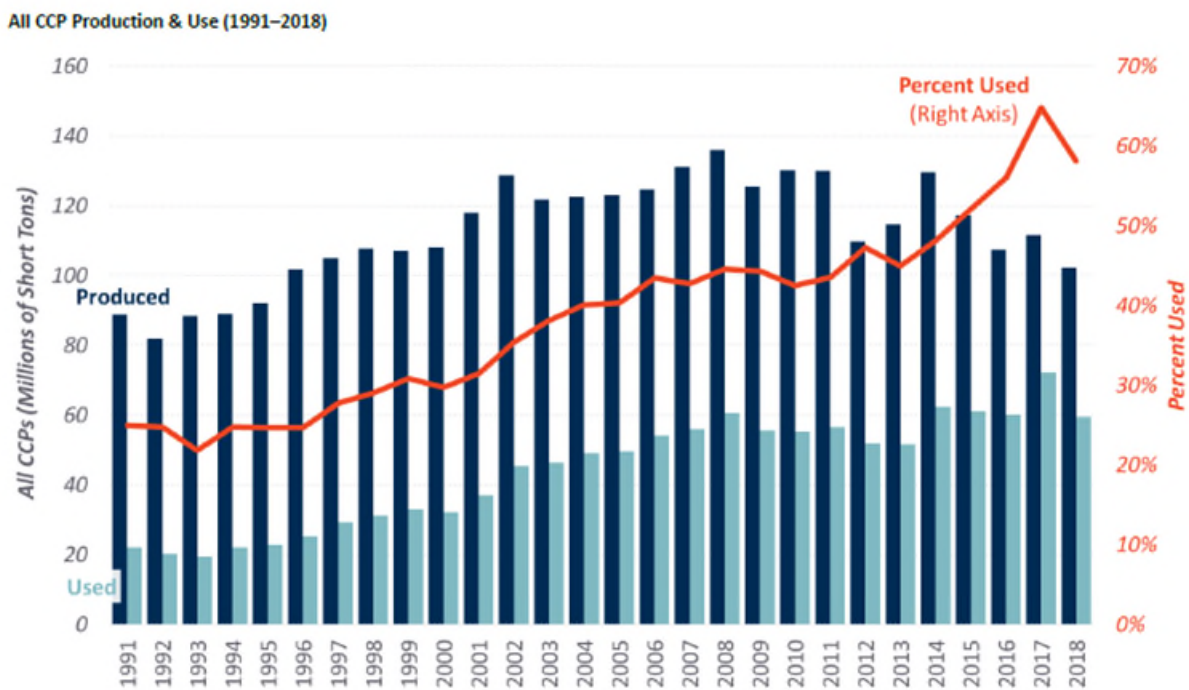


Figure 1-3: Coal fly ash production and consumption over time. [108]

Using the most recent data presented in Figure 1-3, the total fly ash supply for 2016 in the United States was approximately 37 million tons and the total consumption was approximately 22 million tons. In order to make an estimate of how much was consumed in Florida, the cement consumption for Florida was considered. According to the Portland Cement Association, the total apparent cement consumption in the United States in 2017 was approximately 106.5 million tons and 7.2 million in Florida [109]. Therefore, Florida consumes about 7% of the cement produced in the United States. Assuming the proportion of cement consumed in Florida is approximately equivalent to the proportion of fly ash consumed, fly ash consumption in Florida

can be estimated, which would amount to approximately 1.7 million tons. The supply of any supplementary cementitious material acting as a fly ash replacement would have to be comparable or greater than 1.7 million tons to be a single state-wide solution; this is unlikely to be the case and multiple solutions for different regions in the state will likely have to be adopted.

1.8 SURVEY OF SELECT US TRANSPORTATION AGENCIES

The Departments of Transportation (DOTs) covered in the survey focused on states located in regions near Florida (Figure 1-4). These included Alabama, Arkansas, Georgia, Louisiana, Mississippi, North Carolina, Oklahoma, South Carolina, Tennessee, and Texas. Other state DOTs included were California, New York, Virginia, and Washington. Military agencies such as the U.S Army Corps of Engineers (USACE), Naval Facilities Engineering Command (NAVFAC), and Air Force Civil Engineer Center (AFCEC) are responsible for administration of the Unified Facilities Criteria (UFC) system that provides planning, design, construction, and modernization criteria to the Military Departments, the Defense Agencies, and the Department of Defense Field Activities [110].

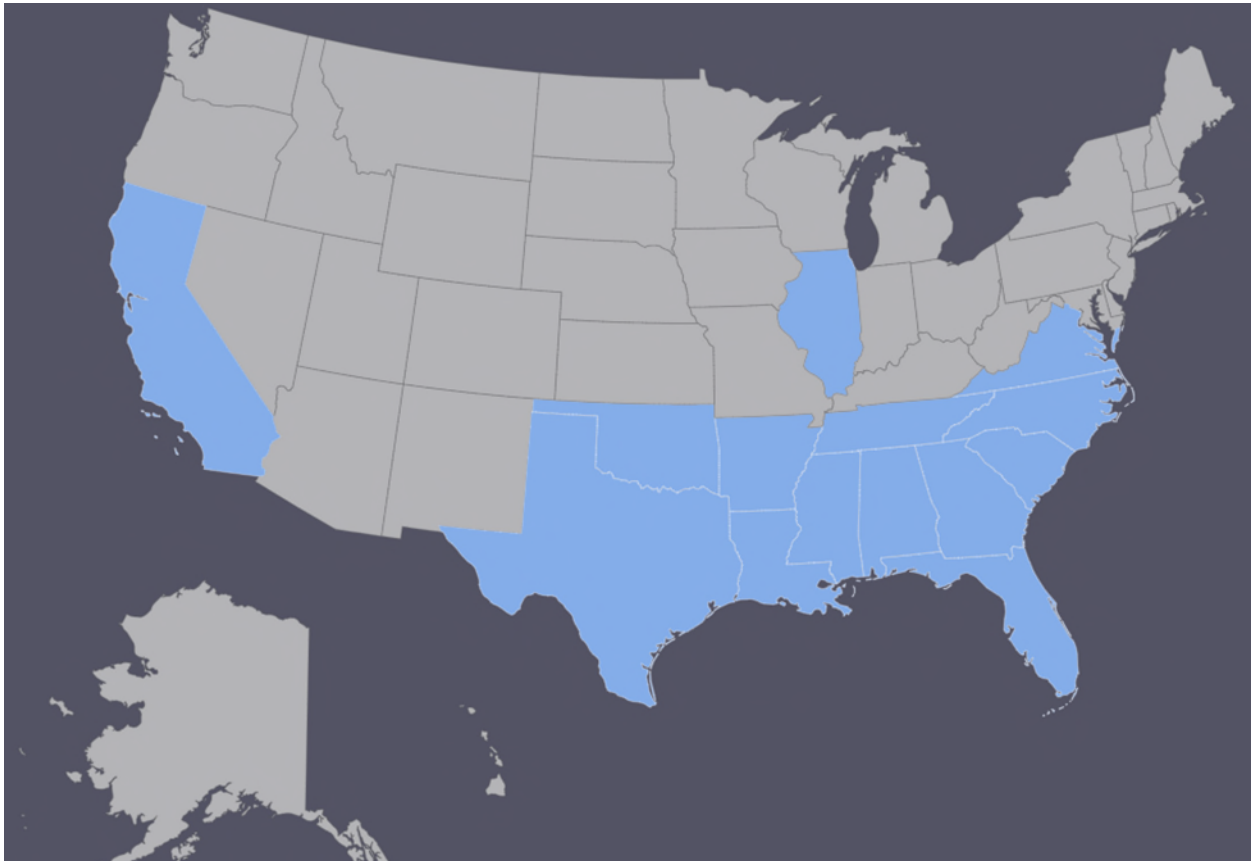


Figure 1-4: State Departments of Transportation included in this survey.

1.8.1 Alabama Department of Transportation (ALDOT)

The Alabama Department of Transportation’s *Standard Specification for Highway Construction* allows for the use of binary or ternary blends of cementitious content containing a maximum of 50% replacement by weight [111]. The only acceptable SCM are coal fly ash (Class C or Class F), slag cement, and silica fume. Table 1-17 below shows the replacement level limits as per ALDOT.

Table 1-17. Supplementary cementitious materials and limits as per ALDOT [111].

Material	Replacement Level	Notes
Class C Fly Ash or Class F Fly Ash	30% maximum	Class F should be used when reduction of heat is required
Slag Cement	50% maximum	25% maximum when ambient temperature is 45°F or below
Microsilica/Silica Fume	10% maximum	
Other	Not Permitted	

1.8.2 Arkansas State Highway and Transportation Department (AHTD)

The Arkansas State Highway and Transportation Department’s *Standard Specifications for Highway Construction* require that most pavement projects use ASTM C150 Type I cement with or without SCM, or an ASTM C595 blended cement [17,20,112]. Mass concrete must use Type II moderate heat (Type II-MH) cement. The blended cements can be a Type IP with 20% or less pozzolan, or Type IS(25) or lower amount of slag cement. For SCM-amended cements, Class C and Class F fly ashes are not allowed to be blended together in the same mixture and neither SCM is allowed for high-early-strength application or in blended cements. These replacement levels apply to pavement and structural concrete with the difference that it requires trial batches for most of structural concrete applications such as mass concrete, retaining walls, and columns. Table 1-18 below shows the replacement level limits as per AHTD.

Table 1-18. Supplementary cementitious materials and limits as per AHTD [112].

Material	Replacement Level	Notes
Class C Fly Ash or Class F Fly Ash	20% maximum	- Cannot be used as a substitute for blended cement, or for high-early-strength cement - Must be grade 100 or higher
Slag Cement	25% maximum	- Cannot be used as a substitute for blended cement, or for high-early-strength cement
Other	Not Permitted	- Ternary mixes are not permitted

1.8.3 California Department of Transportation (Caltrans)

In Section 90-1.02b of the California Department of Transportation’s *Standard Specifications* states that, unless otherwise noted, concrete must be constructed using a Type II with SCM, Type V with SCM, or a Type IS or Type IP blended cement per ASTM C595 (can also be a blended cement using Type II or V) [113]. The available SCM for use in concrete mixes include Class F fly ash, slag cement, ultrafine fly ash, silica fume, metakaolin, or a Class N pozzolan. The limits for each material are dependent upon a set of equations and physical/chemical requirements, and include several options for inclusion; however, a general summary is provided in Table 1-19.

Table 1-19. Supplementary cementitious materials and limits as per Caltrans [113].

Material	Replacement Level ¹	Notes
Class F Fly Ash or Class N Pozzolan	25% maximum	<ul style="list-style-type: none"> - When CaO content is less than 10%, not combined with other SCM, used with reactive aggregate, and has either 1.5% or less available Na₂O_{eq} or 5% total Na₂O_{eq} - All other cases result in a lower maximum content - Maximum replacement includes content in blended cements
Ultrafine Fly Ash	12% maximum	<ul style="list-style-type: none"> - Classified as Class F - Several physical/chemical requirements outlined in specification - When not combined with other SCM and used with reactive aggregate; otherwise, limit decreases
Metakaolin	12% maximum	<ul style="list-style-type: none"> - Several physical/chemical requirements outlined in specification - - When not combined with other SCM and used with reactive aggregate; otherwise, limit decreases
Slag Cement	50% maximum	<ul style="list-style-type: none"> - When not combined with other SCM and used with reactive aggregate; otherwise, limit decreases - Maximum replacement includes content in blended cements - Grade 100 or 120
Silica Fume	12% maximum	<ul style="list-style-type: none"> - Mortar expansion testing required - When not combined with other SCM and used with reactive aggregate; otherwise, limit decreases
Other	Not Permitted	<ul style="list-style-type: none"> - No exclusion on number of SCM, just total quantity

¹ When using non-reactive aggregate, maximum values are reduced to 60% of values shown above.

1.8.4 Florida Department of Transportation (FDOT)

The Florida Department of Transportation’s *Standard Specifications for Road and Bridge Construction* allows for the use of Type I, II, III, IL, IS, and IP cements; as well as ternary blended cements [21]. The use of supplementary cementitious materials is required for each type of structural concrete and include fly ash, slag cement, silica fume, and metakaolin. A general summary of the replacement levels for each allowable supplementary cementitious material is presented below.

Table 1-20. Supplementary cementitious materials and limits as per FDOT [21].

Material	Replacement Level ¹	Notes
Class F Fly Ash	10 – 50%	<ul style="list-style-type: none"> - Different classes of concrete require different ranges of replacement - Different ranges when in combination with slag cement - Cannot be used with Type IP or IS cement
Class C Fly Ash		<ul style="list-style-type: none"> - Must be comparable to Class F fly ash according to a number of performance specifications - Cannot be used with Type IP or IS cement
Ultrafine Fly Ash	8 – 12%	<ul style="list-style-type: none"> - Strength activity index at 7 days must be at least 85% - Strength activity index at 28 days must be at least 95% - 50% of particles must be 3.25 microns or smaller - 90% of particles must be 8.50 microns or smaller - Material retained on 45-micron wet sieve must be less than 6.0% - Moisture content must be less than 1.0% - Loss on ignition must be less than 2.0% - Cannot be used with Type IP or IS cement
Metakaolin	8 – 12%	<ul style="list-style-type: none"> - Must use a high-range water reducer - $\text{SiO}_2 + \text{Al}_2\text{O}_3 + \text{Fe}_2\text{O}_3 > 85\%$ - Loss on ignition must be less than 3.0% - Available alkalis as equivalent Na_2O must be less than 1.0% - Strength activity index at 7 days must be at least 85% - Must be comparable to silica fume according to a number of performance specifications
Slag Cement	25 – 70%	<ul style="list-style-type: none"> - Different classes of concrete require different ranges of replacement - Different ranges when in combination with fly ash - Grade 100 or 120 - Cannot be used with Type IP or IS cement
Silica Fume	7 – 9%	<ul style="list-style-type: none"> - Must use a high-range water reducer

1.8.5 Georgia Department of Transportation (GDOT)

The Georgia Department of Transportation’s *Standard Specifications – Construction of Transportation Systems* allows for the use blended cements, fly ash, slag, and pozzolans for

concrete that is not prestressed [114]. For pre-stressed applications, microsilica (silica fume) is allowed. Additionally, the use of a Type IP or Type IS blended cement is also permitted. A summary table of material and inclusion limits for general portland cement concrete is provided below in Table 1-21.

Table 1-21. Supplementary cementitious materials and limits as per GDOT [114].

Material	Replacement Level	Notes
Class C, F, or N Fly Ash	25% maximum	- Cannot be used with Type IP cement
Slag Cement	50% maximum	- Cannot be used with type IP cement - Has temperature restrictions - Mix design has to be approved before use
Silica Fume	10% maximum	- Only for pre-stressed concrete applications
Other	Not Permitted	

1.8.6 Illinois Department of Transportation (IDOT)

The Illinois Department of Transportation’s *Standard Specifications for Road and Bridge Construction* allows for the use of fly ash, silica fume, metakaolin, and slag [115]. Section 1001.01 of this specification allows for the use of ASTM C595 blended cements containing slag or pozzolan (Class C fly ash, Class F fly ash, or silica fume). A summary of acceptable supplementary cementitious materials and replacement levels are presented in Table 1-22.

Table 1-22. Supplementary cementitious materials and limits as per IDOT [115].

Material	Replacement Level	Notes
Class F Fly Ash	25% maximum	- Limited to specific classes of concrete
Class C Fly Ash	30% maximum	- Limited to specific classes of concrete
Slag Cement	35% maximum	- Limited to specific classes of concrete - Grade 100 or 120
Silica Fume	5% maximum	
Metakaolin	5% maximum	- Must meet AASHTO M321 except maximum residue retained on No. 325 sieve is 15%
Other	Not Permitted	- Only binary and ternary blends are allowed for specific classes of concrete up to 35%

1.8.7 Louisiana Department of Transportation and Development (LaDOTD)

The Louisiana Department of Transportation and Development’s *Standard Specification for Roads and Bridges* allows for the use of Type IL cement, and blended cements [116].

Additionally, for structural concrete, fly ash and slag are permitted for binary or ternary mix designs. There are different replacement levels for structural and pavement concrete mix designs, which are explained in general below in Table 1-23.

Table 1-23. Supplementary cementitious materials and limits as per LaDOTD [116].

Material	Replacement Level	Notes
Class F Fly Ash or Class C Fly Ash	30% maximum	- Limited to binary mixes
Slag Cement	50% maximum	- Limited to binary mixes - Valid for Type I, II, III and IL cement - Blended Type IP and IS cements limited to 40%
Ternary Blends	70% maximum	- Blends of slag cement and fly ash must contain more slag than fly ash - 50% maximum replacement for pavements (above limitations also apply)

1.8.8 Mississippi Department of Transportation (MDOT)

The Mississippi Department of Transportation’s *Standard Specifications for Road and Bridge Construction* permits the usage of fly ash, GGBFS, and silica fume [117]. Furthermore, for concrete exposed to moderate sulfate or seawater, the use of Type IL, IP, or IS cement is allowed in lieu of Type I or II cement. A summary of acceptable supplementary cementitious materials and replacement levels are presented in Table 1-24.

Table 1-24. Supplementary cementitious materials and limits as per MDOT [117].

Material	Replacement Level	Notes
Class F Ash	20 – 25% (Type I/II) ¹ 35% (Type IL) ¹	- 24.5 – 25% when using Type I cement exposed to moderate or severe sulfate
		- 24.5 – 35% when using Type IL cement exposed to moderate sulfate
		- CaO content less than 8%
		- 6% or lower LOI
Class C Ash	20 – 25% (Type I/II) ¹	- 6% or lower LOI
		- Not allowed for sulfate exposure
Slag Cement	45 – 50% ¹	- 49.5 – 50% when using Type I cement exposed to moderate or severe sulfate
		- 49.5 – 50% when using Type II cement exposed to severe sulfate
		- 49.5 – 50% when using Type IL cement exposed to moderate or severe sulfate
		- Grade 100 or 120; no chlorides
Silica Fume	7.5 – 8%	- Only allowed when Type IL cement exposed to moderate sulfate

¹ Replacement levels below the minimum tolerance may be used, but shall not be given special considerations, such as maximum temperature acceptance.

1.8.9 North Carolina Department of Transportation (NCDOT)

The North Carolina Department of Transportation’s *Standard Specifications for Roads and Structures* allows for the use of Type I, II, or III cement for general and pre-cast construction. Blended cements per ASTM C595 are allowed; specifically Type IL, IS, IT, and IP are allowed. Type IS cements shall use 35 – 50% slag, Type IT cements must be approved by The Engineer, Type IP cements shall use 17 – 23% pozzolan, and any blended cements must have interground constituents. A summary of acceptable supplementary cementitious materials and replacement levels are presented in Table 1-25; however, these limits are only placed for use with cements having an alkali content of 0.6 – 1.0%.

Table 1-25. Supplementary cementitious materials and limits as per NCDOT [118].

Material	Replacement Level ¹	Notes
Class F Ash	20 – 30%	- Loss on ignition must be below 4%
Class C Ash ²	Not allowed	
Slag Cement	35 – 50%	- Must be grade 100 or higher
Silica Fume	4 – 8%	
Other	Not Permitted	

¹ These limits are only in place when the cement used has an alkali content of 0.6 – 1.0%.

² Class C fly ash is allowed, as long as the cement used has an alkali content below 0.4%.

1.8.10 Oklahoma Department of Transportation (ODOT)

The Oklahoma Department of Transportation’s *Standard Specifications* allows for the use of any ASTM C150 or ASTM C595 cement type that has a tricalcium aluminate content of less than 15%, and an alkali content less than 0.95% [119]. Additionally, supplementary cementitious materials are permitted at various replacement percentages based upon the inclusion with either ordinary portland cement or blended cements as described in Table 1-26. Additionally, ODOT allows for supplementary cementitious materials to replace portions of blended cements per ASTM C595 as specified in Table 1-27 below.

Table 1-26. Supplementary cementitious materials and limits as per ODOT [119].

Material	Replacement Level	Notes
Class F or C Ash	20% maximum	
Slag Cement	50% maximum	- Grade 100 or 120
Silica Fume	10% maximum	
Fly ash or pozzolans plus silica fume	30% maximum	
Fly ash or pozzolans, slag, plus silica fume	50% maximum	

Notes: ODOT does not define what a “pozzolan” is or what materials are pozzolans

Table 1-27. Supplementary cementitious material replacement of blended cements as per [119].

Cement Substitutes for Blended Hydraulic Cement		
Cement Type	Material	Maximum Percent by Weight
IP (XX)	Fly ash	30 – (XX)
	Silica fume	10
	Slag cement	50 – (XX)
	Combinations	See previous table.
IS (XX)	Fly ash	20
	Silica fume	10
	Slag cement	50 – (XX)
	Combinations	See previous table.

Note: (XX) is the percentage of pozzolan in IP cement or the amount of slag in IS cement.

1.8.11 South Carolina Department of Transportation (SCDOT)

The South Carolina Department of Transportation’s *Standard Specifications for Highway Construction* allow for the use of only Type I, II, III or IS cements [120]; IS cement must contain no more than 25% slag. Any cement used must meet requirements for low-alkali cement ($\text{Na}_2\text{O}_{\text{eq}}$ 0.6% maximum). Additionally, the use of fly ash, slag, and silica fume are allowed as described in Table 1-28 below for concrete structures.

Table 1-28. Supplementary cementitious materials and limits as per SCDOT [120].

Material	Replacement Level	Notes
Class F or C Ash	20% maximum	-
Slag Cement	50% maximum	- Grade 100 or 120
Silica Fume	7.6% maximum	- SCDOT calls for different classes of concrete with either 35 pcy (4,000 psi concrete) or 74 pcy (10,000 psi concrete)

1.8.12 Tennessee Department of Transportation (TDOT)

The Tennessee Department of Transportation’s *Standard Specifications for Road and Bridge Construction* allows for the use of Type I, IL, IP, and IS cement [121]. Unless otherwise specified, the use of Type I, IS, or IL is preferred over the use of Type IP. This document only allows for the use of fly ash and slag as cement replacement materials. The replacement levels are described below in Table 1-29.

Table 1-29. Supplementary cementitious materials and limits as per TDOT [121].

Material	Replacement Level	Notes
Class F or C Ash	25% maximum	<ul style="list-style-type: none"> - Max loss on ignition must be 1.0% - Pozzolanic activity index at 7 days must be 60% minimum ¹ - Pozzolanic activity index at 7 days must be 75% minimum ¹ - Only for use in Type I, Type IL, or Type IS - When used in a ternary blend, fly ash is limited to 20% maximum: 50% portland cement minimum - Cannot blend fly ashes with Type I cement
Slag Cement	35% maximum	<ul style="list-style-type: none"> - Grade 100 or 120 - Only for use in Type I, Type IL, or Type IP - Ternary blends must have 50% portland cement minimum - Cannot blend slags with Type I cement

¹ The specification appears to have a typographic error; it states the pozzolanic activity index at 7 days must be 60% minimum, then states that the pozzolanic activity index at 7 days must be 75%. Most other specifications reference activity index at 28 days having a minimum strength of 75% of control.

1.8.13 Texas Department of Transportation (TxDOT)

The Texas Department of Transportation’s *Standard Specifications for Construction and Maintenance of Highways, Streets, and Bridges* allows for the use of cements that meet ASTM C150 or ASTM C595 with some specific modifications [122]. Type IP cements must have Class F fly ash that is 20% – 40% by mass. Type IIIP must contain Class F fly ash that is 25 – 40% by mass and have specific strength requirements (1,890 psi at 1 day and 3,780 psi at 3 days). Type IS cements must contain at least 35% slag cement. Additionally, cements can be replaced with fly ash, slag cement, silica fume, or metakaolin as described in Table 1-30.

Table 1-30. Supplementary cementitious materials and limits as per TxDOT [122].

Material	Replacement Level	Notes
Class F Ash	20 – 35%	- Maximum 10% replacement when using blended cements
Class C Fly Ash	35% maximum	- When used with at least 6% silica fume, ultrafine fly ash, or metakaolin; must have 35 – 50% cement replacement total and no more than 10% silica fume - Can replace Class F fly ash if total cementitious content is 520 pecy or less for certain classes of concrete
Silica Fume	10% maximum	- Can be used with blended cements, but silica fume content cannot exceed 10% (including composition of Type IT cement)
Slag Cement	35 – 50%	- Maximum 10% replacement when using blended cements
Metakaolin	Used in combination with other SCM	
Ternary Blends	35 – 50%	- Fly Ash limited to 35% - Silica fume limited to 10%

Notes: Each material has separate qualification specifications related to physical properties as well as performance.

1.8.14 Virginia Department of Transportation (VDOT)

The Virginia Department of Transportation’s *Road and Bridge Specifications* allow for the use of Type I, II, III, or blended cements for structures; Type I and Type II cements must contain at most 1.0% total alkalis [123]. Blended cements must be approved by the Engineer of Record prior to implementation. The inclusion of fly ash, slag cement, silica fume, and metakaolin is allowed to replace portions of cement as summarized in Table 1-31 below.

Additionally, VDOT prescribes minimum levels of supplementary cementitious materials dependent on the total alkali content of the cement as described in Table 1-32.

Table 1-31. Supplementary cementitious materials and limits as per VDOT [123].

Material	Replacement Level	Notes
Class F Ash	30% maximum	- Maximum 10% replacement when using blended cements
Class C Fly Ash		- Contractor must demonstrate that replacement level will not produce 0.15% expansion at 56 days according to ASTM C227 using borosilicate aggregate [79]
Slag Cement	50% maximum	- Maximum 10% replacement when using blended cements - Grade 100 or 120
Silica Fume	10% maximum	- Can be used with blended cements, but silica fume content cannot exceed 10% (including composition of Type IT cement)
Metakaolin		- Contractor must demonstrate that replacement level will not produce 0.15% expansion at 56 days according to ASTM C227 using borosilicate aggregate [79]
Others		- Contractor must demonstrate that replacement level will not produce 0.15% expansion at 56 days according to ASTM C227 using borosilicate aggregate [79]

Table 1-32. Minimum level of replacement by supplementary cementitious materials as per [123].

Material	Total alkalis of cement is less than or equal to 0.75%	Total alkalis of cement is between 0.75 – 1.0%
Class F Ash	20% minimum	25% minimum
Slag Cement	40% minimum	50% minimum
Silica Fume	7% minimum	10% minimum
Metakaolin	7% minimum	10% minimum

1.8.15 Unified Facilities Criteria (UFC)

Section 32 13 13.06 2.1.1 of the *Unified Facilities Guide Specifications* used by the United States Army Corps of Engineers (USACE), Naval Facilities Engineering Command (NAVFAC), Air Force Civil Engineer Center (AFCEC), and National Aeronautics and Space Administration (NASA) lists the general design guide for portland cement concrete construction; including materials and recommended levels of inclusion [124]. The UFGS requires that portland

cement comprise 50 – 80% of the total cementitious material content. The cement types allowed include Type I, II, III, V, IS, IP, or general hydraulic cements classified in ASTM C1157 as type MS, HS, or R [125]. A summary of inclusion levels of the various allowable supplementary cementitious materials is presented below in Table 1-33.

Table 1-33. Supplementary cementitious materials and limits as per UFC [124].

Material	Replacement Level	Notes
Class F Ash or Class N Pozzolan	35% maximum	- 25% minimum for $\text{SiO}_2 + \text{Al}_2\text{O}_3 + \text{Fe}_2\text{O}_3 > 70\%$
		- 20% minimum for $\text{SiO}_2 + \text{Al}_2\text{O}_3 + \text{Fe}_2\text{O}_3 > 80\%$
		- 15% minimum for $\text{SiO}_2 + \text{Al}_2\text{O}_3 + \text{Fe}_2\text{O}_3 > 90\%$
Slag Cement	40 – 50%	- Grade 100 or 120; Grade 120 is preferred
Silica Fume	10% maximum	- Can be used with blended cements, but silica fume content cannot exceed 10% (including composition of Type IT cement)
Ultrafine fly ash	7 – 16%	- Must be classified as Class F or Class N according to ASTM C618
		- Average particle size must not exceed 6 microns
Ultrafine pozzolan		- Strength activity index at 28 days must be at least 95% of control
Silica Fume		- The guide describes and links to guidance on the use of silica fume (through the EPA), but does not specifically allow or disallow the material; specifically stating “The Contractor must incorporate these other non-cement materials based on local availability and mixes available at local plants.”

1.8.16 Summary

After an extensive survey of 14 state departments of transportation, and governmental specifications, the following observations can be made:

- Most specifications allow for the use of Class F fly ash, slag cement, and silica fume
- Some specifications allow the use of metakaolin, Class C fly ash, and Class N pozzolans
- Most specifications allow the use of blended Type IS and IP cements; 6 specifications allowed for the use of a Type IL cement
- There were no direct allowances for alternative supplementary cementitious materials that do not conform to standard specifications published by ASTM such as ground

glass, ground rock, ground sand, agricultural ashes, etc. (although some specifications allow for materials that are classified as Class N pozzolans).

- Comparatively, FDOT provides the most latitude with respect to allowable cement types and supplementary cementitious materials combinations. Until recently, except for metakaolin, there was little allowance for Class N pozzolans. However, calcined clay and ground glass have been since allowed [21].

2. Material Acquisition and Characterization

Two different types of sugarcane bagasse ash were acquired for testing. Both were obtained from South Florida. The first type was obtained from Osceola Farm (noted herein as SCBA-A) and the second type was obtained from Okeelanta Farm (noted as SCBA-B). The difference between the two samples is in the processing that takes place. SCBA-A is reclaimed, impounded ash that was incinerated using older equipment, whereas the SCBA-B is fresh and has been processed to burn more completely. This new process results in ash that varies in mineralogical and morphological composition from the SCBA-A. The different sugarcane ashes are shown below in Figure 2-1; the darker SCBA A is the result of a lower temperature, less complete burn.



Figure 2-1. Left: SCBA A. Right: SCBA B.

The ground glass (GG) obtained for this research is a manufactured product referred to as “Pozzotive” and was donated by Urban Mining, a company located in New York that is anticipating opening manufacturing facilities in Florida. This material is ground recycled container glass that is purported to provide results that rival Class F ash-amended concretes in various performance metrics. Ground volcanic rock from a Caribbean source was obtained for evaluation. This material was incorporated into the experimental regime to determine if it could provide a benefit to Florida concretes and mortars.

Based upon the various materials accepted by the state DOTs and federal agencies, Class F fly ash, Class C fly ash, and silica fume were also acquired as comparison materials. Typical Florida aggregates (silica sand for the fine aggregate and oolitic limestone for the coarse aggregate) were acquired for the majority of mixes. For specific durability testing alkali-silica reactive aggregate (Figure 2-2) and high alkali portland cement were obtain. Additionally, for most evaluations, typical Type I/II portland cement as well as Type IL limestone cement were acquired for determining the effects that SCM may have of the various cementitious systems. The complete list of materials acquired for this research are presented below in Table 2-1.

Table 2-1. Materials acquired for this research.

Material Type	Origin	Comments
Type I/II Portland Cement	Gainesville, FL	
Type IL Portland Cement	Tampa, FL	
High Alkali (HA) Type I/II Portland Cement	Slite, Sweden	This cement was barged into Cape Canaveral, Fl and was used for alkali-silica reactivity testing.
Class F Fly Ash	Wilsonville, AL	
Class C Fly Ash	West Jefferson, AL	
Silica Fume		
Sugarcane Bagasse Ash – Facility A	Osceola, FL	
Sugarcane Bagasse Ash – Facility B	Okeelanta, FL	
Ground Waste Glass	New Rochelle, NY	
Ground Volcanic Rock	Roseau, Dominican Republic	
Ground Sand	Gainesville, FL	This material was generated by processing Florida sand in a pulverizer.
Coarse Aggregate	Gainesville, FL	
Fine Aggregate	Gainesville, FL	
Alkali – Reactive Fine Aggregate	El Paso, TX	This material was only used for alkali-silica reactivity and durability testing.



Figure 2-2. Alkali-silica reactive fine aggregate from the Jobe mine in El Paso, Texas.

2.1 ELEMENTAL COMPOSITION

Elemental compositions of materials were determined by x-ray fluorescence. This test method involves creating glass beads from the powdered materials by mixing with a lithium borate flux and heating to over 1,000°C. These glass beads are then subjected to ionizing radiation (“A” in Figure 2-3) which ejects inner shell electrons from atoms (“B” in Figure 2-3). When the inner shell electron is ejected, a higher-shell, higher energy electron drops into the inner shell, but must reduce its energy to do so. The outer shell electron ejects a photon that has characteristic energy related to the element of the atom (“C” in Figure 2-3). The photon energy is then measured by an optical sensor which collects the intensity and quantity of photons that are released, and a composition can be determined. The results of these elemental composition analyses are presented in Table 2-2.

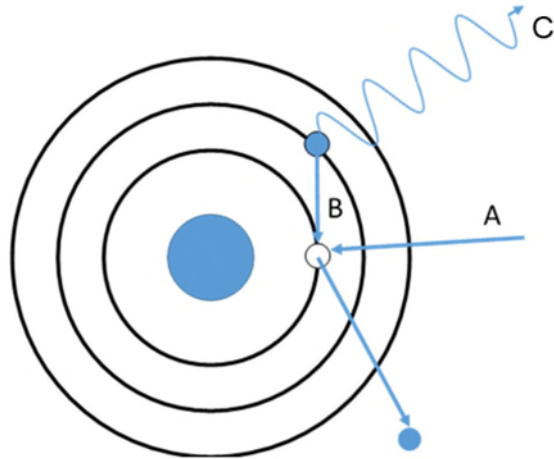


Figure 2-3. Classic photon emission during x-ray fluorescence. A – X-Ray emitted onto an inner-shell electron. B – Inner-shell electron. C – Characteristic energy being emitted from atom.

In addition to elemental oxide composition, loss on ignition was performed on each material. During this evaluation method, a 1-gram sample of material was placed into a crucible and heated to 950°C to remove volatile materials such as bound water (in the form of hydrates in cement), sulfurous compounds, or carbon-based minerals. For cement, this gives an indication of the degree of prehydration, and ASTM C150 limits the loss on ignition (LOI) value to less than 3.0% for Type I/II cement unless limestone is used as a mill addition, then the limit is 3.5%. However, Type IL cements are not bound by ASTM C150, and instead are bound by ASTM C1157, which does not limit loss on ignition due to the varying limestone content. For ashes that are classified by ASTM C618 (coal fly ash and natural pozzolans), the standard acceptable limit for LOI is 6% for Class F and Class C fly ashes, and 10% for Class N pozzolans. The results of the LOI determination are presented in Table 2-2.

Table 2-2. Elemental oxide composition of materials by x-ray fluorescence.

Elemental Oxide	Type I/II PC	Type IL PC	HA PC	Class F Fly Ash	Class C Fly Ash
CaO	65.3%	65.6%	64.4%	2.6%	24.7%
SiO ₂	19.9%	20.3%	20.6%	51.5%	36.1%
Al ₂ O ₃	5.0%	4.9%	5.1%	21.9%	19.3%
Fe ₂ O ₃	3.4%	3.7%	3.2%	13.6%	4.7%
$\bar{S}O_3$	3.2%	2.6%	3.2%	0.8%	2.4%
MnO	0.0%	0.0%	0.1%	0.0%	0.0%
MgO	0.8%	0.9%	3.4%	1.0%	4.9%
Na ₂ O	0.1%	0.1%	0.2%	1.2%	1.6%
K ₂ O	0.3%	0.3%	0.9%	2.6%	0.5%
P ₂ O ₅	0.4%	0.1%	0.0%	0.1%	0.9%
TiO ₂	0.3%	0.2%	0.4%	1.1%	1.5%
Total	98.7%	98.8%	98.6%	95.1%	95.0%
Na ₂ O _{eq}	0.3%	0.3%	0.8%	2.8%	1.9%
LOI	2.3%	4.6%	2.3%	1.4%	0.4%

Table 2-2. Elemental oxide composition of materials by x-ray fluorescence. Continued.

Elemental Oxide	SCBA A	SCBA B	Ground Glass	Ground Volcanic Rock	Silica fume
CaO	9.8%	25.9%	10.7%	6.1%	0.5%
SiO ₂	81.4%	53.8%	70.5%	60.8%	97.0%
Al ₂ O ₃	1.4%	1.8%	1.7%	16.3%	0.6%
Fe ₂ O ₃	1.0%	1.3%	0.3%	7.3%	0.2%
$\bar{S}O_3$	0.6%	4.2%	0.2%	0.1%	0.1%
MnO	0.1%	0.1%	0.0%	0.2%	0.0%
MgO	2.7%	4.1%	2.1%	3.2%	0.5%
Na ₂ O	0.2%	0.4%	13.5%	3.1%	0.1%
K ₂ O	1.4%	4.5%	0.4%	1.3%	0.5%
P ₂ O ₅	1.8%	1.8%	0.0%	0.1%	0.0%
TiO ₂	0.1%	0.1%	0.1%	0.6%	0.0%
Total	100.4%	97.9%	99.5%	98.4%	99.4%
Na ₂ O _{eq}	1.1%	3.4%	13.8%	4.0%	0.4%
LOI	24.2%	12.8%	0.0%	-0.2%	2.3%

2.2 MINERAL COMPOSITION

In addition to elemental oxide composition, the chemical reactivity of a material is driven in part by crystallinity. For siliceous materials, amorphous silica is much more reactive in a high pH environment, such as during cement hydration, due to higher solubility. Therefore, the amount and type of crystalline minerals in a material are of great importance to know. To accomplish the quantitative portion of this determination, powder x-ray diffraction was performed along with a Rietveld refinement to determine the compositional make-up of the crystalline minerals present in each material. Collimated x-rays are directed at a sample and the

individual x-rays are diffracted by the atoms in the crystalline lattice of a material at a specific angle, which is recorded by a detector. As the incident x-ray angle is varied, the diffracted angle also changes. With depth, the lattice spacing contributes to either constructively or destructively interfering x-rays, which change the intensity of the detected diffracted x-rays at a particular angle. As the angle is varied, the intensity changes and this is plotted to form a diffractogram. Once the pattern is plotted, it can be compared to known mineral patterns, and the intensity for each pattern can be adjusted until it closely matches the measured pattern; the adjustments of the mineral patterns are related to the mass portion of that crystalline mineral in the bulk sample measured. Because this method relies on regular crystalline lattice structures, amorphous content produces no discernible peaks; however, the quantity of the amorphous material can be determined if a known amount of a crystalline standard is added to each sample prior to the evaluation. The amorphous material can be present as a glassy phase, possessing no crystalline order, or as a crystalline material that is too fine to be resolved by x-rays. The resulting scans of the materials and a summary table of their mineral compositions are presented below. Appendix I contains the x-ray diffractograms of the materials.

Table 2-3. Mineral composition of materials by x-ray powder diffraction.

Mineral Component	Type I/II PC	Type IL PC	HA PC	Class F Fly Ash	Class C Fly Ash
C3S – Alite	50.2%	51.9%	52.9%	-	-
C2S – Belite	20.4%	14.9%	13.5%	-	-
C3A – Aluminate	4.9%	3.4%	5.3%	1.4%	10.6%
C4AF – Ferrite	12.7%	14.0%	10.4%	-	-
Calcite	4.3%	11.2%	4.5%	-	-
Bassanite	2.7%	1.8%	3.7%	-	-
Syngenite	2.0%	-	3.4%	-	-
Thenardite	1.1%	-	-	-	-
Anhydrite	0.9%	0.4%	0.3%	1.4%	3.4%
Gypsum	0.7%	1.5%	0.5%	-	-
Quartz	-	1.0%	-	6.6%	9.6%
Magnetite	-	-	-	3.5%	-
Periclase	-	-	-	-	2.0%
Lime	-	-	-	-	1.2%
Amorphous Content	Not Measured	Not Measured	Not Measured	87.1%	73.1%

Table 2-3. Mineral composition of materials by x-ray powder diffraction. Continued.

Mineral Component	SCBA A	SCBA B ¹	Ground Glass	Ground Volcanic Rock	Silica fume
Calcite	-	13.0%	-	-	-
Syngenite	-	12.2%	-	-	-
Anhydrite	-	-	-	-	-
Quartz	45.9%	29.3%	-	26.8%	-
Albite	-	-	-	58.6%	-
Augite	-	-	-	5.2%	-
Amorphous Content	51.9%	44.5%	100%	9.5%	100%

¹ This material had a pattern match for mellite, which is an aluminum benzene carboxylate, not naturally found in the US but it assumed to be formed from lignite plant material in aluminum-based clays. This may be a due to the location and processing of the origin material.

2.3 PARTICLE SIZE DISTRIBUTION

In addition to mineralogy, hydration reaction kinetics are affected by particle size as the initial hydration reactions are dissolution controlled. Therefore, it is imperative to determine the particle size distribution of the materials because particle size can give a general indication to surface area of the powders. In order to determine the particle size distribution, a laser light diffractometer is employed whereby lasers are shone through a suspension of a fluid (generally ethanol) and a small amount of powdered sample. The amount of diffraction of the lasers is related to material and particle size. A summary table of results is presented below; the charts for the particle size distribution for each material are presented in Figure 2-4 through Figure 2-11.

The differences in particle size most likely contribute to differences in results as lower particle sizes have higher reactivity rates. The three different cement types have similar particle sizes, which is to be expected. The differences between particle size in both SCBA types is most likely due to the differences in incineration methods. The higher combustion in SCBA-B is likely the main cause of a lower size. Both types of fly ash and GG had smaller particle sizes than cements, which contribute to higher reactivities in the respective mixtures. Ground volcanic rock had a similar particle size to the cements. Therefore, variations in performance would not be attributed to particle size.

Table 2-4. Summary of particle size distribution of materials.

Material	10% Passing Size (μm)	50% Passing Size (μm)	90% Passing Size (μm)
Type I/II OPC	3.1	11.1	28.0
Type IL OPC	1.8	11.4	33.3
HA Type I/II OPC	2.4	11.7	33.1
Class F Fly Ash	1.7	10.6	47.2
Class C Fly Ash	1.0	8.1	60.7
Silica Fume ¹	0.3	5.4	8.8
SCBA A	10.3	45.8	168.4
SCBA B	6.0	20.3	92.2
Ground Glass	3.1	9.2	18.9
Volcanic Rock	2.4	12.3	26.0
Ground Sand	0.8	18.0	43.0

¹The ultrasonic probe was likely not powerful enough to disperse the densified silica fume to entirely discrete particles. The particle size distribution is likely smaller than what is represented here.

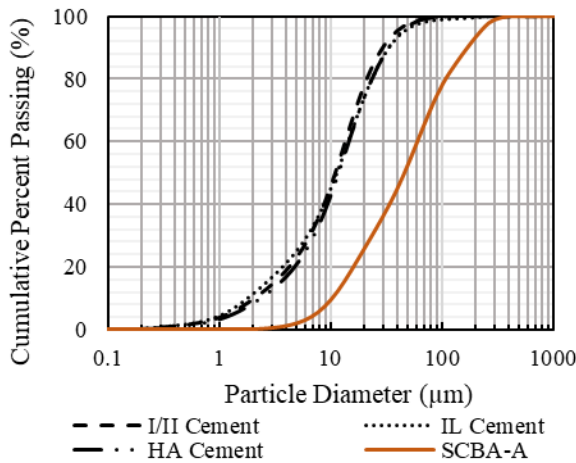


Figure 2-4. Particle size distribution for SCBA-A.

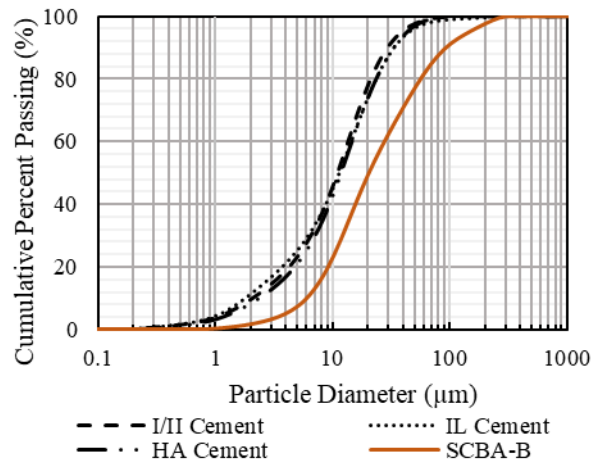


Figure 2-5. Particle size distribution for SCBA-B.

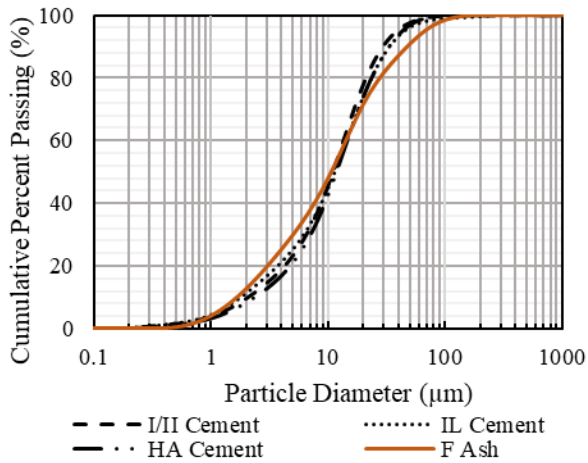


Figure 2-6. Particle size distribution for Class F fly ash.

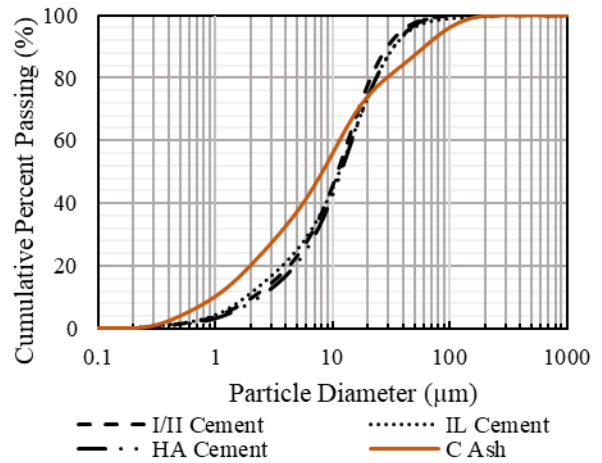


Figure 2-7. Particle size distribution for Class C fly ash.

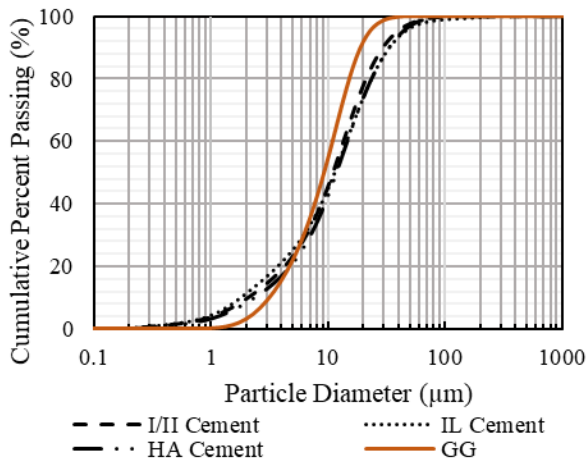


Figure 2-8. Particle size distribution for Ground Glass.

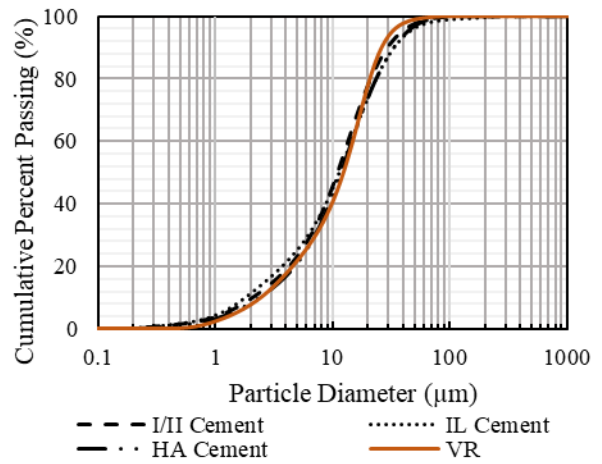


Figure 2-9. Particle size distribution for Volcanic Rock.

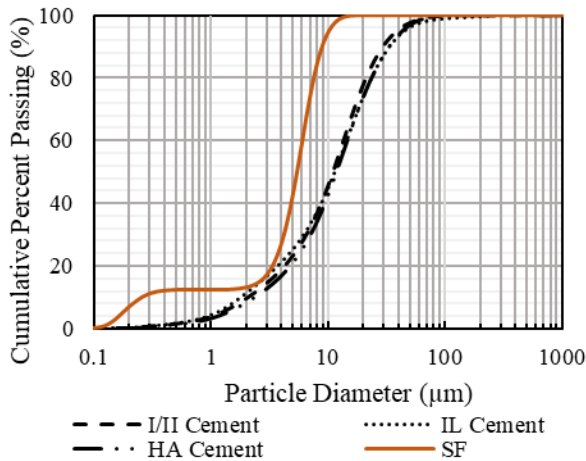


Figure 2-10. Particle size distribution for Silica Fume.

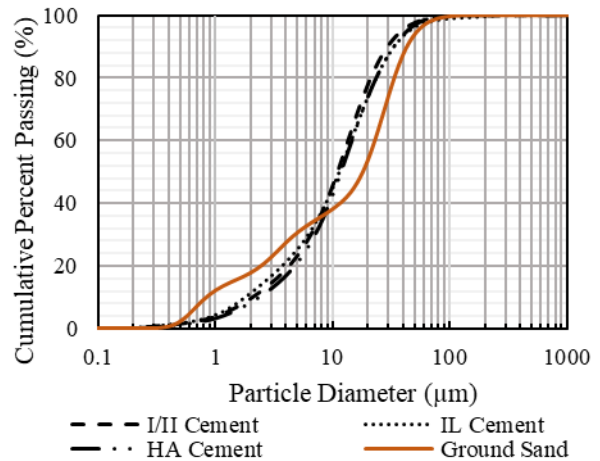


Figure 2-11: Particle size distribution for Ground Sand.

2.4 SPECIFIC HEAT CAPACITY

Specific heat capacity (C_{sp}) for the various materials used for this research was measured using a differential scanning calorimeter at the FDOT State Materials Office. This value measures the amount of heat energy required to raise the temperature of a unit weight of material by one degree. This material property was required to adequately perform isothermal calorimetry (used to measure heat of hydration). In this method, a small (approximately 5 mg) sample is loaded into a machine that simultaneously heats the sample (while measuring the energy input) and measures the temperature rise. This specific heat capacity is then plotted versus temperature. Replicates of each material were evaluated until the coefficient of variation of C_{sp} values at 23°C was less than 5%. Figure 2-12 -Figure 2-21 show the plotted results of replicate evaluations for each material. For isothermal calorimetry, the temperature is held constant at 23°C; therefore, the specific heat capacity of each material is reported in Table 2-5 at 23°C although it was measured from 5.0 – 60.0°C. Additionally, the coefficient of variability is presented along with the data. This metric allows for the evaluation of the variability of the data values regardless of the units; it is computed by taking the standard deviation of the measurements (in this case, at 23°C) and dividing by the mean values. This value is then presented as a percentage where 0% represents data that does not vary at all, and 100% represents data that has no correlation. The coefficient of variation was calculated by dividing the standard deviation of the population of measurements, divided by the mean value, then multiplying by 100%.

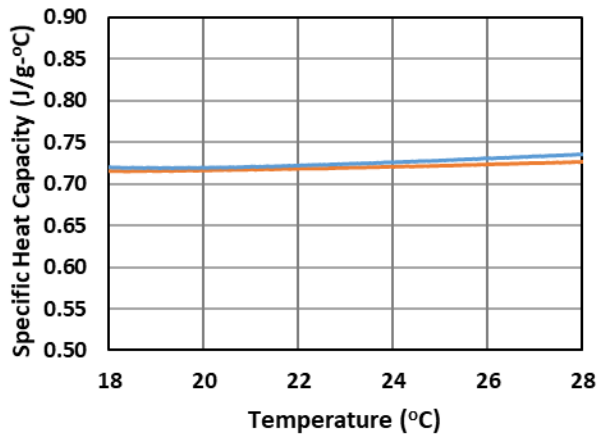


Figure 2-12: Specific heat capacity graph for Type I/II portland cement.

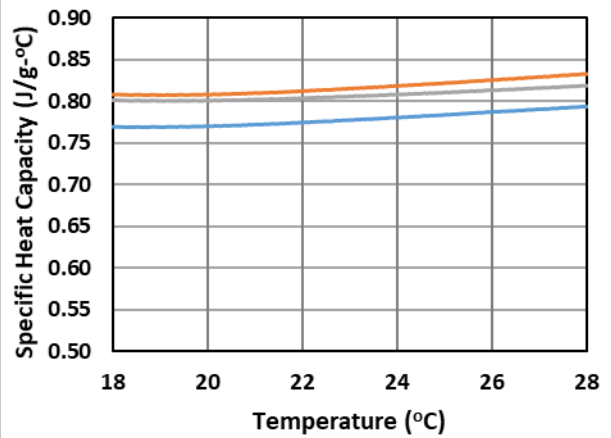


Figure 2-13: Specific heat capacity graph for high alkali Type I/II portland cement.

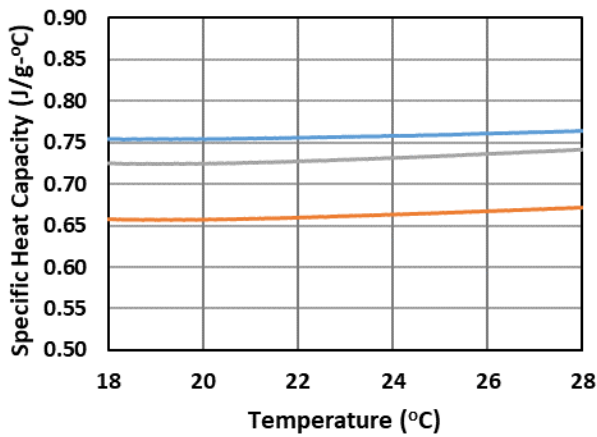


Figure 2-14: Specific heat capacity graph for Type IL limestone cement.

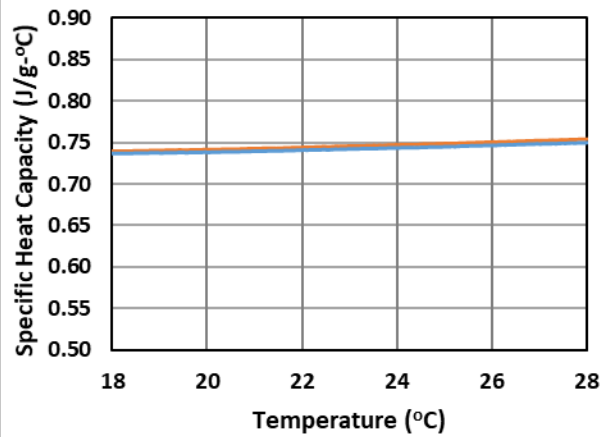


Figure 2-15: Specific heat capacity graph for Class C fly ash.

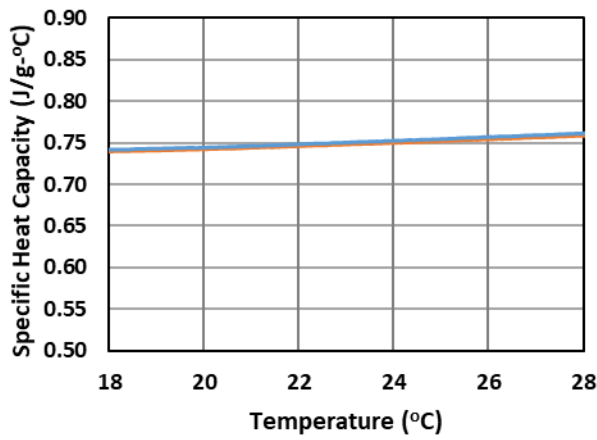


Figure 2-16: Specific heat capacity graph for Class F fly ash.

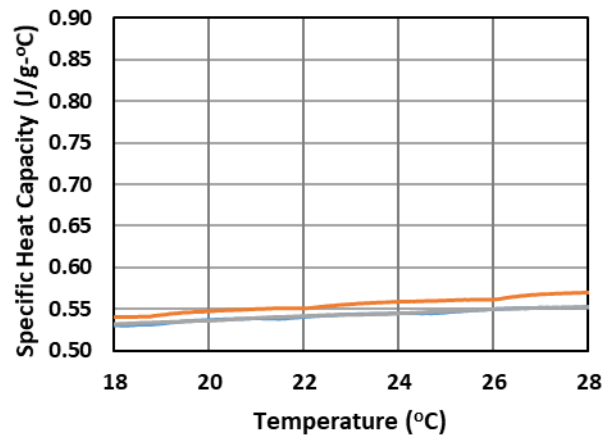


Figure 2-17: Specific heat capacity graph for silica fume.

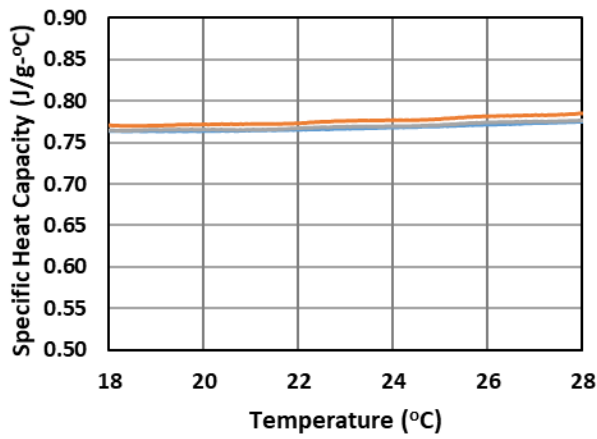


Figure 2-18: Specific heat capacity graph for volcanic rock.

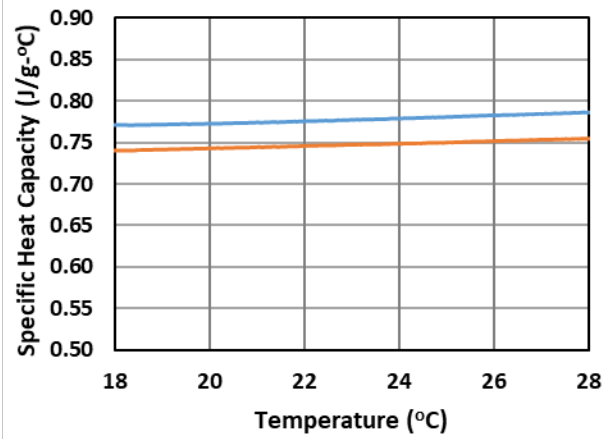


Figure 2-19: Specific heat capacity graph for ground glass.

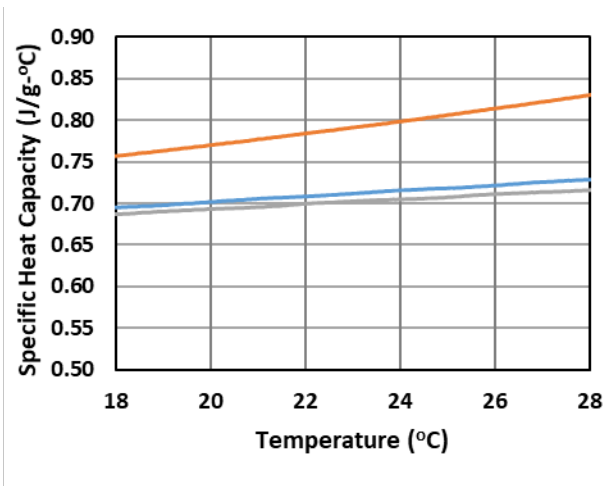


Figure 2-20: Specific heat capacity graph for SCBA-A.

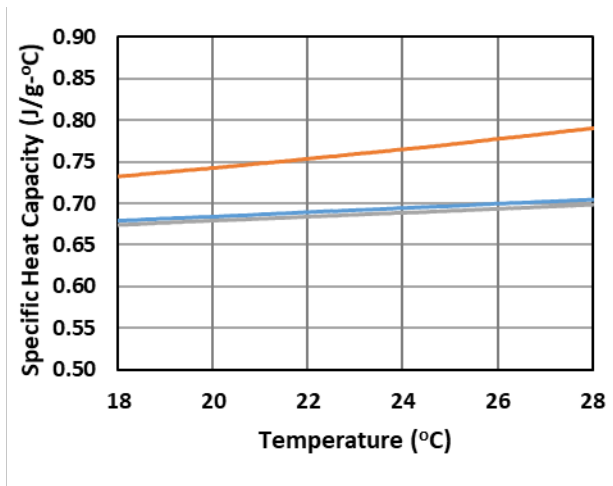


Figure 2-21: Specific heat capacity graph for SCBA-B.

Table 2-5. Specific heat capacity of materials used for this evaluation.

Material	Specific Heat Capacity at 23°C (J/g – °C)	Coefficient of Variation
Type I/II Portland Cement	0.722	0.42%
High-Alkali Type I/II Portland Cement	0.800	1.94%
Type IL Portland Cement	0.716	4.87%
Class C Fly Ash	0.745	0.33%
Class F Fly Ash	0.749	0.08%
Silica Fume	0.771	0.46%
Ground Volcanic Rock	0.548	0.70%
Ground Glass	0.756	1.92%
Sugarcane Bagasse Ash – Facility A	0.735	4.85%
Sugarcane Bagasse Ash – Facility B	0.713	4.04%

The results of this evaluation are consistent with other published values and those previously obtained for other FDOT research [8]. Additionally, the variability of results obtained gives an indication of relative variability of the material itself. The most variable materials tested were the two sugarcane bagasse ashes as well as the limestone cement; however, the sample sizes for this method are very small (approximately 0.005 grams) and therefore any heterogeneity will result in large amounts of variability.

2.5 APPARENT SPECIFIC GRAVITY

The apparent specific gravities of the various materials were evaluated by means of a helium pycnometer at the Florida Department of Transportation's State Materials Office. In this method, a known mass of material is placed into a container of known volume, then the container is filled with helium while the volume and pressure of helium is metered together. As the pressure increases due to the known amount of volume input into the system, using Boyle's law (the ideal gas law), and the volume of helium represents the volume in the container that is not taken up by the sample. Subtracting this volume from the known volume of the container, gives the volume of the sample, which is then used along with the mass of the sample to calculate the apparent specific gravity of the sample. This method will not determine the actual specific gravity, as any voids that are unavailable to the helium will not be accounted for.

This value allows for the appropriate proportioning of mixture components based on the volumetric method. Values represent the ratio of the mass of a unit volume of material, excluding the volume of all open porosity, to the mass of a unit volume of a reference material, which is typically water; thus, for example, a material with a specific gravity of 2.0 is twice as dense as water. A summary of the measured specific gravity for each material is presented in Table 2-6. Similar to the specific heat capacity, the apparent specific gravity values are in line with previous work [8].

Table 2-6. Summary of measured specific gravities of materials.

Material	Apparent Specific Gravity	Coefficient of Variability
Type I/II OPC	3.22	0.18%
Type IL OPC	3.14	0.03%
HA Type I/II OPC	3.11	1.74%
Class F Fly Ash	2.38	0.31%
Class C Fly Ash	2.69	0.31%
Silica Fume	2.26	0.06%
SCBA A	2.50	0.45%
SCBA B	2.37	0.25%
Ground Glass	2.64	0.14%
Volcanic Rock	2.82	0.03%

2.6 CONCRETE AGGREGATE PROPERTIES

For proper concrete mixture design, several aggregate properties needed to be obtained, namely the specific gravity, absorption, and sieve analysis. The specific gravity and absorption of coarse aggregate were determined using ASTM C127. The specific gravity and absorption of

fine aggregate were determined following ASTM C128. Particle gradation of both aggregate types was determined via sieve analysis as per ASTM C136. For this evaluation, #57 Florida limerock was used as coarse aggregate with Florida quartz sand used for fine aggregate; alkali-silica reactivity testing utilized reactive sand from Texas (Jobe mine). The aggregate properties for each material are presented in Table 2-7.

Table 2-7. Measured aggregate properties

	Jobe Sand		Florida Sand		Limestone	
	Sieve Size	% Retained	Sieve Size	% Retained	Sieve Size	% Retained
Sieve Analysis	3/8"	2.4	3/8"	0.0	1 1/2"	0.0
	4	5.2	4	0.0	1"	3.0
	8	5.8	8	4.3	3/4"	21.7
	16	7.2	16	9.6	1/2"	33.3
	30	23.3	30	44.9	3/8"	14.6
	50	40.3	50	30.3	4	18.2
	100	13.6	100	7.9	8	2.6
	200	2.0	200	2.8	10	0.7
	Pan	0.2	Pan	0.2	Pan	5.8
Fineness Modulus	2.67		2.63		-	
Specific Gravity			2.63		2.42	
Absorption			0.15%		5.69%	

2.7 ISOTHERMAL CONDUCTION CALORIMETRY

Isothermal conduction calorimetry measures the heat of hydration of cementitious reactions. The isothermal calorimetry testing was performed with an internal mixing procedure in which the cementitious paste is mixed within the calorimeter, allowing for the measure of the heat of hydration from the beginning of the mixing process. In this method, the mass of a glass vial is recorded, and the mass of cementitious material required (along with the mass of the water) to match the thermal mass of a non-reacting companion cell is metered into the glass vial with a precision of 0.0002g. The water is then weighed within the syringes that are equipped on the internal mixing ampoule (Figure 2-22), the mass of the water in the syringe is adjusted until the desired w/c is correct. The sample is then loaded into the isothermal calorimeter to reach thermal equilibrium (generally at least 18 hours) before the water is introduced to the dry powders.

Once equilibrium is reached, the calorimeter data recording is started, and a baseline measurement is recorded to subtract the signal from to determine only the heat generated by the

hydrating sample. Once the baseline measurement is recorded, the experiment begins and water is dispersed over the course of 30 seconds into the dry material, the material is then manually mixed for 90 seconds at a rate of approximately 120 rpm. The specimen is then allowed to hydrate over the course of 7 days.

The heat produced by the reaction in the paste is measured over 7 days. The heat evolution is measured and reported in mW/g and the total heat output is calculated and reported as J/g. The heat evolution indicates what the instantaneous heat at a certain point in time is, while the total heat output is the total cumulative heat produced by the reaction.



Figure 2-22: Internal mixing ampoule.

Regardless of the SCM replacement used, there was a general decrease in cumulative heat output as replacement increased when using either the Type I/II cement or Type IL cement. This is anticipated as the short duration of the 7-day testing length and relatively small sample size (approximately 6 g of paste) does not allow for adequate measurement of pozzolanic reactivity.

Portland Cement

The presence of limestone in portland cement results in an amplification and acceleration of the main hydration peak of the neat cement pastes when limestone additions as shown in Figure 2-23; this behavior has been reported before Bentz et al. [126]. However, the total heat generation of the limestone cement was lower than the ordinary portland cement at 7 days as seen in Figure 2-24. The mechanism behind the acceleration and amplification of instantaneous heat of the hydration curve is presumed to be that the limestone provides a beneficial surface for C3S formation to occur. Bentz et al. reported that limestone powder having median particle sizes of 1.6 microns or 16 microns both showed characteristic acceleration and amplification (although to different degrees) compared to the control cement when replaced at 10% [126].

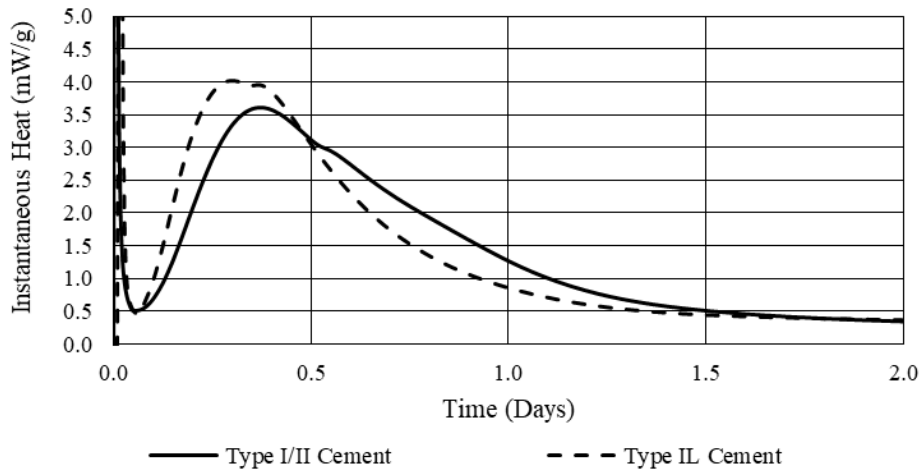


Figure 2-23. Instantaneous heat curve of Type I/II and Type IL cement pastes.

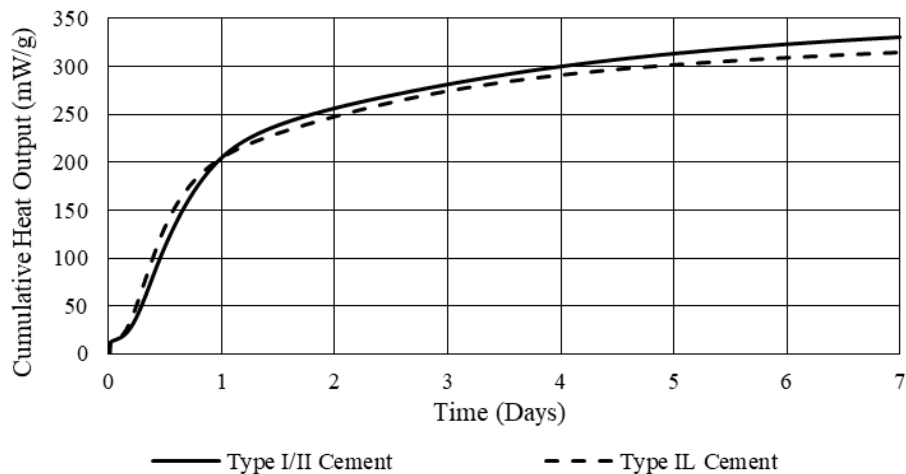


Figure 2-24. Cumulative heat curve of Type I/II and Type IL cement pastes.

2.7.1 Class F Fly Ash

The isothermal heat rises of mixes incorporating 20% fly ash replacement of either Type I/II portland cement (Figure 2-25) or Type IL limestone cement (Figure 2-26) show typical reductions in reactivity at early ages due to the incorporation of Class F fly ash [127,128]. The inclusions at early ages do not have sufficient time in the highly alkaline systems to dissolve the silica to take part in the hydration reactions and therefore appear as nearly inert materials where the reduction in heat evolution is closely tied to replacement percentage [127,128]. The shape, relative intensity to the maximum peak, and time to hydration of each peak within the curves do not appear to be materially affected by the inclusion of Class F fly ash at early ages.

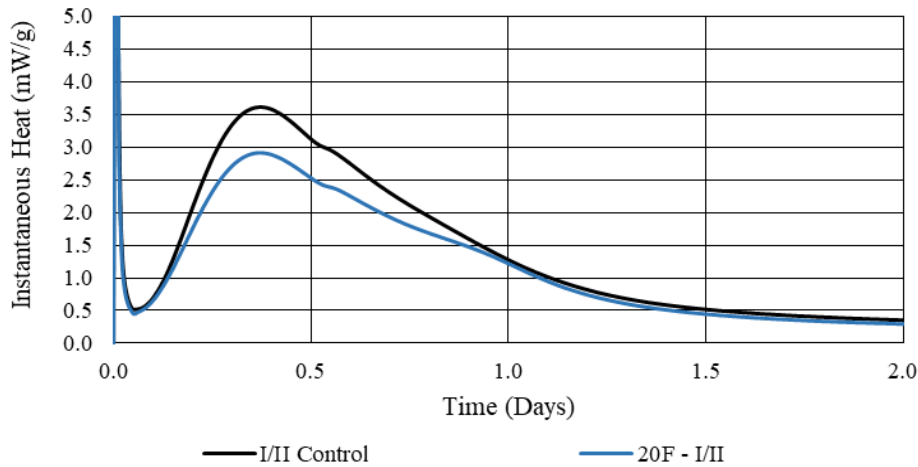


Figure 2-25. Instantaneous heat curve of cement paste with a 20% replacement of Class F Fly ash compared to a Type I/II cement paste.

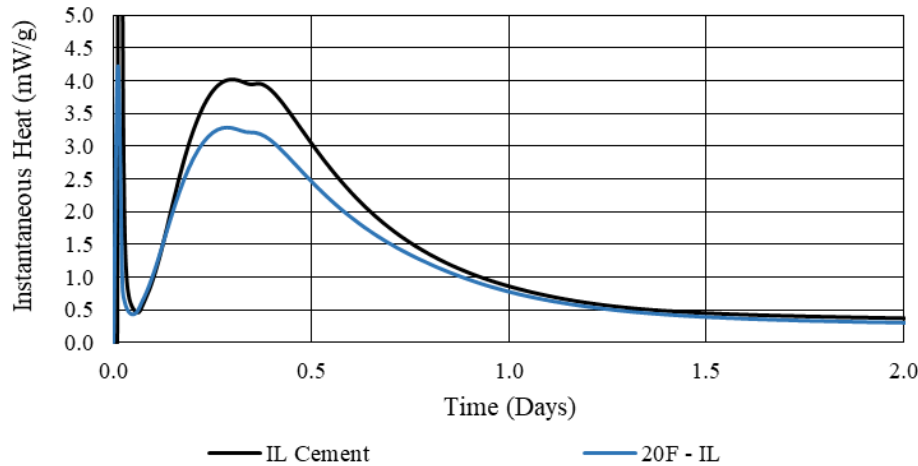


Figure 2-26. Instantaneous heat curve of cement paste with a 20% replacement of Class F Fly ash compared to a Type IL cement paste.

The cumulative heat generation curves developed from cement amended with fly ash where Figure 2-27 and Figure 2-28, show little deviation from the control curves beyond a 20% reduction at any point indicating that the heat evolution curves follow the same general shape (and therefore, hydration profile).

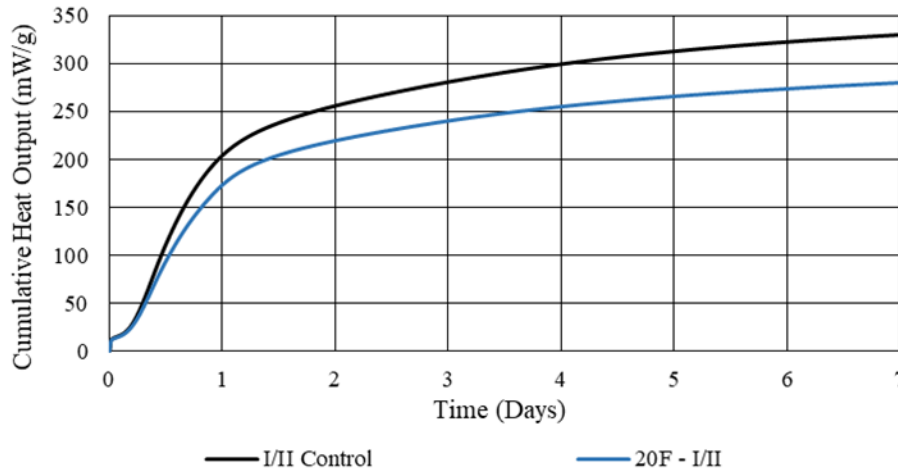


Figure 2-27. Cumulative heat curve of cement paste with a 20% replacement of Class F Fly ash compared to a Type I/II cement paste.

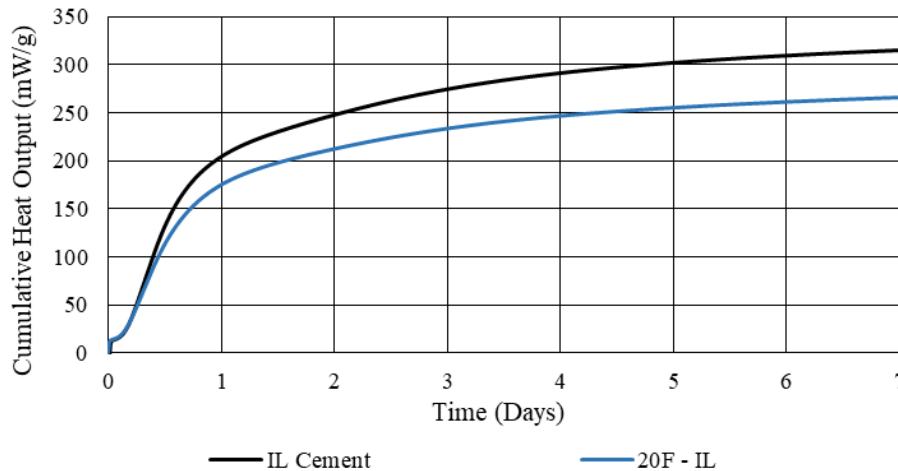


Figure 2-28. Cumulative heat curve of cement paste with a 20% replacement of Class F Fly ash compared to a Type IL cement paste

2.7.2 Class C Fly Ash

As can be seen in Figure 2-29, the addition of Class C fly ash into a Type I/II portland cement system results in not only the typical primary (C_3S) and secondary (C_3A) hydration peaks, but also a distinct third peak that was also reported in a 50% Class C fly ash replacement

(with 2% gypsum addition) by Bentz et al [129]. Additionally, the lower amount of available reactive silica and lower amount of sulfate in the Class C fly ash forces less C_3S hydration and less aluminate retardation as sulfate depletion occurs [130]; this results in the aluminate reaction becoming more pronounced as the replacement level increases as can be seen in Figure 2-29. With the Type IL cement, the sulfate content is lower than the Type I/II cement allowing for less aluminate retardation resulting in an aluminate reaction that supersedes the silicate reaction in intensity (Figure 2-30).

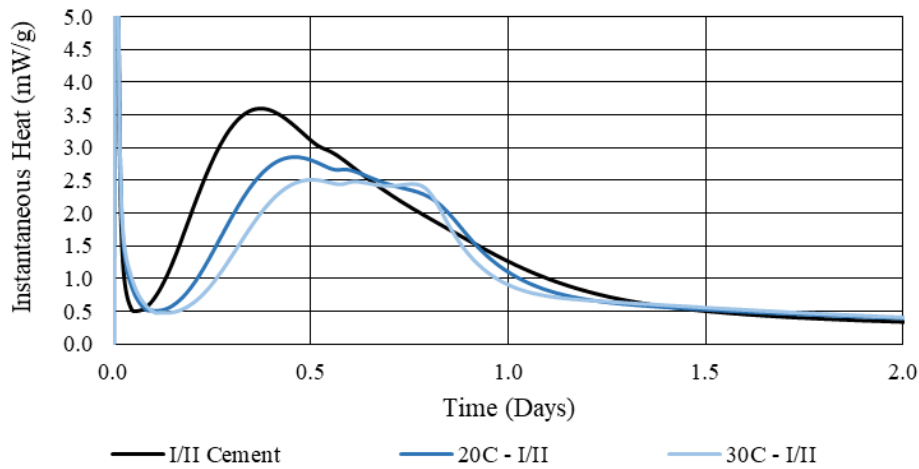


Figure 2-29. Instantaneous heat curve of cement paste with 20 and 30% replacements of Class C Fly ash compared to a Type I/II cement paste.

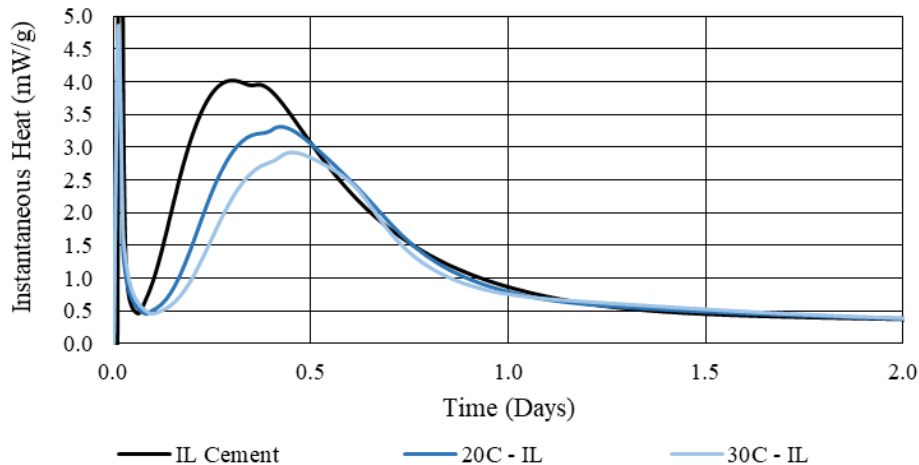


Figure 2-30. Instantaneous heat curve of cement paste with 20 and 30% replacements of Class C Fly ash compared to a Type IL cement paste.

The cumulative heat curves shown in Figure 2-31 and Figure 2-32 exhibit higher relative heat evolution over time; for instance, at 2 days, the difference between the Type I/II cement and 20% Class C fly ash replacement is approximately 40 mW/g, whereas at 7 days, the difference between the two is approximately 20 mW/g, indicating that the Class C fly ash reacts slower but does so over a longer time period [127]. This characteristic is shown not only in the 30% replacement of the Type I/II cement, but also for both replacements in the Type IL cement system as well and is indicative of longer-term reactions.

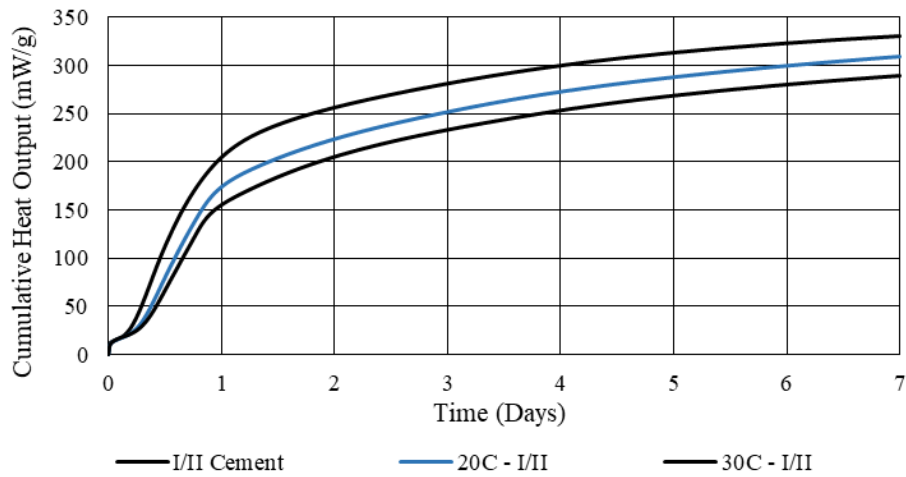


Figure 2-31. Cumulative heat curve of cement paste with 20 and 30% replacements of Class C Fly ash compared to a Type I/II cement paste.

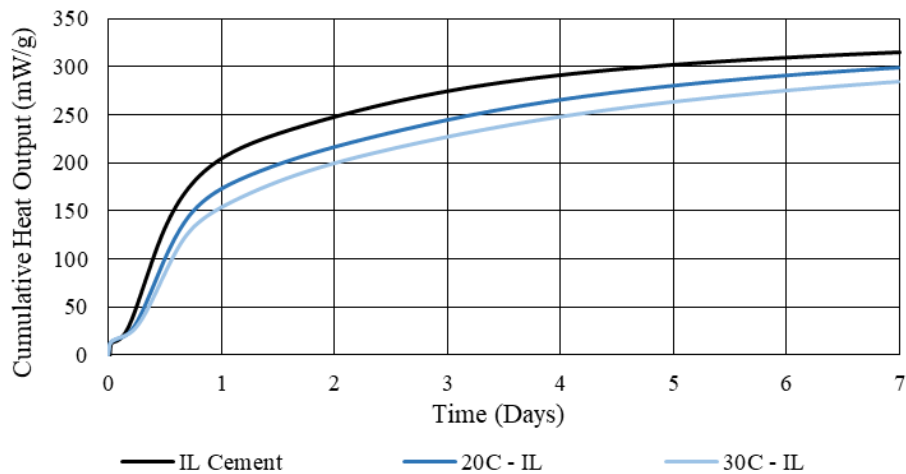


Figure 2-32. Cumulative heat curve of cement paste with 20 and 30% replacements of Class C Fly ash compared to a Type IL cement paste.

2.7.3 Silica Fume

The instantaneous heat evolution hydration curves for 4% silica fume are presented in Figure 2-33 and Figure 2-34; silica fume is a highly reactive material with large amounts of amorphous silica. However, the material is densified prior to packaging, thus, there is insufficient shearing action to break up agglomerations and achieve proper dispersion of silica fume in isothermal calorimetry using internal mixing. Therefore, the reactivity of the silica fume is reduced for these results. Ultimately, the silica fume reduced the instantaneous heat and cumulative heat, which would be uncharacteristic of a silica fume mixture that is mechanically mixed with high shearing action.

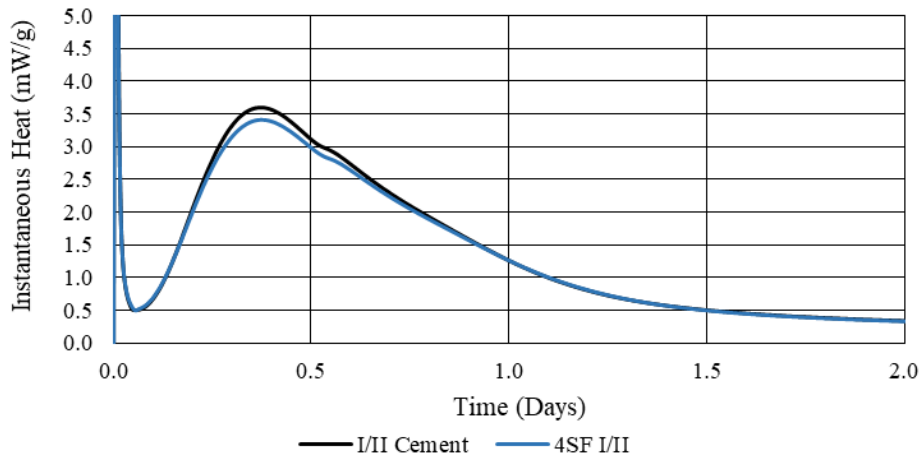


Figure 2-33. Instantaneous heat curve of cement paste with a 4% replacement of Silica Fume compared to a Type I/II cement paste.

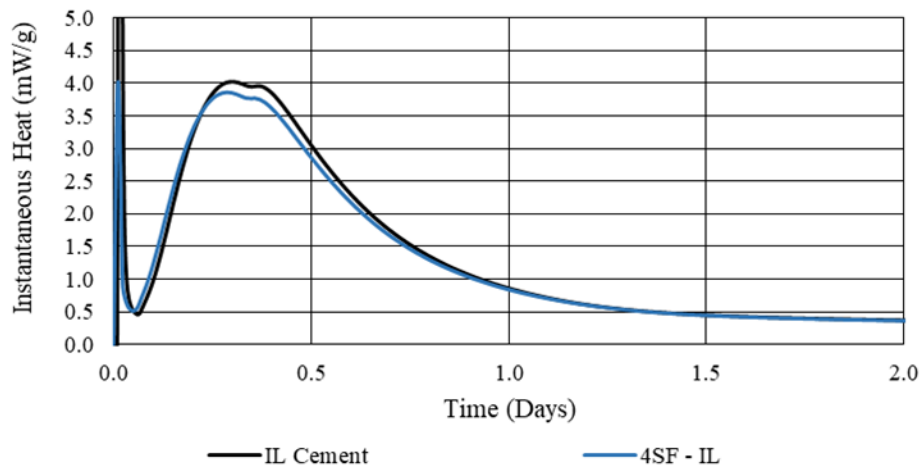


Figure 2-34. Instantaneous heat curve of cement paste with a 4% replacement of Silica Fume compared to a Type IL cement paste.

The cumulative heat generation curves shown in Figure 2-35 and Figure 2-36 show that the silica fume mixes provided more heat than would be expected for an inert material, but did not provide an excess of heat over the control cements in either Type I/II or Type IL systems [131]. In the Type IL cement system, the total heat output of the 4% silica fume mix is slightly higher (as a percentage of the control) than in the Type I/II cement system; however, this is well within the margin of error of the method and nothing definitive can be said about this.

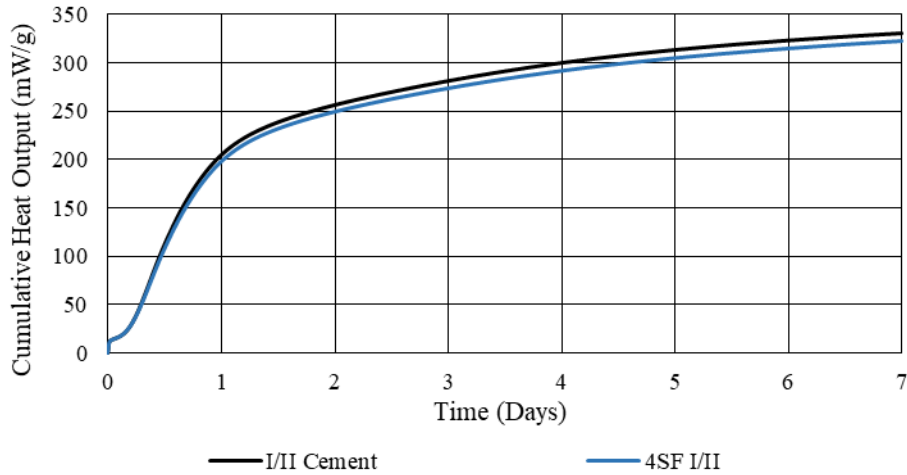


Figure 2-35. Cumulative heat curve of cement paste with a 4% replacement of Silica Fume compared to a Type I/II cement paste.

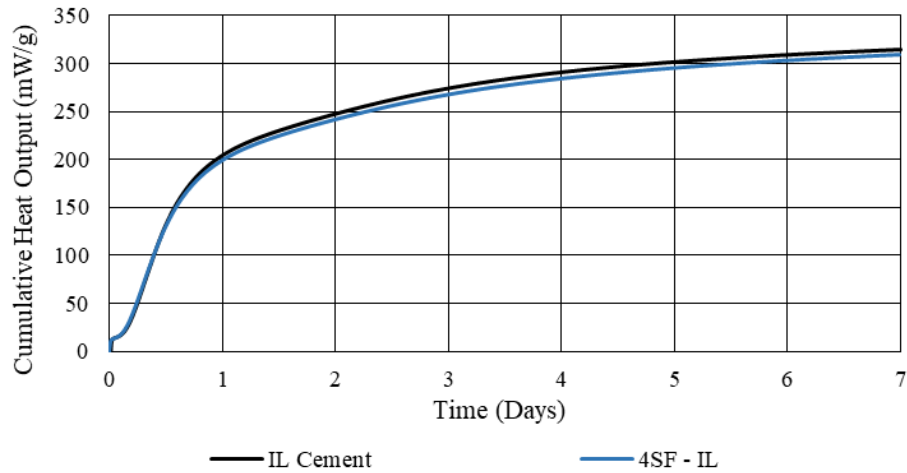


Figure 2-36. Cumulative heat curve of cement paste with a 4% replacement of Silica Fume compared to a Type IL cement paste.

2.7.4 Sugarcane Bagasse Ash

Similar to the Class F Fly ash, the SCBA-A in the Type I/II cement system, Figure 2-37, exhibited essentially no changes to the shape or timing of the hydration curve; only the intensities of the peaks were affected. This indicates that the SCBA-A is initially largely unreactive and behaves like Class F fly ash, which required at least 7 days of hydration for beneficial reactions to initiate. However, for the SCBA-B material, the main peak maximum intensities were slightly accelerated (shifted to earlier times) with increased additions and, similar to the SCBA-A results, the peak intensities decreased with increased additions along with slight retardations of the aluminate peak. The acceleration of the silicate peak is most likely due to the elevated levels of chlorides present in the SCBA-B (approximately 0.55%) whereas the aluminate peak delay is caused by the additional sulfate brought with the SCBA-B (approximately 4.2%). This delay in the aluminate peak can be seen in Figure 2-38, where the four curves converge at approximately 22 hours compared to at approximately 40+ hours for the Type I/II system with SCBA-A. The SCBA-A results are consistent with those found in FDOT BDV-31-977-06 [8].

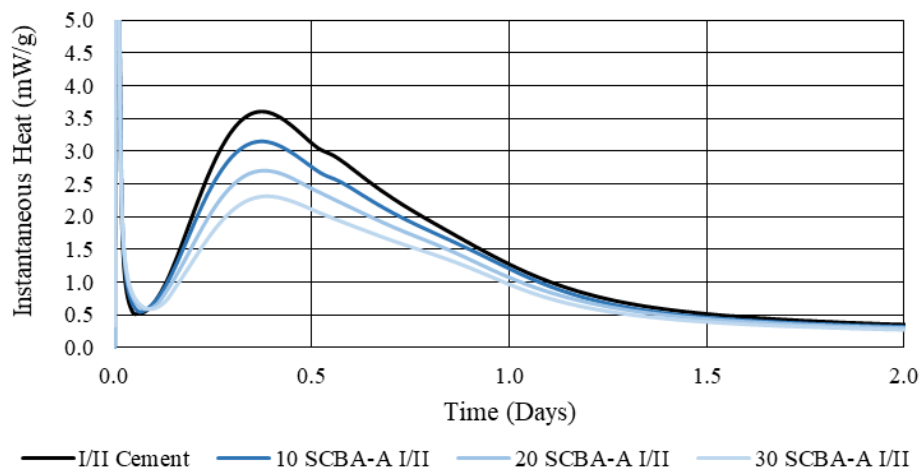


Figure 2-37. Instantaneous heat curve of cement paste with 10% – 30% replacements of SCBA-A compared to a Type I/II cement paste.

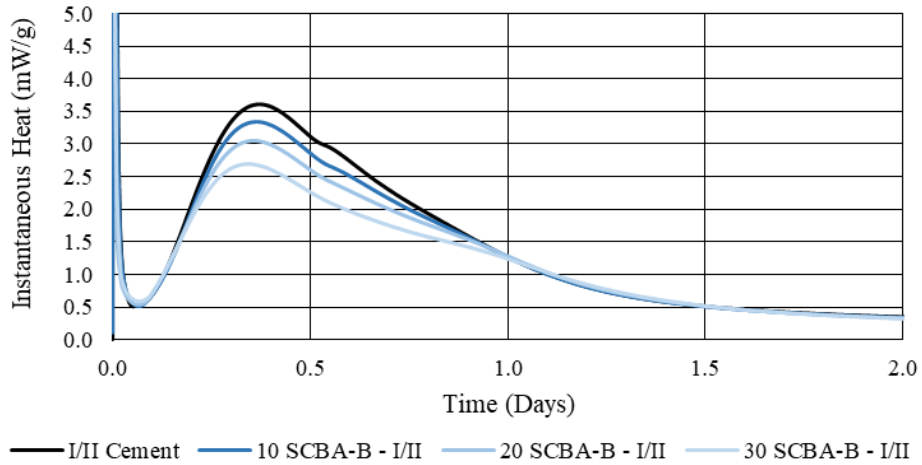


Figure 2-38. Instantaneous heat curve of cement paste with 10% – 30% replacements of SCBA-B compared to a Type I/II cement paste.

The performance of SCBA-A and SCBA-B in a Type IL system was consistent with that of the performance in the Type I/II system as can be seen in Figure 2-39 and Figure 2-40. The same acceleration of the silicate peak and delay of the aluminate peak can be seen with the additions of SCBA-B; but otherwise the differences in the performance due to increased additions were unremarkable.

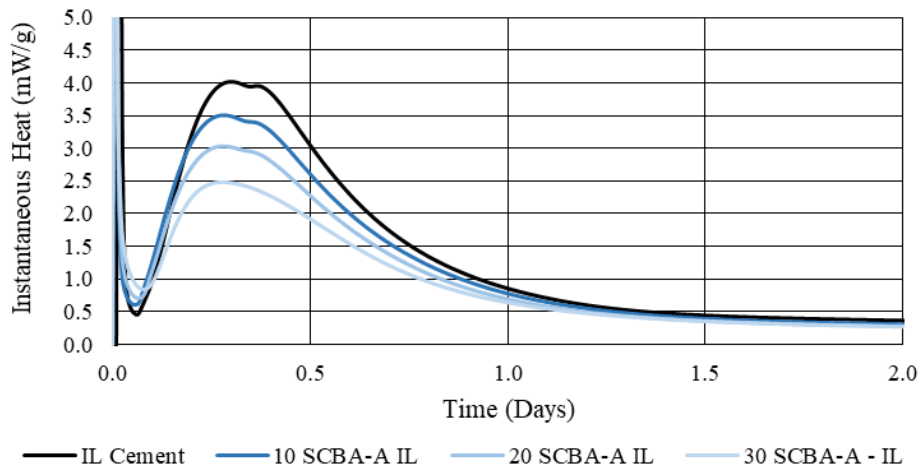


Figure 2-39. Instantaneous heat curve of cement paste with 10% – 30% replacements of SCBA-A compared to a Type IL cement paste.

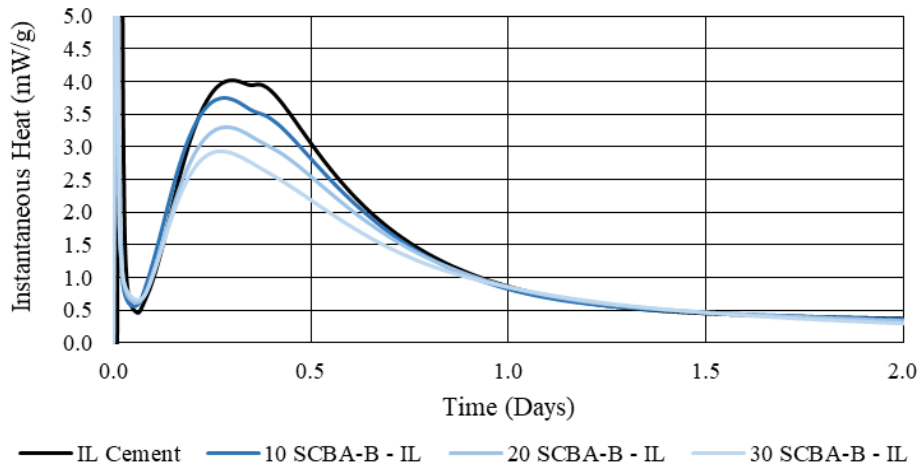


Figure 2-40. Instantaneous heat curve of cement paste with 10% – 30% replacements of SCBA-B compared to a Type IL cement paste.

The cumulative heat output of the isothermal calorimetry for the SCBA-A in the Type I/II cement system shows consistent reductions in total heat output as replacements increased from 10% to 30% (Figure 2-41). However, with SCBA-B (Figure 2-42), the 7-day heat values for the replacements were more “condensed” from 0 – 20% replacement than from 20% to 30% replacement, indicating that the chloride acceleration caused additional heat generation. However, there appeared to be no accelerating effect for the 30% addition.

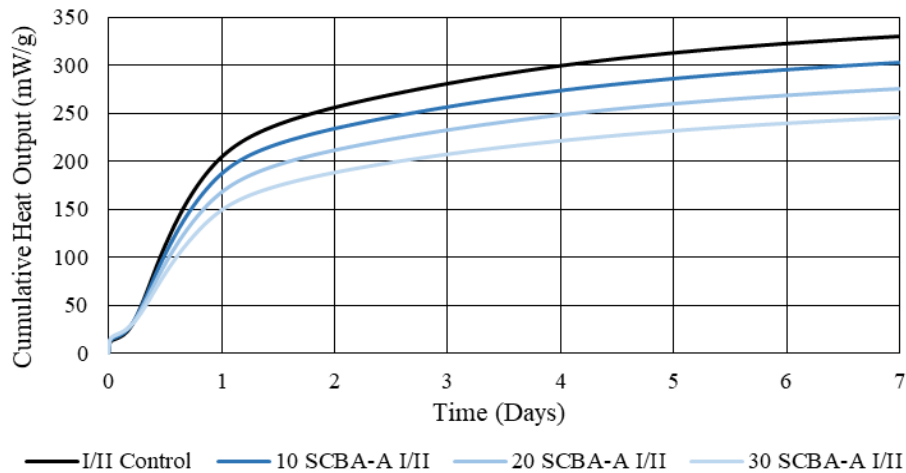


Figure 2-41. Cumulative heat curve of cement paste with 10% – 30% replacements of SCBA-A compared to a Type I/II cement paste.

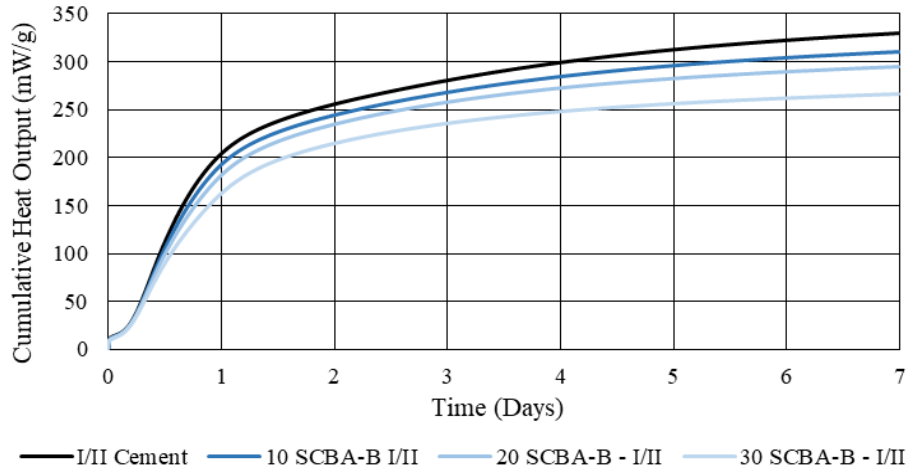


Figure 2-42. Cumulative heat curve of cement paste with 10% – 30% replacements of SCBA-B compared to a Type I/II cement paste.

SCBA-A additions to Type IL cement did not show much variability based on the instantaneous heat curves (Figure 2-39) and the cumulative heat curves (Figure 2-43). The curves are evenly spaced indicating consistent reactivity with differential additions. When utilizing Type IL cement, the acceleration caused by chlorides are less pronounced, and when looking at Figure 2-44, this is confirmed by the relatively even spacing of the curves with each replacement percentage.

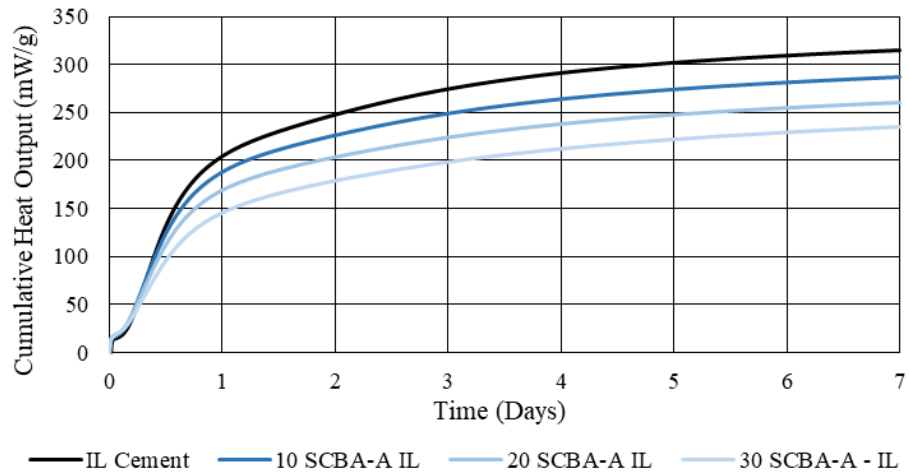


Figure 2-43. Cumulative heat curve of cement paste with 10% – 30% replacements of SCBA-A compared to a Type IL cement paste.

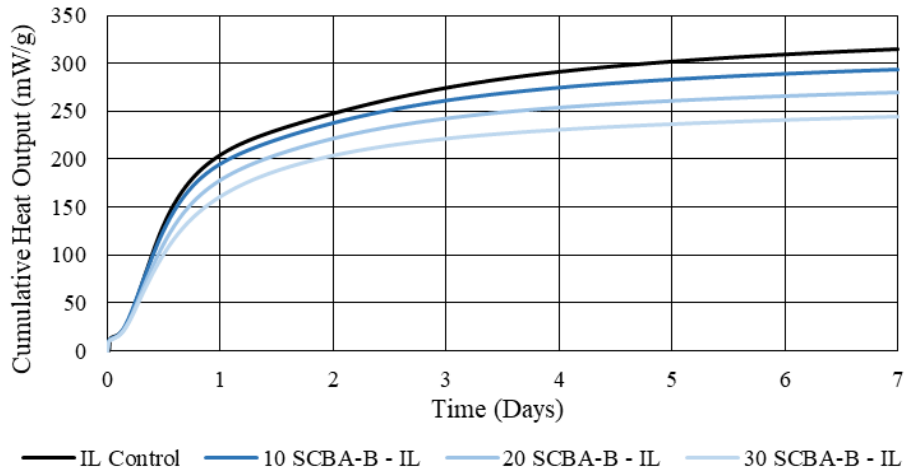


Figure 2-44. Cumulative heat curve of cement paste with 10% – 30% replacements of SCBA-B compared to a Type IL cement paste.

2.7.5 Ground Glass

There was a notable decrease in heat generation when ground glass replaced portland cement. Figure 2-45 shows that the curves for 20% and 30% are similar to both Class F fly ash and SCBA-A in terms of shape and peak location; however, at 40% GG replacement, the end of the aluminate curve (right before the hydration period) occurs at a later time and involves a lower instantaneous heat. The sulfate content of ground glass was low, a delay in aluminate peak was not expected nor observed. The replacement of portland cement with GG lowered the total sulfate content, which accelerated the aluminate reaction in the early stages of hydration [75]. The alkali content of the glass was approximately 13%; therefore the shift is most likely due to the alkali content driving sulfate (ettringite and monosulfate) reactions at the end of the aluminate hydration curve [132]. It is presumed that the alkalis do not immediately leach out of the glass upon contact with water (or the glass would have been leached of alkalis during use as containers or processing); therefore, the alkalis, if available for reaction, would only be present after some amount of contact time in the highly alkaline environment. This aluminate hydration discrepancy was not observed when the ground glass was incorporated into the Type II cementitious system as shown in Figure 2-46. This indicates that a sulfate balancing issue may arise with the usage of ground glass and precautions should be taken prior to use to avoid issues. Precautions include limiting replacement percentages or amending with additional sulfate to bolster the overall sulfate-to-aluminate ratio.

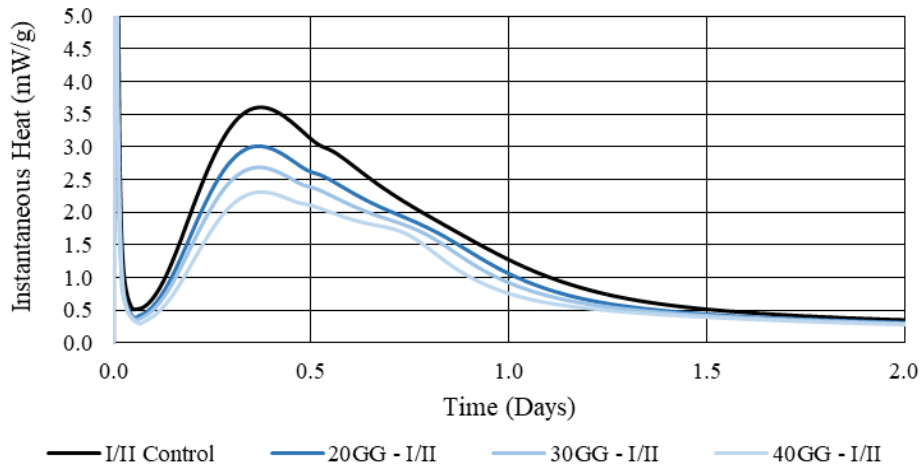


Figure 2-45. Instantaneous heat curve of cement paste with 20% – 40% replacements of GG compared to a Type I/II cement paste.

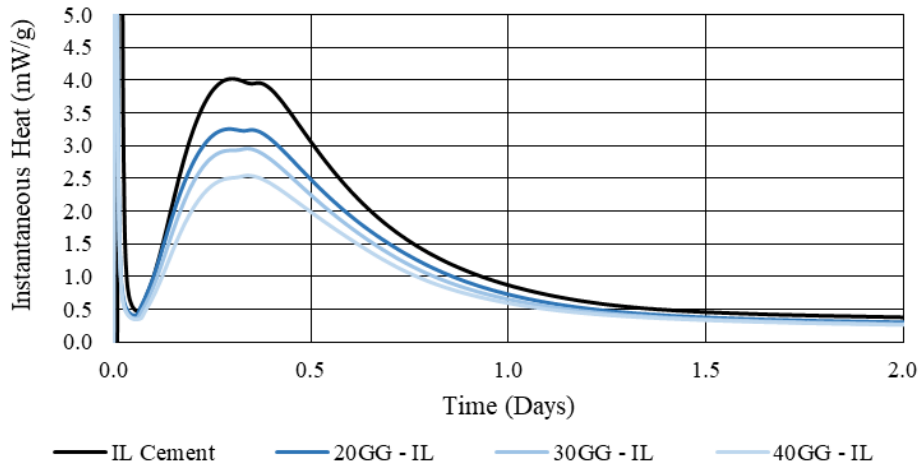


Figure 2-46. Instantaneous heat curve of cement paste with 20% – 40% replacements of GG compared to a Type IL cement paste.

As anticipated, the cumulative heat curves shown in Figure 2-47 and Figure 2-48 show relatively low reactivity with diminishing cumulative generation as the ground glass replacement increases. This is owed to the relative non-reactivity of the glass at early ages observed in this testing method. There was not a significant difference in the performance of the ground glass from one cementitious system to another with regards to isothermal heat generation over seven days.

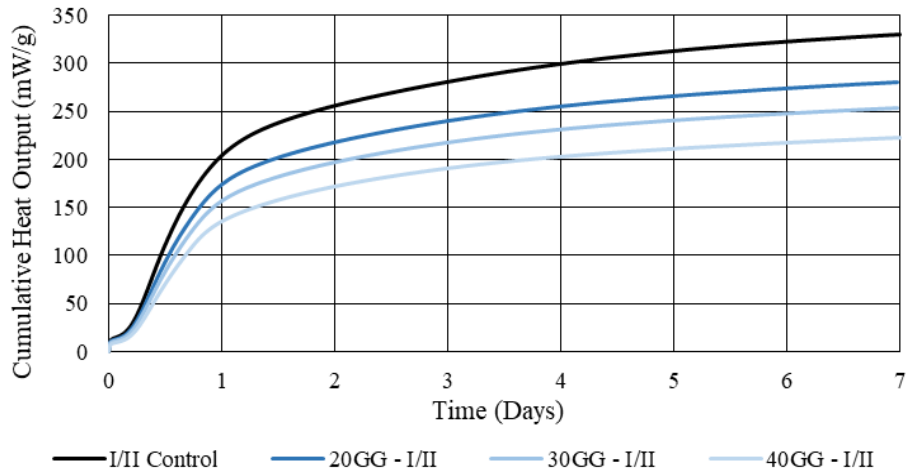


Figure 2-47. Cumulative heat curve of cement paste with 20% – 40% replacements of GG compared to a Type I/II cement paste.

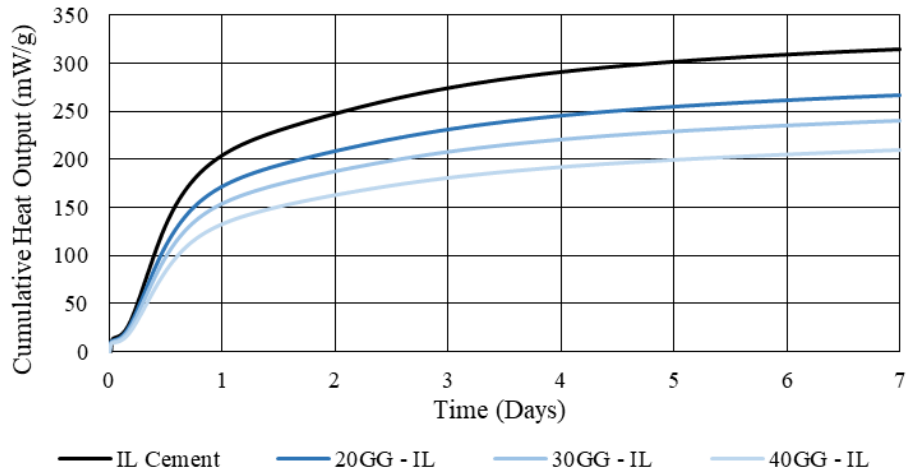


Figure 2-48. Cumulative heat curve of cement paste with 20% – 40% replacements of GG compared to a Type IL cement paste.

2.7.6 Volcanic Rock

The volcanic rock has a similar particle size distribution to the ground glass as well as a similar chemical composition. However, the volcanic rock has considerably lower alkali content but much higher iron and aluminum content. If the aluminum content is available for reaction, it is expected to cause a shift in the aluminate hydration peak due to an imbalance in the sulfate content. However, as can be observed in Figure 2-49 and Figure 2-50, regardless of cementitious system, the presence of 20% ground volcanic rock showed virtually no effect beyond dilution compared to the control. This would indicate that the aluminum content of the volcanic rock is not able to contribute to hydration. The general non-reactivity of this material is further

supported by the relatively small amount of amorphous material (approximately 10%) determined during x-ray diffraction. In general, when a material has more crystalline content, the dissolution of that material takes more chemical, thermal, or physical energy and therefore amorphous content is preferred for reactivity. As the volcanic rock amounts to over 90% crystalline material, it would be generally expected to have a low degree of reactivity unless the crystalline phases were particularly susceptible to dissolution in highly alkaline environments [133], which is not the case with ground volcanic rock.

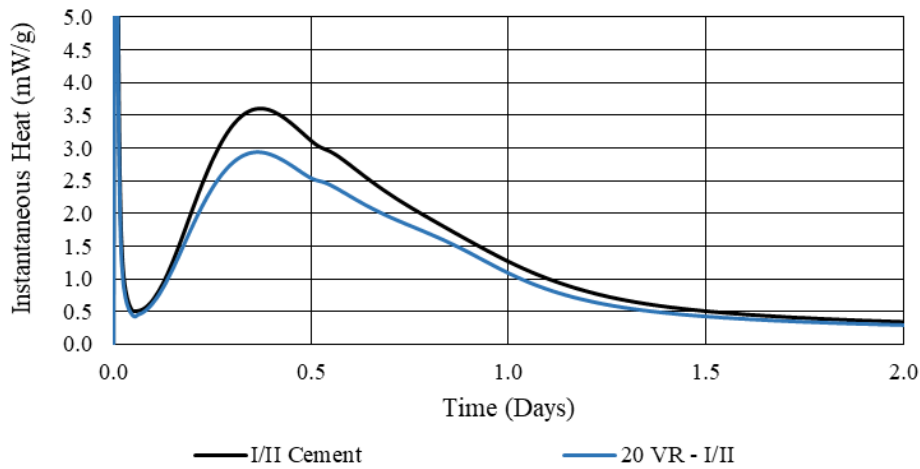


Figure 2-49. Instantaneous heat curve of cement paste with a 20% replacement of VR compared to a Type I/II cement paste.

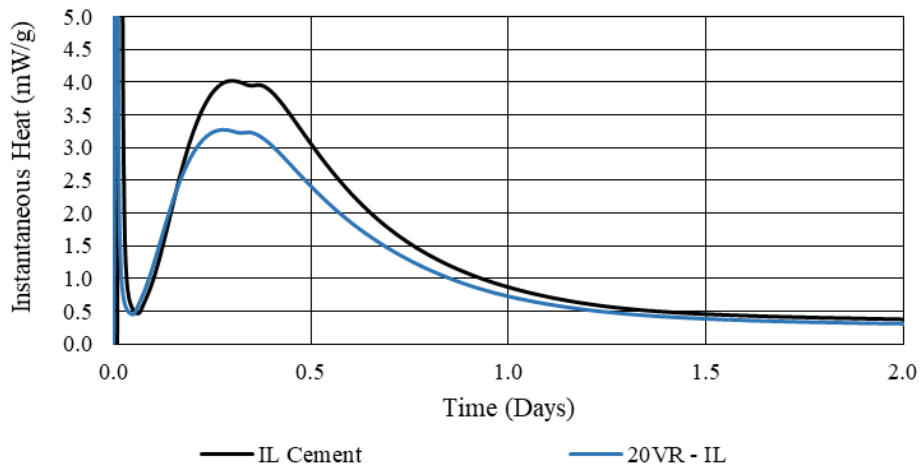


Figure 2-50. Instantaneous heat curve of cement paste with a 20% replacement of VR compared to a Type IL cement paste.

Similarly, the cumulative heat curves shown in Figure 2-51 and Figure 2-52 present data and comparison to Paris and Ferraro 2018, indicates the volcanic rock acts as little more than an inert filler, at least for the first seven days during hydration, as far as exothermic reactions are concerned (Reference Paris and Ferraro 2018).

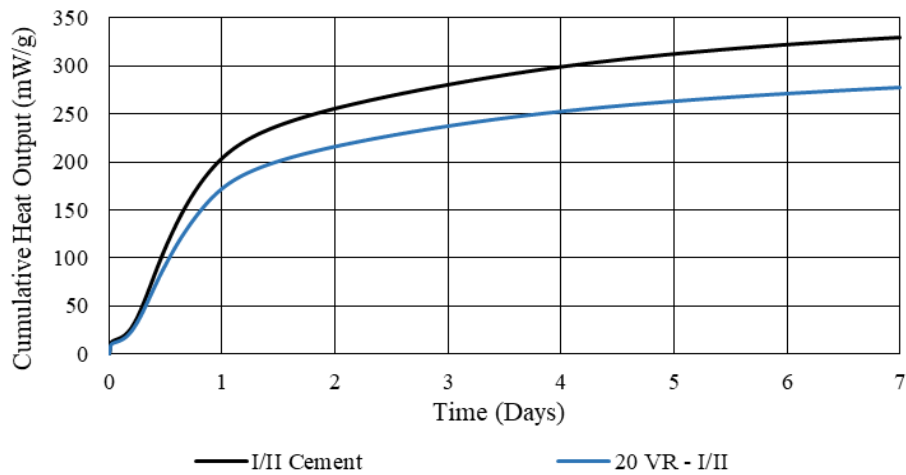


Figure 2-51. Cumulative heat curve of cement paste with a 20% replacement of VR compared to a Type I/II cement paste.

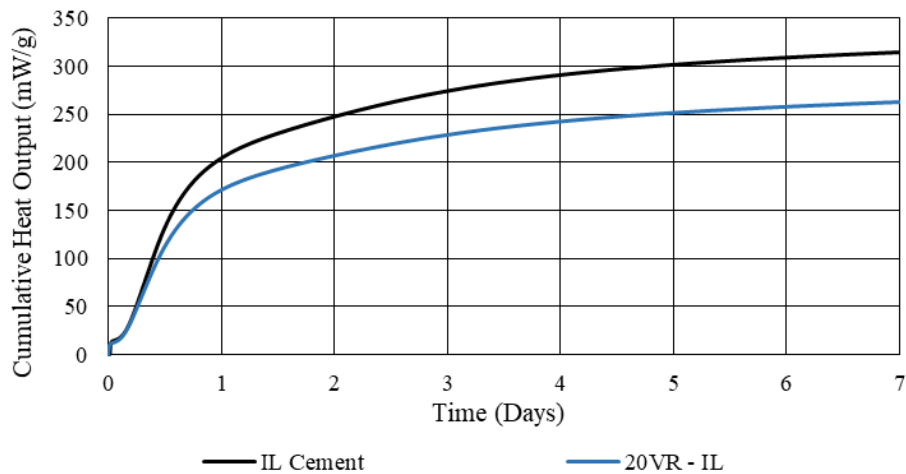


Figure 2-52. Cumulative heat curve of cement paste with a 20% replacement of VR compared to a Type IL cement paste.

A summary table of the peak instantaneous heat (peak power) and 7-day cumulative heat production for each mixture along with the values normalized to the Type I/II control cement are

presented in Table 2-8. A similar summary table for the Type II cementitious system mixtures is presented in Table 2-9.

Table 2-8: Summary table of isothermal data for Type I/II cement with SCM replacements.

Type I/II Cement				
Mix	Peak Instantaneous Heat (mW/g)	7-Day Heat (mW/g)	Nominalized Instantaneous Heat	Nominalized 7-Day Cumulative Heat
OPC - Type I/II	3.62	332	100%	100%
Binary Mixes				
10SCBA-A	3.17	302	88%	91%
20SCBA-A	2.67	272	74%	82%
30SCBA-A	2.30	246	64%	74%
10SCBA-B	3.36	312	93%	94%
20SCBA-B	3.15	293	87%	88%
30SCBA-B	2.69	266	74%	80%
20GG	3.00	281	83%	85%
30GG	2.67	252	74%	76%
40GG	2.31	223	64%	67%
20VR	2.93	276	81%	83%
20C	2.87	310	79%	93%
30C	2.52	290	70%	87%
20F	2.71	284	75%	86%
4SF	3.43	324	95%	98%
Ternary Mixes				
30C+5SCBA-A	2.35	271	65%	82%
30C+10SCBA-A	2.26	256	62%	77%
30C+5SCBA-B	2.47	283	68%	85%
30C+10SCBA-B	2.40	276	66%	83%
20C+5GG	2.72	295	75%	89%
20C+10GG	2.58	280	71%	84%
30C+10VR	2.32	254	64%	77%
30C+5F	2.41	273	67%	82%
30C+10F	2.36	254	65%	77%
30C+4SF	2.34	274	65%	83%

Table 2-9: Summary table of isothermal data for Type IL cement with SCM replacements

Type IL Cement				
Mix	Peak Instantaneous Heat (mW/g)	7-Day Heat (mW/g)	Nominalized Instantaneous Heat	Nominalized 7-Day Cumulative Heat
OPC - Type IL	3.98	312	100%	100%
Binary Mixes				
10SCBA-A	3.52	287	88%	92%
20SCBA-A	3.03	260	76%	83%
30SCBA-A	2.52	236	63%	76%
10SCBA-B	2.90	243	73%	78%
20SCBA-B	3.73	295	94%	95%
30SCBA-B	3.32	272	83%	87%
20GG	3.29	267	83%	86%
30GG	2.92	239	73%	77%
40GG	2.57	212	65%	68%
20VR	3.28	265	82%	85%
20C	3.31	299	83%	96%
30C	2.93	284	74%	91%
20F	3.29	266	83%	85%
4SF	3.86	310	97%	99%
Ternary Mixes				
30C+5SCBA-A	2.73	272	69%	87%
30C+10SCBA-A	2.49	255	63%	82%
30C+5SCBA-B	2.77	280	70%	90%
30C+10SCBA-B	2.56	273	64%	88%
20C+5GG	3.17	289	80%	93%
20C+10GG	3.02	276	76%	88%
30C+10VR	2.57	257	65%	82%
30C+5F	2.78	273	70%	88%
30C+10F	2.59	261	65%	84%
30C+4SF	2.76	276	69%	88%

2.7.7 Ground Sand – R³ Method

The reactivity of the ground sand was evaluated using isothermal conduction calorimetry and the R³ method, the results of which are shown in Figure 2-53. The R³ method involves the use of external mixing instead of internal mixing with a w/cm ratio of 0.5. The dry materials and water were weighed separately, with the water being added over 15-20 seconds. Once the water was added, the paste was mixed at a rate of 1600 rpm for 2 minutes [134]. The paste was then inserted into the isothermal vials, the vials were crimped, and added into the isothermal calorimeter.

The test was conducted at 40°C for 7 days and the cumulative heat produced was measured. The ground sand samples were compared to control samples as well as slag cement samples. Figure 2-54 shows a reactivity curve compared to the ground sand and slag cement total heat output. The reactivity of the ground sand is comparable to that of a non-reactive filler such as diamond [133]. Additionally, quartz has a hardness of 7 on the Mohs hardness scale, compared to clinker, which typically has a hardness of 5-6, depending on the alite and belite content [135–138]. Due to the lack of reactivity exhibited by ground sand and the increased energy requirements needed for particle size reduction [137,138], there was no further investigation into the material performance.

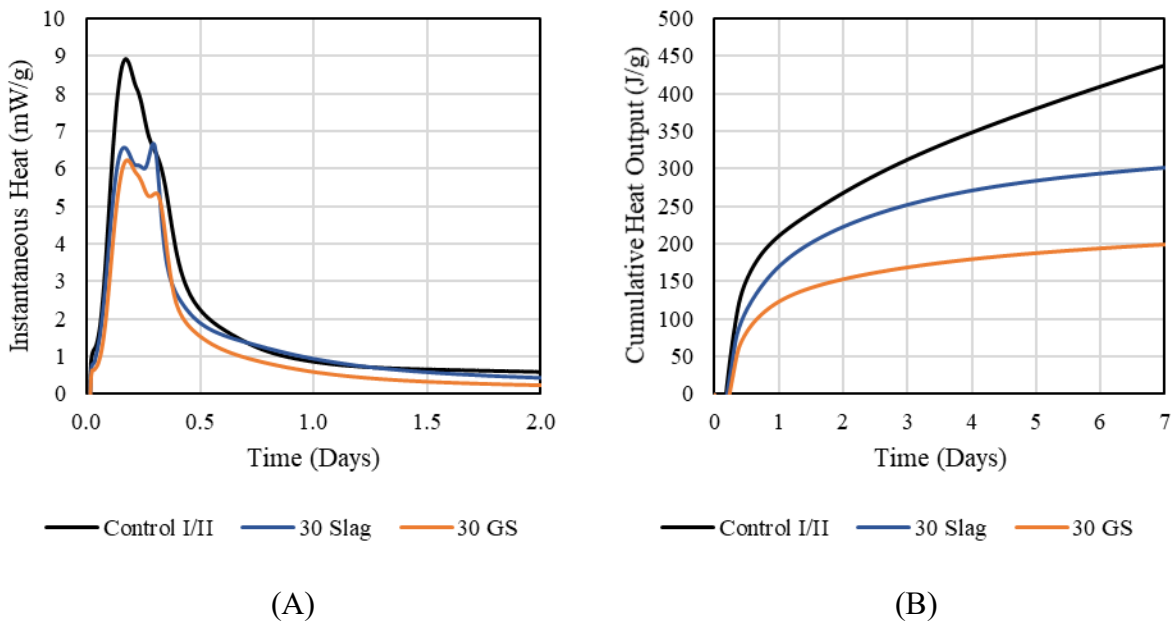


Figure 2-53: Instantaneous heat (A) and cumulative heat output (B) results from the R³ method comparing 30% slag and 30% GS replacements to control.

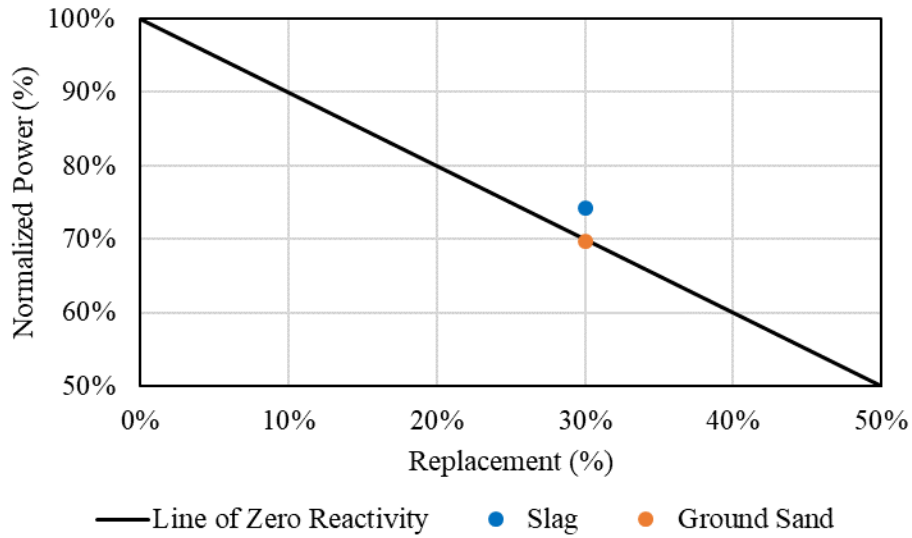


Figure 2-54: Reactivity curve comparing 30% slag cement and 30% ground sand mixtures.

2.8 CHLORIDE CONCENTRATION

Chloride concentration in the various materials has been measured utilizing the Florida Method of Test for Determining Low-Levels of Chloride in Concrete and Raw Materials [139]. The FDOT has guidelines limiting the amount of chlorides (lb/yd³) in a reinforced concrete system [21]. Knowing the chloride concentration of each material is useful to comply with these limits and avoid any materials that could result in the concrete potentially exceeding them. The chloride concentrations in Table 2-10 are presented as a percentage of total mass and in lb/yd³ of raw material. SCBA-B has an elevated level of chlorides present, which is greater than SCBA-A. The most likely reason for the differing levels is due to the impoundment of SCBA-A. During the impoundment period, SCBA-A is stored in water, which causes the alkalis and chlorides to leach and therefore significantly reduce the total chloride content; whereas SCBA-B is not impounded and has a higher chloride content. Additionally, the emissions controls vary by the processing facility which may result in initial chloride and alkali concentrations varying.

Table 2-10. Summary of acid soluble chlorides present in each material.

Material	Chloride Content (%)	Chloride Content (lb/yd ³ of concrete)
I/II Cement	0.010	0.54
IL Cement	0.007	0.37
F Fly Ash	0.009	0.36
C Fly ash	0.003	0.14
Silica Fume	0.016	0.60
SCBA-A	0.009	0.38
SCBA-B	0.550	21.96
Ground glass	0.005	0.22
Volcanic Rock	0.122	5.80

Using the specifications given by the FDOT and summarized in Figure 2-55 and the values in Table 2-10, if a mix were to include 752 lb/yd³ of total cementitious content, the maximum allowable replacement of SCBA-B would be 8% replacement with Type I/II portland cement, and 8.5% with Type IL cement with a total chloride content of 0.40 lb/yd³. If the total allowable chloride content was increased to 0.70 lb/yd³ for non-reinforced concrete, the replacements can be increased to 15.25% and 15.75% for Type I/II and Type IL cements, respectively. Reducing the total cementitious content would allow for larger replacements of SCBA-B; it should be noted that these calculations also presume no chloride contributions from the water or aggregates.

Application/Exposure Environment		Maximum Allowable Chloride Content, (pounds per cubic yard of concrete)
Non-Reinforced Concrete		No Test Needed
Reinforced Concrete	Slightly Aggressive Environment	0.70
	Moderately or Extremely Aggressive Environment	0.40
Prestressed Concrete		0.40

Figure 2-55: Chloride content limits for concrete construction (Table 346-5 from [107])

3. Mortar Testing

Two of the largest costs associated with concrete installations are labor and materials costs, including chemical admixture costs [140,141]. The placement of concrete by skilled laborers can be hindered due to stiff or "unworkable" concrete mixes, or cause workers to add additional water to the mixture or finished surface. Materials compatibility testing performed on mortars ensure that the mixture proportions proposed are appropriate for further investigation into concrete.

The testing methods performed on the mortars were selected to encompass a range of quality controls used in industry. The methods of testing the mortars for plastic property compatibility included mortar flow and time of setting. Following plastic property testing, the mortars were tested for physical/mechanical strength with compressive strength determination on 2” cube specimens. Finally, a detailed durability examination of the mortars was executed by testing the mortars investigating dimensional stability using length change, sulfate resistance, and potential for alkali-silica reactivity using accelerated length change testing procedures.

3.1 MIXTURE DESIGN AND COMPOSITION

The mortar mixtures created for mortar flow, ASTM C1437 [142], were the same batches of mortar used for time of setting, ASTM C403 [143], and compressive strength of mortar, ASTM C109 [144]. These batches used a sand-to-cementitious material ratio of 2.25:1 and a water-to-cement ratio of 0.47:1. The complete mixture proportions of each mix design for these mortars, in terms of lb/yd³ are presented in Table 3-1 and Table 3-2. These mix designs were further used for accelerated alkali-silica reactivity, ASTM C1567 [82], and dimensional stability, ASTM C157 [145]. The mortar mixture designs for ASTM C1567 using alkali reactive Jobe sand will be provided in Section 3.2.5.2, while the mixture proportions for the sulfate durability testing, ASTM C1012 [146], are provided in Section 3.2.6.

Table 3-1: Mortar mix proportions (lb/yd³) with Type I/II cement and Florida sand for ASTMs C109, C157, C403, C1437, and C1567.

Mix	I/II Cement	Sand	Water	SCBA-A	SCBA-B	GG	F Ash	C Ash	VR	SF
1	1034	2326	486	-	-	-	-	-	-	-
2	925	2313	483	103	-	-	-	-	-	-
3	818	2301	481	205	-	-	-	-	-	-
4	712	2289	478	305	-	-	-	-	-	-
5	924	2310	483	-	103	-	-	-	-	-
6	816	2295	479	-	204	-	-	-	-	-
7	709	2279	476	-	304	-	-	-	-	-
8	820	2307	482	-	-	205	-	-	-	-
9	715	2297	480	-	-	306	-	-	-	-
10	610	2288	478	-	-	407	-	-	-	-
11	816	2295	479	-	-	-	204	-	-	-
12	821	2309	482	-	-	-	-	205	-	-
13	716	2300	481	-	-	-	-	307	-	-
14	823	2314	483	-	-	-	-	-	206	-
15	989	2318	484	-	-	-	-	-	-	41
16	711	2460	514	55	-	-	-	328	-	-
17	654	2453	512	109	-	-	-	327	-	-
18	710	2458	514	-	55	-	-	328	-	-
19	653	2449	512	-	109	-	-	327	-	-
20	804	2413	504	-	-	54	-	214	-	-
21	749	2408	503	-	-	107	-	214	-	-
22	710	2458	514	-	-	-	55	328	-	-
23	653	2450	512	-	-	-	109	327	-	-
24	656	2460	514	-	-	-	-	328	109	-
25	721	2458	513	-	-	-	-	328	-	44

Table 3-2: Mortar mix proportions (lb/yd³) with Type IL cement and Florida sand for ASTMs C109, C157, C403, C1437, and C1567.

Mix	IL Cement	Sand	Water	SCBA-A	SCBA-B	GG	F Ash	C Ash	VR	SF
26	1,029	2,315	484	-	-	-	-	-	-	-
27	921	2,303	481	102	-	-	-	-	-	-
28	815	2,292	479	204	-	-	-	-	-	-
29	710	2,281	476	304	-	-	-	-	-	-
30	920	2,300	481	-	102	-	-	-	-	-
31	813	2,286	478	-	203	-	-	-	-	-
32	707	2,272	475	-	303	-	-	-	-	-
33	817	2,298	480	-	-	204	-	-	-	-
34	712	2,290	478	-	-	305	-	-	-	-
35	608	2,281	477	-	-	406	-	-	-	-
36	813	2,287	478	-	-	-	203	-	-	-
37	818	2,300	480	-	-	-	-	204	-	-
38	713	2,293	479	-	-	-	-	306	-	-
39	819	2,305	481	-	-	-	-	-	205	-
40	984	2,307	482	-	-	-	-	-	-	41
41	708	2,452	512	54	-	-	-	327	-	-
42	652	2,445	511	109	-	-	-	326	-	-
43	708	2,450	512	-	54	-	-	327	-	-
44	651	2,442	510	-	109	-	-	326	-	-
45	801	2,404	502	-	-	53	-	214	-	-
46	746	2,399	501	-	-	107	-	213	-	-
47	708	2,450	512	-	-	-	54	327	-	-
48	651	2,442	510	-	-	-	109	326	-	-
49	654	2,453	512	-	-	-	-	327	109	-
50	719	2,450	512	-	-	-	-	327	-	44

3.2 TESTING RESULTS

3.2.1 Mortar Flow – ASTM C1437

The mortar flow was determined using a modified version of ASTM C1437 [142]. In ASTM C1437, the flow table is prescribed to be dropped a total of 25 times in 15 seconds (a rate of 100 drops/minute). However, a large portion of the mixtures evaluated contain a high replacement percentage of fly ash and had a tendency to flow off the table within 25 drops. To remedy this, the drop count was changed to 15 total drops instead of 25, using the same drop rate. The mortar flow results are summarized in Table 3-3 and are separated by cement type. Additionally, the scope of ASTM C1437 is to measure the water content required for a mortar to

provide a specified flow level. This constraint was also removed, as it was not perceived to be germane to the investigation of the effects on flow that these materials would present (water demand was not investigated). Furthermore, adjusting the water content of the mortar mixes to a constant flow value would result in an exceedingly high number of total mixes investigated; therefore, the water to cement ratio was held constant at 0.47. The precision of ASTM C1437 states that the flow of similar batches should not differ by more than 11%.

Two sugarcane bagasse ashes were used for this research; one is burned less completely (SCBA-A) and another that is burned to a greater extent (SCBA-B). The structure of SCBA-A is shown in Figure 3-1 which is a function of the combustion process affecting the hemicellulose and lignin structures of the plants; this process also changes the amorphous content and surface area as noted with other agricultural residual ashes by Ataie and Riding [147]. While both sugarcane bagasse ashes have elevated levels of carbon, SCBA-B has a lower level than SCBA-A, which was determined by LOI in Table 2-2 and the effect can be observed in the differences of flow between mixes using the two materials. Similar effects are observed in the ternary mixes. However, the incorporation of C fly ash mitigated the negative effects on flow caused by both SCBAs as the ternary mixtures have comparable or greater flow than both controls.

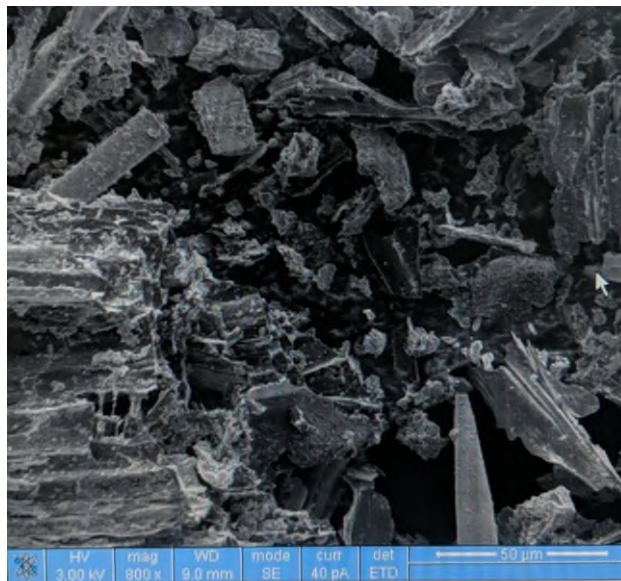


Figure 3-1: Scanning electron microscopy (SEM) image of SCBA-A.

The flow of the ground glass (GG) in the mixtures was greater than control in the Type I/II cement system and comparable to control in the Type IL cement system. The ternary mixtures using GG had comparable flow to the mixtures using F ash, even with 10% less C ash.

The improvement in flow is most likely due to the lack of water demand associated with the use of GG [148,149].

The volcanic rock and fly ash mixtures increased flow by approximately the same amount compared to control in both cement systems. The silica fume mixtures had little to no effect on mortar flow, which is most likely due to the low replacement level. Silica fume typically causes a decrease in workability at higher replacement levels [150]. As observed with the other materials, the flow of the ternary mixtures was influenced by the C ash addition and led to increased flow.

Table 3-3: Summary of flow of mortars using Type I/II or Type IL cement with SCM.

Type I/II Cement Mixes	Flow	Type IL Cement Mixes	Flow
Control	94%	Control	117%
10% - SCBA-A	86%	10% - SCBA-A	63%
20% - SCBA-A	52%	20% - SCBA-A	25%
30% - SCBA-A	0%	30% - SCBA-A	0%
10% - SCBA-B	93%	10% - SCBA-B	88%
20% - SCBA-B	62%	20% - SCBA-B	59%
30% - SCBA-B	0%	30% - SCBA-B	0%
20% - GG	114%	20% - GG	114%
30% - GG	111%	30% - GG	112%
40% - GG	116%	40% - GG	111%
20% - VR	125%	20% - VR	120%
20% - C Ash	122%	20% - C Ash	127%
30% - C Ash	130%	30% - C Ash	133%
20% - F Ash	128%	20% - F Ash	123%
4% - SF	102%	4% - SF	100%
Type I/II Cement Ternary Mixes		Type IL Ternary Mixes	
30C + 5SCBA-A	118%	30C + 5SCBA-A	120%
30C + 10SCBA-A	95%	30C + 10SCBA-A	104%
30C + 5SCBA-B	120%	30C + 5SCBA-B	122%
30C + 10SCBA-B	111%	30C + 10SCBA-B	113%
20C + 5GG	123%	20C + 5GG	127%
20C + 10GG	131%	20C + 10GG	130%
30C + 5F	136%	30C + 5F	137%
30C + 10F	137%	30C + 10F	139%
30C + 10VR	133%	30C + 10VR	133%
30C + 4SF	123%	30C + 4SF	121%

3.2.2 Time of Set – ASTM C403

Time of setting of mortar was performed in accordance with ASTM C403 [143] in which prepared mortars had a composition matching that given in ASTM C1567 [82]. Each mortar was

prepared using a benchtop stand mixer and placed into a water-tight steel cubic container in three lifts using tamping compaction for each lift. The mortars were then allowed to cure while periodically being evaluated for penetration resistance using a plunger and interchangeable needles with a range of diameters. In this fashion, the resistance stress over time was computed and the time at which initial setting (500 psi of resistance) and final setting (4,000 psi of resistance) was interpolated from the readings. The time of set for each mixture is presented in Figure 3-2 through Figure 3-13 where penetration resistance over time (red and black dashed lines on the figures represent the initial and final setting time conditions, respectively) as well as a summary table detailing the computed initial and final setting times for each mix.

3.2.2.1 Type I/II cement

An investigation on siliceous powders published by Bentz. et al. [151] showed that highly siliceous materials accelerate the hydration and time of setting of cementitious pastes. It was presumed then, that SCBA may have a similar effect when retarding admixtures are not used, as the material has a large surface area and is mostly siliceous. This material appears to have little retardation of setting in either system as shown in Figure 3-2. When the replacement percentage was increased to 30%, the final setting time was reduced by over one hour for SCBA-A and approximately 30 minutes for SCBA-B. This may be a side effect of the reduced workability of high replacement SCBA absorbing much of the water resulting in 1.) stiffer mortar from the outset, and 2.) lower effective w/c once mixed as the water is absorbed by the SCBA.

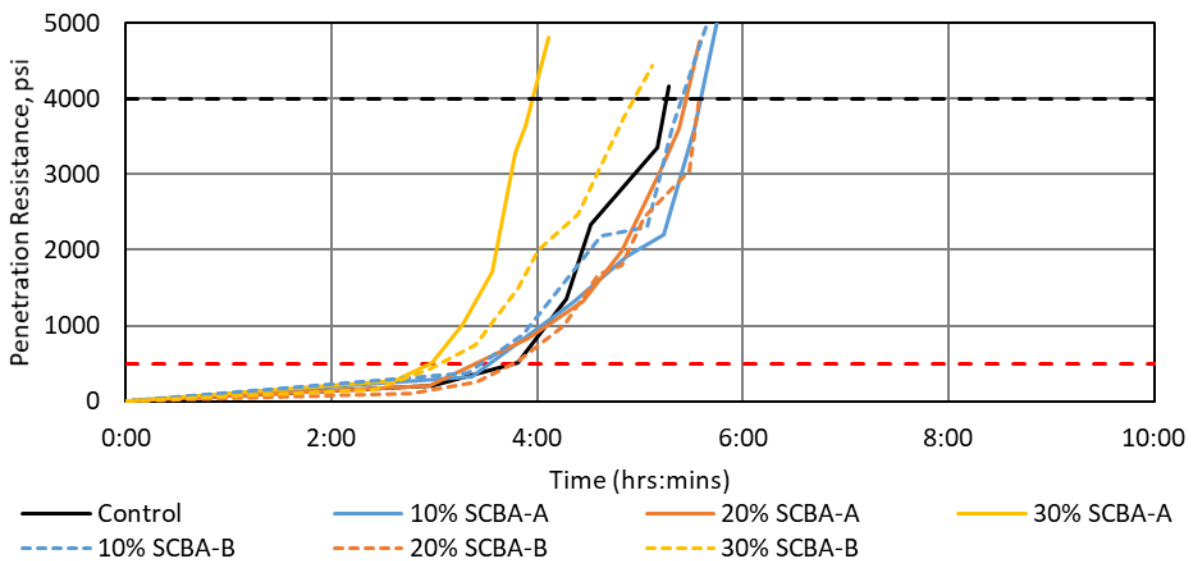


Figure 3-2: Time of set of mortar containing SCBA replacement of Type I/II cement.

Ground glass (GG) has the next highest silica content but exhibited set retardation of approximately 40-50 minutes with replacements of 20% – 40% (Figure 3-3). With nearly identical XRF elemental chemistry to SCBA with the exception of silica and alkali content. The disparity is most likely a result of a combination of the amount of siliceous amorphous phase, which is more reactive than the siliceous crystalline phases, and the relatively large particle size of the glass, which would have lower reactivity due to lower exposed surface area. Based upon the evaluation done in Section 2.3, the median particle size is larger and the crystalline content higher for the SCBA-A, which would both lead to a longer time of set. As the materials are generated from different waste streams (the glass from ground solid glass and the SCBA a burned plant material), the surface morphology of the particles plays the largest role because it is known that the SCBA has a much larger surface area for reaction than the glass particles. Additionally, it has been reported that as alkali content increases, so does the rate of hydration [152]. This would lead one to estimate that glass would react more at early ages compared to SCBA; however, it may be that the alkalis present are inaccessible in the glass matrix at very early ages.

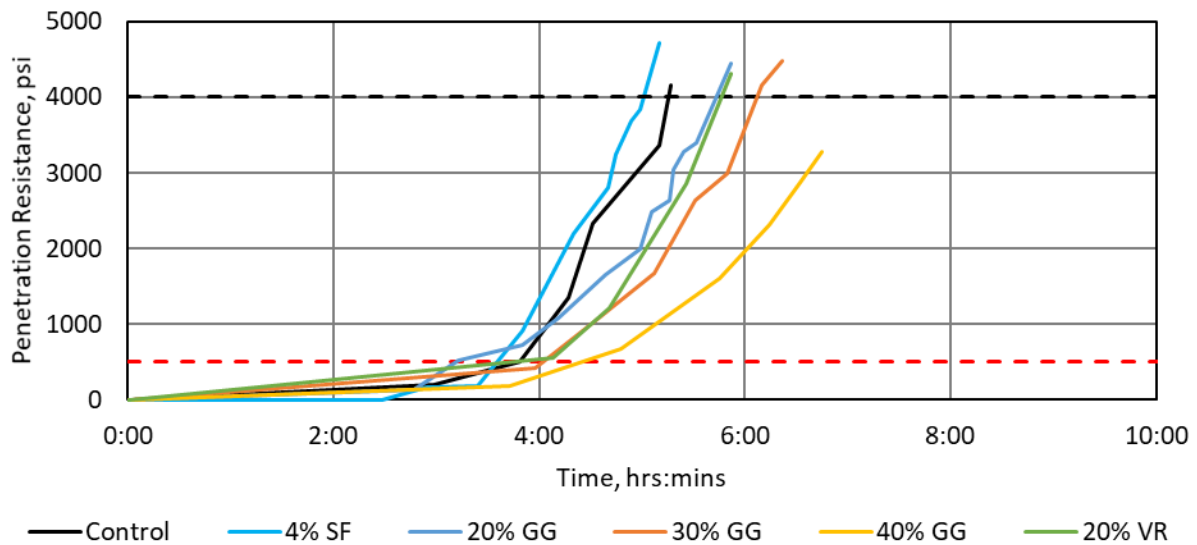


Figure 3-3: Time of set of mortar containing GG, SF, or VR replacement of Type I/II cement.

There was a large disparity in the performance of Class F fly ash compared to Class C fly ash. Since Class C fly ash also has hydraulic properties, it would be expected to have shorter final set times than Class F fly ash. The 20% Class F fly ash mixtures resulted in final set retardations of 11 minutes, whereas the 20% Class C fly ash mix resulted in final set delays of 90

minutes. Increasing the Class C fly ash content from 20% to 30% had only a minor effect on final setting time (6-minute reduction for Type III and 1-minute delay for Type II). As the particle size distribution of the two fly ash types are very similar, the chemical effects dominate the performance differences. This is most likely due to the unusually high phosphorus content of the Class C fly which was nearly 1%, and it is known that phosphorus drastically reduces the rate of hydration in portland cement systems [153]. Research by Holanda et al. shows that P_2O_5 amounts above 0.8% will incur several hours of hydration retardation. Other discrepancies between the elemental compositions in the Class F and Class C fly ash are the calcium and silica contents with the C ash having approximately 22% more calcium and 15% less silica (as well as more magnesium and less iron); these differences were unlikely to have a large contributing effect on the time of set for each mixture.

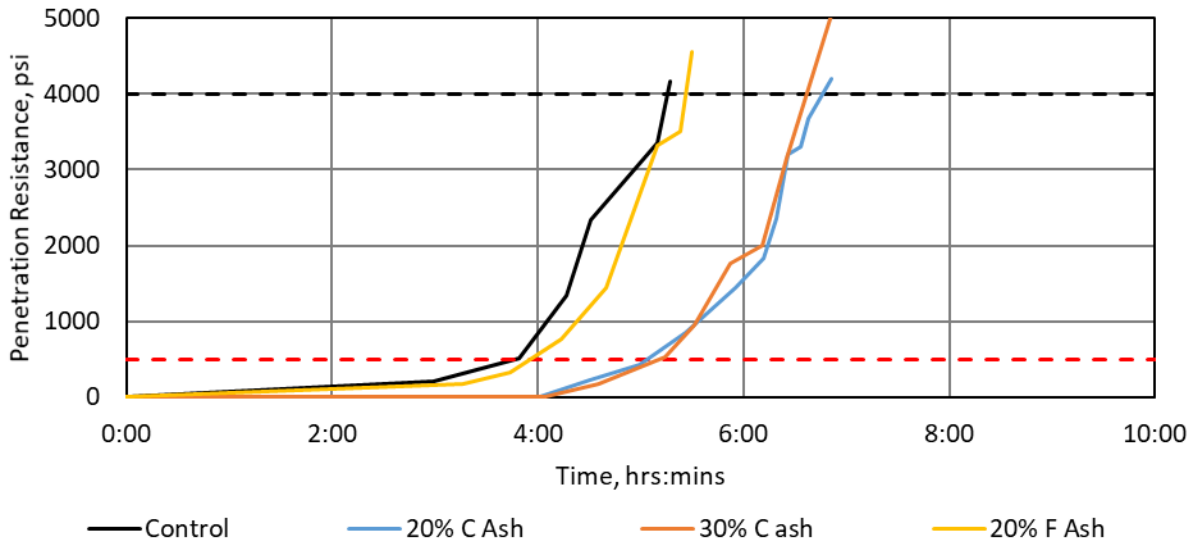


Figure 3-4: Time of set of mortar containing C ash or F ash replacement of Type I/II cement.

Ternary blended mixtures had extended time of set values regardless of SCM utilized. This is attributed to the incorporation of at least 20% Class C fly ash in each ternary mixture. The mixture which took the longest time to reach final set was the 30% C ash + 10% SCBA-A at 10 hours (91% longer than control).

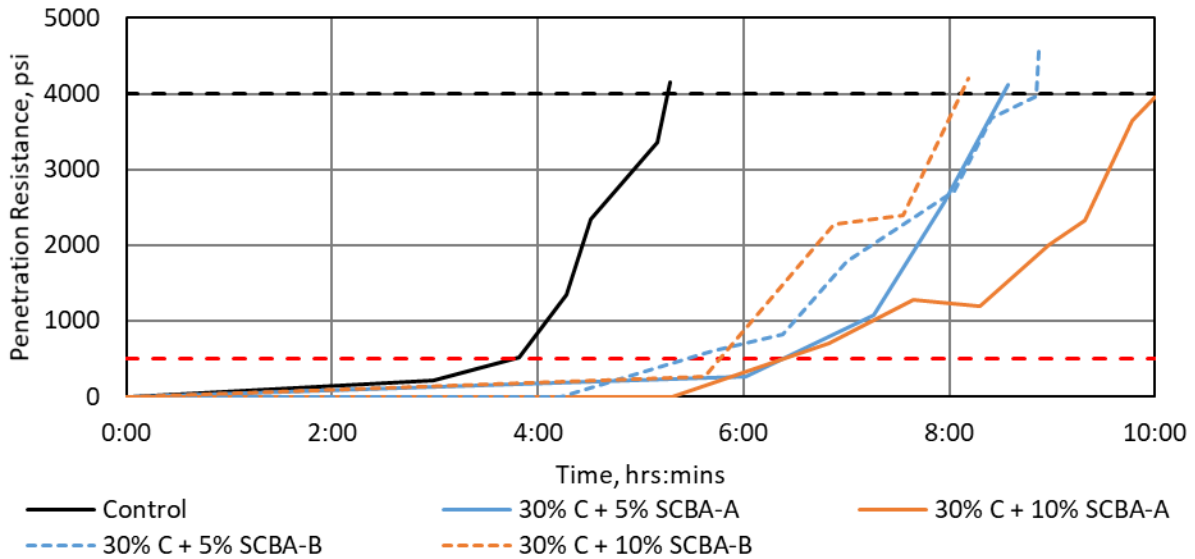


Figure 3-5: Time of set of mortar containing a ternary blend of C ash and SCBA replacement of Type I/II cement.

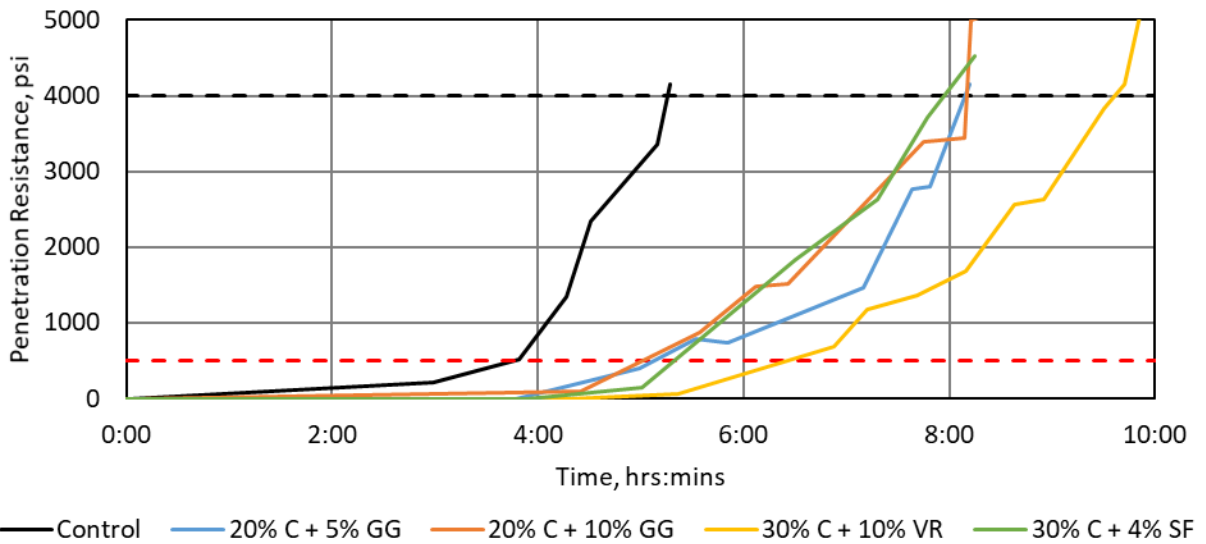


Figure 3-6: Time of set of mortar containing a ternary blend of C ash and GG, VR, or SF replacement of Type I/II cement.

The mixture that had the least amount of set retardation compared to control was the 30% C ash + 5% F ash having a final setting time 7 hours and 49 minutes compared to the 5 hours and 15 minutes of the control (49% longer). On average, the ternary blends took approximately 65% longer than the control mix for the Type I/II system (39-91% range) to reach final setting time. A summary of the initial and final setting times determined by penetration resistance for mortars containing one or two SCM in a Type I/II cement system are presented in Table 3-4.

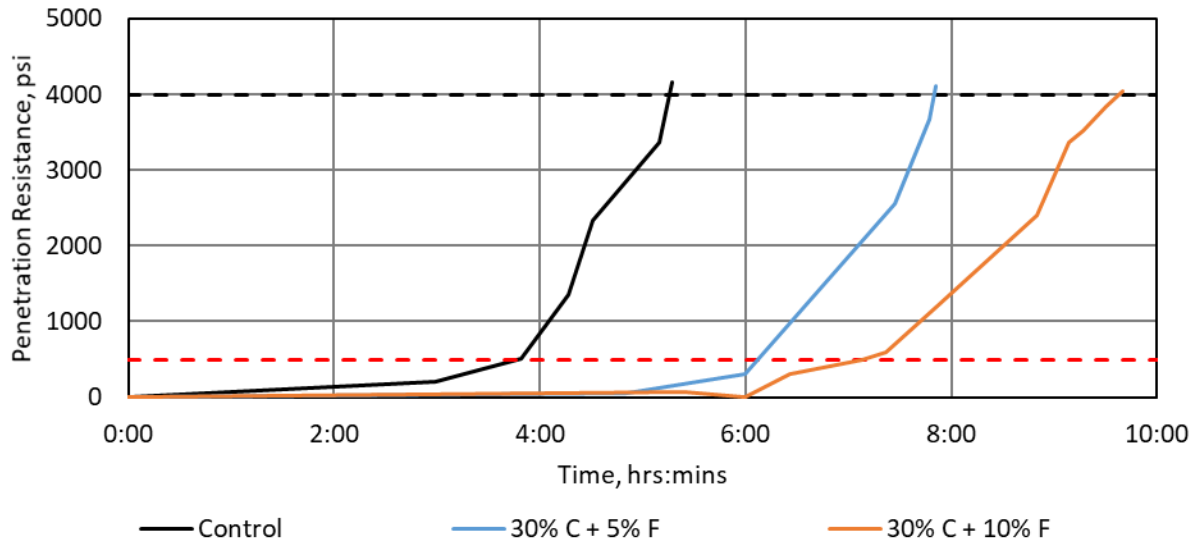


Figure 3-7: Time of set of mortar containing a ternary blend of C ash and F ash replacement of Type I/II cement.

Table 3-4: Summary of time of set of mortars using a Type I/II cement with SCM.

Type I/II Cement Mixes	Initial Set, h:min	Final Set, h:min
Control	3:47	5:15
10% - SCBA-A	3:32	5:35
20% - SCBA-A	3:33	5:27
30% - SCBA-A	2:58	3:57
10% - SCBA-B	3:28	5:24
20% - SCBA-B	3:46	5:34
30% - SCBA-B	3:06	4:46
20% - GG	3:11	6:12
30% - GG	4:02	6:07
40% - GG	4:24	7:12
20% - VR	4:05	5:47
20% - C Ash	5:03	6:42
30% - C Ash	5:10	6:36
20% - F Ash	3:56	5:26
4% - SF	3:35	5:01
Ternary Mixes		
30C + 5SCBA-A	6:22	8:31
30C + 10SCBA-A	6:23	10:02
30C + 5SCBA-B	5:25	8:51
30C + 10SCBA-B	5:45	8:06
20C + 5GG	5:07	8:09
20C + 10GG	5:01	8:10
30C + 5F	6:07	7:49
30C + 10F	7:08	9:38
30C + 10VR	6:26	9:36
30C + 4SF	5:19	7:18

3.2.2.2 Type II cement

The mortar systems utilizing a Type II cement with one or two supplementary cementitious materials performed as expected with no large deviations from what was expected with large amounts of SCM requiring longer times to reach initial and final setting times. This effect was exacerbated when ternary blends incorporated up to 40% cement replacement.

Figure 3-8 shows the time of setting of mortars using SCBA-A and SCBA-B at replacements of 10%, 20%, or 30% in the Type II cement system. The mortars showed comparable setting times to the control mixture with the exception of the 30% SCBA-A mixture, which had a final setting time that was retarded by 59 minutes (or 22% of the control). The large

replacements of SCBA did not exhibit set acceleration as seen in the Type I/II mixtures. This is attributed to the lack of calcium oxide (CaO) in the cementitious system which utilized IL cement, demonstrating that the optimal replacement of portland cement with pozzolan may be different for systems that utilize type IL cement.

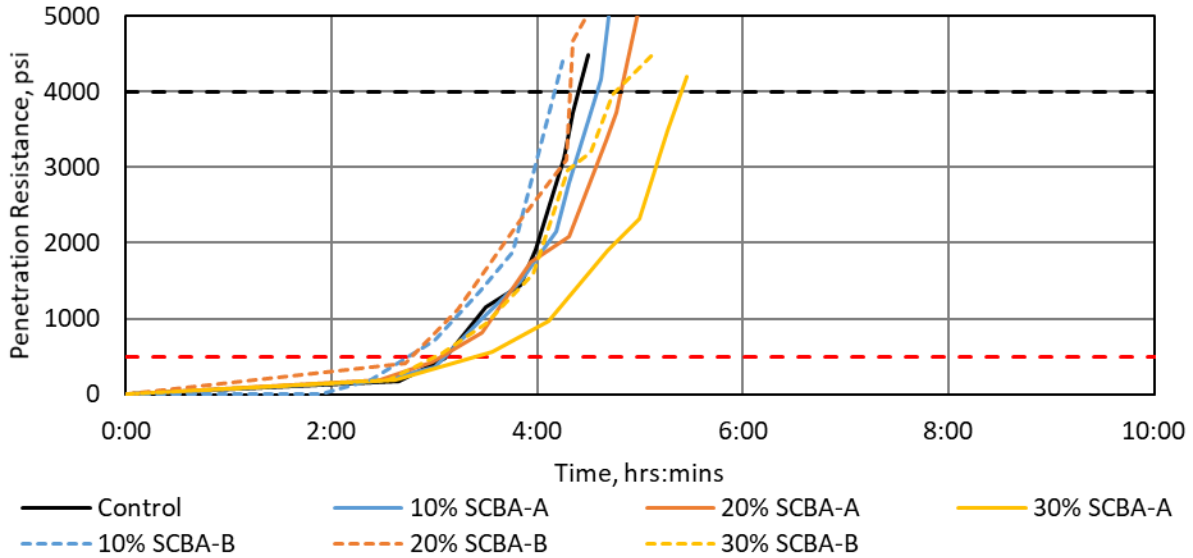


Figure 3-8: Time of set of mortar containing SCBA replacement of Type IL cement.

The silica fume replacement mix had virtually identical performance to the control, with the ground glass mixtures exhibiting set retardation that became more prominent as the replacement percentage increased; a trend that is mirrored in the Type I/II systems. The volcanic rock mixture exhibited a final setting time that was statistically comparable for the equivalent level of replacement of ground glass (20%) indicating similar levels of early-age reactivity.

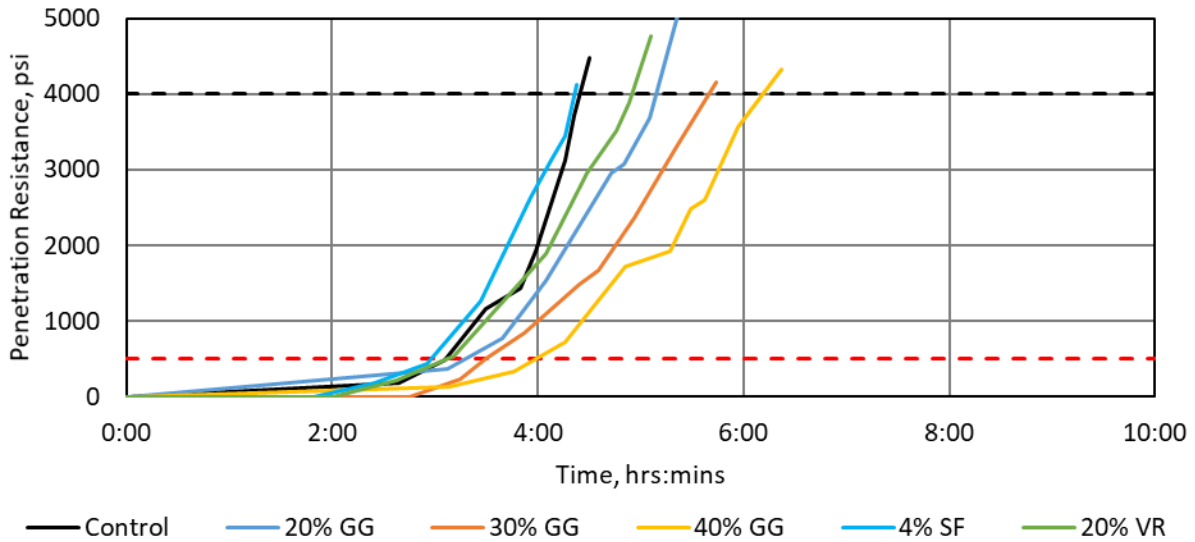


Figure 3-9: Time of set of mortar containing GG, SF, or VR replacement of Type II cement.

The Class C fly ash replacements of Type II cement exhibited the largest amounts of final set retardation of any of the binary mixes with both mixes reaching final set within 1 minute of the other. These mixes extended final setting by over two and a half hours or approximately 60% of the control final set time for the Type II mix as can be seen in Figure 3-10. The 20% Class F ash replacement extended the final setting time by 35 minutes, or approximately 13%.

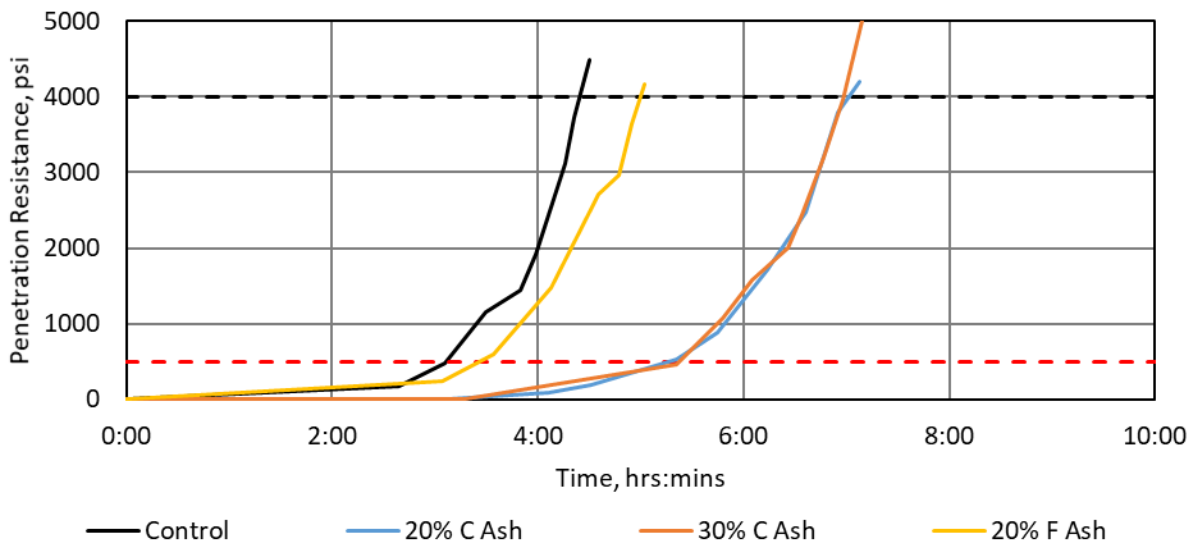


Figure 3-10: Time of set of mortar containing C ash or F ash replacement of Type II cement.

On average, the ternary blends took approximately 60% longer than the control in the Type II system (31-80% range) to reach final setting time as shown in Figure 3-11 through Figure 3-13.

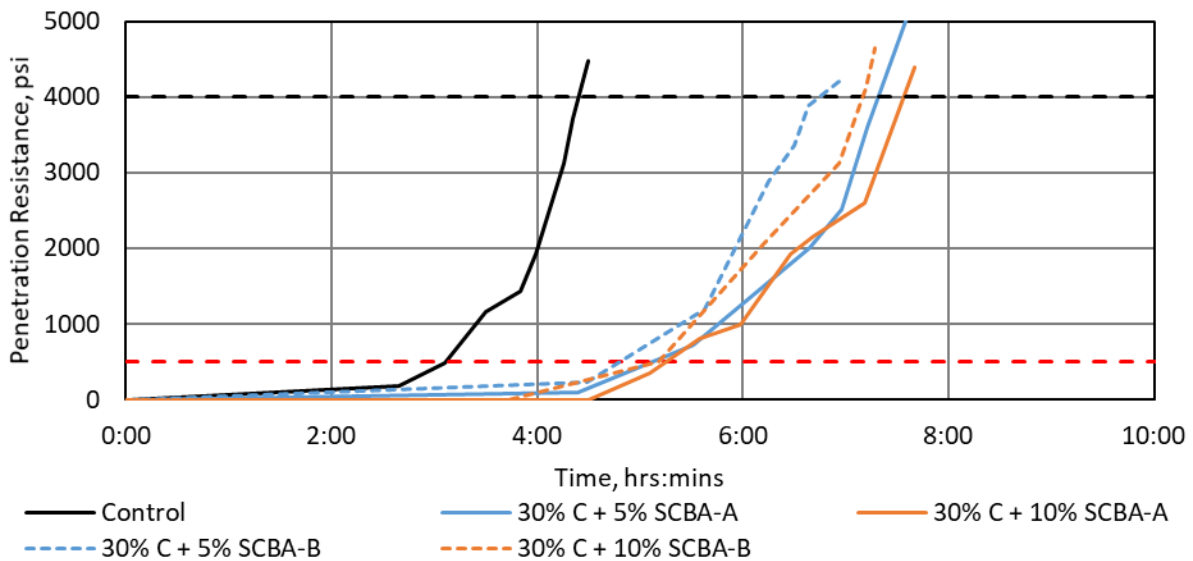


Figure 3-11: Time of set of mortar containing a ternary blend of C ash and SCBA replacement of Type II cement.

As with the Type I/II cement systems, the Type II ternary blended mixes exhibited final setting times that were in excess of the control; the mix that exhibited the least amount of set retardation was the 20% C ash and 5% GG mixture having a final setting time of 5 hours and 45 minutes (31% longer than control), and the mixture that had the longest setting time was the 20% C ash and 10% GG mixture having a final setting time of 7 hours and 53 minutes (80% longer than control).

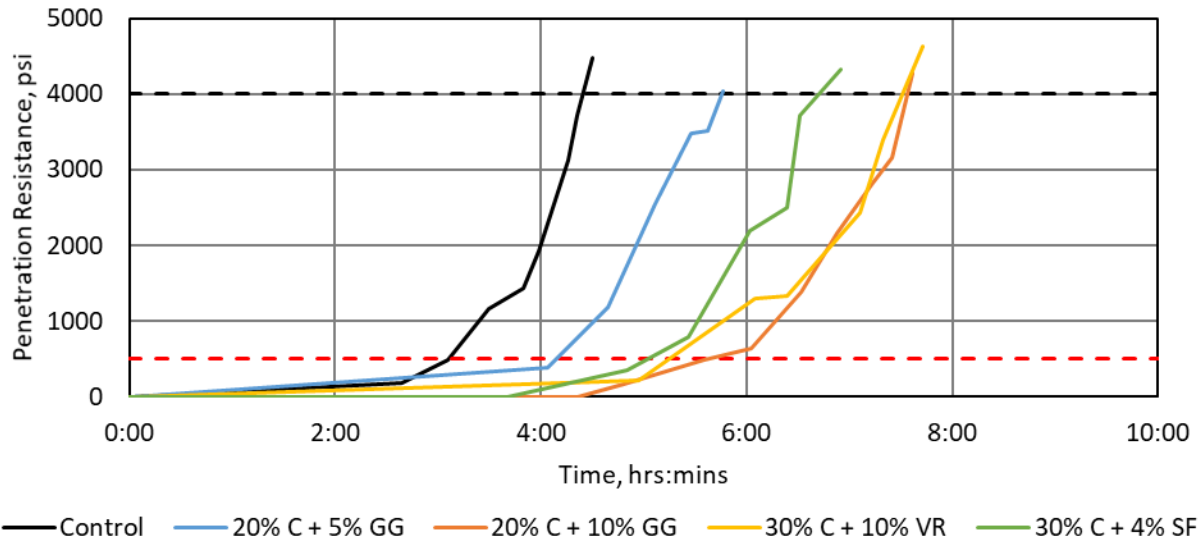


Figure 3-12: Time of set of mortar containing a ternary blend of C ash and GG, VR, or SF replacement of Type IL cement.

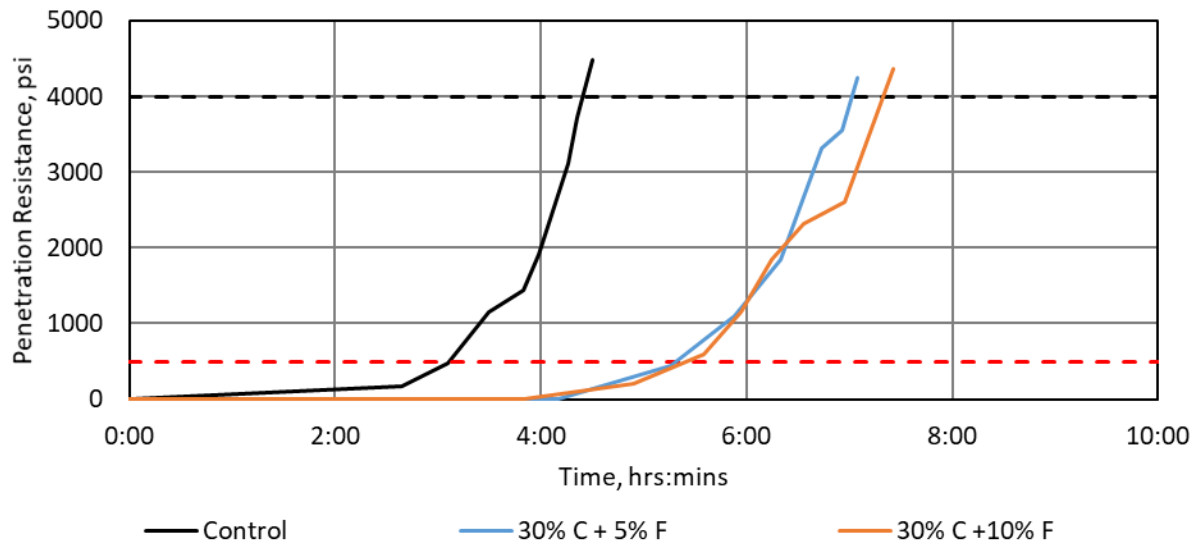


Figure 3-13: Time of set of mortar containing a ternary blend of C ash and F ash replacement of Type IL cement.

A summary of the initial and final setting times determined by penetration resistance for mortars containing one or two SCM in a Type I/II cement system are presented in Table 3-5.

Table 3-5: Summary of time of set of mortars using a Type IL cement with SCM.

Type IL Cement Mixes	Initial Set, h:min	Final Set, h:min
Control	3:06	4:24
10% - SCBA-A	3:06	4:34
20% - SCBA-A	3:04	4:48
30% - SCBA-A	3:24	5:23
10% - SCBA-B	2:44	4:10
20% - SCBA-B	2:46	4:19
30% - SCBA-B	3:01	4:45
20% - GG	3:16	5:08
30% - GG	3:30	5:39
40% - GG	3:58	6:11
20% - VR	3:06	4:54
20% - C Ash	5:16	6:57
30% - C Ash	5:22	6:58
20% - F Ash	3:25	4:59
4% - SF	2:57	4:21
Ternary Mixes		
30C + 5SCBA-A	5:07	7:19
30C + 10SCBA-A	5:15	7:33
30C + 5SCBA-B	4:48	6:44
30C + 10SCBA-B	5:11	7:10
20C + 5GG	4:09	5:45
20C + 10GG	5:38	7:53
30C + 5F	5:19	7:01
30C + 10F	5:25	7:20
30C + 10VR	5:14	7:31
30C + 4SF	5:02	6:42

3.2.3 Compressive Strength – ASTM C109

3.2.3.1 Type I/II cement

Mortar cube specimens were prepared and evaluated for compressive strength in accordance with ASTM C109 [144]. The cube specimens were prepared in a benchtop mortar mixer, placed and tamped in brass molds, and then cured in a 23°C and 95% relative humidity fog room in accordance with ASTM C192 [154]. At ages 7, 28, 56, and 91 days after casting, the cubes were removed from the fog room and immediately placed into a compression machine to evaluate their strength.

The sugarcane bagasse ash that was burned less completely (SCBA-A), when replacing Type I/II cement, showed a consistent reduction in compressive strength as replacement percentage increased. Additionally, for each replacement, the 91-day strength values were lower than the 56-day compressive strength values. This phenomenon was also reported in strengths beyond 28 days utilizing the same material for FDOT BDV31-977-06 [8]. The more completely burned SCBA-B exhibited reduced compressive strengths for the 10% and 20% replacements compared to the SCBA-A; this trend is likely due to the increased crystalline composition of SCBA-B being less reactive in the cementitious system. The SCBA-B did not exhibit a pronounced drop in compressive strength at later ages, however. The results of both sugarcane ash replacements on the mortar strength are presented in Figure 3-14.

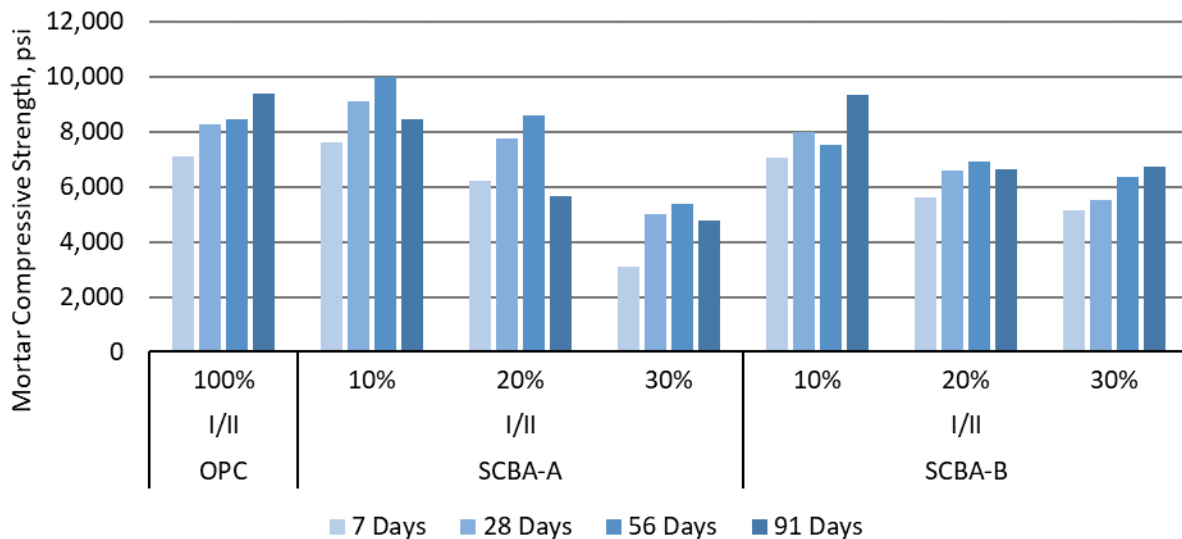


Figure 3-14: Compressive strength of mortar containing SCBA replacement of Type I/II cement.

Mixes incorporating ground glass similarly produced reduced compressive strength as the replacement percentage increased, with replacement percentages having 56- and 91-day strengths significantly lower than that for the control. Significance of results were evaluated using a two-tailed T-test assuming unequal variances and a confidence interval of 95%. The silica fume, SF, mix showed statistically lower strength compared to the control until the 91-day testing age, at which point the average strength was identical to control. The ground volcanic rock, GR, mix had lower strength than the control mix at each age tested with nominal strengths being from 84% at 7 days to 74% at 91 days. The results of the GG, SF and VR replacements can be found in Figure 3-15.

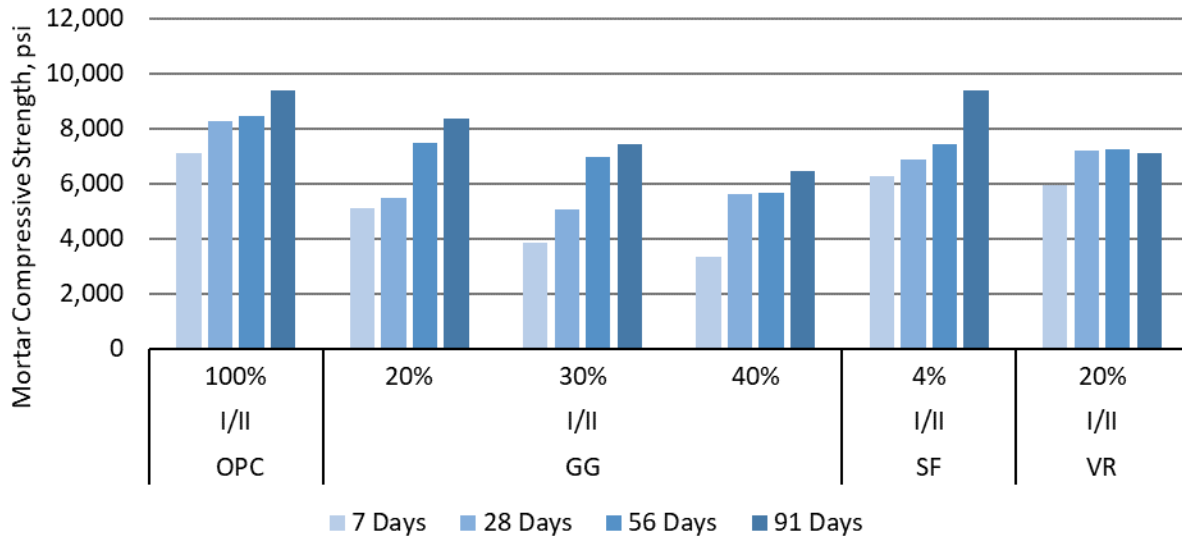


Figure 3-15: Compressive strength of mortar containing GG, SF, or VR replacement of Type I/II cement.

The binary mixtures containing fly ash replacements performed similar to the control mix with most 28-day and later strengths being statistically comparable or higher than the control, with the exception of the 56-day 20% F ash mix, which had a normalized strength of 85% of the control mixture at the same age. The reduction in strength of the C ash mixtures at 56 days was consistent with both replacement percentages; however, both mixes recovered and showed increased strength at 91 days. This dip in strength is unlikely to be sample bias as it occurred in both specimens, and there was not an outlier detected in either group as per ASTM C109; furthermore, the distribution of strength values for the 30% C ash mix at 56 days was 3.5% of the control, indicating consistent performance across the specimens. The results of the fly ash replacement mixes are presented in Figure 3-16.

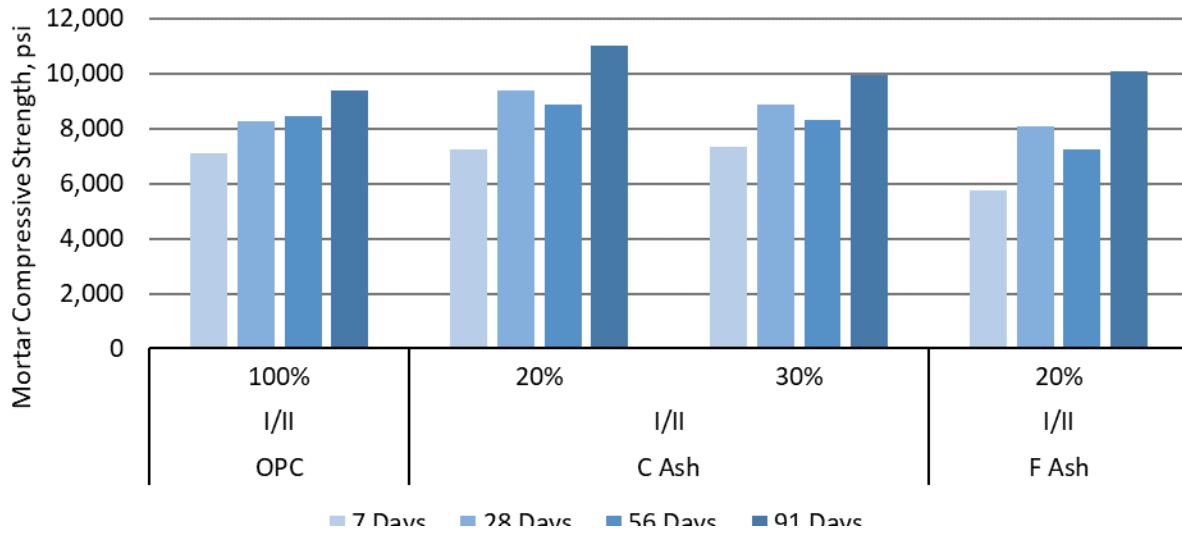


Figure 3-16: Compressive strength of mortar containing C ash or F ash replacement of Type I/II cement.

The ternary blend of 30% C ash with 5% or 10% of SCBA-A resulted in a reduction of strength at each of the ages as shown in Figure 3-17. Conversely, the addition of SCBA-B to 30% C ash produced statistically similar compressive strengths at each age beyond 28 days, except for 91 days in the 30% C ash and 10% SCBA-B mixture, which was statistically lower than the control, having a normalized strength of 71%. However, given that these mixes utilize 40% cement replacements, the performance of these mixes was adequate for consideration in structural use. Interestingly, it appears that adding SCBA-B to the C-ash caused a late-age reaction which reduced strength over time.

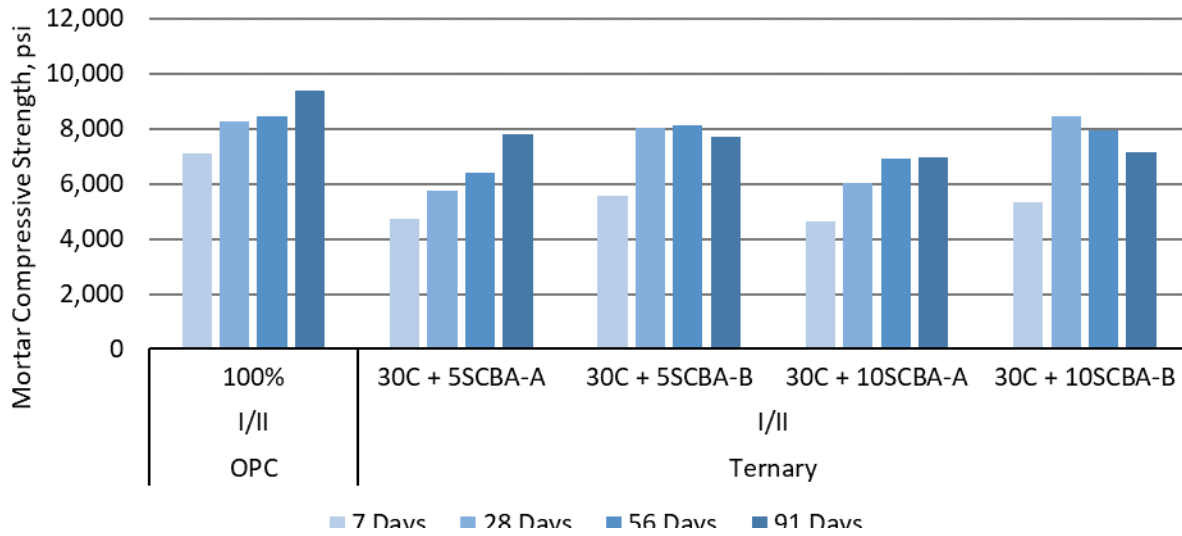


Figure 3-17: Compressive strength of mortar containing a ternary blend of C ash and SCBA replacement of Type I/II cement.

The ternary mixtures incorporating ground glass were comparable to control at and beyond 28 days of curing, as shown in Figure 3-18. Similar performance was observed for ternary blends of 30% C ash with either VR or SF, with the exception being a statistically lower strength for the 30% C ash and 10% VR at 91 days. The distribution of the strength values of the specimens representing this group was relatively small and thus indicates similar performance amongst each specimen tested; there were no outliers in this group.

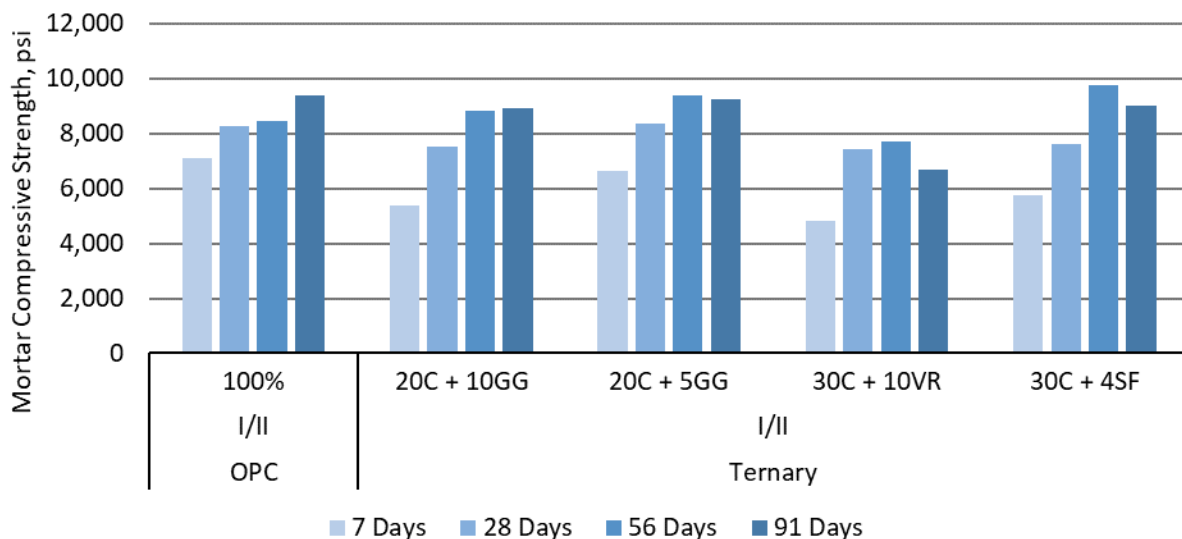


Figure 3-18: Compressive strength of mortar containing a ternary blend of C ash and GG, VR, or SF replacement of Type I/II cement.

Combining 30% C ash and 5% F ash resulted in mortar strengths that were comparable to control at each age except for 7 days as shown in Figure 3-19. However, when the replacement percentage of F ash was increased to 10%, the strength of the mortar was statistically lower at each testing age, having a nominal strength of only 65% at 7 days and 78% at 91 days.

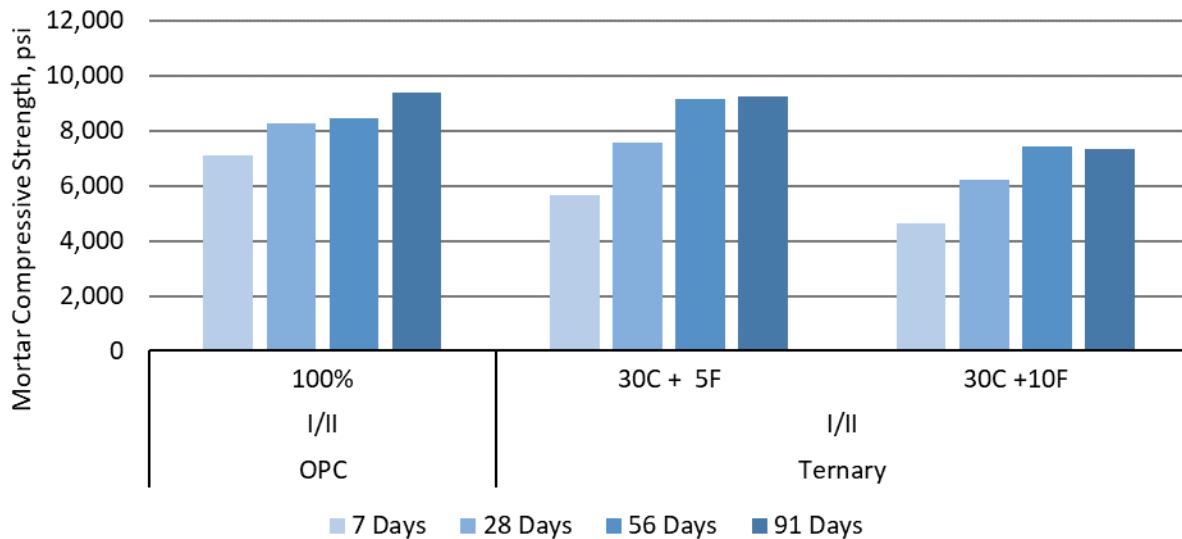


Figure 3-19: Compressive strength of mortar containing a ternary blend of C ash and F ash replacement of Type I/II cement.

There were no mixtures in the Type I/II system that were statistically stronger than the control mix at 7 days as shown in Table 3-6. This lack of strength gain, even at later ages, for materials presumed to have high pozzolanic activity, is likely due to lack of shearing action provided by the ASTM method for mixing mortars. For instance, the 4% silica fume replacement performed statistically worse than control at 7, and 56 days which is uncharacteristic of that material. The worst performing mixture was the 40% GG binary mixture having a normalized compressive strength of 47% at 7 days and only 68% of control at 91 days. Reduction in early age strength is due to the reduced activity from the replacement of the more reactive portland cement which is responsible for early age strength gain. While the reduced strength at later ages is likely due to the reduced reactivity by exhausting the available calcium hydroxide in the system by overloading the reactive silica resulting in effectively very fine aggregate rather than a pozzolanic material at high replacement percentages.

Table 3-6: Summary of compressive strength of mortars using Type I/II cement and SCM.

Mix	7-Day	28-Day	56-Day	91-Day	7-Day	28-Day	56-Day	91-Day
Control	7,080	8,250	8,450	9,390	100%	100%	100%	100%
10% - SCBA-A	7,600	9,080	9,960*	8,430	107%	110%	118%	90%
20% - SCBA-A	6,200*	7,750	8,570	5,670	88%	94%	101%	60%
30% - SCBA-A	3,080*	5,020	5,170*	4,790*	44%	61%	61%	51%
10% - SCBA-B	7,060	7,980	7,530	9,350	100%	97%	89%	100%
20% - SCBA-B	5,610*	6,580	6,910*	6,610*	79%	80%	82%	70%
30% - SCBA-B	5,110*	5,440	6,340*	6,700*	73%	66%	75%	71%
20% - GG	5,120*	5,490	7,490*	8,160*	72%	67%	89%	87%
30% - GG	3,840*	5,040	6,940*	7,420*	54%	61%	82%	79%
40% - GG	3,340*	5,610*	5,670*	6,430*	47%	68%	67%	68%
20% - VR	5,920*	6,960	7,260*	6,910*	84%	84%	86%	74%
20% - C Ash	7,240	9,380	8,880	10,980*	102%	114%	105%	117%
30% - C Ash	7,320	8,850	8,290	9,930	103%	107%	98%	106%
20% - F Ash	5,760*	8,080	7,220*	10,070	81%	98%	85%	107%
4% - SF	6,270*	6,860	7,410*	9,390	89%	83%	88%	100%
Ternary Mixes				Ternary Mixes				
30C + 5SCBA-A	4,730*	5,730	6,400*	7,790*	67%	69%	76%	83%
30C + 10SCBA-A	4,620*	6,010	6,920	6,970*	65%	73%	82%	74%
30C + 5SCBA-B	5,570*	8,020	8,140	7,520	79%	97%	96%	80%
30C + 10SCBA-B	5,320*	8,440	7,910	7,130*	75%	102%	94%	76%
20C + 5GG	6,610	8,340	9,360	9,220	93%	101%	111%	98%
20C + 10GG	5,360*	7,510	8,830	8,900	76%	91%	104%	95%
30C + 5F	5,650*	7,550	9,120	9,230	80%	92%	108%	98%
30C + 10F	4,630*	6,220*	7,440*	7,340*	65%	75%	88%	78%
30C + 10VR	4,830*	7,410	7,680	6,690*	68%	90%	91%	71%
30C + 4SF	5,740*	7,620	9,750	8,980	81%	92%	115%	96%

Values that are appended with an asterisk (*) denote a mix that exhibits a strength value that is statistically different than control based on a two-tailed T-test using two unequal variances and a 95% confidence interval.

3.2.3.2 Type II cement

The compressive strengths of mortars incorporating SCM as Type II cement replacements are shown in Figure 3-20 through Figure 3-25. The strength increases in ternary blends at 28 days and beyond is indicative of the large inclusion of Class C fly ash which similarly performed well in the binary mixes having statistically better performance than control at 28 and 56 days, and comparable performance at 91 days, regardless of replacement percentage as shown in Figure 3-20. The inclusion of Class F fly ash at 20% replacement of Type II cement

resulted in comparable performance at each age tested, having a nominal strength of 89% at 7 days and 95% at 91 days.

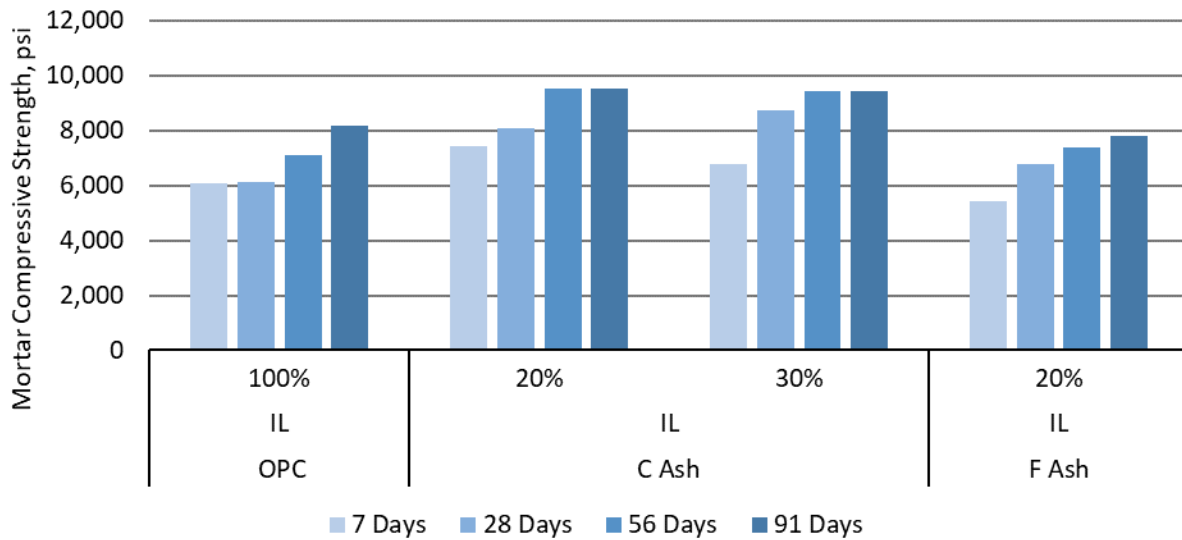


Figure 3-20: Compressive strength of mortar containing C ash or F ash replacement of Type IL cement.

Sugarcane bagasse ash in the Type IL cement systems showed similar trends as observed for the Type I/II systems with the SCBA-A ash. Resulting mixes had slightly higher compressive strength at a 10% replacement and comparable strength up to 56 days for 20% replacement. Later ages and higher replacements generally produced lower strength mixes. For SCBA-B mixes, as shown in Figure 3-21, strengths were comparable up to 28 days but did not exhibit strong pozzolanic reaction, and later-age strengths were statistically lower than the control mix, with 65% and 76% relative strengths at 91 days for the 20% and 30% replacements, respectively.

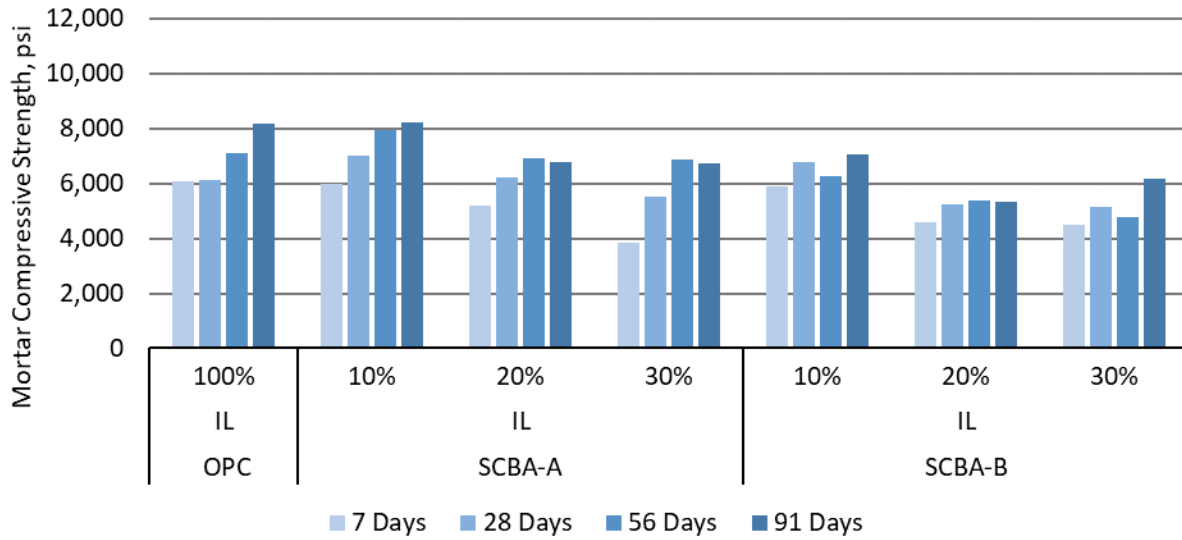


Figure 3-21: Compressive strength of mortar containing SCBA replacement of Type IL cement.

The compressive strengths of mixes with ground glass replacements in the Type IL cementitious systems were generally lower than the control strength, which was similar to the Type I/II mixes as shown in Figure 3-22. The inclusion of silica fume at 4% increased the strength at each testing age but was only statistically significant at 28 days. The normalized strength of the 4% silica fume mixes varied from 106% at 7 days, to a maximum of 133% at 28 days, and then 99% at 91 days.

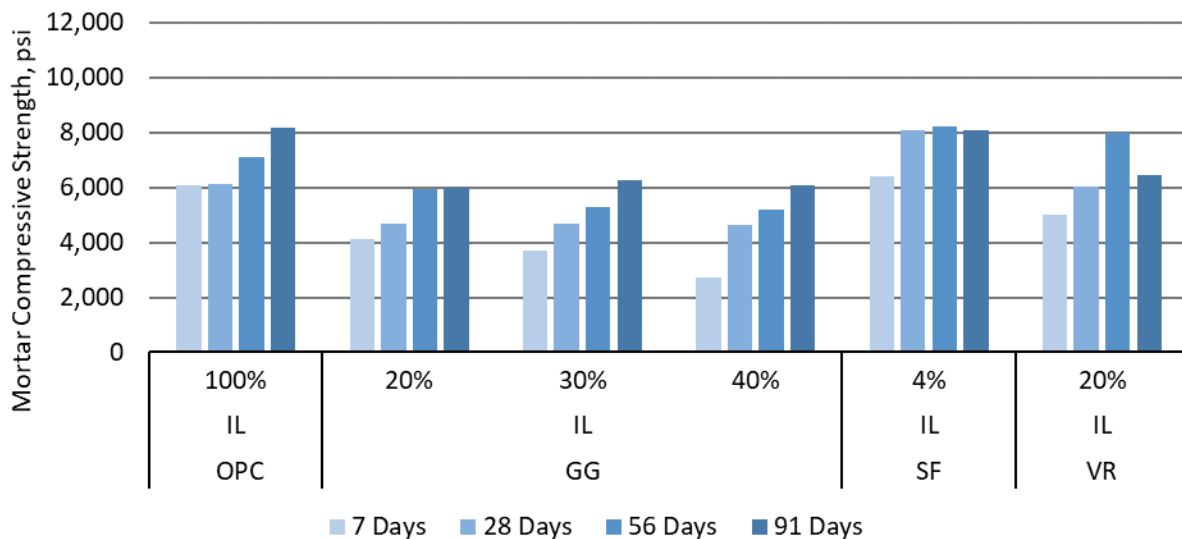


Figure 3-22: Compressive strength of mortar containing GG, SF, or VR replacement of Type IL cement.

Amending the mortars with 30% C ash and 5% or 10% sugarcane bagasse ash improved compressive strength after 7 days, with the mixes being either comparable to the control mix (for 30% C ash and 10% SCBA-B) or higher than control as shown in Figure 3-23. As stated earlier, each of the ternary blended mixtures performed well; this is largely due to the inclusion of the 30% C ash, which performed slightly better than any of the ternary mixtures.

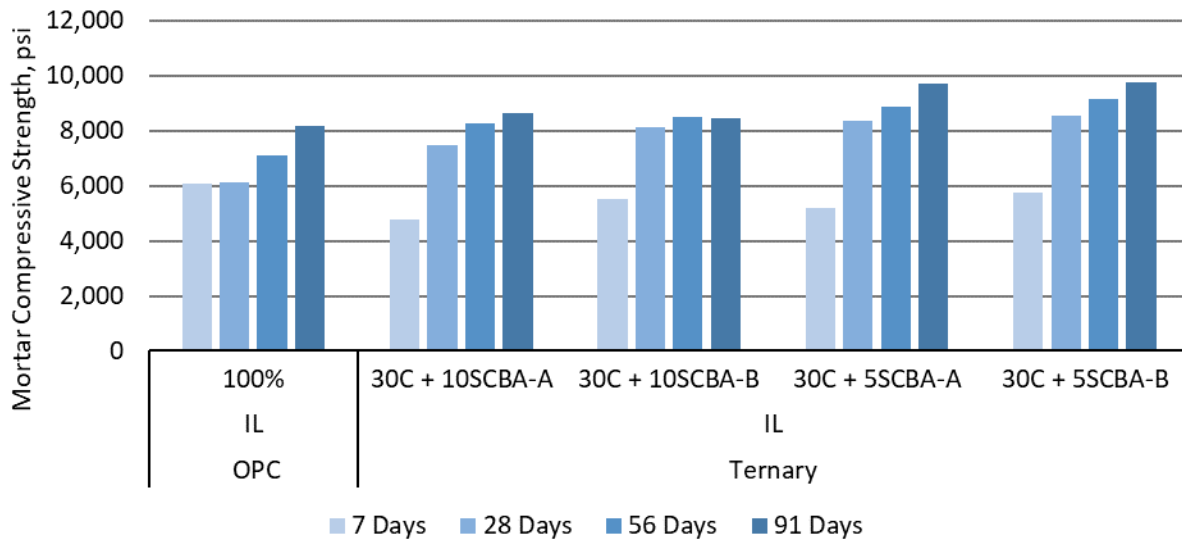


Figure 3-23: Compressive strength of mortar containing a ternary blend of C ash and SCBA replacement of Type IL cement.

The results from the compressive strength testing of ternary blends of C ash and F ash, GG, VR and SF are shown in Figure 3-24 and Figure 3-25. These results further describe the effectiveness of adding high volumes of Class C fly ash to the Type IL cement system. Regardless of the secondary supplementary cementitious material, the performance was comparable or better than control at each age tested.

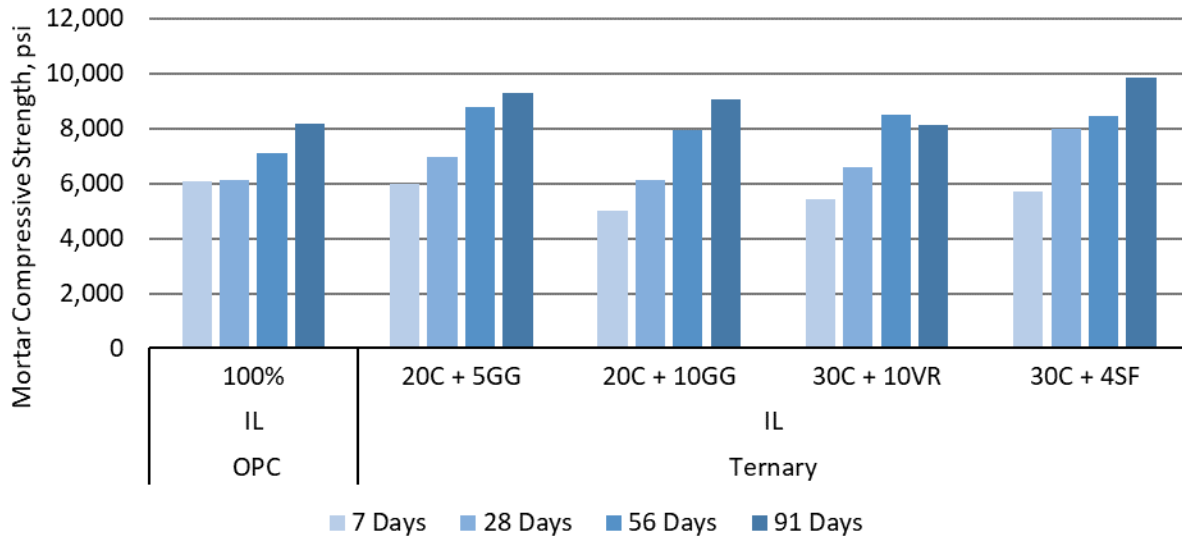


Figure 3-24: Compressive strength of mortar containing a ternary blend of C ash and GG, VR, or SF replacement of Type IL cement.

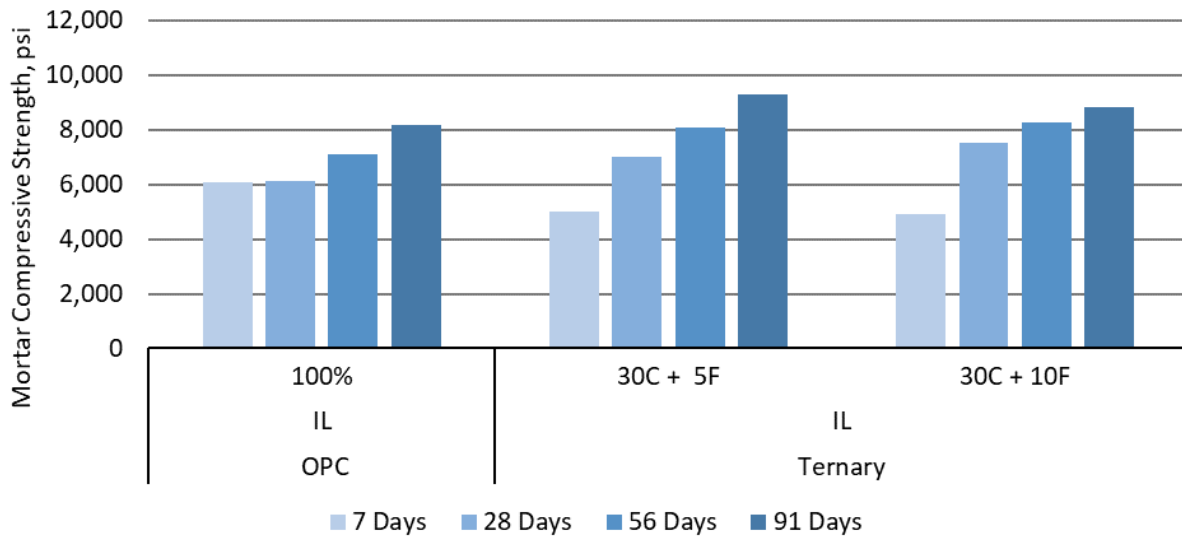


Figure 3-25: Compressive strength of mortar containing a ternary blend of C ash and F ash replacement of Type IL cement.

Based on the strength results, it appears that the addition of the limestone filler in the cement results in appreciably better strength gain at later ages for SCM amended mortars. The addition of fine limestone particles provides nucleation sites for the reactants forming calcium carboaluminates [151,155].

Incorporating SCM into the Type II system produced higher strengths for the majority of the mixes, particularly the ternary blends, with each of the ternary mixes having comparable or higher strength than the control mixes at and beyond 28 days as shown in Table 3-7.

Table 3-7: Summary of compressive strength of mortars using Type II cement and SCM.

Mix	7-Day	28-Day	56-Day	91-Day	7-Day	28-Day	56-Day	91-Day
Control	6070	6100	7100	8160	100%	100%	100%	100%
10% - SCBA-A	5970	7010*	7950*	8220	98%	115%	112%	101%
20% - SCBA-A	5200	6200	6890	6770*	86%	102%	97%	83%
30% - SCBA-A	3820*	5530	6880	6720*	64%	91%	97%	82%
10% - SCBA-B	5890	6780	6250*	7030*	97%	111%	88%	86%
20% - SCBA-B	4570	5230	5370*	5340*	75%	86%	76%	65%
30% - SCBA-B	4480	5130	4750	6170*	74%	84%	67%	76%
20% - GG	4120	4680*	5950	6000*	68%	77%	84%	74%
30% - GG	3710	4690*	5270*	6250*	61%	77%	74%	77%
40% - GG	2730*	4610*	5210	6070*	45%	76%	73%	74%
20% - VR	5020	6040	6210*	6430*	83%	99%	87%	79%
20% - C Ash	7430	8090*	9520*	9520	122%	133%	134%	117%
30% - C Ash	6770	8730*	9400*	9420	112%	143%	132%	115%
20% - F Ash	5410	6770	7360	7770	89%	111%	104%	95%
4% - SF	6420	8090*	7960	8050	106%	133%	112%	99%
Ternary Mixes				Ternary Mixes				
30C + 5SCBA-A	5170	8340*	8870*	9710*	85%	137%	125%	119%
30C + 10SCBA-A	4760	7480*	8270*	8630	78%	123%	116%	106%
30C + 5SCBA-B	5740	8560*	9150*	9740*	95%	140%	129%	119%
30C + 10SCBA-B	5520	8100	8500	8450	91%	133%	120%	104%
20C + 5GG	5970	6970	8750*	9270*	98%	114%	123%	114%
20C + 10GG	5020	6110	7950*	9030*	83%	100%	112%	111%
30C + 5F	5310	6990	8060	9280*	83%	115%	114%	114%
30C + 10F	4930	7510	8240*	8820	81%	123%	116%	108%
30C + 10VR	5400	6600	8490*	8100	89%	108%	120%	99%
30C + 4SF	5700	8000	8430	9840*	94%	131%	119%	121%

Note: Values that are appended with an asterisk (*) denote a mix that exhibits a strength value that is statistically different than control based on a two-tailed T-test using two unequal variances and a 95% confidence interval.

3.2.4 Length Change – ASTM C157

Length change of mortar was performed in accordance with the standard test as prescribed in ASTM C157 [125]. As can be seen in Figure 3-26 through Figure 3-29, the SCBA-A and SCBA-B mixes performed similar to the control when stored in water, exhibiting no

deleterious expansion out to 64 weeks of storage in either a Type I/II or Type II cement system. Additionally, when stored in air, the majority of the mortar mixes exhibited which utilized the combination of Type I/II cement with SCBA, experienced slightly higher shrinkage compared to control, with only the 30% SCBA-A replacement of Type I/II cement having approximately 0.050% more shrinkage than control at 64 weeks after curing. The mortar mixtures which use Type II cement with SCBA experienced less shrinkage when compared to the systems that used Type I/II and SCBA. The mortar combination of Type II and SCBA-B experienced the least amount shrinkage which is due to the crystalline nature of SCBA-B (compared to SCBA-A).

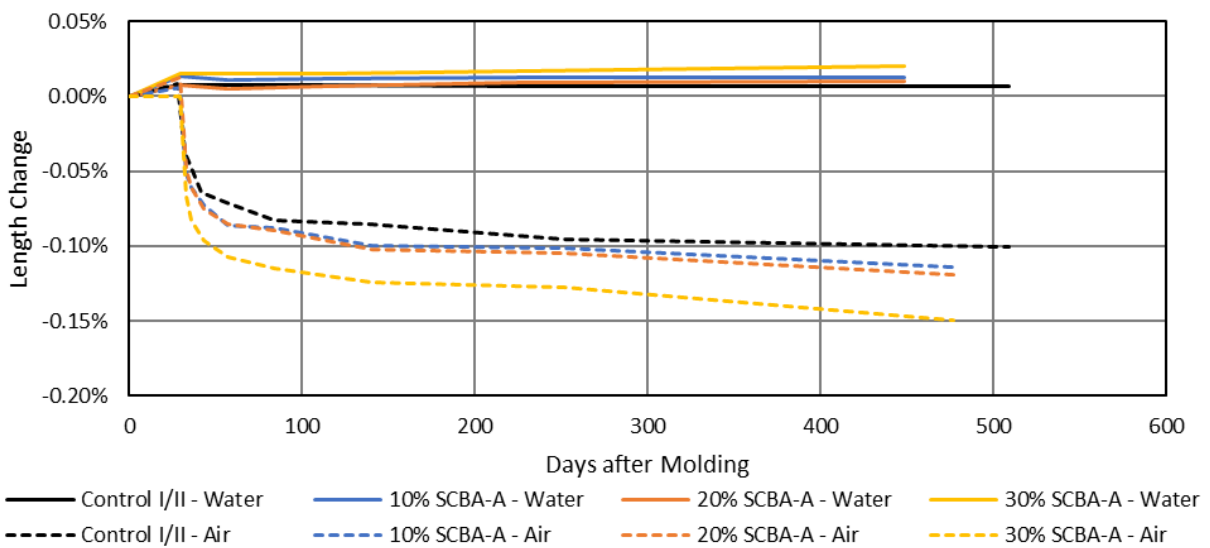


Figure 3-26: Length change of mortar containing SCBA-A replacement of Type I/II cement.

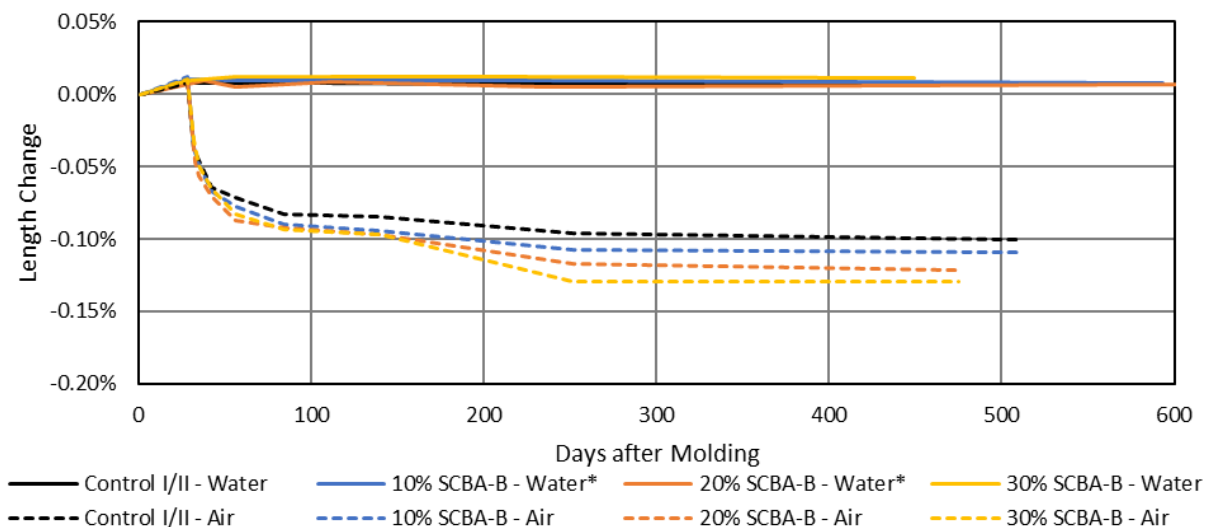


Figure 3-27: Length change of mortar containing SCBA-B replacement of Type I/II cement.

Note, due to the laboratory shutdown as a result of COVID-19, mixtures with * were measured by a different (authorized) user as part of the laboratory protocols at the University of Florida (the last measurement shown was performed by the original researcher).

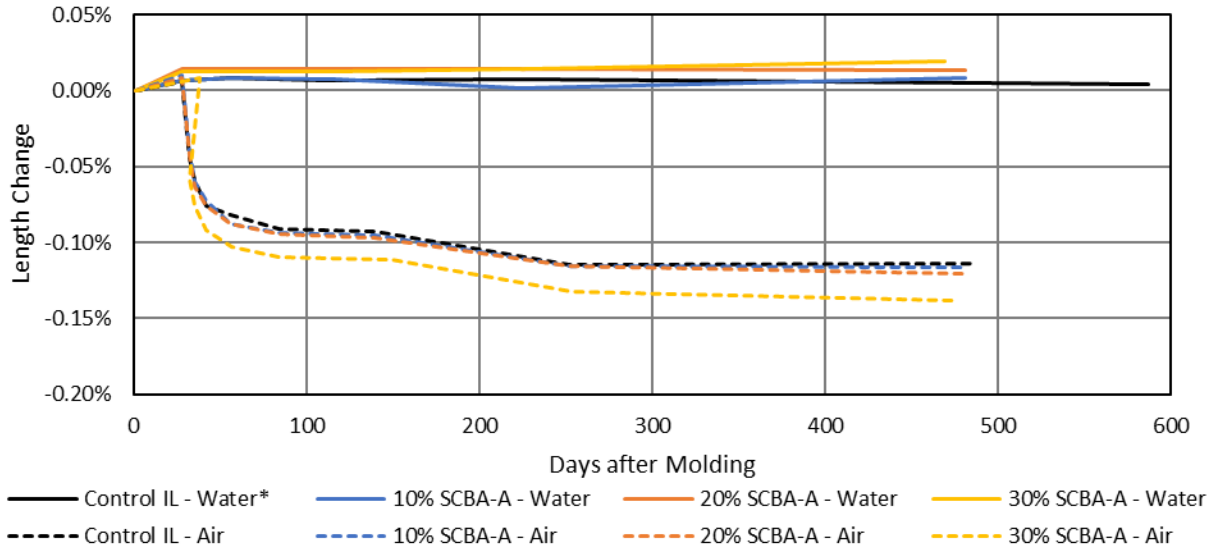


Figure 3-28: Length change of mortar containing SCBA-A replacement of Type II cement.

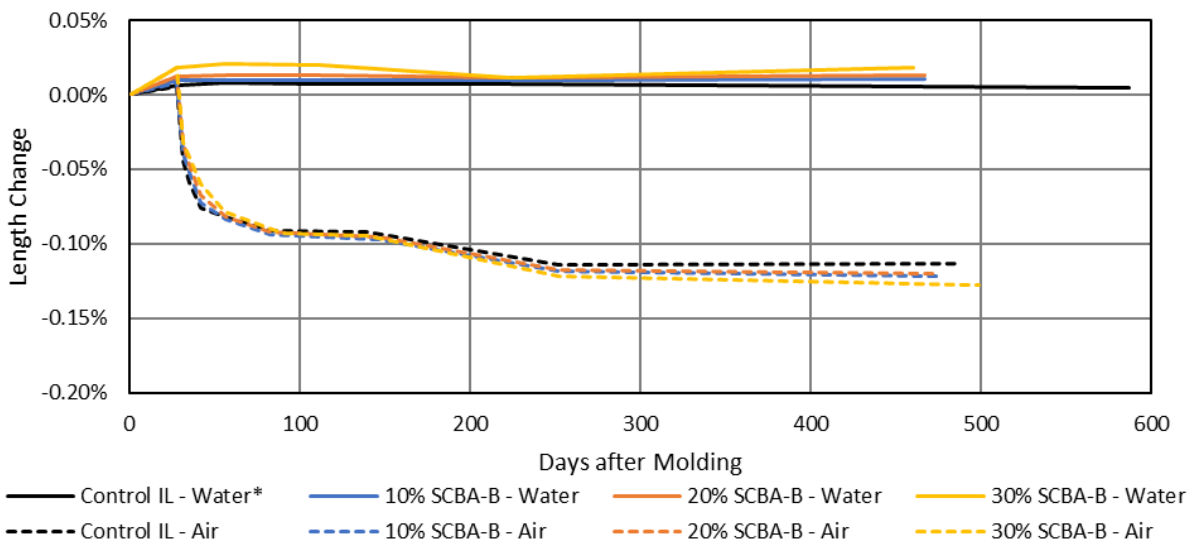


Figure 3-29: Length change of mortar containing SCBA-B replacement of Type II cement

When incorporated into a ternary blended cementitious system along with 30% Class C ash fly ash, the 5% and 10% additions of SCBA-A or SCBA-B performed virtually identically

when stored in water compared to the control, exhibiting no expansive behavior in either a Type I/II or Type IL cement system as seen in Figure 3-30 through Figure 3-33. When stored in air, the ternary blends in Type I/II cement tended to shrink more (Figure 3-30 and Figure 3-31), with three of the blended mixtures having a deviation of approximately 0.04% at 64 weeks post curing. In the Type IL replacement mixes, the shrinkage deviation from control was approximately 0.025 – 0.030% at 64 weeks across the four mixes.

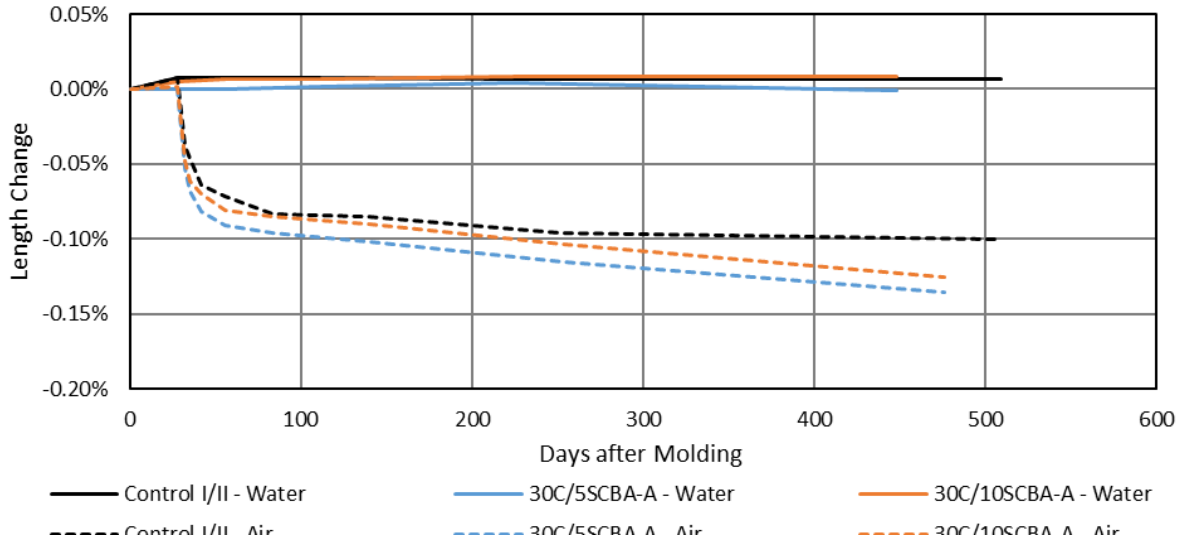


Figure 3-30: Length change of mortar containing a ternary blend of C ash and SCBA-A replacement of Type I/II cement.

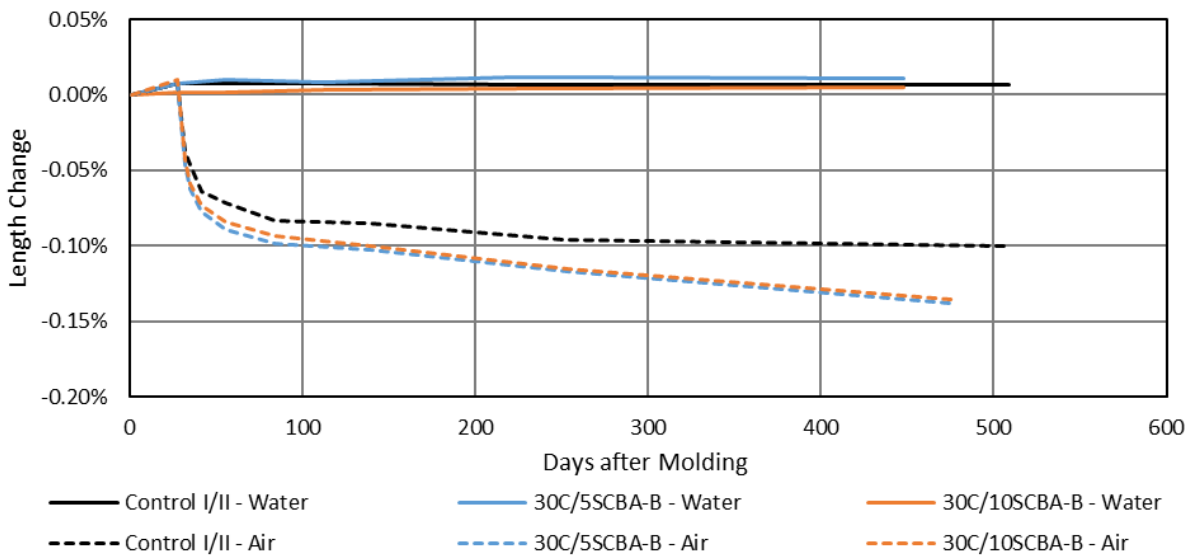


Figure 3-31: Length change of mortar containing a ternary blend of C ash and SCBA-B replacement of Type I/II cement.

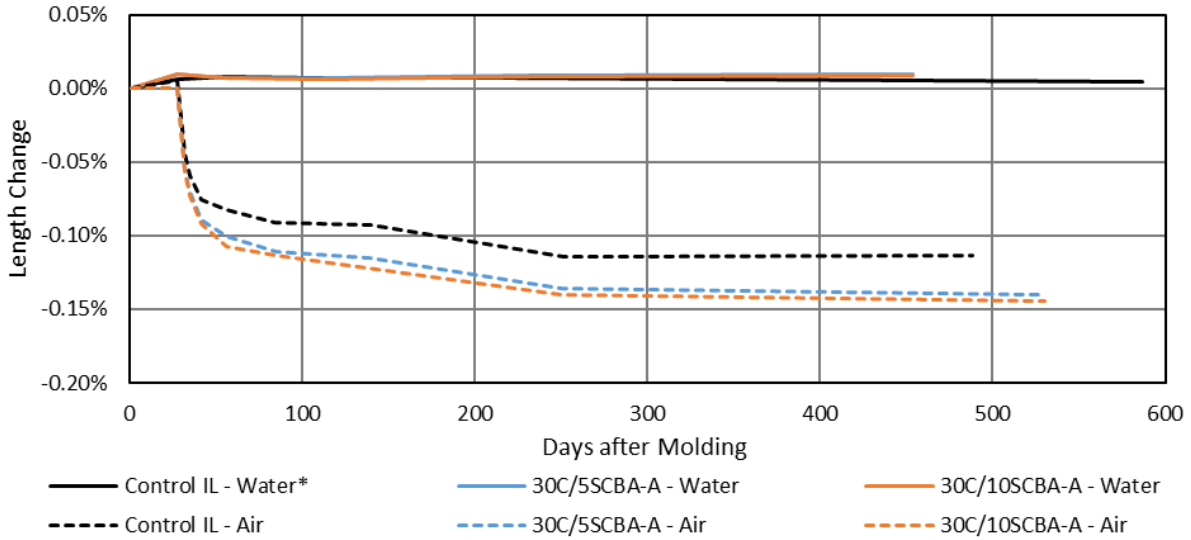


Figure 3-32: Length change of mortar containing a ternary blend of C ash and SCBA-A replacement of Type IL cement.

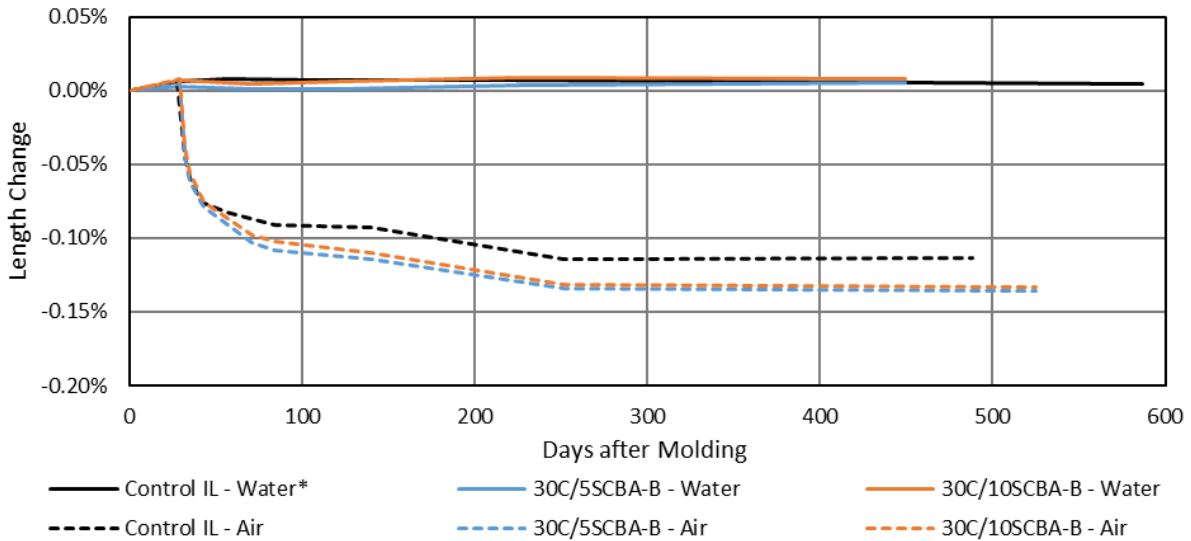


Figure 3-33: Length change of mortar containing a ternary blend of C ash and SCBA-B replacement of Type IL cement.

In both Type I/II and Type IL binary replacement systems, the 30% glass mixture exhibited the least amount of shrinkage, followed by the 20% mixture, and finally the 40% mixture, as seen in Figure 3-34 and Figure 3-35. The 40% glass mixture exhibited shrinkage in excess of 0.04% more than the control at 64 weeks post curing in either cementitious system. While this behavior of 40% GG is not indicative of deleterious behavior, it would be cause for concern that may warrant further investigation in durability testing.

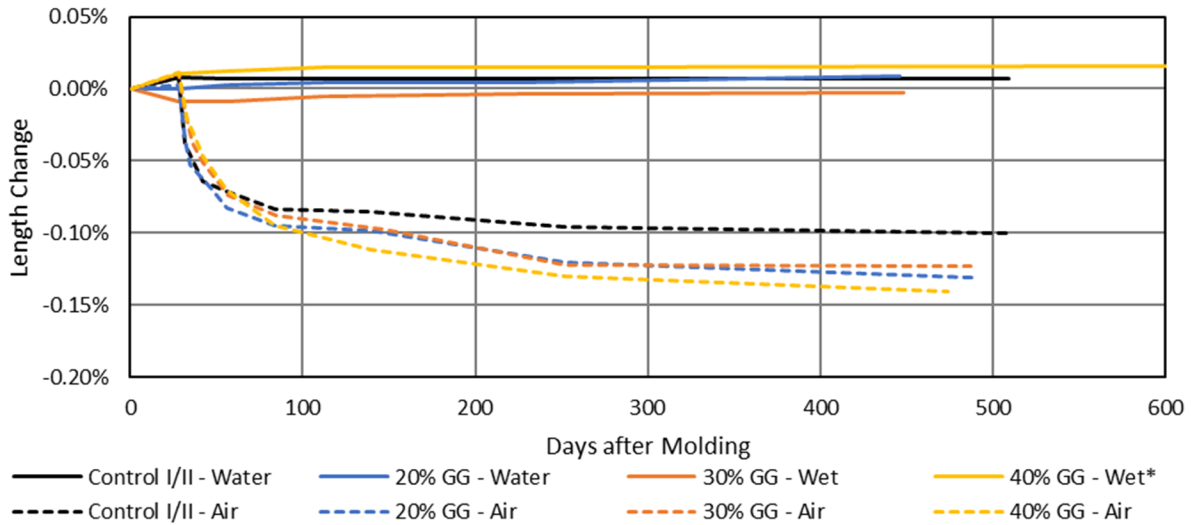


Figure 3-34: Length change of mortar containing GG replacement of Type I/II cement.

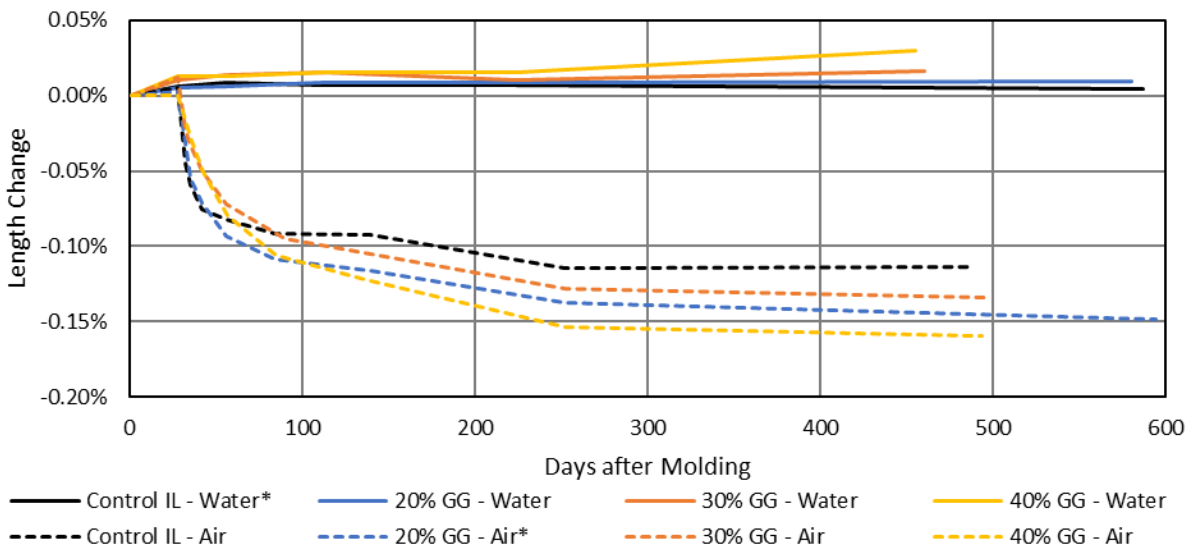


Figure 3-35: Length change of mortar containing GG replacement of Type IL cement.

Conversely, when the ground glass replacement was limited to 5% or 10% and amended with higher amounts of Class C fly ash, the dimensional instability exhibited in binary mixtures was greatly reduced as shown in Figure 3-36 and Figure 3-37. The combinatory effect of ground glass and C ash ends up being more beneficial in terms of dimensional stability than either SCM in a binary system, likely due to increased stability from long-term pozzolanic activity between the SCM of different elemental chemistries.

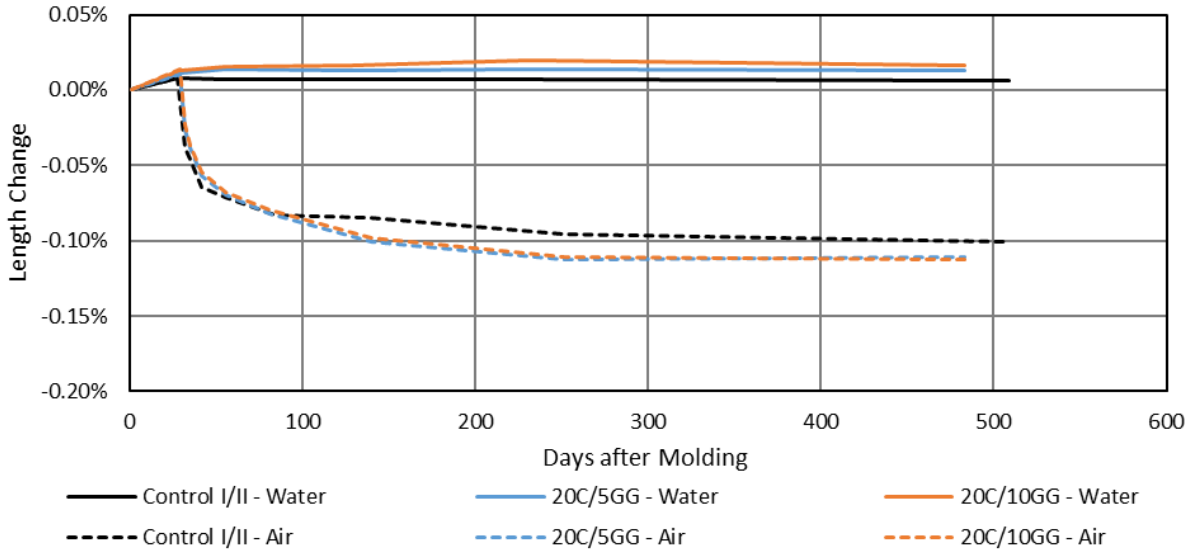


Figure 3-36: Length change of mortar containing a ternary blend of C ash and GG replacement of Type I/II cement.

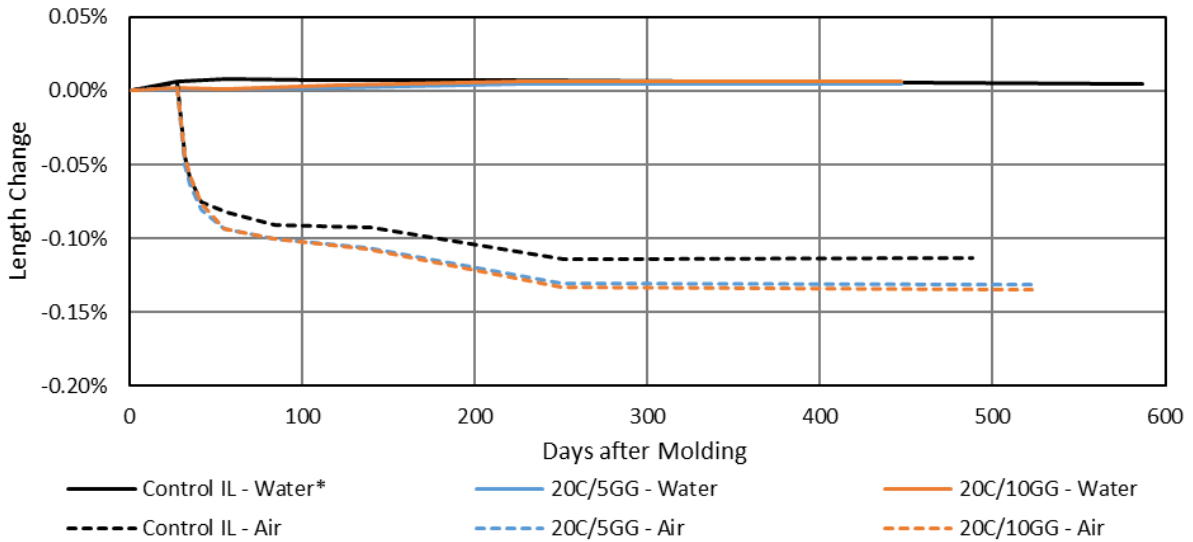


Figure 3-37: Length change of mortar containing a ternary blend of C ash and GG replacement of Type IL cement.

The binary mixtures containing 4% silica fume in both the Type I/II and Type IL system had minimal effect on the dimensional stability of the mortar. This performance was expected as the presence of silica fume in a non-aggressive environment is not anticipated to have a large effect on mortars; only when in an aggressive environment are the benefits of silica fume generally realized. Similarly, the addition of volcanic rock had minimal effect on the dimensional stability of the mortar; however, based upon other evaluation methods such as

compressive strength, isothermal calorimetry, and durability testing, it is presumed that this is due to the non-reactive nature associated with ground volcanic rock. Neither material exhibited expansion or shrinkage deviations from control by more than 0.010% as shown in Figure 3-38 and Figure 3-39.

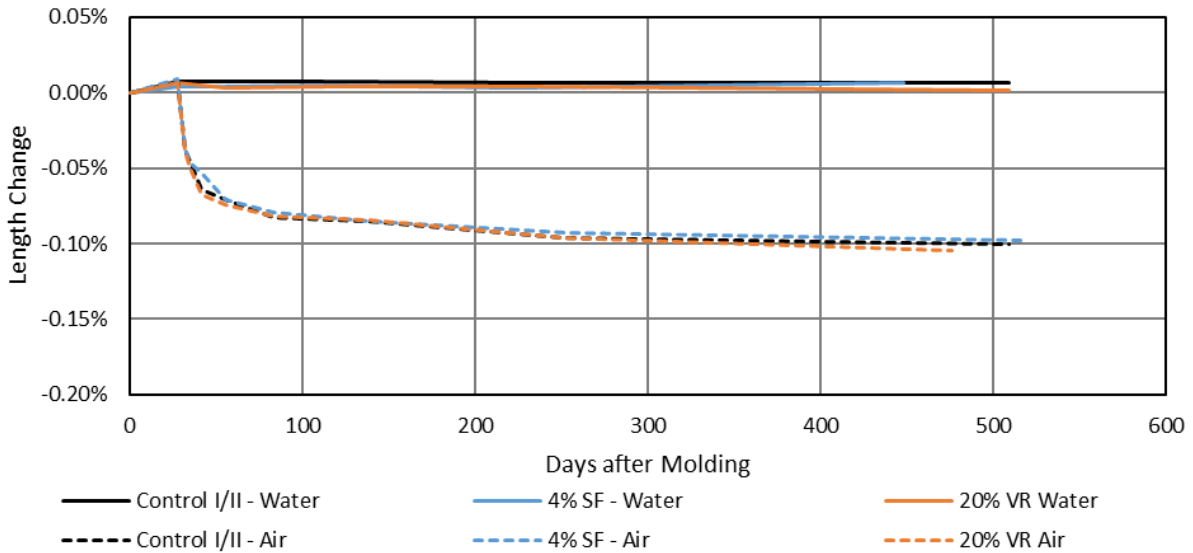


Figure 3-38: Length change of mortar containing SF or VR replacement of Type I/II cement.

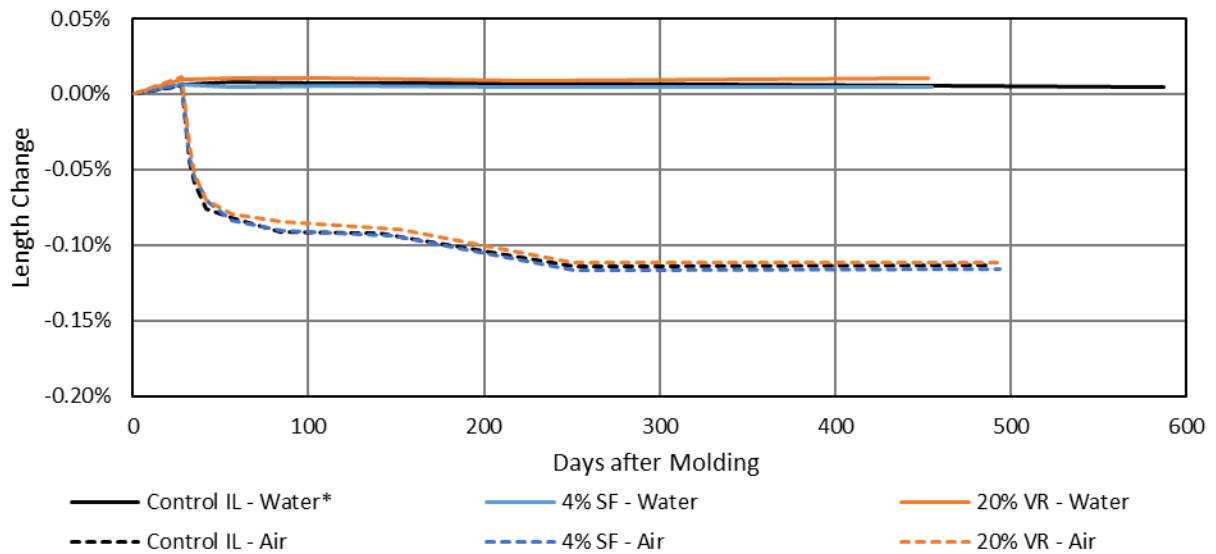


Figure 3-39: Length change of mortar containing SF or VR replacement of Type IL cement.

Interestingly, when the ground volcanic rock was included into a ternary blended system with 30% Class C fly ash as a replacement for Type I/II cement, the results showed less shrinkage in the air-cured bars and more expansion in the water-cured bars than the control.

While these differences are not more than 0.04%, this indicates the potential for cracking in the system between these three materials as the expansion of volcanic rock and Class C fly ash in binary systems was virtually identical to control; whereas when combined together, resulted in expansion. This is further supported by the reduction in compressive strength of the same mix as denoted in Figure 3-18. The silica fume additions in the ternary blended systems did not appear to significantly alter the dimensional stability of the mortars.

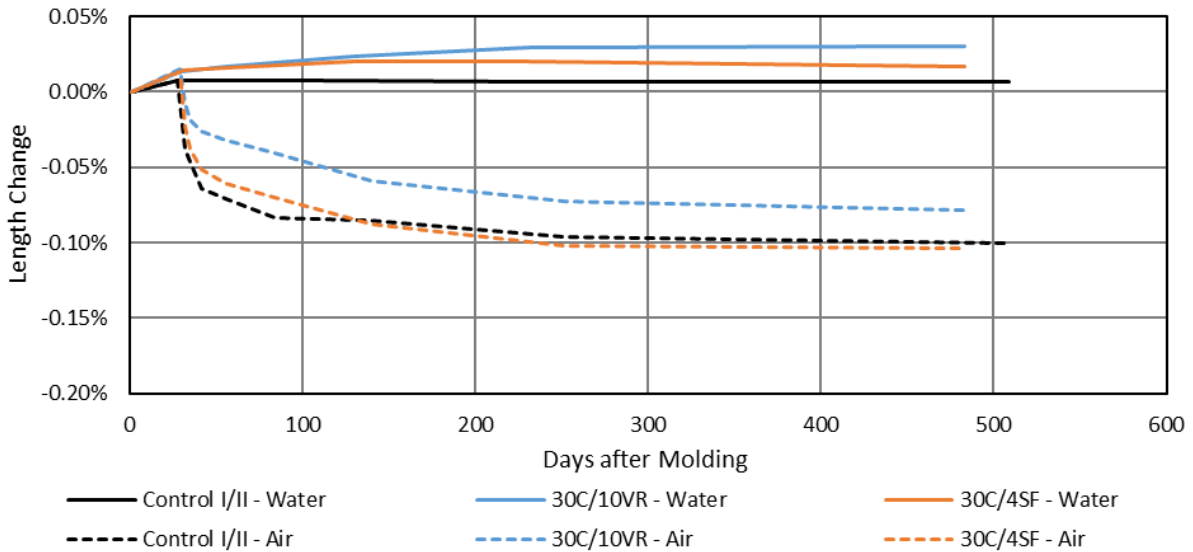


Figure 3-40: Length change of mortar containing a ternary blend of C ash and VR or SF replacement of Type I/II cement.

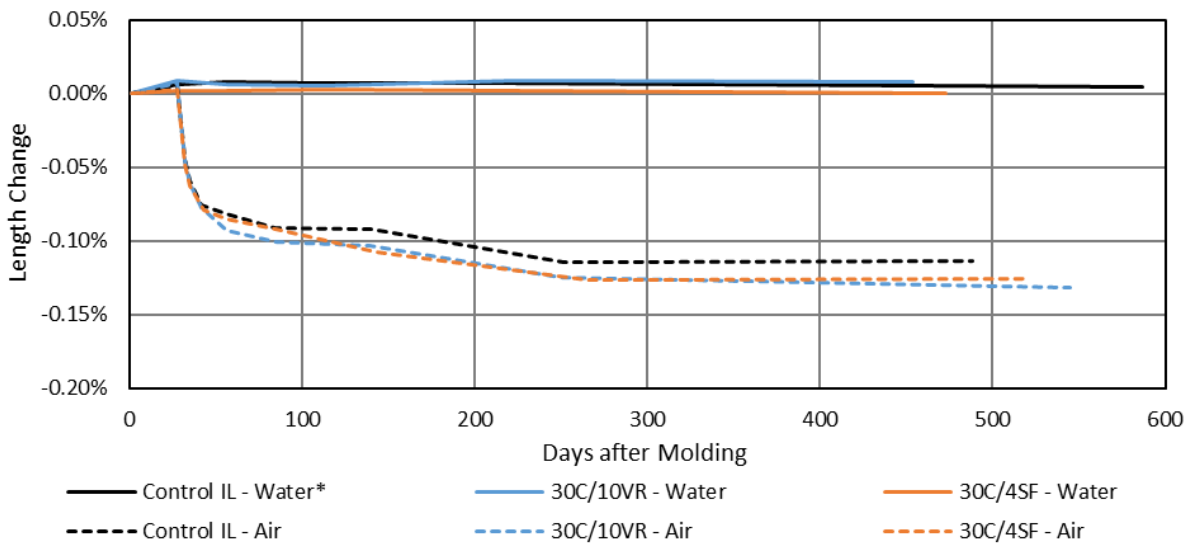


Figure 3-41: Length change of mortar containing a ternary blend of C ash and VR or SF replacement of Type IL cement.

The addition of Class F fly ash as a binary replacement for Type I/II and Type IL cement performed as anticipated with the inclusion having essentially no effect on the dimensional stability of the mortar in a non-aggressive environment, similar to silica fume, as evidenced in Figure 3-42 and Figure 3-43. The same cannot be said of the 20% Class C fly ash replacements, which exhibited 0.042% more shrinkage in the Type I/II cement system than the control; 30% replacement of C ash exhibited 0.036% more shrinkage. Neither replacement percentage in either cement system exhibited significant expansion after 64 weeks of curing.

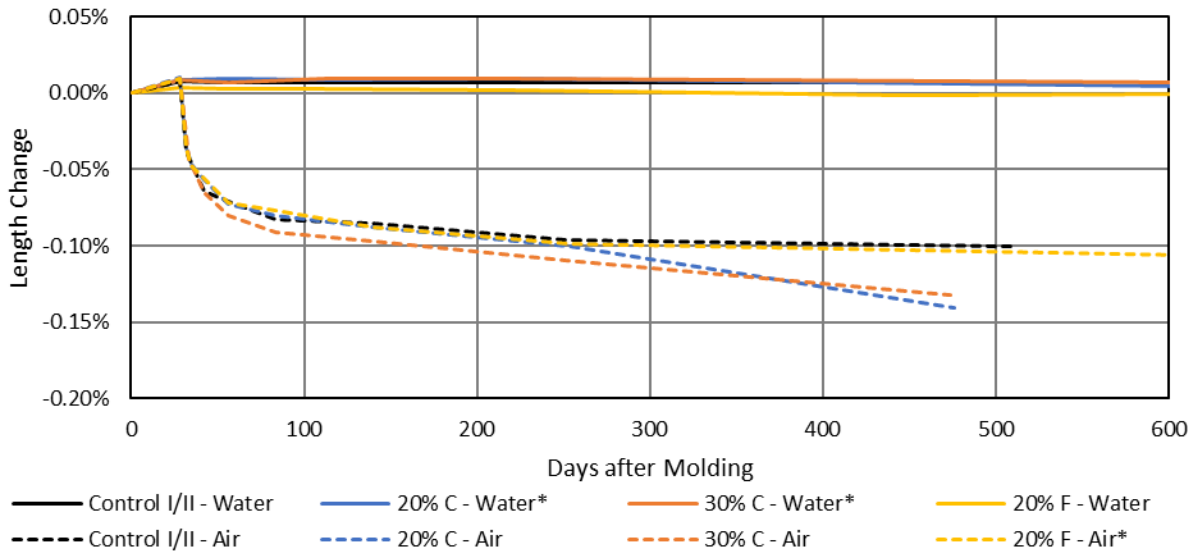


Figure 3-42: Length change of mortar containing C ash or F ash replacement of Type I/II cement.

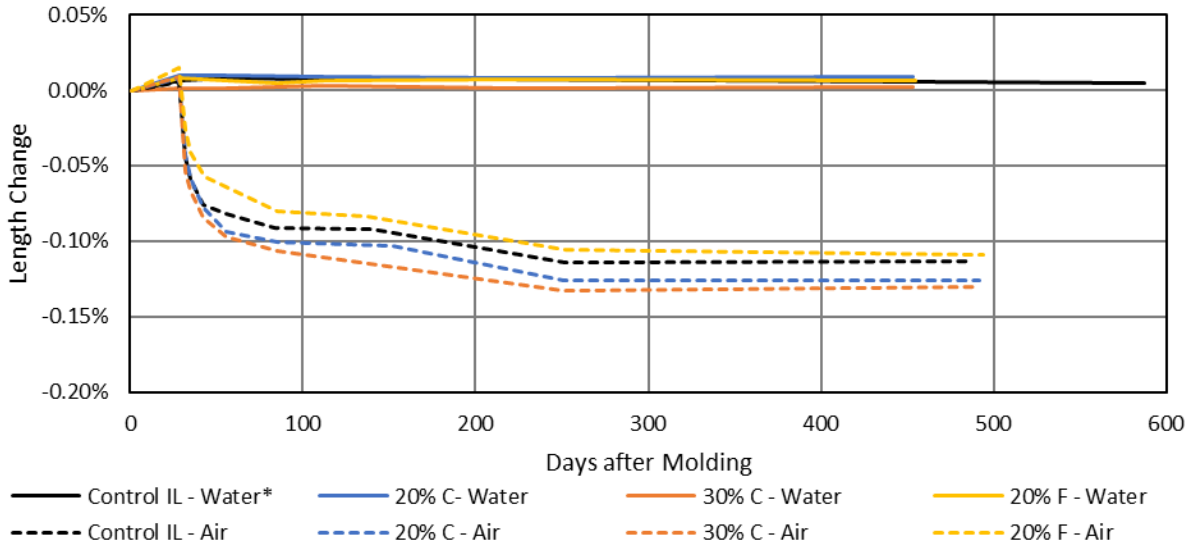


Figure 3-43: Length change of mortar containing C ash or F ash replacement of Type IL cement.

For mixes where a 5% or 10% replacement of Class F fly ash was blended along with 30% Class C fly ash (Figure 3-44 and Figure 3-45), the shrinkage associated with the binary replacements compared to the use of Class C fly ash alone was almost entirely diminished. The largest deviation from control, shown in Figure 3-45, was 0.014% more shrinkage exhibited by the 30% C ash and 5% F ash blend in the Type IL mixture.

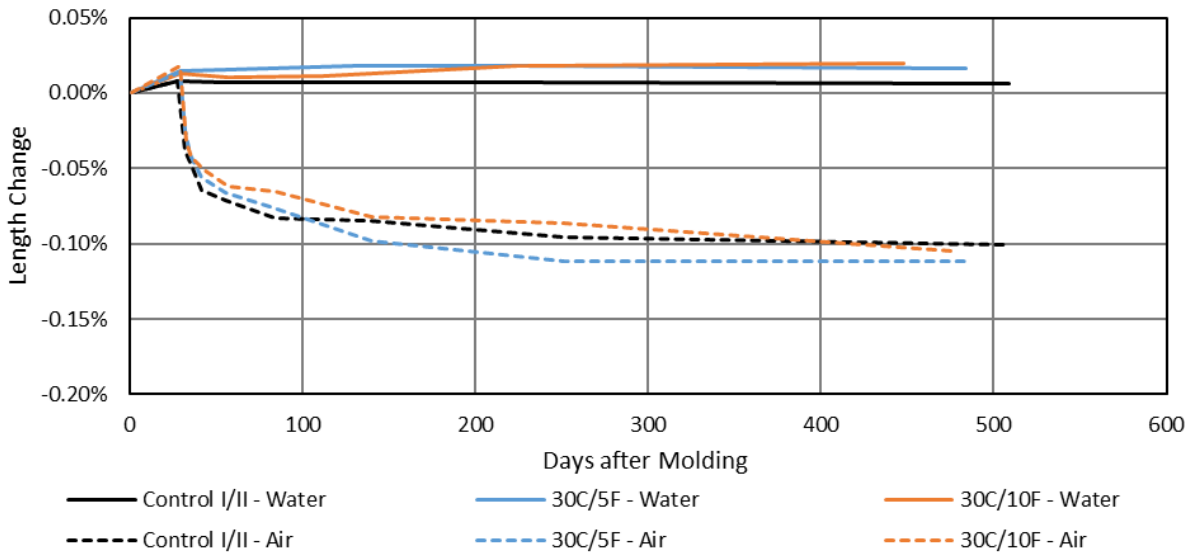


Figure 3-44: Length change of mortar containing a ternary blend of C ash and F ash replacement of Type I/II cement.

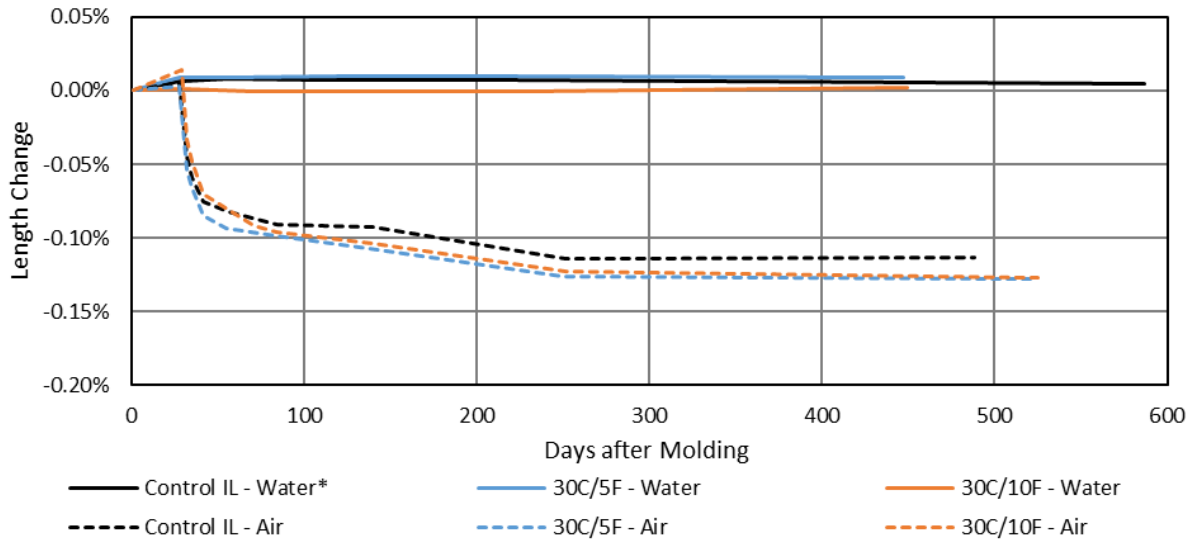


Figure 3-45: Length change of mortar containing a ternary blend of C ash and F ash replacement of Type IL cement.

A potential reason for the drying shrinkage in many of the mixtures being greater than the control can be found in the modulus of elasticity results. A lower value for modulus often results in a higher level of drying shrinkage [156]. Most of the mixes incorporating SCM had a lower modulus of elasticity than the respective control. However, it is difficult to directly compare the mortar mixtures with the concrete mixtures, as there are several variables that are different between the two. A potential reason for the drying shrinkage in many of the mixtures being greater than the control can be found in the modulus of elasticity results. A lower value for modulus often results in a higher level of drying shrinkage [156]. Most of the mixes incorporating SCM had a lower modulus of elasticity than the respective control. However, it is difficult to directly compare the mortar mixtures with the concrete mixtures, as there are several variables that are different between the two

3.2.5 Alkali-Silica Reaction – ASTM C1567

This test method can detect the potential for alkali-silica reaction in a cementitious material and aggregate combination. The accelerated mortar bar method can also be compared with the concrete prism test (ASTM C1293) in order to evaluate its adequacy with respect to unconventional SCM. The accelerated mortar bar method is conducted for 14 days of exposure but can be extended. It involves sieving the aggregate to develop a specific gradation prescribed by the test method. The bars are demolded and measured, put into a 1N sodium hydroxide

solution, and measured over time at 80°C. The percent expansion is calculated and reported. A range of expansion values is given as a guideline to determine if a material is deleterious. If the mortar expands beyond 0.10%, it indicates that the aggregate used may be alkali-silica reactive.

Alkali silica reaction (ASR) is a deleterious chemical interaction between alkali ions in concrete pore solution and reactive silica in aggregates. The reaction produces a gel, which expands in the presence of water, causing the concrete to crack [157–159]. The use of SCM can reduce the expansion caused by ASR through the densification of the concrete microstructure and reduction of permeability, thus reducing the potential for the gel to absorb water. Additionally, the alumina supplied by some SCM can bind to the alkalis in the pore solution, which decreases the production of expansive gel [73]. Two of the most well-known methods for evaluating the potential for ASR are ASTM C1567 and ASTM C1293; ASTM C1567 is an accelerated mortar bar test that is completed at 80°C for a period of 14 days, while ASTM C1293 is evaluated at 40°C for 24 months if the concrete contains SCM. Alkali-silica reaction (ASR) is a deleterious chemical interaction between alkali ions in concrete pore solution and reactive silica in aggregates. The reaction produces a gel, which expands in the presence of water, causing the concrete to crack [157–159]. The use of SCM can reduce the expansion caused by ASR through the densification of the concrete microstructure, thus reducing the potential for the gel to absorb water. Additionally, the alumina supplied by some SCM can bind to the alkalis in the pore solution, which decreases the production of expansive gel [73]. Two of the most well-known methods for evaluating the potential for ASR are ASTM C1567 and ASTM C1293; ASTM C1567 is an accelerated mortar bar test that is completed at 80°C for a period of 14 days while ASTM C1293 is evaluated at 40°C for 24 months if the concrete contains SCM.

3.2.5.1 Accelerated Mortar Bar Method using Florida Sand

The mixtures in this section use Florida sand, which is a non-reactive aggregate. Florida sand was used to determine if these materials or replacement levels can induce ASR. The accelerated mortar bar method was used for the mixes below, with the exception of grading the Florida sand, because it is meant to be an application with typical Florida sand which is naturally much finer than the gradation allows for in the testing specification.

3.2.5.1.1 Portland Cement

As anticipated, the control mixture with Florida sand showed essentially no expansion and is not indicative of a mix that would be expected to have the potential to be susceptible to alkali-silica reactivity. The control mixtures for the Type I/II cement and the Type IL cement are shown together in Figure 3-46.

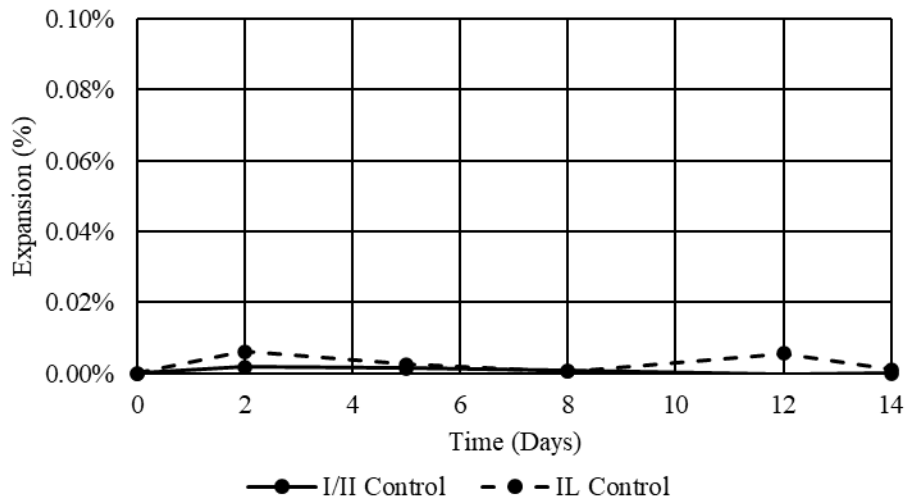


Figure 3-46: Accelerated ASR results using Florida sand and Type I/II and Type IL cements.

3.2.5.1.2 Class F Fly Ash

The inclusion of Class F fly ash showed a marginal level of expansion, but this level of expansion is not of concern as the threshold for potentially concerning expansion is 0.10% and the 20% Class F fly ash mix expanded to approximately 0.01% as shown in Figure 3-47.

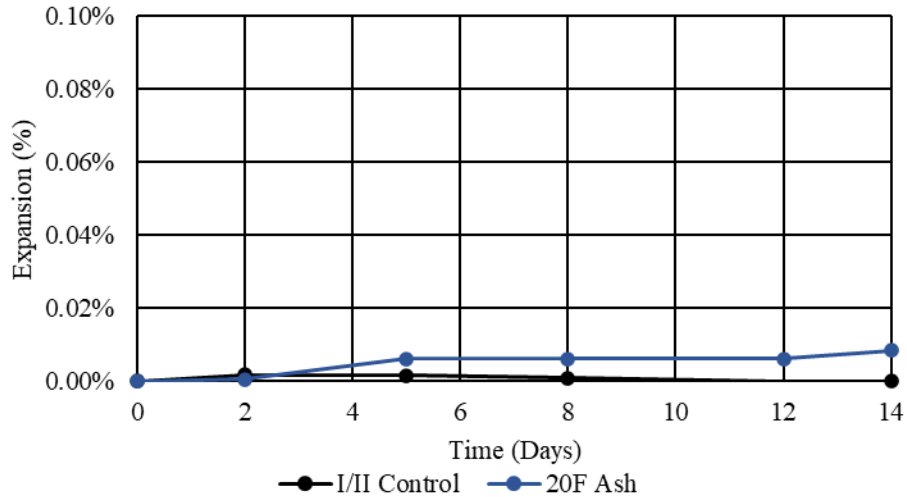


Figure 3-47: Accelerated ASR results using Florida sand and F ash with Type I/II cement.

The expansion of the Class F fly ash as 20% Type IL cement replacement showed marginally more expansion than in the Type I/II cementitious system as seen in Figure 3-48; however, this level of expansion is negligible and below the threshold of potentially deleterious.

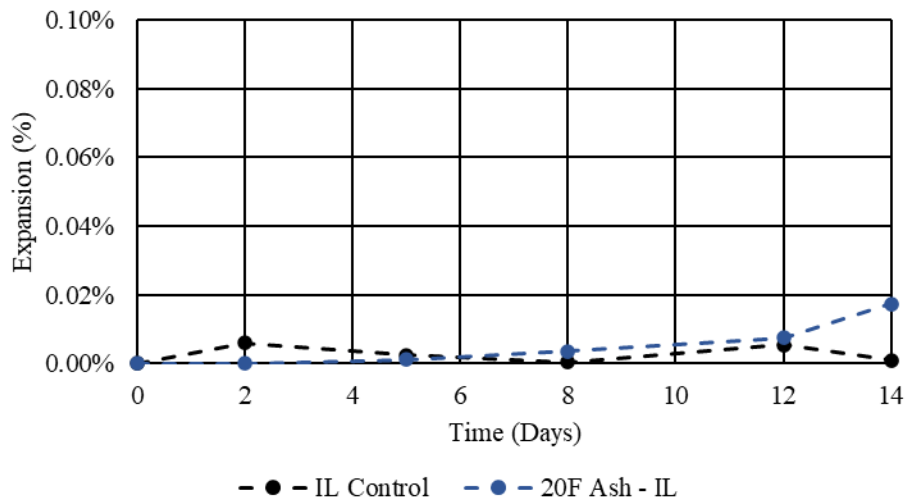


Figure 3-48: Accelerated ASR results using Florida sand and F ash with Type IL cement.

3.2.5.1.3 Class C Fly Ash

The addition of Class C fly ash performed similarly to the Class F fly ash mixtures even at 30% replacement. Despite the larger particles at the high end of the particle size distribution curve for Class C fly ash and the amorphous content, it would appear that the benefits from having finer particles toward the lower end of the particle size distribution reduced permeability

allowing for increased resistance to ASR. The total expansion of the 30% Class C fly ash mix expanded to 0.02%, which is below the 0.10% expansion threshold (Figure 3-49).

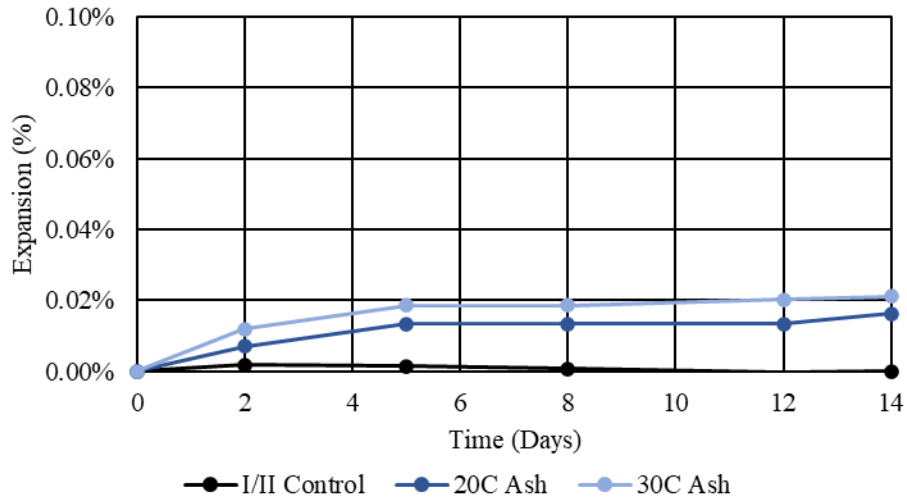


Figure 3-49: Accelerated ASR results using Florida sand and C ash with Type I/II cement.

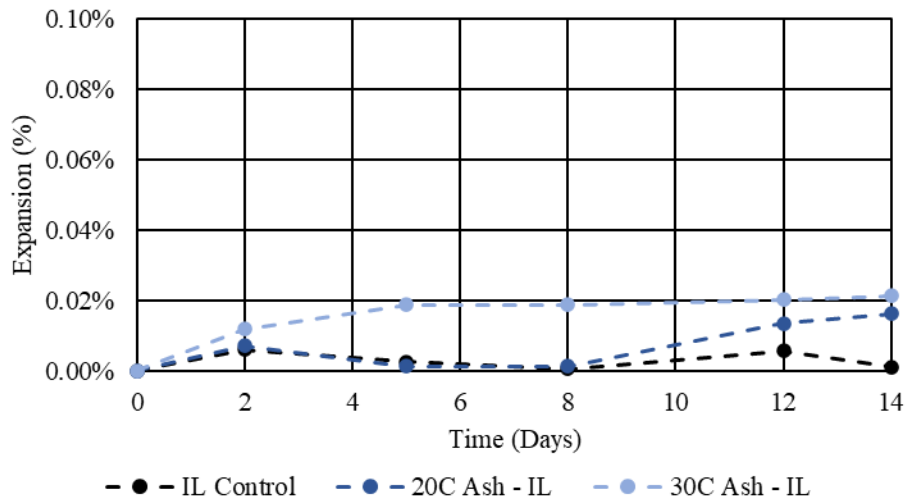


Figure 3-50: Accelerated ASR results using Florida sand and C ash with Type IL cement.

3.2.5.1.4 Silica Fume

The addition of the silica fume, Figure 3-51, showed similar expansion to the fly ash mixes. This result was not surprising as the chemical composition of the silica fume is most similar to the fly ash mixes (amorphous silica) and the ground glass, although the ground glass mixture contains significant quantities of alkalis as well. The maximum expansion at 14 days of 0.02% was well below the threshold of concern and does not present any issues of compatibility

in the Type I/II cementitious system when combined with Florida sand as a fine aggregate. The addition of silica fume to the limestone cement reduced expansion further as seen in Figure 3-52; again, this reduces the level of expansion even further below the threshold level of concern.

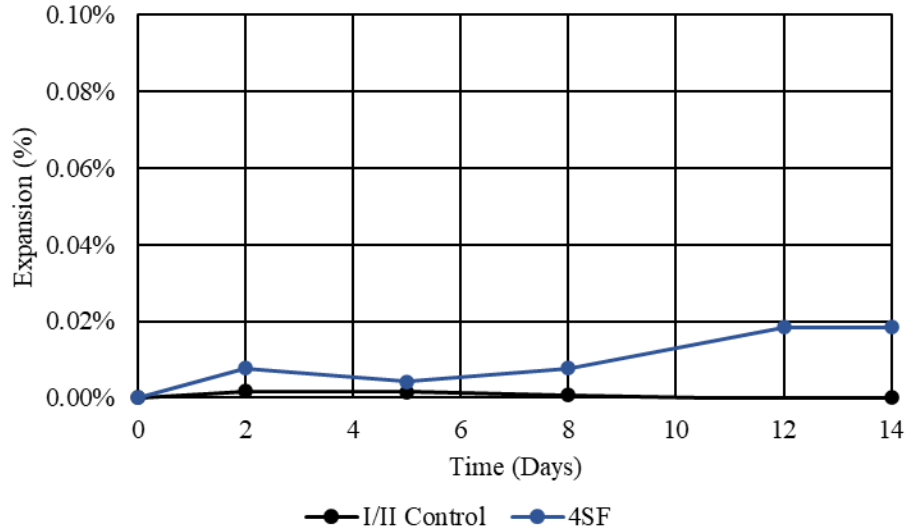


Figure 3-51: Accelerated ASR results using Florida sand and SF with Type I/II cement.

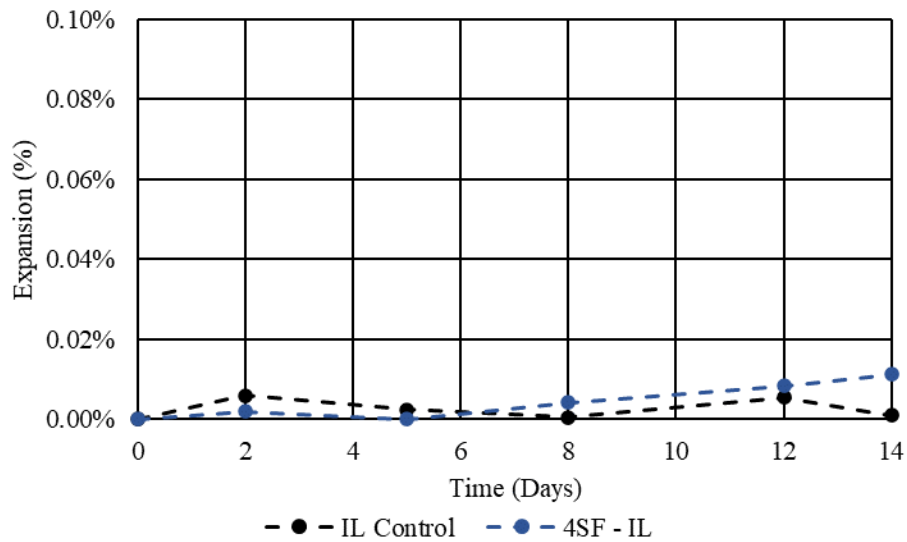


Figure 3-52: Accelerated ASR results using Florida sand and SF with Type IL cement.

3.2.5.1.5 Sugarcane Bagasse Ash

The incorporation of 10% SCBA-A resulted in approximately 0.015% expansion, but the 20% and 30% SCBA-A mixtures showed approximately 0.04% and 0.08% expansions as shown in Figure 3-53. While these values are not above the threshold level of 0.10%; it is conceivable

that higher levels of inclusion, while not tested nor confirmed, may result in expansions beyond 0.10% in this test method. This behavior was noted by Ferraro et al. and was attributed to the potential for the SCBA-A to agglomerate and create large pockets of concentrated reactive silica [8].

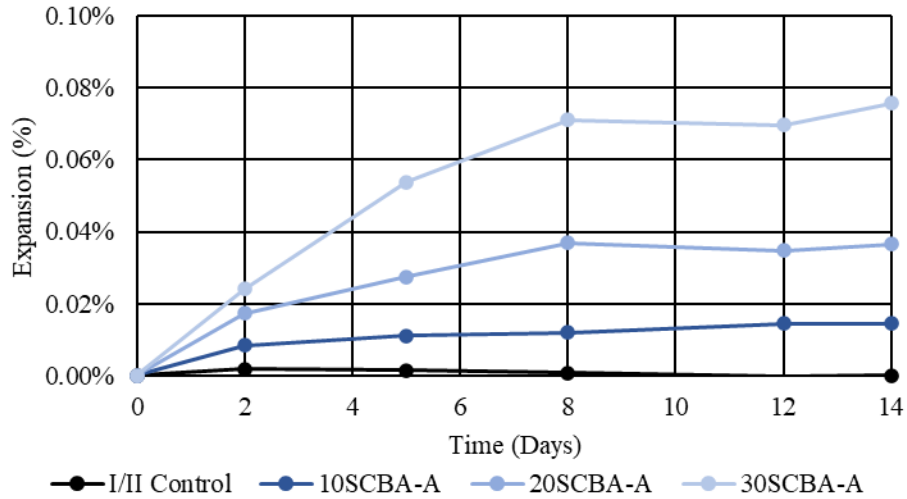


Figure 3-53: Accelerated ASR results using Florida sand and SCBA-A with Type I/II cement.

The higher concentration of crystalline material in the SCBA-B resulted in less alkali-silica reactivity even at 30%, with 14-day expansions of approximately 0.02%, Figure 3-54. With a replacement of 10% SCBA-B, the expansion at 14 days was 0.0%, identical to the control mixture. It is clear that the processing of the sugarcane bagasse ashes led to performance differences between the two materials not only in workability as seen by the mortar flow results, but also with respect to potential for alkali-silica reactivity.

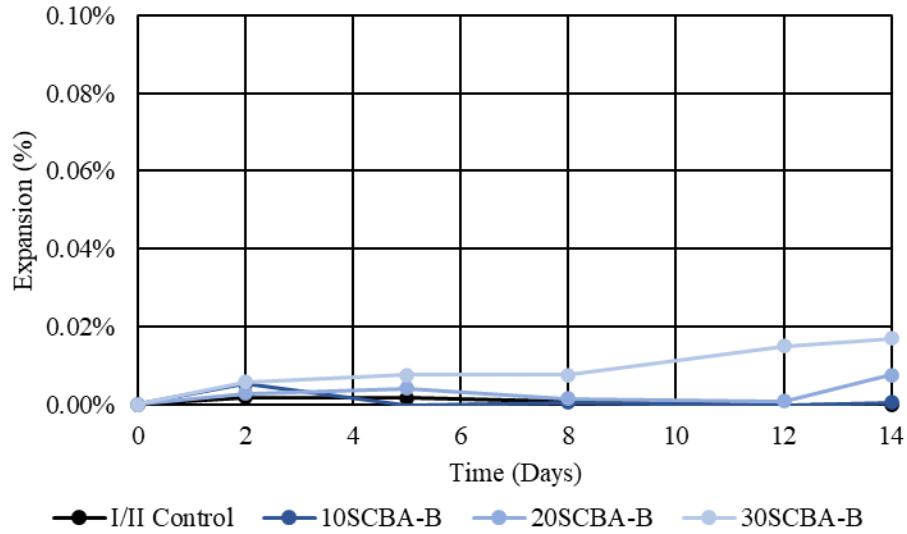


Figure 3-54: Accelerated ASR results using Florida sand and SCBA-B with Type I/II cement.

For binary Type IL- SCBA-A, the tendency for an alkali-silica reaction appeared to be reduced compared to the Type I/II cementitious system as can be seen in Figure 3-55 compared to the expansion in the Type I/II cementitious system. Hooton et al. reported that little research has been done on the effects of limestone cement on ASR, with research showing delays, but not mitigation of ASR; however, it would be expected that the use limestone cement would result a slight increase in resistance due to the dilution of cement alkalis [160].

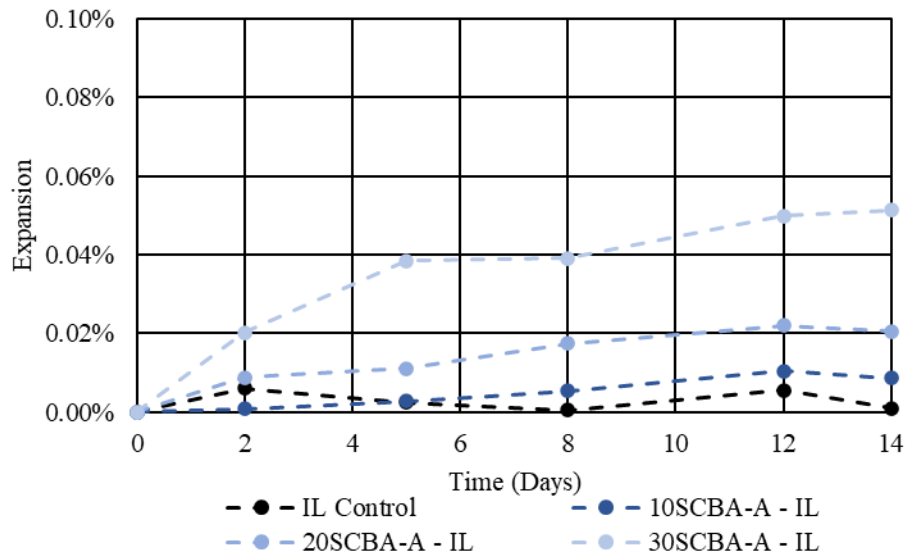


Figure 3-55: Accelerated ASR results using Florida sand and SCBA-A with Type IL cement.

The performance of SCBA-B in the Type IL cementitious system follows a similar trend of the SCBA-A wherein the expansion in the Type IL cement is slightly reduced compared to that of the Type I/II cement as can be seen in Figure 3-56.

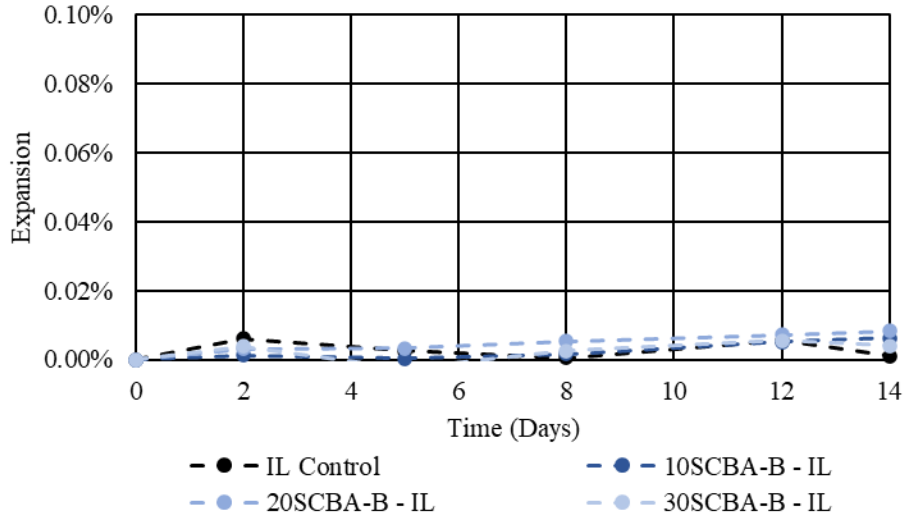


Figure 3-56: Accelerated ASR results using Florida sand and SCBA-B with Type IL cement.

3.2.5.1.6 Ground Glass

The inclusion of the ground glass into the mortar mixes in both cementitious systems of Type I/II cement and Type IL cement are provided for completeness, however, they do not follow the ASTM specification as the alkali content of the SCM is too high (13%). ASTM C1567 notes that ASTM C1293 should be used for mortars containing SCM with alkali contents above 4% because ASTM C1567 may incorrectly indicate a low probability for ASR. Figure 3-57 and Figure 3-58 show expansions that are very low, however these results are unreliable and must be confirmed by ASTM C1293 prior to being accepted as valid.

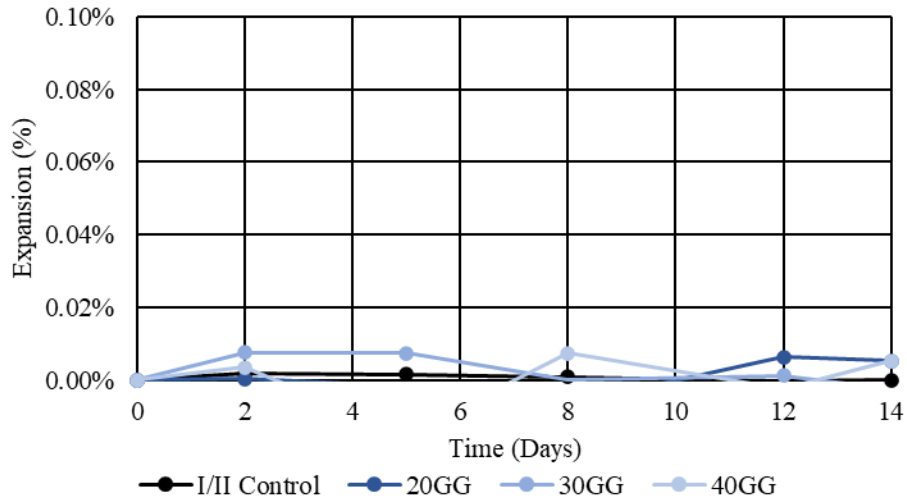


Figure 3-57: Accelerated ASR results using Florida sand and GG with Type I/II cement.

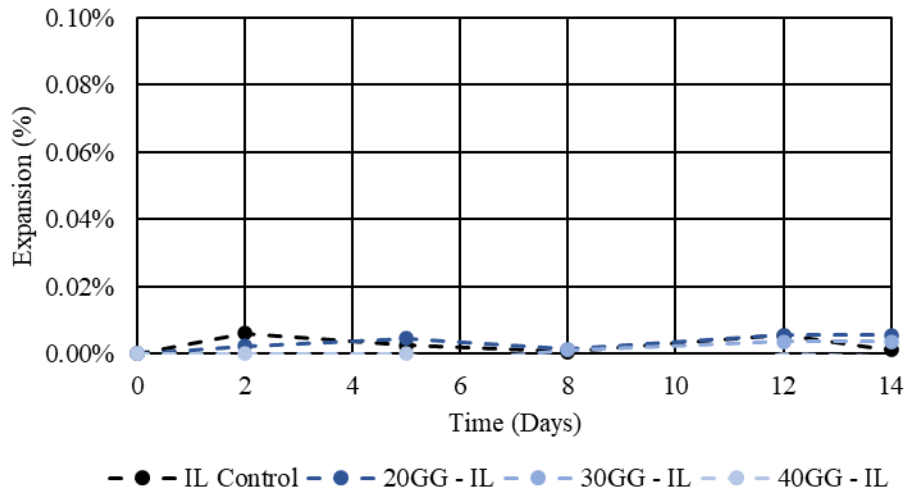


Figure 3-58: Accelerated ASR results using Florida sand and GG with Type IL cement.

3.2.5.1.7 Volcanic Rock

The ground volcanic rock showed no expansion in either cementitious system owing largely to the crystalline nature of the material, which leads to very low reactivity as shown in Figure 3-59 and Figure 3-60.

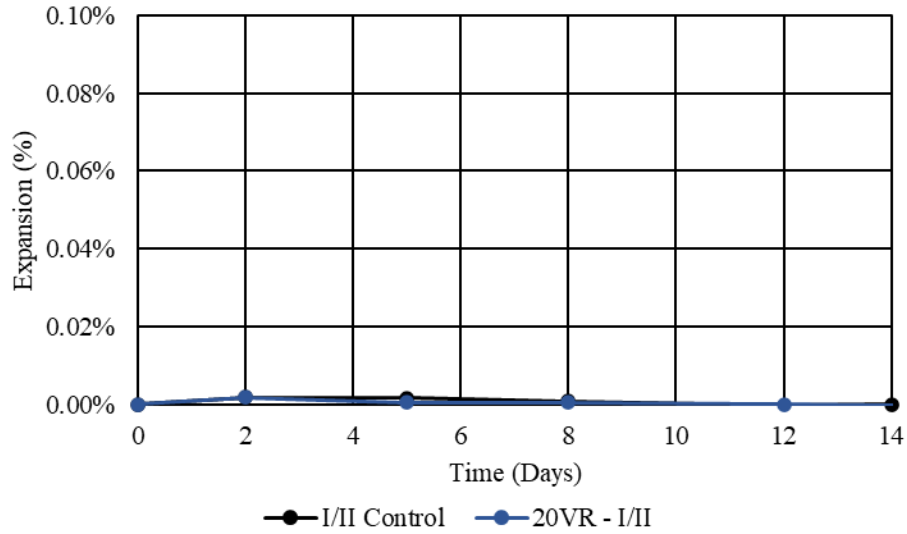


Figure 3-59: Accelerated ASR results using Florida sand and VR with Type I/II cement.

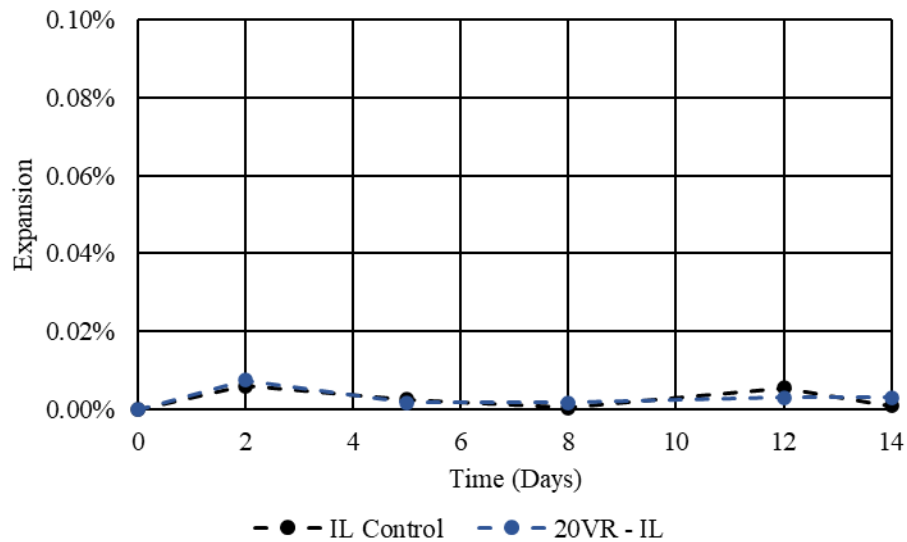
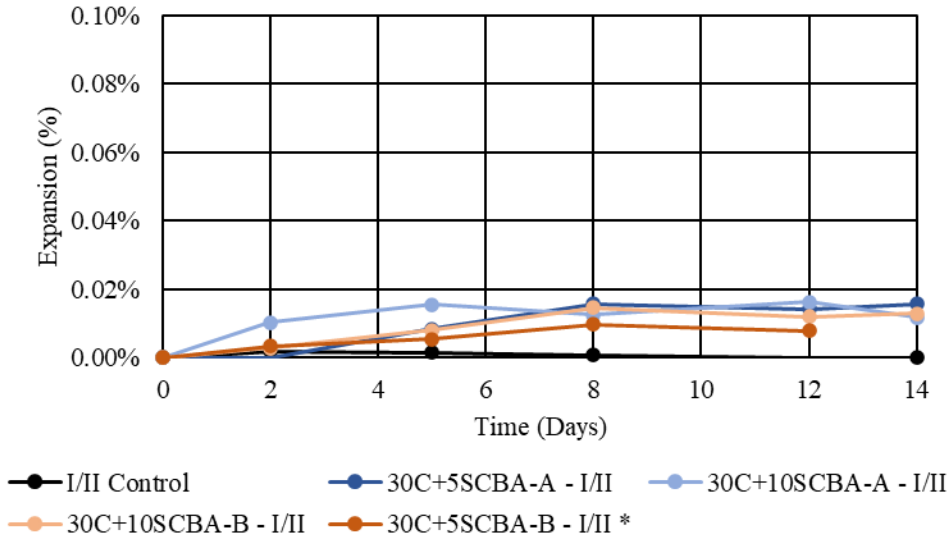


Figure 3-60: Accelerated ASR results using Florida sand and VR with Type IL cement.

3.2.5.1.8 Ternary Mixtures

As to be expected from combining several materials that did not produce deleterious reactions, the ternary blended mortars using 20 – 30% Class C fly ash with other SCM did not produce expansions in excess of 0.04% in any mixture, regardless of the cement type used, as can be seen in Figure 3-61 through Figure 3-63. Unsurprisingly, the largest expansions were caused by ternary blends incorporating sugarcane bagasse ash; however, the amount of SCBA was limited to 10% maximum, and therefore the expansion was mild.



*Results plotted until day 12 due to container failure on day 14.

Figure 3-61: Accelerated ASR results using Florida sand for ternary mixes incorporating SCBA with Type I/II cement.

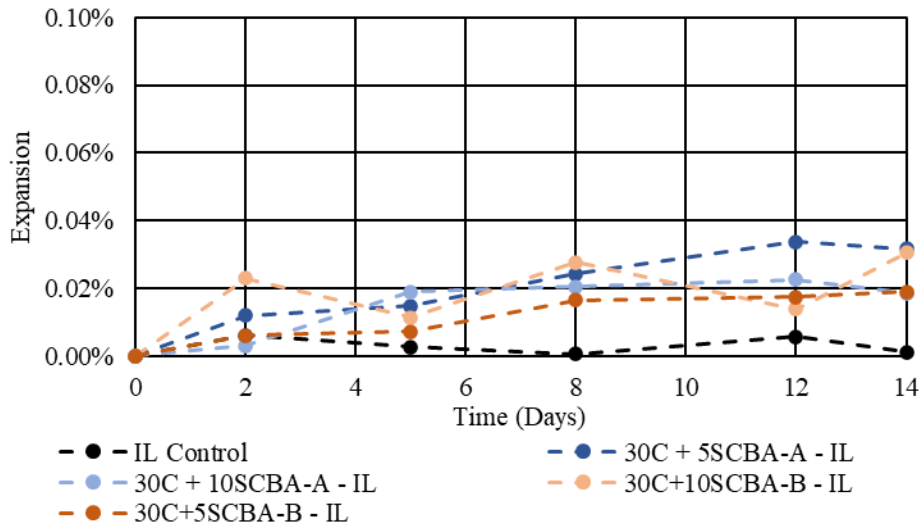


Figure 3-62: Accelerated ASR results using Florida sand for ternary mixes incorporating SCBA with Type IL cement.

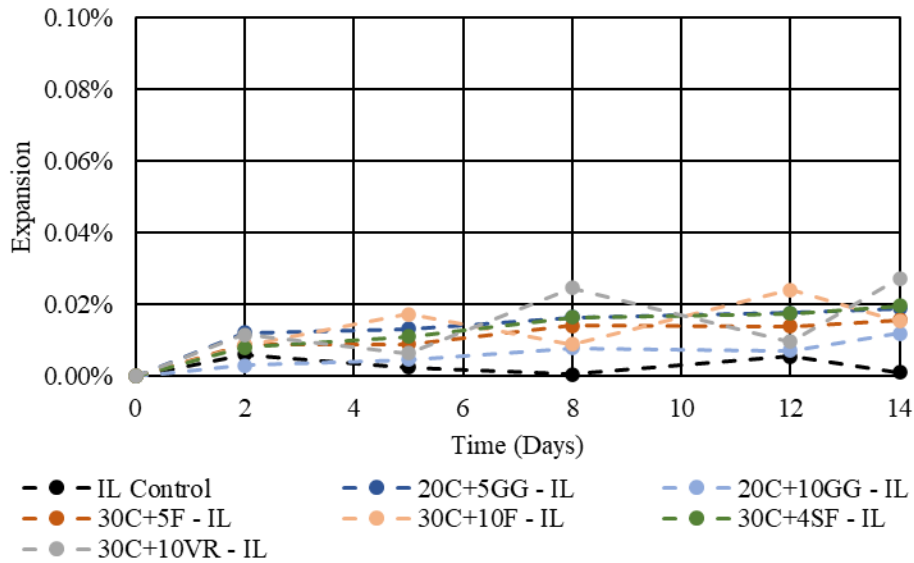


Figure 3-63: Accelerated ASR results using Florida sand for ternary mixes incorporating GG, F ash, VR, and SF with Type IL cement.

A summary of the 14-day expansion of the of the mortar mixes containing either Type I/II or Type IL cement with Florida fine aggregate in modified ASTM C1567 is presented in Table 3-8. The largest expansion observed was the 30% SCBA-A replacement of the Type I/II cement, which had a final expansion of 0.08% that is below the 0.10% threshold for potentially deleterious expansion. Therefore, based upon the evaluation, each of the material combinations would be deemed to not pose a threat of producing damaging expansion due to alkali-silica reactivity.

With the potential for alkali-silica reactivity of the supplementary cementitious materials likely to be negligible, the next step of evaluation was to investigate the efficacy of the materials to prevent alkali-silica reactivity when combined with known reactive aggregate. This experimentation was performed on Jobe sand instead of Florida sand in the following section.

Table 3-8: ASTM C1567 14-day expansions of mortars with Florida sand using Type I/II or Type IL cement and SCM.

Mix	14 Day Expansion	Mix	14 Day Expansion
OPC - Type I/II	0.00%	OPC - Type IL	0.00%
Binary Mixes		Binary Mixes	
10SCBA-A	0.01%	10SCBA-A	0.01%
20SCBA-A	0.04%	20SCBA-A	0.02%
30SCBA-A	0.08%	30SCBA-A	0.05%
10SCBA-B	0.00%	10SCBA-B	0.01%
20SCBA-B	0.01%	20SCBA-B	0.01%
30SCBA-B	0.02%	30SCBA-B	0.00%
20GG	0.01%*	20GG	0.01%*
30GG	0.00%*	30GG	0.00%*
40GG	0.01%*	40GG	0.00%*
20VR	0.00%	20VR	0.00%
20C	0.02%	20C	0.02%
30C	0.02%	30C	0.02%
20F	0.01%	20F	0.02%
4SF	0.02%	4SF	0.01%
Ternary Mixes		Ternary Mixes	
30C+5SCBA-A	0.02%	30C+5SCBA-A	0.03%
30C+10SCBA-A	0.02%	30C+10SCBA-A	0.02%
30C+5SCBA-B	0.00%	30C+5SCBA-B	0.02%
30C+10SCBA-B	0.01%	30C+10SCBA-B	0.03%
20C+5GG	0.01%*	20C+5GG	0.02%*
20C+10GG	0.01%*	20C+10GG	0.01%*
30C+10VR	0.01%	30C+10VR	0.03%
30C+5F	0.01%	30C+5F	0.02%
30C+10F	0.02%	30C+10F	0.02%
30C+4SF	-	30C+4SF	0.02%

*Note: The results of the ground glass expansion in ASTM C1567 with Jobe sand are presented for completeness. The results are not valid due to the high alkali content of the glass. The mitigation potential of the glass must be evaluated with a different method that does not restrict the alkali content, such as ASTM C1293.

3.2.5.2 Accelerated Mortar Bar Method using Jobe Sand

The mixtures in this section only involve the alternative SCM. The purpose of using Jobe sand is to determine the ability of each material/replacement to decrease expansion caused by alkali-silica reactivity and the conventional materials (fly ashes and silica fume) are known to reduce permeability enough to mitigate ASR. The mixture proportions of the ASR mixes containing Type I/II cement and Jobe sand with the alternative supplementary cementitious materials is provided in Table 3-9. While the mixture proportions of the ASR mixes containing

Type II cement and Jobe sand with the alternative supplementary cementitious materials is provided in Table 3-10.

Table 3-9: Mortar mix proportions (in lb/yd³) with Type I/II cement and Jobe sand for ASTM C1567.

Mix	I/II Cement	Sand	Water	SCBA-A	SCBA-B	GG	VR
Control	1,032	2,322	485	-	-	-	-
10SCBA-A	924	2,309	483	103	-	-	-
20SCBA-A	817	2,296	480	204	-	-	-
30SCBA-A	711	2,284	478	305	-	-	-
10SCBA-B	922	2,306	481	-	102	-	-
20SCBA-B	814	2,290	478	-	204	-	-
30SCBA-B	708	2,275	475	-	303	-	-
20GG	814	2,290	478	-	-	204	-
30GG	708	2,275	475	-	-	303	-
40GG	603	2,260	472	-	-	402	-
20VR	821	2,309	482	-	-	-	205

Table 3-10: Mortar mix proportions (in lb/yd³) with Type II cement and Jobe sand for ASTM C1567.

Mix	II Cement	Sand	Water	SCBA-A	SCBA-B	GG	VR
Control	1027	2310	483	-	-	-	-
10SCBA-A	920	2299	480	102	-	-	-
20SCBA-A	813	2288	478	203	-	-	-
30SCBA-A	708	2276	476	304	-	-	-
10SCBA-B	918	2296	479	-	102	-	-
20SCBA-B	811	2282	477	-	203	-	-
30SCBA-B	705	2268	473	-	302	-	-
20GG	815	2294	479	-	-	204	-
30GG	711	2285	478	-	-	305	-
40GG	607	2277	476	-	-	405	-
20VR	818	2300	480	-	-	-	204

The majority of the evaluated mixtures containing Jobe sand and alternative SCM (SCBA, GG, and VR) exceeded the expansion limit of 0.10% at 14 days. The only mixtures that exhibited expansions below 0.10% at 14 days were GG. However, the test method highlights that the results of ASTM C1567 are invalid when using an SCM with an alkali content of 4% or more. Therefore, the results of the GG mixtures are not valid, but indicate the necessity for evaluation with ASTM C1293.

3.2.5.2.1 Portland Cement

The expansion of the Jobe sand in the two different cementitious systems is presented in Figure 3-64. As seen previously with the Florida sand experiments, the Type IL cement expanded slightly less than the Type I/II cement. Both systems exhibit expansion well beyond what was observed with Florida sand (0.68% expansion for the Type I/II and 0.60% expansion for the Type IL cement); confirming that the Jobe sand is a known reactive aggregate and sufficient for use in this evaluation.

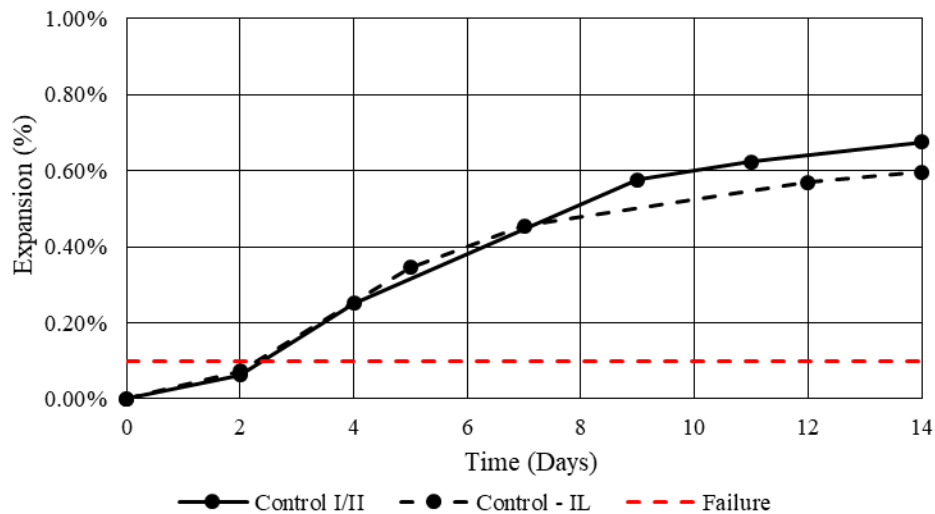


Figure 3-64: Accelerated ASR results using Jobe sand with Type I/II or Type IL cement.

3.2.5.2.2 Sugarcane Bagasse Ash (SCBA-A and SCBA-B)

The inclusion of the sugarcane bagasse ash at a 10% replacement resulted in expansion levels that were higher than the control; however, based on the precision and bias statement of the method, expansions within approximately 8% of each other are not statistically significant and the additional expansion caused by the 10% SCBA-A addition was on the borderline of that amount. This may be due to the SCBA-A providing a small amount of additional reactive silica without much benefit. Yet, when the replacement was increased to 20% or even 30% SCBA-A, the expansion level decreased considerably as seen in Figure 3-65. This level of expansion is beyond the threshold but does show that SCBA-A has some mitigating potential when incorporated.

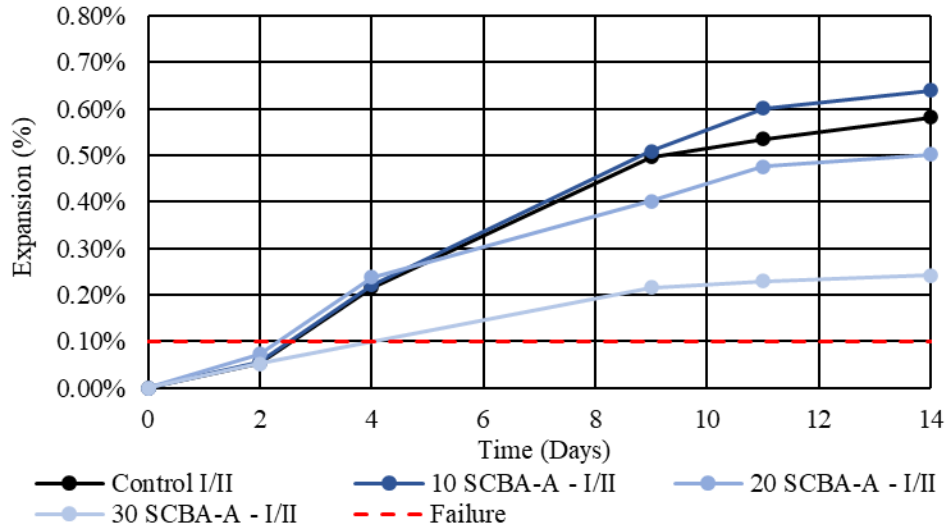


Figure 3-65: Accelerated ASR results using Jobe sand and SCBA-A with Type I/II cement.

When using SCBA-A and Type IL cement with the Jobe cement the overall expansions were less, which was the same trend that was observed when looking at the SCBA-A with Florida sand in the previous section, however, the total expansion even at 30% replacement was still considerably above the 0.10% threshold expansion limit for the method. The expansion of the 10%, 20%, and 30% SCBA-A additions to Type IL cement with Jobe sand are shown in Figure 3-66.

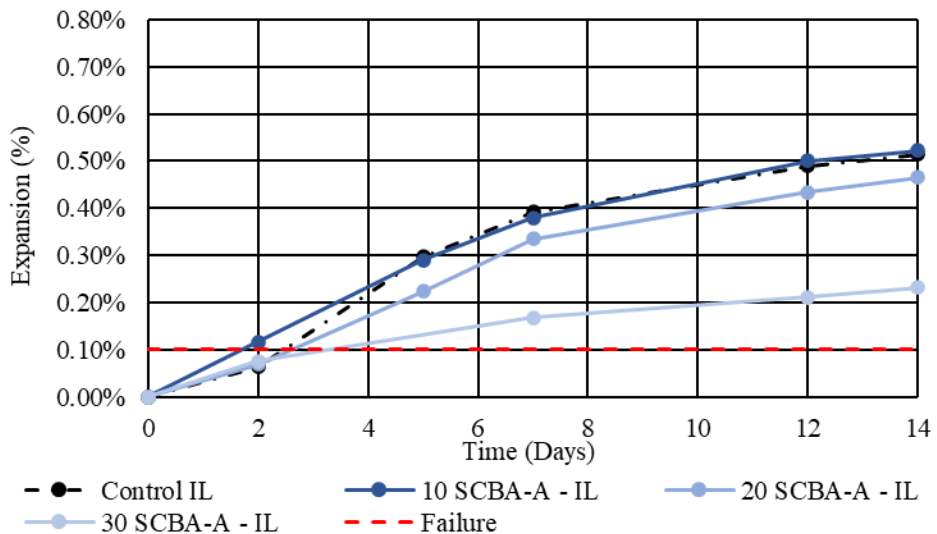


Figure 3-66: Accelerated ASR results using Jobe sand and SCBA-A with Type IL cement.

The inclusion of SCBA-A mitigated but did not completely suppress the expansion caused by ASR, as shown in Figure 3-65 and Figure 3-66. However, when evaluating SCBA-B

for ASR suppression, Figure 3-67 and Figure 3-68, the mitigating potential was considerably reduced.

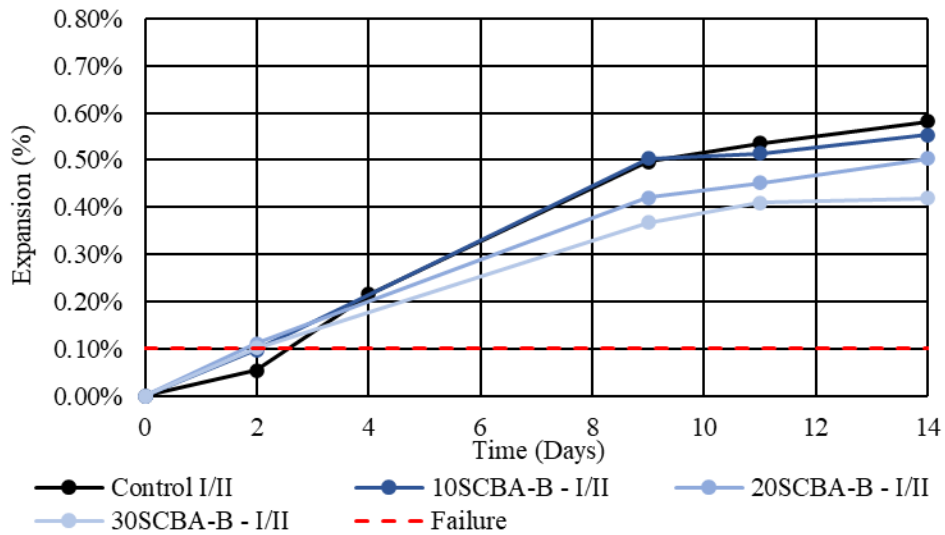


Figure 3-67: Accelerated ASR results using Jobe sand and SCBA-B with Type I/II cement.

As with the Type I/II cementitious system, when replacing Type IL cement with SCBA-B, the total expansion is reduced marginally, but not enough to consider the mixtures to have a low risk of expansion due to alkali-silica reactivity, as seen in Figure 3-68. The performance is indicative of some reactive silica being present; however, the lower amount of amorphous content detected in x-ray diffraction lends credence to the lower ASR resistance of the SCBA-B compared to SCBA-A in this test method.

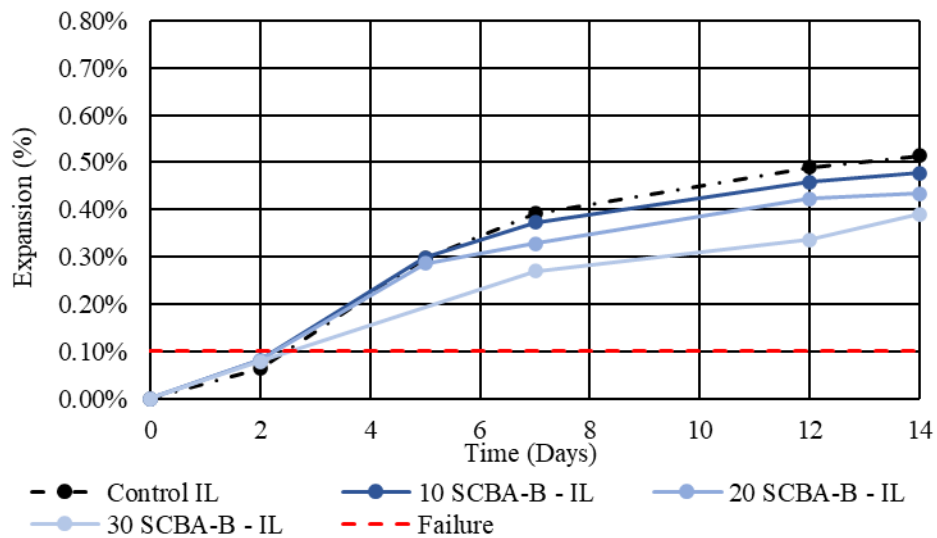


Figure 3-68: Accelerated ASR results using Jobe sand and SCBA-B with Type IL cement.

3.2.5.2.3 Ground Glass (GG)

Similar to the performance with the Florida sand, the ground glass experimentation results (Figure 3-69 and Figure 3-70) are being presented for completeness. However, the results are not valid per the method and no observed trend should be taken as indicative of field performance until a method that does not have a restriction on alkali content is evaluated. ASTM C1567 limits alkali content of SCM to 4.0% maximum, and the ground glass has more than three times this amount, invalidating the results.

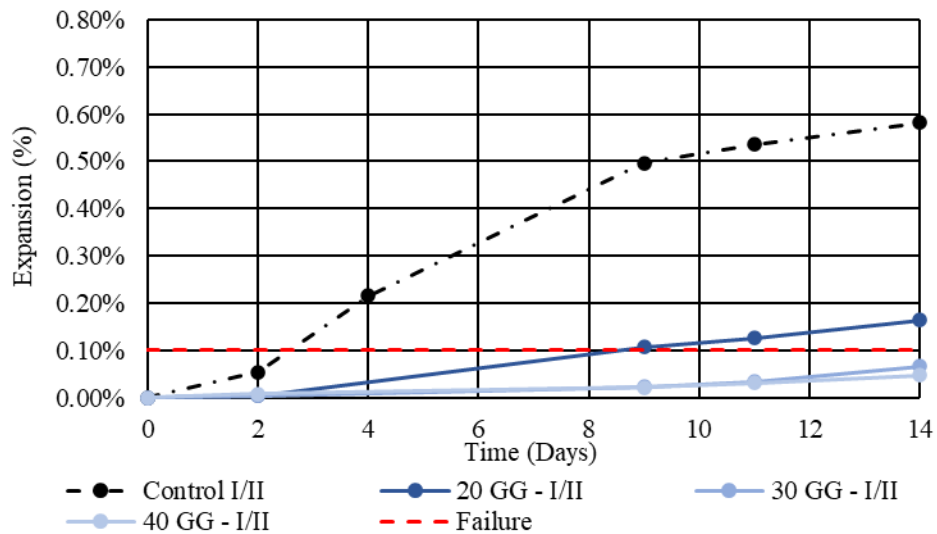


Figure 3-69: Accelerated ASR results using Jobe sand and GG with Type I/II cement.

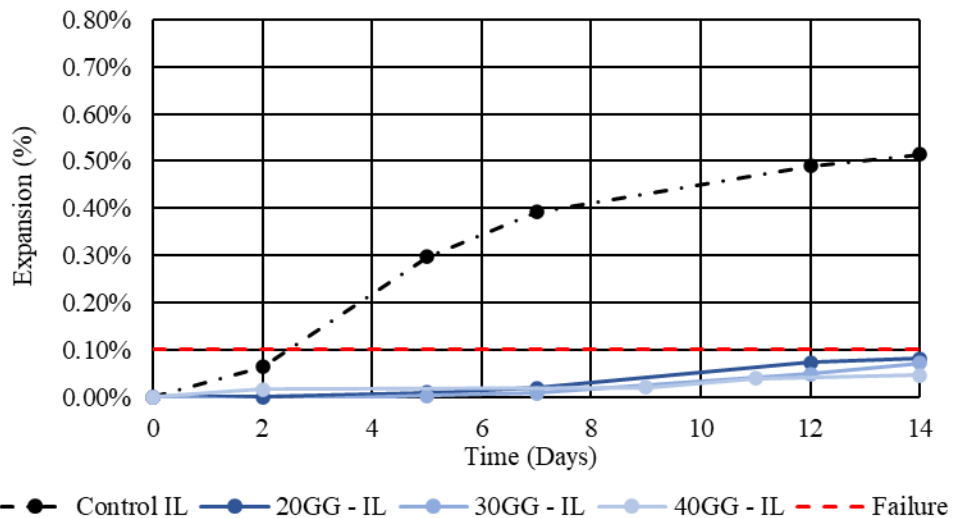


Figure 3-70: Accelerated ASR results using Jobe sand and GG with Type IL cement.

3.2.5.2.4 Volcanic Rock (VR)

The performance of volcanic rock in Type I/II cement, Figure 3-71, and Type IL cement, Figure 3-72, are similar whereby the 20% replacement results in approximately a 45% reduction in total expansion compared to the control. This level of mitigation is not sufficient in either system to consider it a low risk of ASR expansion. So, while the volcanic rock does not pose a threat of expansion as observed when combined with Florida sand, the material does not provide much benefit as an SCM with respect to preventing alkali-silica reaction.

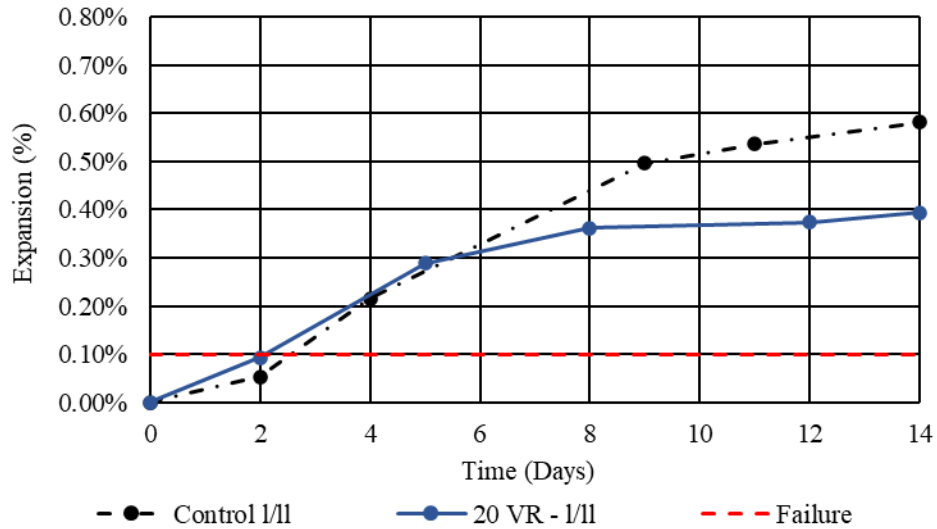


Figure 3-71: Accelerated ASR results using Jobe sand and VR with Type I/II cement.

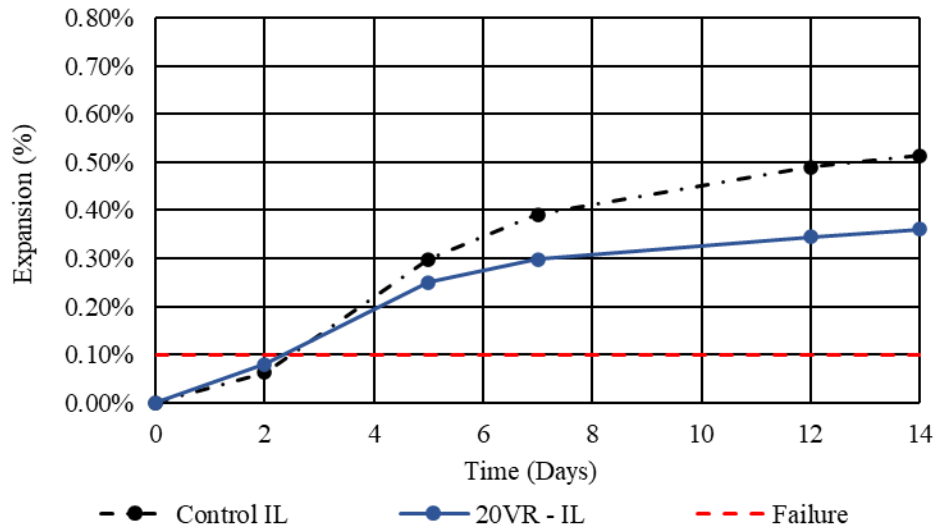


Figure 3-72: Accelerated ASR results using Jobe sand and VR with Type IL cement.

A final summary of the 14-day expansions of each of the mixes containing either Type I/II cement or Type IL cement, along with Jobe sand and alternative supplementary cementitious materials, is presented in Table 3-11. As stated previously, the only mixes that arrest expansion below the test method failure threshold of 0.10% were the glass mixes; however, these results are not valid due to the high alkali content of the ground glass.

Table 3-11: ASTM C1567 14-day expansions of mortars with Jobe sand using Type I/II or Type IL cement and SCM.

Mix	14 Day Expansion	Mix	14 Day Expansion
OPC - Type I/II	0.68%	OPC - Type IL	0.60%
Binary Mixes		Binary Mixes	
10SCBA-A	0.74%	10SCBA-A	0.61%
20SCBA-A	0.58%	20SCBA-A	0.54%
30SCBA-A	0.28%	30SCBA-A	0.25%
10SCBA-B	0.64%	10SCBA-B	0.56%
20SCBA-B	0.59%	20SCBA-B	0.50%
30SCBA-B	0.49%	30SCBA-B	0.45%
20GG	0.19%*	20GG	0.09%*
30GG	0.08%*	30GG	0.08%*
40GG	0.06%*	40GG	0.05%*
20VR	0.39%	20VR	0.35%

*Note: The results of the ground glass expansion in ASTM C1567 with Jobe sand are presented for completeness. The results are not valid due to the high alkali content of the glass. The mitigation potential of the glass must be evaluated with a different method that does not restrict the alkali content, such as ASTM C1293.

3.2.6 Sulfate Resistance – ASTM C1012

The sulfate resistance of mortar test method, ASTM C1202, prescribes a sand-to-cementitious materials ratio of 2.75:1 and a water-to-cementitious materials ratio of 0.485:1 [146]. This mixture design was followed for each mixture, and the mixture proportions, in terms of lb/yd³, are presented in Table 3-12 for mixtures using Type I/II cement. For mortars using Type IL cement, the mixture proportions are presented in Table 3-13.

Table 3-12: Mortar mix proportions (in lb/yd³) for sulfate testing with I/II cement

Mix	I/II Cement	Sand	Water	SCBA-A	SCBA-B	GG	F Ash	C Ash	VR	SF
1	919	2527	446	-	-	-	-	-	-	-
2	823	2515	444	91	-	-	-	-	-	-
3	728	2503	441	182	-	-	-	-	-	-
4	634	2491	439	272	-	-	-	-	-	-
5	822	2512	443	-	91	-	-	-	-	-
6	726	2497	440	-	182	-	-	-	-	-
7	632	2482	438	-	271	-	-	-	-	-
8	730	2509	442	-	-	182	-	-	-	-
9	636	2499	441	-	-	271	-	-	-	-
10	543	2490	439	-	-	362	-	-	-	-
11	727	2497	440	-	-	-	182	-	-	-
12	730	2510	443	-	-	-	-	183	-	-
13	637	2502	441	-	-	-	-	273	-	-
14	732	2515	444	-	-	-	-	-	183	-
15	879	2519	444	-	-	-	-	-	-	37
16	590	2496	440	45	-	-	-	272	-	-
17	543	2490	439	91	-	-	-	272	-	-
18	590	2495	440	-	45	-	-	272	-	-
19	543	2487	439	-	90	-	-	271	-	-
20	683	2506	442	-	-	46	-	182	-	-
21	637	2501	441	-	-	91	-	182	-	-
22	590	2495	440	-	-	-	45	272	-	-
23	543	2487	439	-	-	-	90	271	-	-
24	545	2496	440	-	-	-	-	272	91	-
25	599	2494	440	-	-	-	-	272	-	36

Table 3-13: Mortar mix proportions (in lb/yd³) for sulfate testing with IL cement

Mix	IL Cement	Sand	Water	SCBA-A	SCBA-B	GG	F Ash	C Ash	VR	SF
26	915	2516	444	-	-	-	-	-	-	-
27	820	2505	442	91	-	-	-	-	-	-
28	726	2494	440	181	-	-	-	-	-	-
29	632	2483	438	271	-	-	-	-	-	-
30	819	2502	441	-	91	-	-	-	-	-
31	724	2488	439	-	182	-	-	-	-	-
32	630	2475	436	-	270	-	-	-	-	-
33	727	2500	441	-	-	182	-	-	-	-
34	634	2492	439	-	-	272	-	-	-	-
35	542	2484	438	-	-	361	-	-	-	-
36	724	2489	439	-	-	-	181	-	-	-
37	728	2502	441	-	-	-	-	182	-	-
38	635	2495	440	-	-	-	-	272	-	-
39	729	2507	442	-	-	-	-	-	182	-
40	876	2509	442	-	-	-	-	-	-	36
41	588	2489	439	45	-	-	-	272	-	-
42	542	2484	438	90	-	-	-	271	-	-
43	588	2488	439	-	45	-	-	271	-	-
44	541	2481	438	-	90	-	-	271	-	-
45	681	2498	441	-	-	45	-	182	-	-
46	635	2494	440	-	-	91	-	181	-	-
47	588	2488	439	-	-	-	45	271	-	-
48	541	2481	438	-	-	-	90	271	-	-
49	543	2490	439	-	-	-	-	272	91	-
50	597	2487	439	-	-	-	-	271	-	36

This test method evaluates the performance of the pozzolans with respect to mitigating external sulfate attack. The mechanism of sulfate attack involves the reaction of sulfate ions with calcium hydroxide and calcium aluminate hydrate, producing gypsum and ettringite [161–163]. The ettringite formation causes expansion and weakens the concrete. In general, the SCM mitigate the sulfate degradation mechanism in two ways: 1.) the consumption of calcium hydroxide during the pozzolanic reaction leaves fewer chemical reactants for gypsum and ettringite formation, and 2.) the pozzolanic reaction leads to a denser microstructure preventing sulfate transport into the concrete from the environment.

Mortars exposed to sulfate solution as per ASTM C1012 were crushed, sieved to remove aggregate particles, then ground in a mortar and pestle to a fine powder. The powdered

specimens were analyzed for sulfate mineral formation using semi-quantitative x-ray diffraction. Sulfate minerals were detected, and Rietveld refinement was performed on the concrete mortars to ascertain if thaumasite was formed in addition to ettringite. The determination is complicated by the presence of several overlapping peaks shown in Figure 3-73.

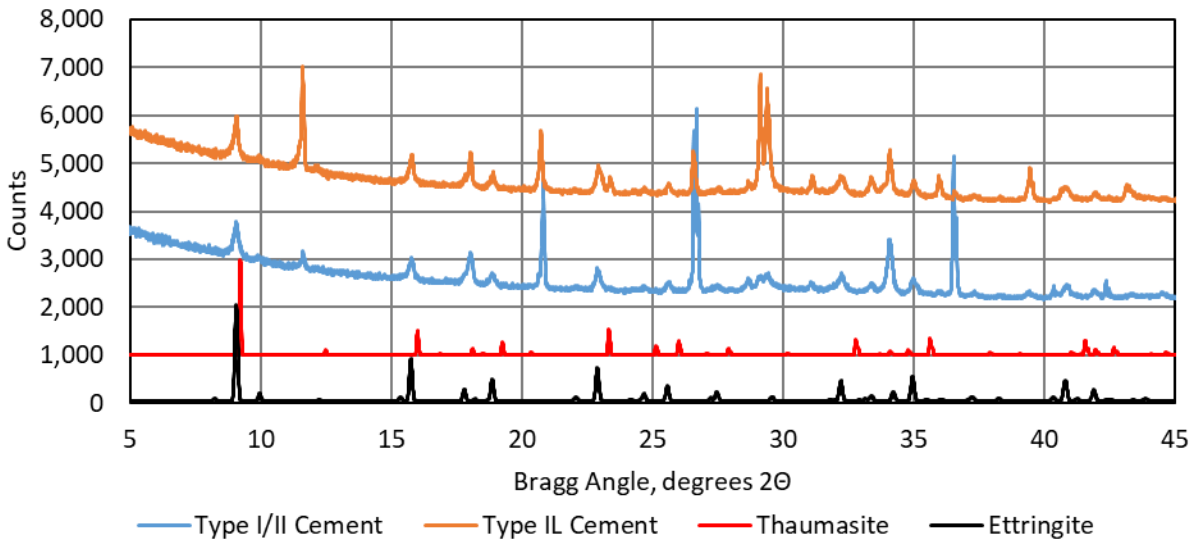


Figure 3-73: X-ray diffractogram showing the scans of cement powders using Type I/II and Type IL cements along with the reference scans for ettringite and thaumasite.

The three most intense peaks for thaumasite occur at about 9.2°, 16.0°, and 23.4° 2θ, and only one matches a peak on the scan for Type IL cement and none have a match on the Type I/II cement. Based on this, the presence of thaumasite is inconclusive. All the major peaks for ettringite match peaks on both the Type IL and Type I/II cements indicating its presence in both.

Identifying materials that provide the benefit of high sulfate resistance to concrete mixes would prove useful, especially in Florida due to the high levels of sulfates present in the soil and along the coasts [164]. Measurements are conducted over the course of 18 months and reported as a percentage of the initial measurement. A higher resistivity to sulfates would lead to a decrease in the number of repairs done on bridges and roadways. Figure 3-74 - Figure 3-92 show the expansion caused by external sulfate attack compared to the limits in ACI 201.2R-16 [71].

3.2.6.1 Portland Cement

The Type I/II mortar used in this study expanded less than the Type IL mortar by 0.24% at 12 months (approximately 0.18% and 0.42% for Type I/II and Type IL, respectively), and

0.4% at 18 months of exposure (0.45% and 0.85% for Type I/II and Type IL, respectively). Although it has been noted that when exposed to sulfate conditions, blended limestone cements are much more susceptible to sulfate attack brought on by the formation of thaumasite, a sulfate mineral which incorporates carbonate into the structure, significant thaumasite formation occurs at temperatures below typical laboratory testing conditions [97,165,166].

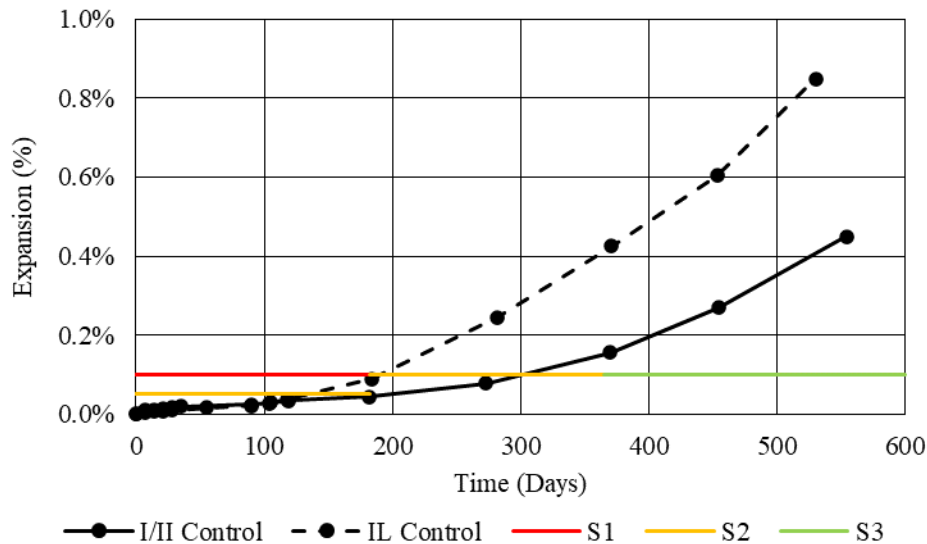


Figure 3-74: Sulfate attack induced expansion results comparing Type I/II with Type IL cement mixtures.

3.2.6.2 Coal Fly Ash (C ash and F ash)

The performance of both the fly ash mixes, regardless of replacement percentage, was as expected. With the typical mechanism of mitigation of sulfate attack being to reduce available portlandite and permeability, both fly ashes would be well suited to do both consuming calcium hydroxide during the pozzolanic reaction as well as reducing permeability from increased hydrated phases, but unreactive particles would also function as mineral fillers creating particle packing.

While there is no expansion limit stated in ASTM C1012, it is clear that the inclusion of the fly ash, particularly the 20% Class F fly ash replacement, dramatically reduces the effects of external sulfate exposure. This is largely due to the high silica content readily consuming excess calcium hydroxide during the pozzolanic reaction. However, with increasing amounts of Class C fly ash addition, the sulfate resistance is lowered due to the Class C fly ash bringing along calcium with the silica, therefore the material is less likely to consume the calcium hydroxide

byproduct of the cement hydration compared to Class F fly ash. The performance of the Type I/II cementitious blends with Class C or Class F fly ash is shown in Figure 3-75.

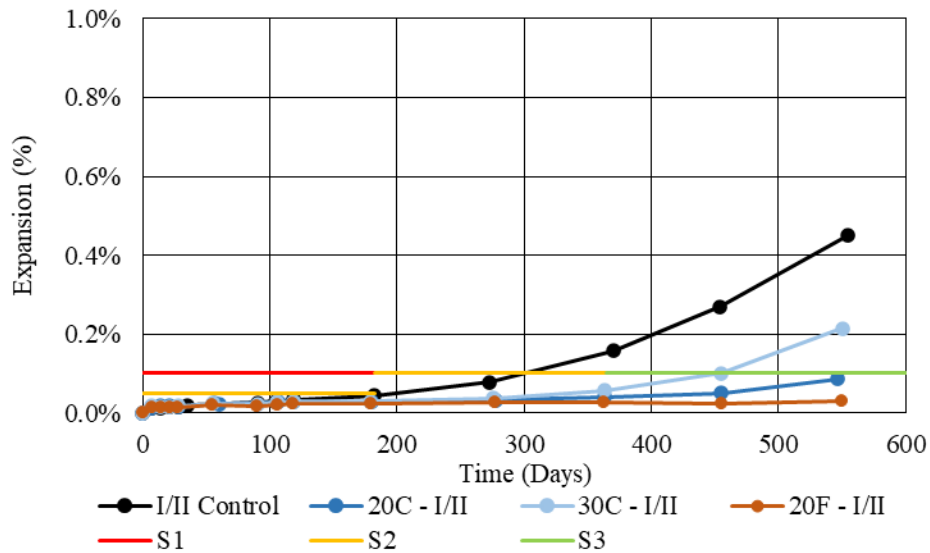


Figure 3-75: Sulfate attack induced expansion results comparing C ash and F ash mixtures in Type I/II systems to control.

As the thaumasite formation is a degradation of calcium carbonate, the consumption of calcium hydroxide is less effective at mitigation and only reduction of permeability can reduce the likelihood of degradation for this mortar; as such, the SCMs do not perform as well as can be seen in Figure 3-76. However, the Class F fly ash mixture does perform well even with the Type IL cement.

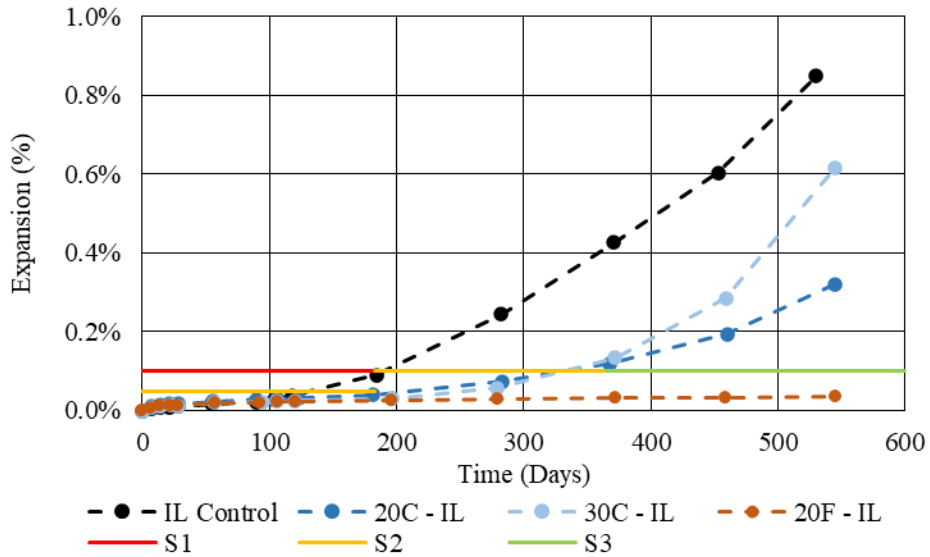


Figure 3-76: Sulfate attack induced expansion results comparing C ash and F ash mixtures in Type IL systems to control.

3.2.6.3 Silica Fume

Based upon previous research, it was anticipated that the silica fume would mitigate or minimize the sulfate damage due to the pozzolanic reactivity and reduction in permeability [167]. However, there was anomalous expansion beyond 1-year of exposure, Figure 3-77, which is atypical of silica fume mixes exposed to sodium sulfate solutions. The expansion was approximately 2% at the end of measuring. This was not observed in the Type IL cementitious system as observed in Figure 3-78. The expansion seen in the Type I/II system was observed in each of the seven mortar bars, so it was not a sampling/averaging bias.

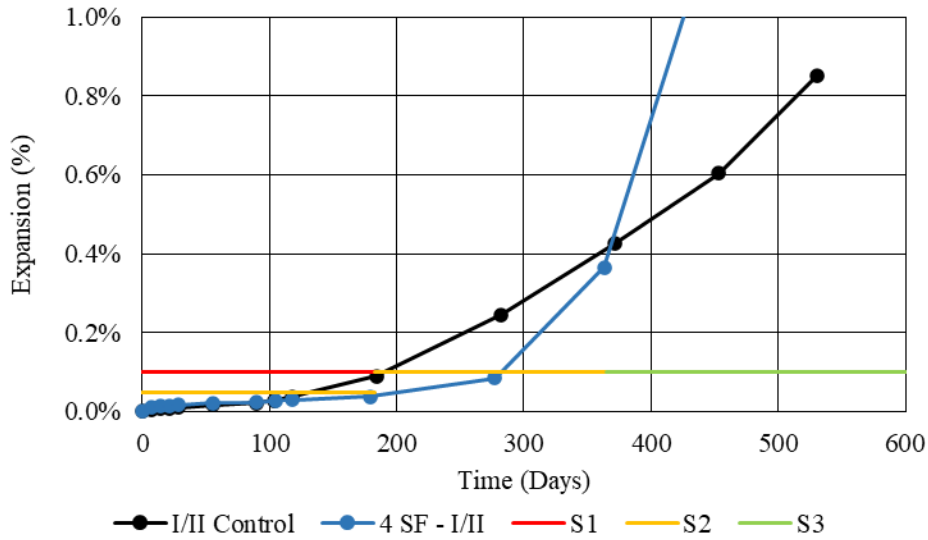


Figure 3-77: Sulfate attack induced expansion results comparing the SF mixture in a Type I/II system to control.

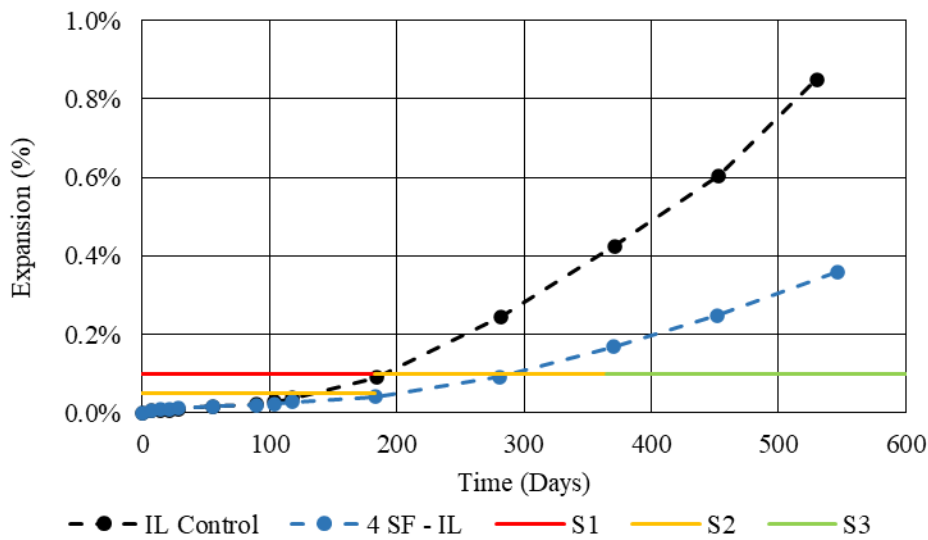


Figure 3-78: Sulfate attack induced expansion results comparing the SF mixture in a Type IL system to control.

3.2.6.4 Sugarcane Bagasse Ash

The mixing and curing procedure of this method involves mixing the cementitious materials with water, followed by the fine aggregate, then molding mortar bars and companion mortar cubes. When the cubes have reached a specific strength, the mortar bars are then exposed to a sulfate solution. This method presented an issue when using sugarcane bagasse ash; when mixed in accordance with ASTM C305, the mixes would not meet the strength requirement of

3,000 psi. Mortars containing 30% SCBA prepared in this method would cure for over six months without reaching the target strength. Several replicate mortar mixes were prepared with the same results. When the bagasse mixes were blended with the aggregate and cement first, then had water introduced, the mortars would reach the target strength in less than three days of curing. The only difference in the mixing procedure was that instead of mixing water with cement and SCBA, then sand, the dry materials were blended before exposure to water. The results for the SCBA mixes presented herein represent this mixing regime.

The strength requirements of ASTM C1012 were not met by the SCBA mixtures containing 30% replacements, regardless of SCBA type or cement type. The mixtures incorporating SCBA-A show a higher expansion in the 20% replacements compared to the 10% replacements in both Type I/II and IL systems, while the opposite is observed for SCBA-B mixtures. The sulfate resistance of mixes showing sugarcane bagasse ash replacements of Type I/II cement can be seen in Figure 3-79 and Figure 3-80.

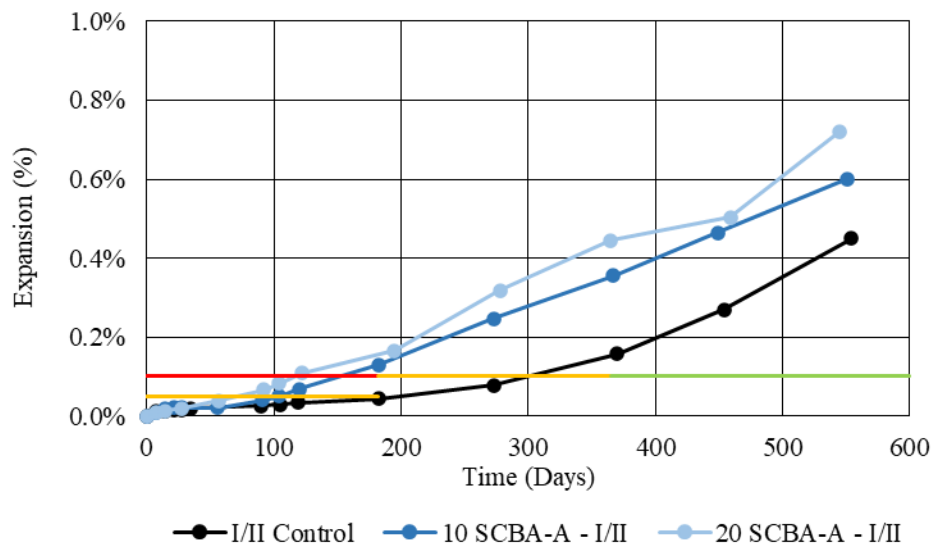


Figure 3-79: Sulfate attack induced expansion results comparing SCBA-A mixtures in Type I/II systems to control.

Reduced expansion due to incorporation of SCBA-A would be expected rather than SCBA-B due to the higher reactivity of the SCBA-A leading to increased pozzolanic activity. This is likely attributed to the differences in SO_3 content; 4.2% SO_3 for SCBA-A and 0.6% SO_3 for SCBA-B.

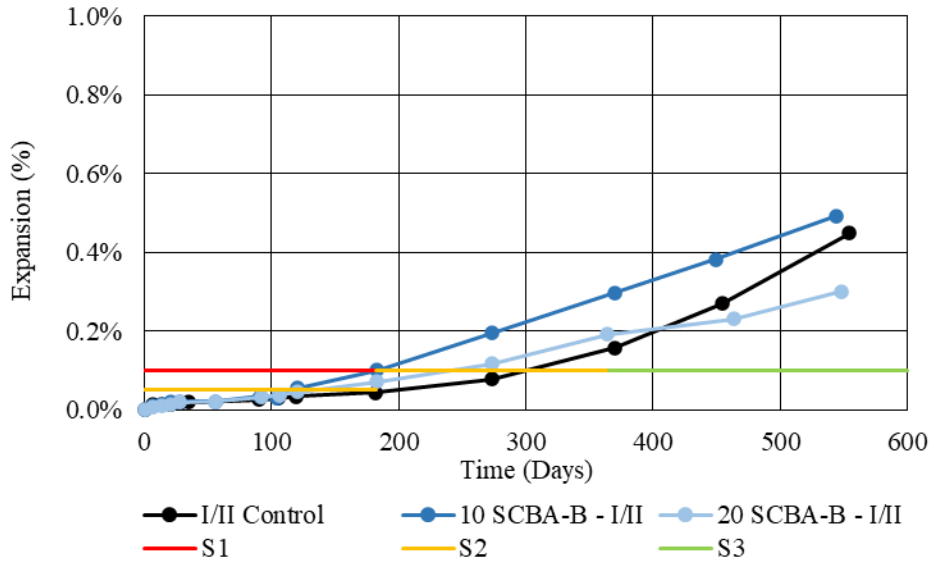


Figure 3-80: Sulfate attack induced expansion results comparing SCBA-B mixtures in Type I/II systems to control.

The sugarcane bagasse ash mixes generally expanded to the same final level at 18 months of exposure regardless of cement type. The sulfate resistance of mortars containing sugarcane bagasse ash replacements of Type IL cement are found in Figure 3-81 and Figure 3-82.

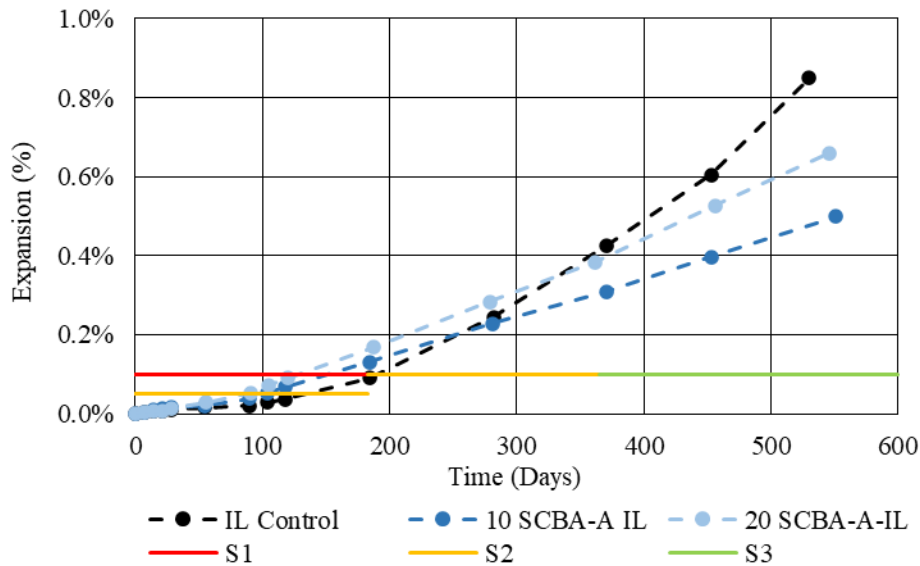


Figure 3-81: Sulfate attack induced expansion results comparing SCBA-A mixtures in Type IL systems to control.

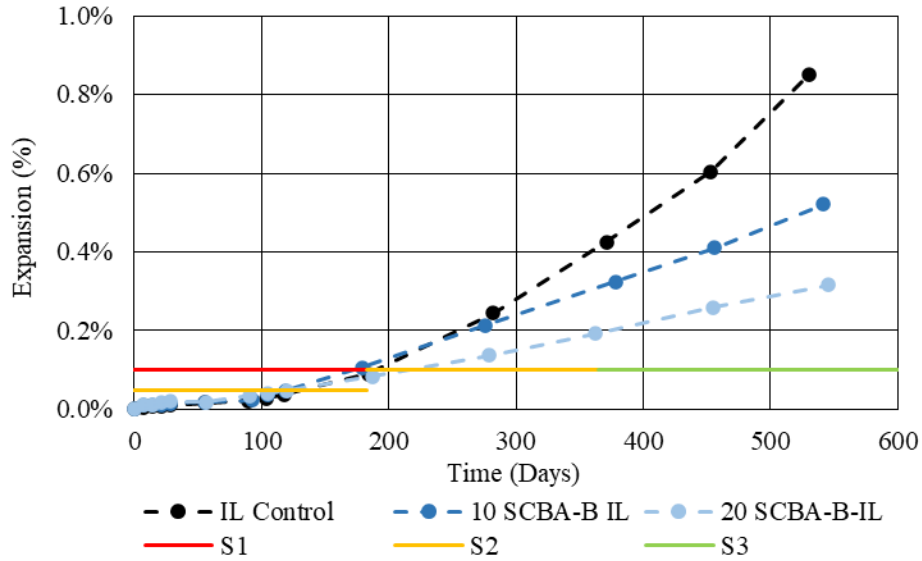


Figure 3-82: Sulfate attack induced expansion results comparing SCBA-B mixtures in Type IL systems to control.

3.2.6.5 Ground Glass

The ground glass mixtures significantly reduced the expansion caused by sulfate attack, even in mixtures with a 20% replacement in both Type I/II and Type IL systems. Similar performance has been observed in other studies [58,168,169]. Even when compared to the fly ash mixtures, the expansion observed in ground glass mixtures was lower. The pozzolanic reaction induced by ground glass reduces the calcium hydroxide in the mortar, which reduces the potential for sulfate ions to react with excess calcium hydroxide. The ground glass mixture likely performed better than the fly ash mixtures due to differences in calcium aluminate hydrate formation; ground glass has an alumina content of 1.7%.

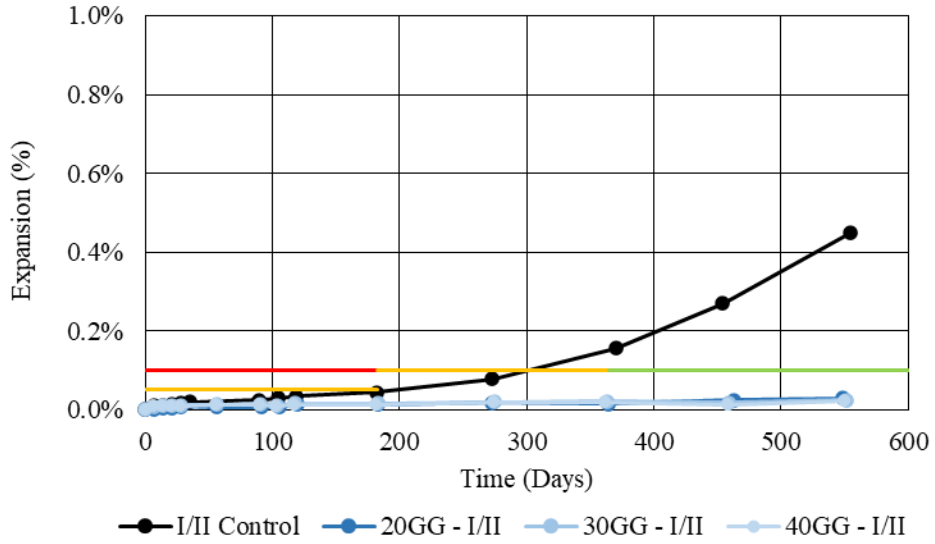


Figure 3-83: Sulfate attack induced expansion results comparing GG mixtures in Type I/II systems to control.

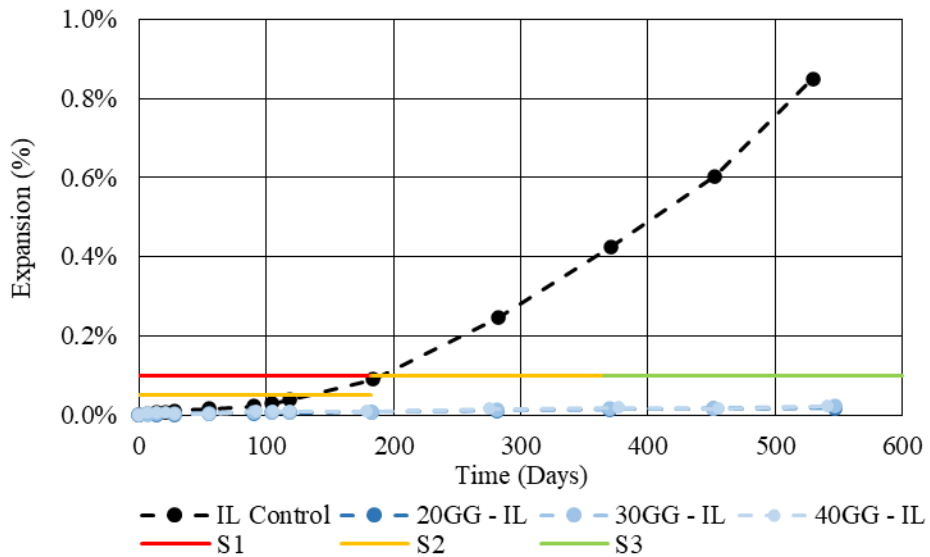


Figure 3-84: Sulfate attack induced expansion results comparing GG mixtures in Type IL systems to control.

3.2.6.6 Ground Volcanic Rock

The expansions observed in the mixtures incorporating volcanic rock in the Type I/II cementitious system expanded greater than control as shown in Figure 3-85. Additionally, in the Type IL cementitious system, 20% volcanic rock had comparable expansion to the control indicating that volcanic rock had low pozzolanic reactivity, as shown in Figure 3-86.

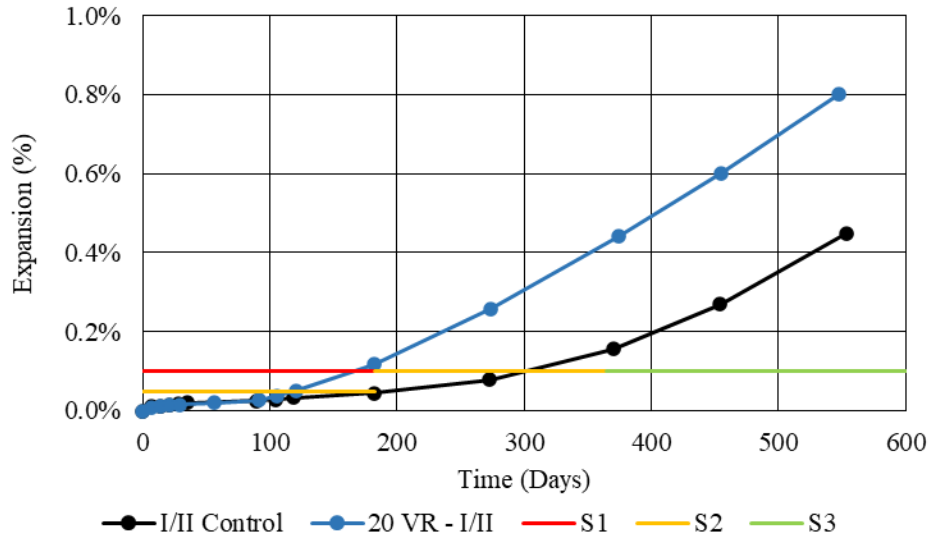


Figure 3-85: Sulfate attack induced expansion results comparing VR mixtures in Type I/II systems to control.

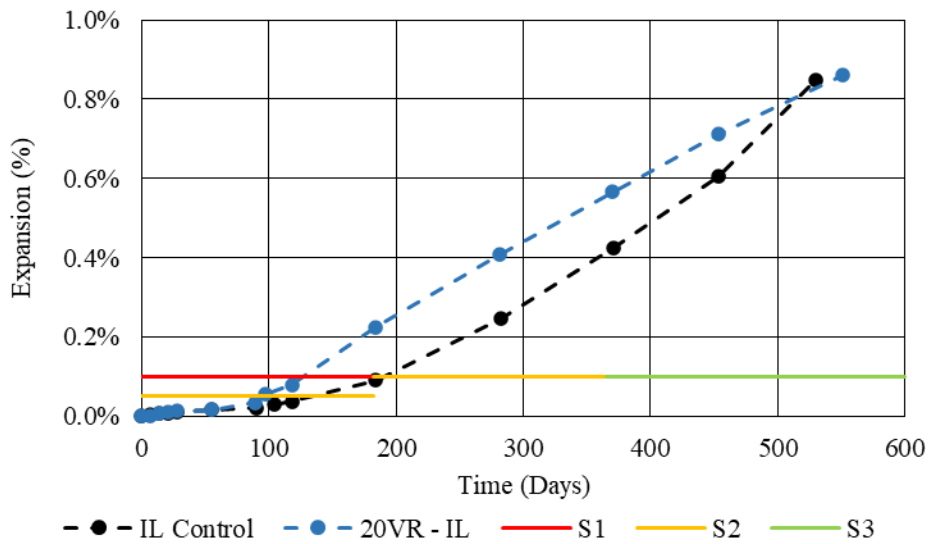


Figure 3-86: Sulfate attack induced expansion results comparing VR mixtures in Type IL systems to control.

3.2.6.7 Ternary Mixes

In ternary blended mortars incorporating sugarcane bagasse ash as a Type I/II or Type IL cement replacement, Figure 3-87 and Figure 3-88, the ternary blends were either comparable to control or expanded more than the control. The mixtures failed to control expansion due to the sulfate exposure.

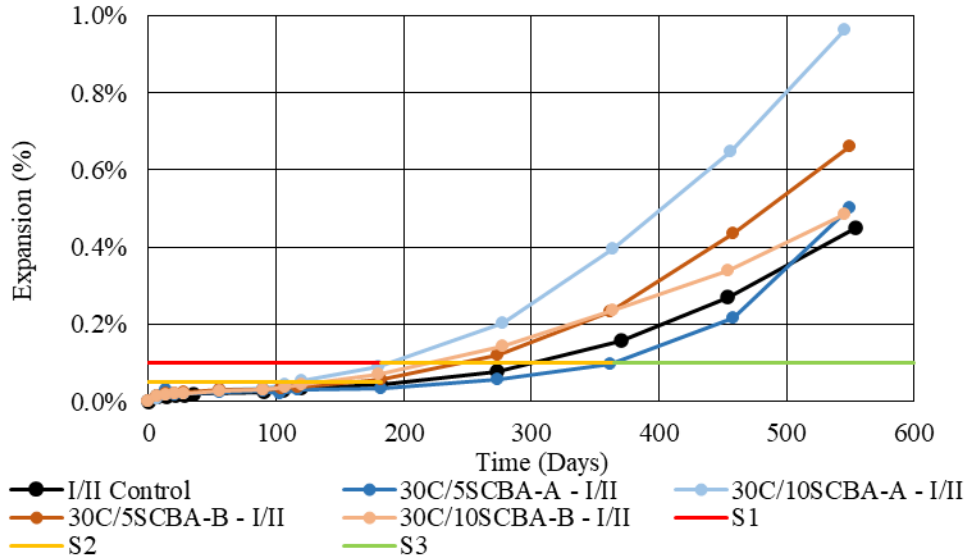


Figure 3-87: Sulfate attack induced expansion results comparing ternary SCBA mixtures Type I/II systems to control.

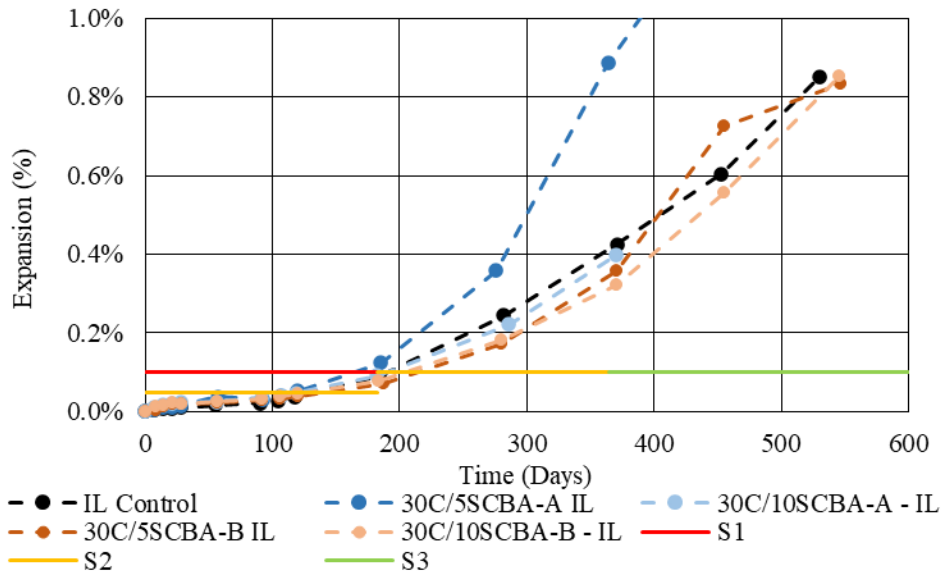


Figure 3-88: Sulfate attack induced expansion results comparing ternary SCBA mixtures Type IL systems to control.

Each of the ternary mixes containing Class C fly ash blended with either ground glass or Class F fly ash as replacements for either Type I/II cement (Figure 3-89) or Type IL cement (Figure 3-90) exhibited considerable reduction in expansion compared to the respective controls. Each of the mixes that replaced Type IL cement were able to limit the total expansion to less than 0.10% at 18 months compared to 0.85% expansion for the control.

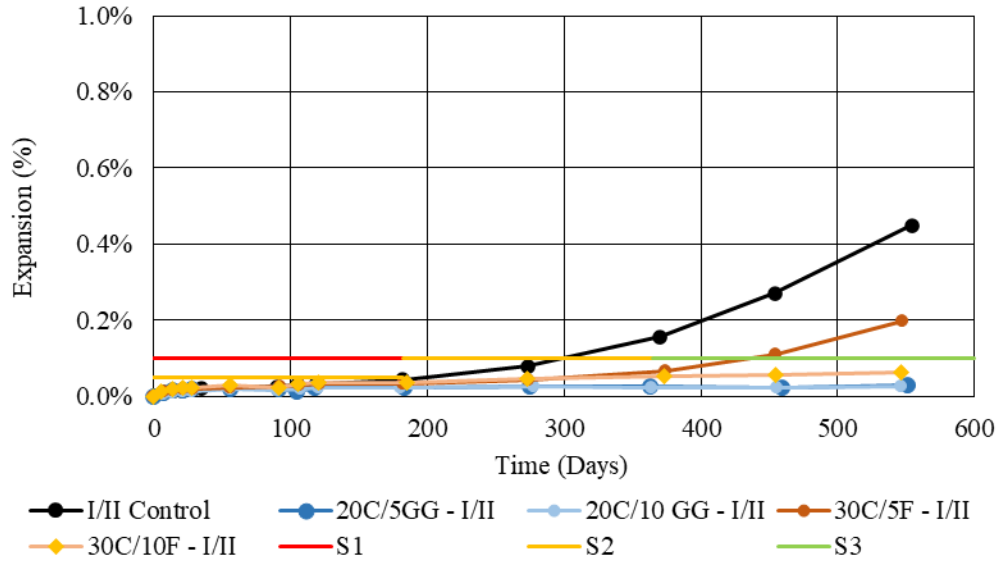


Figure 3-89: Sulfate attack induced expansion results comparing ternary mixtures with GG or F ash with C ash in Type I/II systems to control.

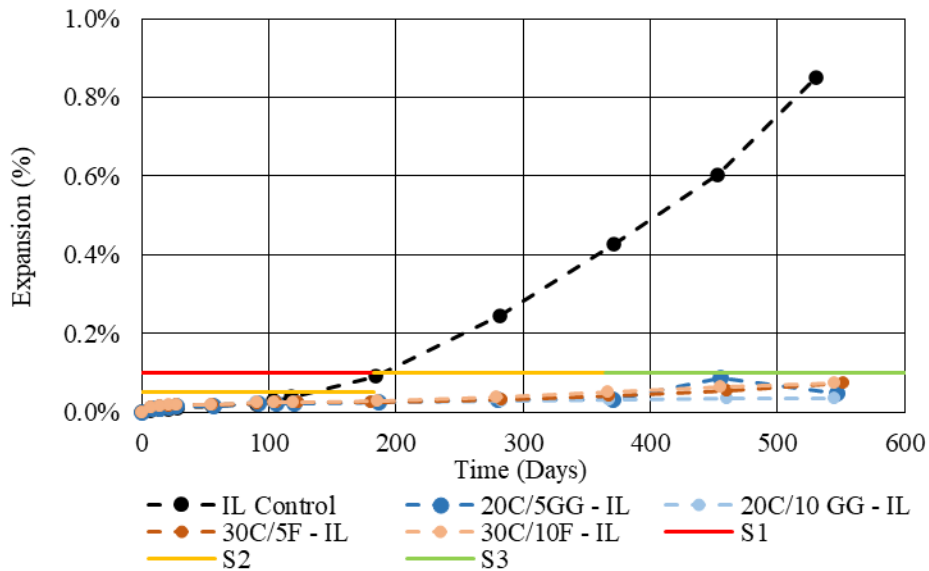


Figure 3-90: Sulfate attack induced expansion results comparing ternary mixtures with GG or F ash with C ash in Type IL systems to control.

The ternary mixes combining Class C fly ash with either ground volcanic rock or silica fume as replacement for the Type I/II cement (Figure 3-91) exhibited comparable expansion to the control. The ternary blend of Class C fly ash and silica fume in the Type IL cementitious system performed much better than control (Figure 3-92); however, the ternary blend of the volcanic rock had failed due to specimens breaking and the specimens could no longer be measured.

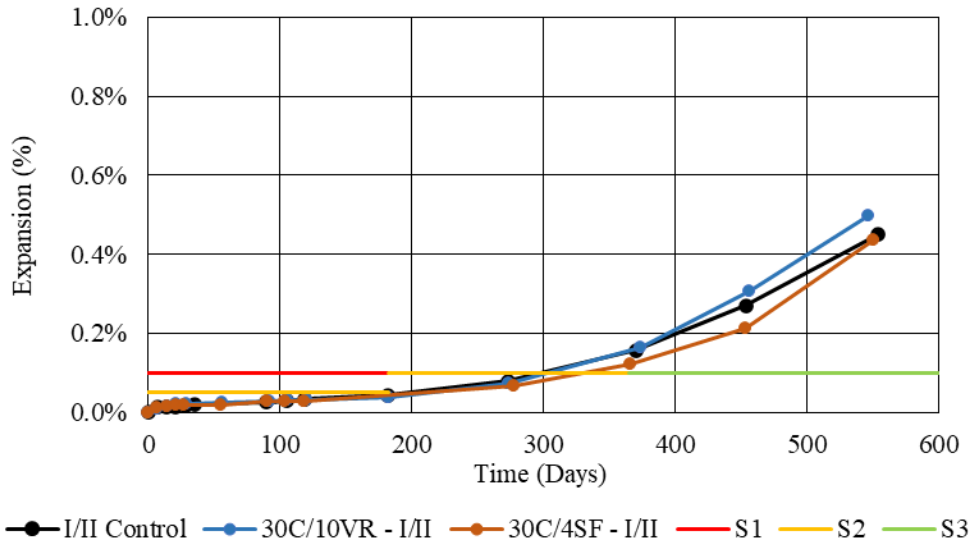


Figure 3-91: Sulfate attack induced expansion results comparing ternary mixtures with VR or SF with C ash in Type I/II systems to control.

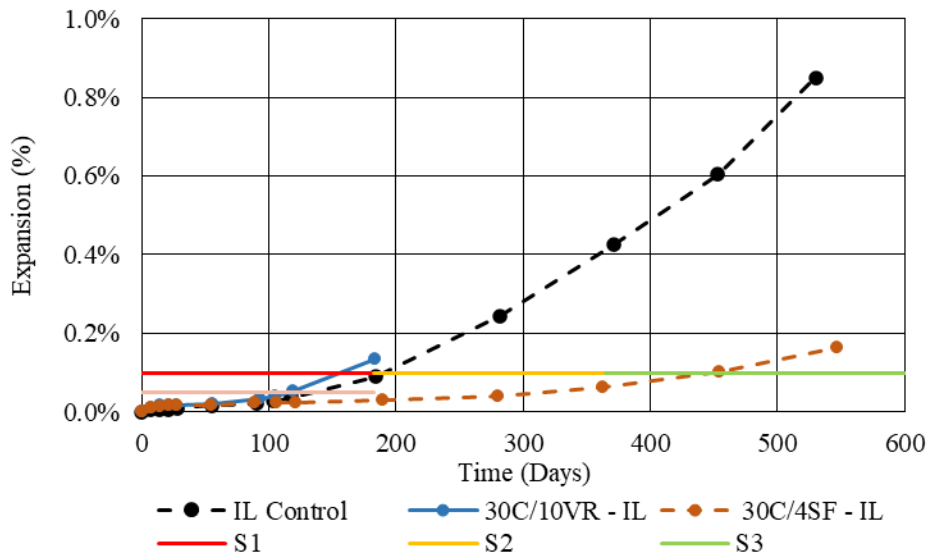


Figure 3-92: Sulfate attack induced expansion results comparing ternary mixtures with VR or SF with C ash in Type IL systems to control.

A summary of the 12-month and 18-month expansion due to sulfate exposure for each of the mixes utilizing Type I/II cement with supplementary cementitious materials is presented in Table 3-14. A summary of the 12-month and 18-month expansion due to sulfate exposure for each of the mixes utilizing Type I/II cement with supplementary cementitious materials is presented in Table 3-15.

Table 3-14: Summary of sulfate expansion values at 12 months and 18 months for Type I/II cementitious mixtures.

Mix	12-Month Expansion	18-Month Expansion
OPC - Type I/II	0.16%	0.45%
Binary Mixes		
10SCBA-A	0.36%	0.60%
20SCBA-A	0.44%	0.72%
30SCBA-A	-	-
10SCBA-B	0.30%	0.49%
20SCBA-B	0.19%	0.30%
30SCBA-B	-	-
20GG	0.02%	0.03%
30GG	0.02%	0.02%
40GG	0.02%	0.02%
20VR	0.44%	0.80%
20C	0.04%	0.09%
30C	0.06%	0.21%
20F	0.03%	0.03%
4SF	0.37%	2.00%
Ternary Mixes		
30C+5SCBA-A	0.10%	0.50%
30C+10SCBA-A	0.40%	0.95%*
30C+5SCBA-B	0.23%	0.66%*
30C+10SCBA-B	0.24%	0.48%
20C+5GG	0.03%	0.03%
20C+10GG	0.02%	0.03%
30C+10VR	0.17%	0.48%*
30C+5F	0.07%	0.20%
30C+10F	0.05%	0.06%
30C+4SF	0.12%	0.44%

*Mix with one or more broken bars by 18-month measurement.

Table 3-15: Summary of sulfate expansion values at 12 months and 18 months for Type IL cementitious mixtures.

Mix	12-Month Expansion	18-Month Expansion
OPC - Type IL	0.43%	0.85%
Binary Mixes		
10SCBA-A	0.31%	0.50%
20SCBA-A	0.39%	0.66%
30SCBA-A	-	-
10SCBA-B	0.32%	0.52%
20SCBA-B	0.19%	0.32%
30SCBA-B	-	-
20GG	0.01%	0.02%
30GG	0.02%	0.02%
40GG	0.02%	0.02%
20VR	0.57%	0.86%
20C	0.12%	0.32%
30C	0.13%	0.62%
20F	0.03%	0.04%
4SF	0.17%	0.36%
Ternary Mixes		
30C+5SCBA-A	0.885%*	1.309%*
30C+10SCBA-A	0.40%	*
30C+5SCBA-B	0.36%	0.83%
30C+10SCBA-B	0.03%	0.85%
20C+5GG	0.03%	0.05%
20C+10GG	0.03%	0.03%
30C+10VR	*	*
30C+5F	0.04%	0.07%
30C+10F	0.05%	0.07%
30C+4SF	0.06%	0.17%

*Mix with one or more broken bars by 18-month measurement.

Some mortar bars could not be measured once cracks propagated through the cross section of the bars. A summary of the mixes this occurred to, along with the number of bars that were damaged and when they were damaged, is presented in Table 3-16.

Table 3-16: Summary of damaged mortar bars.

Mixture	Bars	Age (Days)
30C - IL	1 Bar	545
30C + 10SCBA-A - I/II	1 Bar	546
30C + 10SCBA-A - IL	7 Bars	455
30C + 5SCBA-B - IL	5 Bars	547
30C + 10VR - IL	7 Bars	365
30C + 10VR - I/II	3 Bars	547
30C + 5SCBA-B - I/II	1 Bar	458
	3 Bars	550
30C + 5SCBA-A - IL	1 Bar	276
	1 Bar	364
	4 Bars	457
	2 Bars	546

4. Concrete Testing

Mortar testing allowed for the initial characterization and identification of compatibility issues that may arise during the fabrication of concrete with the alternative supplementary cementitious materials. The results obtained guided the evaluation of the properties of concrete with respect to areas of concern such as workability and durability. With this in mind, the concrete experimentation regime was designed to evaluate the concrete with respect to plastic properties, mechanical strength, and durability aspects that were not necessarily quantified during the mortar testing phase.

4.1 MIXTURE DESIGN AND COMPOSITION

For the concrete test methods described below, a total of 125 different mixes were created. The concrete mixes used for physical testing were designed based on FDOT's *Standard Specifications for Road and Bridge Construction* Section 346 [21]. Class IV concrete has a minimum cementitious content of 658 lb/yd³ and a maximum water-to-cementitious ratio (w/cm) of 0.41 based on Table 4-1. Class I pavements require a minimum cementitious content of 470 pounds per cubic yard and maximum w/cm of 0.50.

A portion of this research involved determining the effects of adding alternative SCM to portland-limestone cements (Type IL). As such, each mixture was tested with Type I/II cement and Type IL cement. Each material or replacement was incorporated into FDOT Class I (Pavement) concrete and Class IV concrete mix designs. The Type IL cement was used in FDOT Class I and Class IV concrete mix designs, while Type I/II cement was only used to evaluate Class IV concrete because it has already been evaluated as a Class I concrete in a previous FDOT research project, FDOT BDV31-977-06 [8]. The water-to-cementitious materials (w/cm) ratios for the mix designs were determined based on "Table 3" in Section 346-4 of the FDOT *Standard Specifications for Road and Bridge Construction* [21], which is reproduced as Table 4-1 in this document. For the selected Class I (Pavement) designs, a w/cm ratio of 0.5 was chosen, along with 500 pounds of total cementitious material per cubic yard of concrete. For the selected Class IV concrete designs, a w/cm ratio of 0.4 was selected with 670 pounds of total cementitious material per cubic yard of concrete. Table 4-2 through Table 4-3 outline the mix designs that were chosen for each class of concrete and each type of cement.

Table 4-1. Minimum cement content and maximum w/cm as per FDOT [21]

Class of Concrete	Minimum Total Cementitious Materials Content (lb/yd ³)	Maximum Water-to-Cementitious Materials Ratio*
I	470	0.53
I (Pavement)	470	0.50
II	470	0.53
II (Bridge Deck)	611	0.44
III	611	0.44
III (Seal)	611	0.53
IV	658	0.41**
IV (Drilled Shaft)	658	0.41
V (Special)	752	0.37**
V	752	0.37**
VI	752	0.37**

*Calculation of water-to-cementitious materials ratio (w/cm) is based on the total cementitious material including cement and supplemental cementitious materials.

**When silica fume or metakaolin is used, the maximum w/cm will be 0.35, and when the use of ultrafine fly ash is required, the maximum w/cm will be 0.30.

4.2 CONCRETE MIX PROPORTIONS

The concrete mix program was developed to determine whether alternative pozzolans investigated in this research project perform comparably to the currently accepted pozzolans allowed in the Florida Department of Transportation's *Standard Specifications for Road and Bridge Construction* [21]. There is little research available for concrete mixtures for Class I pavement mixes that utilize IL portland cement with limestone addition. Although this research project was focused on the study of alternative pozzolans in concrete, the scope was expanded to study the compatibility of standardized and alternative pozzolans for replacement of IL cement. The literature regarding the reactivity of portland cement systems incorporating limestone is not fully agreed upon. The general consensus is that the reactivity and strength is reduced in concrete systems with more than 10% limestone [170–177]. However, there is some disagreement; some research concludes that limestone replacements greater than 10% can increase strength; this result is likely due to the limestone inclusions being very finely ground to increase reactivity [178–180]. In the case of Bentz et al. [178], the limestone was treated as an inert filler (although it was stated that it was not inert) and the w/c was kept constant (0.40); however, when accounting for limestone as a cementitious material the w/cm was lowered to 0.25, effectively increasing the compressive strength. Soroka and Setter [179] and Soroka and Stern [180] used limestone fillers having specific surface areas ranging from 1,150 cm²/g to 10,300 cm²/g (with

the majority of the fillers being over 6,500 cm²/g); however, the specific surface area of the cement used was not reported in either case. The fineness of the limestone fillers used are considerably higher than cements of recent years, and historically cements in the mid-1970's were much coarser than the fillers being evaluated [181,182]. Table 4-2 and Table 4-4 show the mixture proportions for Class IV concretes using Type I/II cement and Type IL cement, respectively. While Table 4-4 provides the mixture proportions for Class I concretes using Type IL cement.

Table 4-2: Class IV concrete proportions (lb/yd³) using Type I/II cement

Mix	I/II Cement	SCBA-A	SCBA-B	GG	F Ash	C Ash	VR	SF	Coarse Agg.	Fine Agg.	Water
1	670	-	-	-	-	-	-	-	1729	1153	268
2	603	67	-	-	-	-	-	-	1727	1151	268
3	536	134	-	-	-	-	-	-	1718	1145	268
4	469	201	-	-	-	-	-	-	1709	1139	268
5	603	-	67	-	-	-	-	-	1724	1150	268
6	536	-	134	-	-	-	-	-	1713	1142	268
7	469	-	201	-	-	-	-	-	1702	1135	268
8	603	-	-	134	-	-	-	-	1711	1141	268
9	536	-	-	201	-	-	-	-	1702	1135	268
10	469	-	-	268	-	-	-	-	1708	1139	268
11	536	-	-	-	134	-	-	-	1714	1142	268
12	536	-	-	-	-	134	-	-	1723	1149	268
13	469	-	-	-	-	201	-	-	1717	1145	268
14	536	-	-	-	-	-	134	-	1727	1151	268
15	643	-	-	-	-	-	-	27	1730	1153	268
16	436	34	-	-	-	201	-	-	1713	1142	268
17	402	67	-	-	-	201	-	-	1708	1139	268
18	436	-	34	-	-	201	-	-	1712	1141	268
19	402	-	67	-	-	201	-	-	1706	1137	268
20	503	-	-	34	-	134	-	-	1720	1147	268
21	469	-	-	67	-	134	-	-	1717	1144	268
22	402	-	-	-	-	201	67	-	1713	1142	268
23	436	-	-	-	34	201	-	-	1712	1141	268
24	402	-	-	-	67	201	-	-	1706	1138	268
25	228	-	-	-	-	201	-	27	1712	1141	268

Table 4-3: Class IV concrete proportions (lb/yd³) using Type II cement

Mix	IL Cement	SCBA-A	SCBA-B	GG	F Ash	C Ash	VR	SF	Coarse Agg.	Fine Agg.	Water
26	670	-	-	-	-	-	-	-	1729	1153	268
27	603	67	-	-	-	-	-	-	1729	1147	268
28	536	134	-	-	-	-	-	-	1712	1141	268
29	469	201	-	-	-	-	-	-	1704	1136	268
30	603	-	67	-	-	-	-	-	1718	1145	268
31	536	-	134	-	-	-	-	-	1707	1138	268
32	469	-	201	-	-	-	-	-	1697	1131	268
33	603	-	-	134	-	-	-	-	1711	1141	268
34	536	-	-	201	-	-	-	-	1702	1135	268
35	469	-	-	268	-	-	-	-	1693	1129	268
36	536	-	-	-	134	-	-	-	1707	1138	268
37	536	-	-	-	-	134	-	-	1717	1145	268
38	469	-	-	-	-	201	-	-	1712	1141	268
39	536	-	-	-	-	-	134	-	1721	1147	268
40	643	-	-	-	-	-	-	27	1723	1149	268
41	436	34	-	-	-	201	-	-	1707	1138	268
42	402	67	-	-	-	201	-	-	1703	1136	268
43	436	-	34	-	-	201	-	-	1706	1138	268
44	402	-	67	-	-	201	-	-	1701	1134	268
45	503	-	-	34	-	134	-	-	1714	1143	268
46	469	-	-	67	-	134	-	-	1711	1141	268
47	402	-	-	-	-	201	67	-	1708	1139	268
48	436	-	-	-	34	201	-	-	1706	1138	268
49	402	-	-	-	67	201	-	-	1701	1134	268
50	228	-	-	-	-	201	-	27	1706	1137	268

Table 4-4: Class I concrete proportions (lb/yd³) using Type IL cement

Mix	IL Cement	SCBA-A	SCBA-B	GG	F Ash	C Ash	VR	SF	Coarse Agg.	Fine Agg.	Water
51	500	-	-	-	-	-	-	-	1836	1224	250
52	450	50	-	-	-	-	-	-	1830	1220	250
53	400	100	-	-	-	-	-	-	1824	1216	250
54	350	150	-	-	-	-	-	-	1818	1212	250
55	450	-	50	-	-	-	-	-	1829	1219	250
56	400	-	100	-	-	-	-	-	1821	1214	250
57	350	-	150	-	-	-	-	-	1812	1209	250
58	400	-	-	100	-	-	-	-	1827	1218	250
59	350	-	-	150	-	-	-	-	1823	1215	250
60	300	-	-	200	-	-	-	-	1818	1212	250
61	400	-	-	-	100	-	-	-	1821	1214	250
62	400	-	-	-	-	100	-	-	1828	1219	250
63	350	-	-	-	-	150	-	-	1824	1216	250
64	400	-	-	-	-	-	100	-	1831	1221	250
65	480	-	-	-	-	-	-	20	1832	1221	250
66	325	25	-	-	-	150	-	-	1821	1214	250
67	300	50	-	-	-	150	-	-	1818	1212	250
68	325	-	25	-	-	150	-	-	1820	1213	250
69	300	-	50	-	-	150	-	-	1816	1211	250
70	375	-	-	25	-	100	-	-	1826	1217	250
71	350	-	-	50	-	100	-	-	1823	1216	250
72	300	-	-	-	-	150	50	-	1821	1214	250
73	325	-	-	-	25	150	-	-	1820	1213	250
74	300	-	-	-	50	150	-	-	1816	1211	250
75	330	-	-	-	-	150	-	20	1820	1213	250

4.3 TESTING RESULTS

4.3.1 Slump – ASTM C143

The slump evaluations of concrete produced similar trends compared to the mortar flow evaluations. Admixture was needed to improve the slump performance of the SCBA mixtures for each class of concrete and cement type. The slump results for each class of concrete and cement type are shown in Table 4-5 through 4-7. The amount of admixture to ensure workability increased as SCBA replacement increased. Much like the flow results though, SCBA-B mixtures required lower admixture doses than SCBA-A mixtures to achieve minimal flow properties. When used in a ternary system, the introduction of SCBA did not require the use of water

reducing admixtures to produce an adequate slump. The potential for agglomerations in SCBA-A was observed for mortar, but not in concrete. This is attributed to the differences in shearing action during mixing caused by the coarse aggregate in concrete as compared to mortar where elevated shear force in concrete mixing adequately breaks up any potential agglomerations.

The use of water reducing admixtures was limited in the mixtures incorporating ground glass in Class IV concrete with Type I/II cement. The Type D mid-range water-reducing admixture dosage used was rather minimal at less than 2 oz/cwt; this dosage produced mixes that were acceptable in the laboratory with slumps ranging from 2.0" to 3.25". However, larger doses of the Type D admixture would be necessary for the higher slumps required for field applications.

The volcanic rock (VR) mixtures exhibited varying results depending on the class of concrete and type of cement used. For the Class IV concrete with Type I/II cement, the incorporation of VR improved slump from control (4.75" in. slump) to 5.5", while the Type IL cement system had a comparable slump of 3.0" without admixtures compared to the 3.25" for the control mix. The Class I concrete with Type IL cement required 2 oz/cwt of Type D admixture to produce a slump of 2.25". The need for elevated doses of water-reducing admixtures in the Class I concrete to achieve minimum slump requirements was consistently observed across different SCM, which was due to the lower cement content in Class I concrete. The lower cement content reduced slump by decreasing the paste volume and also reduced the efficacy of the admixture.

The fly ash mixtures increased the slump without the use of any admixtures as anticipated from previous research [1–3]. Additionally, much like the flow results, the ternary mixtures were beneficially affected by the C ash addition and produced increased slump across the evaluated mixes without admixture addition. The silica fume mixtures produced adequate slump for each concrete mixture, which shows that the replacement of portland cement with 4% silica fume into concrete had little effect on concrete workability as seen in the flow table evaluation.

Table 4-5: Slump of Class IV concrete mixes using Type I/II concrete

Binary Mix	Slump (in)	Water-Reducing Admixtures Used, (oz/cwt)
Control	4.75	1.8 oz Type D
10% - SCBA-A	2.5	8.6 oz Type D
20% - SCBA-A	2.0	8 oz Type D & 5.1 oz Type F
30% - SCBA-A	2.0	6.9 oz Type D & 10.3 oz Type F
10% - SCBA-B	2.75	8.6 oz Type D
20% - SCBA-B	7.0	3.4 oz Type D & 4 oz Type F
30% - SCBA-B	3.75	10 oz Type D & 10.3 oz Type F
20% - GG	2.5	1.8 oz Type D
30% - GG	2.0	1.8 oz Type D
40% - GG	3.25	1.7 oz Type D
20% - VR	5.5	
20% - C Ash	7.0	
30% - C Ash	8.5	
20% - F Ash	7.75	
4% - SF	2.75	
Ternary Mix	Slump (in)	
30C + 5SCBA-A	8.25	
30C + 10SCBA-A	3.75	
30C + 5SCBA-B	8.25	
30C + 10SCBA-B	5.0	
20C + 5GG	7.75	
20C + 10GG	7.5	
30C + 5F	9.5	
30C + 10F	9.25	
30C + 10VR	9.0	
30C + 4SF	8.25	

Note: Due to the fly ash content, ternary blends did not require the use of water-reducing admixtures.

Table 4-6: Slump of Class IV concrete mixes using Type II concrete

Binary Mix	Slump (in)	Water-Reducing Admixtures Used (oz/cwt)
Control	3.25	
10% - SCBA-A	2.25	5.3 oz Type D
20% - SCBA-A	3.0	7.9 oz Type D60 & 3.5oz Type F
30% - SCBA-A	2.25	7 oz Type D & 7oz Type F
10% - SCBA-B	3.75	7 oz Type D
20% - SCBA-B	5.75	9.9 oz Type D & 3.4oz Type F
30% - SCBA-B	4.5	10 oz Type D
20% - GG	2.75	
30% - GG	3.25	
40% - GG	2.5	
20% - VR	3.0	
20% - C Ash	8.25	
30% - C Ash	8.75	
20% - F Ash	7.75	
4% - SF	4.75	
Ternary Mix	Slump, in	
30C + 5SCBA-A	6.5	
30C + 10SCBA-A	3.0*	
30C + 5SCBA-B	7.75	
30C + 10SCBA-B	3.75	
20C + 5GG	7.5	
20C + 10GG	8.0	
30C + 5F	7.25	
30C + 10F	7.75	
30C + 10VR	8.5	
30C + 4SF	4.5	

Note: Due to the fly ash content, ternary blends did not require the use of water-reducing admixtures *with the exception of the 30 + 10SCBA-A mixture which required 1.9 oz/cwt of Type D admixture.

Table 4-7: Slump of Class I concrete mixes using Type II concrete

Binary Mix	Slump (in)	Water-Reducing Admixtures Used (oz/cwt)
Control	6.5	6.8 oz Type D & 3.4 oz Type F
10% - SCBA-A	3.0	10 oz Type D
20% - SCBA-A	3.25	10 oz Type D & 5 oz Type F
30% - SCBA-A	2.0	10 oz Type D
10% - SCBA-B	2.75	5 oz Type D
20% - SCBA-B	3.75	10 oz Type D & 1 oz Type F
30% - SCBA-B	4.5	10 oz Type D & 4 oz Type F
20% - GG	2.5	
30% - GG	4.25	
40% - GG	5.0	
20% - VR	2.25	2 oz Type D
20% - C Ash	3.0	
30% - C Ash	3.75	
20% - F Ash	8.25	
4% - SF	2.75	
Ternary Mix	Slump (in)	
30C + 5SCBA-A	2.5	
30C + 10SCBA-A	2.75*	
30C + 5SCBA-B	7.75	
30C + 10SCBA-B	6.0	
20C + 5GG	8.5	
20C + 10GG	6.5	
30C + 5F	8.5	
30C + 10F	5.5	
30C + 10VR	6.5	
30C + 4SF	5.0	

Note: Due to the fly ash content, ternary blends did not require the use of water-reducing admixtures *with the exception of the 30 + 10SCBA-A mixture which required 2 oz/cwt of Type D admixture.

4.3.1 Temperature – ASTM C1064

Concrete temperature can give an indication of complications that may arise in mass concrete placements. For example, a concrete mix that is much higher in temperature than the control is more likely to have issues arising from thermal cracking. Therefore, an SCM that lowers the heat generated by hydration would be useful, as Florida primarily places concrete in hot weather compared to the rest of the United States. The temperature of freshly mixed concrete

is measured by inserting a thermometer into the concrete. After two to five minutes, the temperature of the concrete is recorded to the nearest 1°F [183].

In accordance with ASTM C511 the laboratory mixing room is kept at $23^{\circ}\text{C} \pm 4^{\circ}\text{C}$ and the mixing water is $23^{\circ} \pm 2^{\circ}\text{C}$. From these values, each of the concrete mixtures fresh temperatures would fall within the acceptable range of the room temperature ($66.2^{\circ}\text{F} - 80.6^{\circ}\text{F}$). Prior to mixing, the materials were batched out the day before and were allowed to thermally equilibrate in the mixing laboratory (in sealed buckets) for approximately 24 hours. Based on the ranges of fresh temperatures ($68^{\circ}\text{F} - 76^{\circ}\text{F}$), there were no mixes that appeared to present an issue with regards to excessive heat generation. The fresh temperature of each class of concrete is summarized in Table 4-8 and Table 4-9.

Table 4-8: Fresh temperature of Class IV concrete using Type I/II or Type IL cement with SCM

Class IV – Type I/II Cement		Class IV – Type IL Cement	
Mix	Temperature (°F)	Mix	Temperature (°F)
OPC	72	OPC	71
Binary Mixes		Binary Mixes	
10SCBA-A	74	10SCBA-A	72
20SCBA-A	74	20SCBA-A	72
30SCBA-A	76	30SCBA-A	75
10SCBA-B	75	10SCBA-B	74
20SCBA-B	75	20SCBA-B	74
30SCBA-B	73	30SCBA-B	76
20GG	74	20GG	76
30GG	74	30GG	71
40GG	71	40GG	73
20VR	71	20VR	68
20C	72	20C	72
30C	73	30C	73
20F	72	20F	73
4SF	71	4SF	74
Ternary Mixes		Ternary Mixes	
30C+5SCBA-A	73	30C+5SCBA-A	75
30C+10SCBA-A	72	30C+10SCBA-A	75
30C+5SCBA-B	73	30C+5SCBA-B	72
30C+10SCBA-B	74	30C+10SCBA-B	73
20C+5GG	72	20C+5GG	71
20C+10GG	73	20C+10GG	71
30C+10VR	73	30C+10VR	72
30C+5F	72	30C+5F	72
30C+10F	73	30C+10F	72
30C+4SF	72	30C+4SF	74

Table 4-9: Fresh temperature of Class I concrete using Type II cement with SCM

Class I – Type II Cement	
Mix	Temperature (°F)
OPC	72
Binary Mixes	
10SCBA-A	75
20SCBA-A	76
30SCBA-A	75
10SCBA-B	75
20SCBA-B	75
30SCBA-B	74
20GG	72
30GG	75
40GG	75
20VR	68
20C	72
30C	73
20F	72
4SF	73
Ternary Mixes	
30C+5SCBA-A	72
30C+10SCBA-A	72
30C+5SCBA-B	72
30C+10SCBA-B	73
20C+5GG	72
20C+10GG	73
30C+10VR	72
30C+5F	73
30C+10F	72
30C+4SF	71

4.3.2 Density (Unit Weight) – ASTM C138

The density of concrete is used as a form of quality control. If the density of the concrete differs significantly compared to what is expected, it can be indicative that the concrete mix may not be batched correctly. For determining the density of freshly made concrete, a steel bucket of known volume is filled with concrete in three layers. Each layer is rodded, and the entrapped air is removed by tapping the bucket with a mallet. After the third layer is placed, the surface is finished, and the bucket is weighed. The density is then determined by dividing the weight of the concrete in the bucket by the volume of the bucket. The results of the unit weight/density measurements of each concrete batch are presented below in Table 4-10 and Table 4-11. The results indicate that there are not large deviations between concrete mixes, although the inclusion

of sugarcane bagasse ash or ground glass will tend to make the concrete slightly less dense. This is not surprising as the apparent specific gravity of these materials were on the lower end of the materials investigated.

Table 4-10: Unit weight of Class IV concrete using Type I/II or Type IL cement with SCM

Class IV – Type I/II Cement		Class IV – Type IL Cement	
Mix	Unit Weight (lb/ft ³)	Mix	Unit Weight (lb/ft ³)
OPC	145	OPC	145
Binary Mixes		Binary Mixes	
10SCBA-A	143	10SCBA-A	146
20SCBA-A	141	20SCBA-A	143
30SCBA-A	141	30SCBA-A	141
10SCBA-B	143	10SCBA-B	143
20SCBA-B	143	20SCBA-B	143
30SCBA-B	144	30SCBA-B	143
20GG	144	20GG	142
30GG	143	30GG	141
40GG	143	40GG	141
20VR	144	20VR	144
20C	145	20C	144
30C	145	30C	145
20F	145	20F	144
4SF	143	4SF	143
Ternary Mixes		Ternary Mixes	
30C+5SCBA-A	145	30C+5SCBA-A	144
30C+10SCBA-A	143	30C+10SCBA-A	144
30C+5SCBA-B	145	30C+5SCBA-B	144
30C+10SCBA-B	144	30C+10SCBA-B	143
20C+5GG	145	20C+5GG	144
20C+10GG	144	20C+10GG	143
30C+10VR	145	30C+10VR	145
30C+5F	145	30C+5F	145
30C+10F	144	30C+10F	145
30C+4SF	144	30C+4SF	144

Table 4-11: Unit weight of Class I concrete using Type IL cement with SCM

Class I – Type IL Cement	
Mix	Unit Weight (lb/ft ³)
OPC	144
Binary Mixes	
10SCBA-A	143
20SCBA-A	141
30SCBA-A	140
10SCBA-B	142
20SCBA-B	141
30SCBA-B	142
20GG	141
30GG	138
40GG	138
20VR	144
20C	144
30C	144
20F	143
4SF	143
Ternary Mixes	
30C+5SCBA-A	143
30C+10SCBA-A	143
30C+5SCBA-B	144
30C+10SCBA-B	143
20C+5GG	144
20C+10GG	143
30C+10VR	144
30C+5F	144
30C+10F	144
30C+4SF	143

4.3.3 Air Content – ASTM C231

Much like the density test, air content is another form of quality control. If results from other performance tests are indicative of a poor-quality concrete, the air content can potentially help explain why the results are skewed. This test method is used to determine the air content of freshly made concrete with the use of a pressure meter. Once the density of concrete is measured, an air chamber is attached to the steel bucket. The chamber is pressurized, and the air content is measured. Determining the air content of a concrete mix can help with its evaluation. The durability and strength characteristics affected by air content are freeze-thaw resistance and permeability [9,73], which affects chloride ion penetration and, to a lesser extent, alkali silica reactivity, and sulfate resistance [184,185]. A higher air content results in a higher resistance to

freeze-thaw damage [11,186] and a higher permeability [9]. If the concrete being placed is reinforced, a lower air content and corresponding permeability reduces the susceptibility of corrosion [187–189].

One additional area of concern was the fact that the sugarcane bagasse ashes had considerable amounts of carbon left from incomplete incineration. With fly ashes that have high amounts of carbon, the highly absorptive carbon can absorb air-entraining admixtures and reduce air entrainment. Therefore, it was imperative to determine whether the SCBA mixtures had acceptable air content. From the FDOT's *Standard Specifications for Road and Bridge Construction* Section 346, the air content of concrete should be between 1-6% [21]. Each mixture evaluated, including the sugarcane bagasse ash mixes had sufficient air content as can be seen in Table 4-12 and Table 4-13. After accounting for the precision of the test method, mixes incorporating ground glass were slightly higher compared to control. This can be explained by the differences in slump between the controls and the GG mixtures. A mixture with higher slump typically has a lower air content compared to a mixture with lower slump; most of the GG mixtures had a lower slump than control [190,191].

Table 4-12: Air content of Class IV concrete mixes using Type I/II or Type IL cement with SCM

Class IV – Type I/II		Class IV – Type IL	
Mix	Air Content (%)	Mix	Air Content (%)
OPC – Type I/II	2.3%	OPC – Type IL	3.0%
Binary Mixes		Binary Mixes	
10SCBA-A	2.6%	10SCBA-A	2.3%
20SCBA-A	3.2%	20SCBA-A	2.7%
30SCBA-A	3.1%	30SCBA-A	2.9%
10SCBA-B	2.8%	10SCBA-B	2.8%
20SCBA-B	2.4%	20SCBA-B	2.8%
30SCBA-B	2.3%	30SCBA-B	2.8%
20GG	3.3%	20GG	3.8%
30GG	3.3%	30GG	3.7%
40GG	2.8%	40GG	3.3%
20VR	2.2%	20VR	3.1%
20C	1.5%	20C	1.4%
30C	1.6%	30C	1.4%
20F	1.8%	20F	1.8%
4SF	2.9%	4SF	2.7%
Ternary Mixes		Ternary Mixes	
30C+5SCBA-A	1.6%	30C+5SCBA-A	1.9%
30C+10SCBA-A	2.1%	30C+10SCBA-A	2.3%
30C+5SCBA-B	1.8%	30C+5SCBA-B	1.9%
30C+10SCBA-B	2.0%	30C+10SCBA-B	2.1%
20C+5GG	1.7%	20C+5GG	1.9%
20C+10GG	1.8%	20C+10GG	1.9%
30C+10VR	1.5%	30C+10VR	1.5%
30C+5F	1.3%	30C+5F	1.6%
30C+10F	1.2%	30C+10F	1.6%
30C+4SF	1.6%	30C+4SF	2.1%

Table 4-13: Air content of Class I concrete mixes using Type II cement with SCM

Class I - II	
Mix	Air Content (%)
OPC – Type II	3.0%
Binary Mixes	
10SCBA-A	3.0%
20SCBA-A	3.4%
30SCBA-A	3.5%
10SCBA-B	3.6%
20SCBA-B	4.0%
30SCBA-B	3.5%
20GG	4.8%
30GG	5.3%
40GG	5.2%
20VR	2.8%
20C	2.1%
30C	2.1%
20F	1.8%
4SF	3.1%
Ternary Mixes	
30C+5SCBA-A	2.4%
30C+10SCBA-A	2.3%
30C+5SCBA-B	1.9%
30C+10SCBA-B	1.9%
20C+5GG	2.3%
20C+10GG	2.4%
30C+10VR	1.2%
30C+5F	1.8%
30C+10F	1.8%
30C+4SF	2.0%

4.4 MECHANICAL PROPERTIES

The only mechanical property evaluated with mortars was compressive strength, and while there were no mixes that exhibited gross incompatibility within cementitious systems, it is prudent to determine if the higher shearing action provided by tumbling aggregate in a concrete mixture would provide additional benefit compared to mortar mixing. Additionally, for concrete structural design, tensile strength and elastic modulus are design characteristics of concern. Evaluating concrete for these characteristics allows for a more robust evaluation of the potential of each material.

4.4.1 Compressive Strength – ASTM C39

The compressive strengths for the concrete mixes for Class I and Class IV are presented below. The results are organized by concrete class, SCM type, and then cement type. The figures compare SCM to the respective control for the type of cement used and the Class of concrete produced. The red dotted line indicates the specified minimum compressive strength at 28 days (f'_c) for each class of concrete. The compressive strength for each mixture was measured and computed using a minimum of three cylindrical 4" x 8" specimens in accordance with ASTM C39 [192]. The specimens were demolded after $23 \frac{1}{2} \pm \frac{1}{2}$ hours after casting and stored in a fog room at $73^\circ \pm 3^\circ\text{F}$ and 95% RH as per ASTM C511 [193]. The specimens were stored in the fog room until the time of testing.

Figure 4-1 compares Type I/II cement and Type IL cement in an FDOT Class IV concrete. The general mix design for the Class IV concrete included 670 lb/yd³ of cementitious content, which could include 100% portland cement, or up to 40% supplementary cementitious material content, a water-to-cementitious material ratio (w/cm) of 0.40, an aggregate ratio of 0.40, target slump of three inches, and a 28-day target strength of 5,500 psi. Liquid admixtures were used to adjust air content and workability as needed.

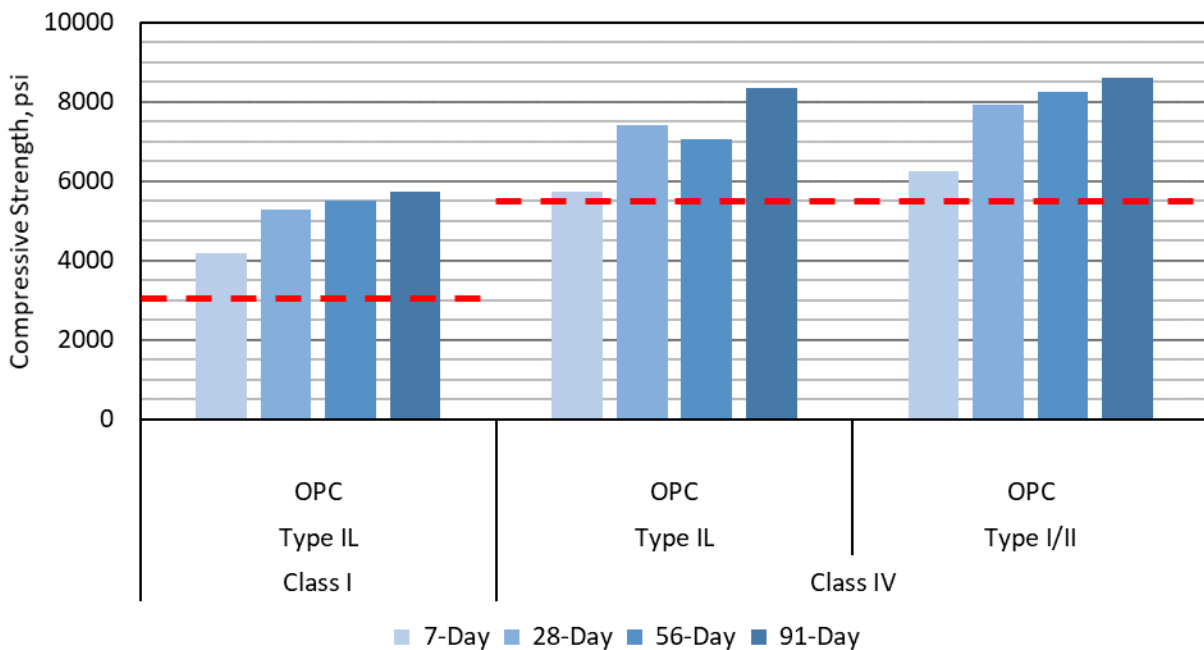


Figure 4-1: Compressive strength of Type IL Class I concrete, Type IL Class IV concrete, and Type I/II Class IV concrete mixes.

The mix design for the Class I concrete included 500 lb/yd³ of total cementitious content, a w/cm of 0.50, an aggregate ratio of 0.40, target slump of two inches, and a 28-day target strength of 3,000 psi. Liquid admixtures were used to adjust air content and workability as needed.

The minimum cement content required by the FDOT for a Class IV concrete is 658 lb/yd³ and a Class I concrete is 470 lb/yd³. The specified minimum 28-day compressive strengths ($f'c$) for a Class IV (5,500 psi) and a Class I (3,000 psi) concrete were exceeded at 7 days by the three control mixes [21].

4.4.1.1 Class IV Concrete

4.4.1.1.1 Sugarcane Bagasse Ash (SCBA-A and SCBA-B)

The compressive strength results of sugarcane bagasse ash as a cement replacement are presented in Figure 4-2 and Figure 4-3. The results indicated a general decrease in strength as SCBA replacements increased. However, most of the mixes containing sugarcane bagasse ash met the specified minimum 28-day compressive strength ($f'c$) of 5,500 psi, with the exception of the 30% replacement of IL cement with SCBA-B.

With Type I/II cement, SCBA-A had lower early-age strength than SCBA-B; but the SCBA-A mixes exhibited strengths that were comparable or higher than SCBA-B amended mixes beyond 28 days. SCBA-A mixes exhibited higher early-age strength than SCBA-B mixes when using Type IL cement. The SCBA-A mixes decreased in strength as replacement increased. The SCBA mixes, regardless of type, had decreasing compressive strength as the replacement percentage increased.

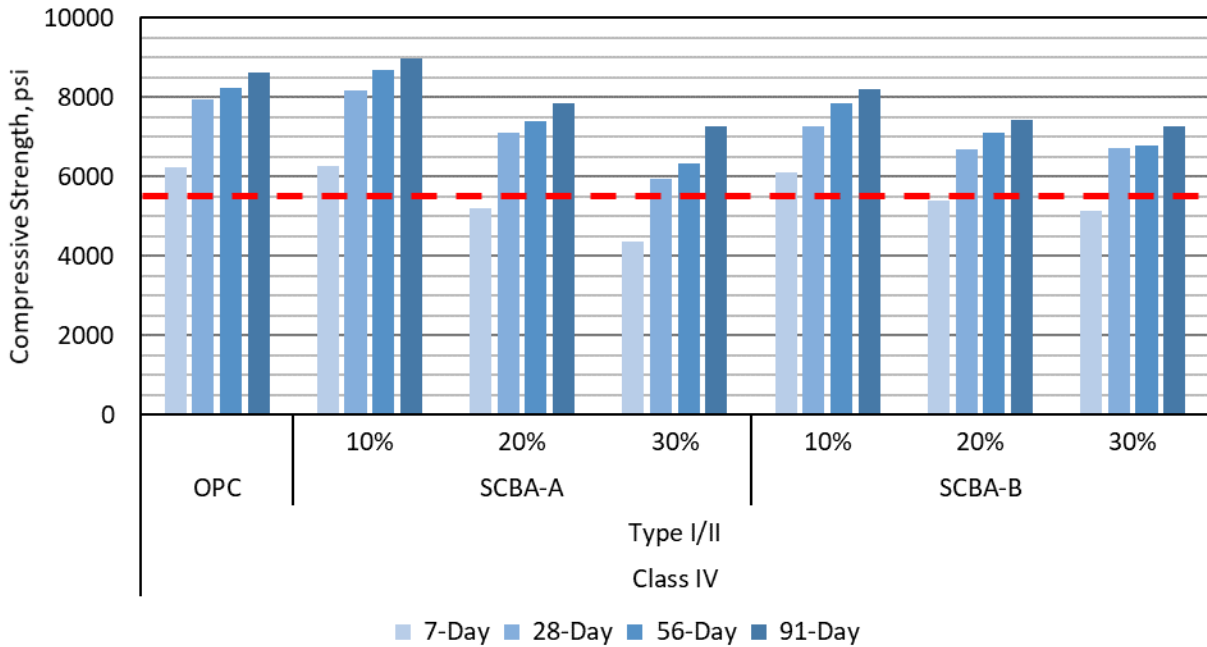


Figure 4-2: Compressive strength of concrete with 10% – 30% SCBA-A or SCBA-B as Type I/II cement replacements.

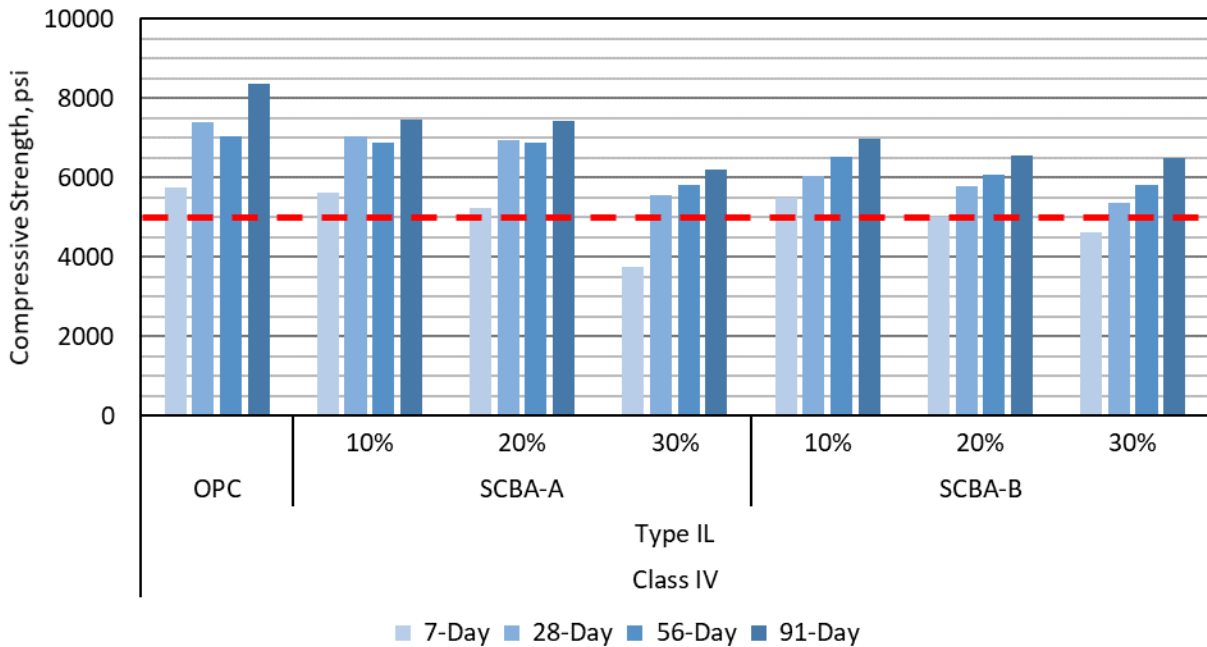


Figure 4-3: Compressive strength of concrete with 10% – 30% SCBA as Type IL cement replacements.

4.4.1.1.2 Ground Glass (GG) and Volcanic Rock (VR)

The compressive strength results from the incorporation of post-consumer ground waste glass (GG) and ground volcanic rock (VR) in Class IV concrete are presented in Figure 4-4 and Figure 4-5. The general trend observed with the use of GG was decreasing 28-day strength as the replacement increased. However, at 91 days, the three glass replacements exhibited comparable strengths to each other. The behavior of glass in concrete was similar to that of Class F fly ash in that the early strength (7 and 28 days) was statistically significantly lower than control (using a two-tailed T-test with unequal variances and a 95% confidence interval), but at later ages (56 and 91 days), the difference in strength was less pronounced. Ground volcanic rock exhibited a lower strength at each age for a 20% replacement of cement. The GG and VR mixes met the FDOT specified minimum 28-day compressive strength ($f'c$) except for 30 and 40% Type II cement replacements with GG.

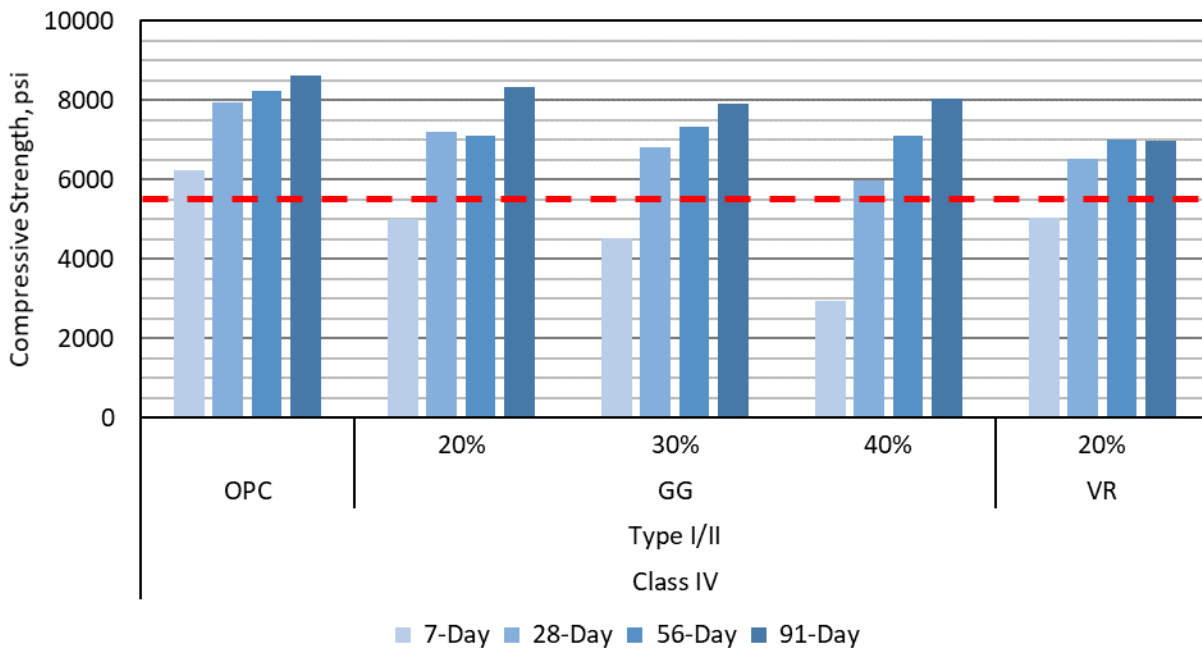


Figure 4-4: Compressive strength of concrete with 20% – 40% GG or 20% VR as I/II cement replacements.

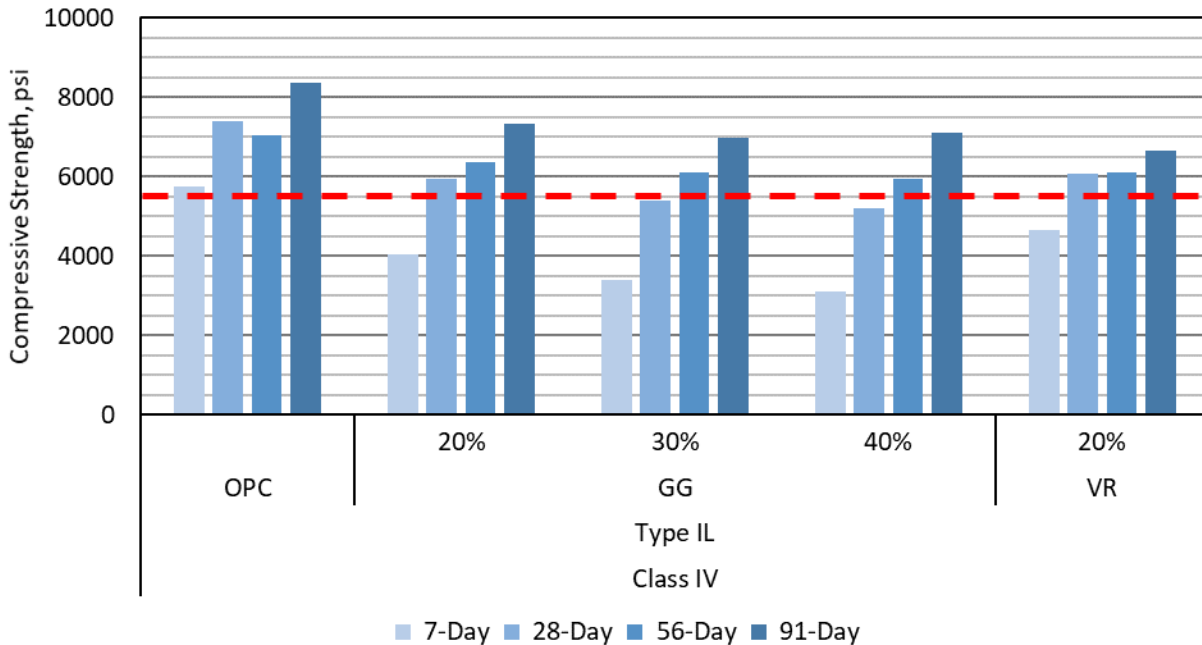


Figure 4-5: Compressive strength of concrete with 20% – 40% GG or 20% VR as IL cement replacements.

4.4.1.1.3 Class F and C Fly Ash (F Ash and C Ash), and Silica Fume (SF)

The compressive strength results from the incorporation of Class F fly ash (F ash), Class C fly ash (C ash), and silica fume (SF) in Class IV concrete are presented in Figure 4-6 and Figure 4-7. The fly ashes and silica fume were used as benchmarks for the performance of alternative SCM. Each of the mixes presented below exceeded the specified minimum 28-day compressive strength (f'_c) of 5,500 psi. As expected, the strength gain in the fly ash mixes was more pronounced at later ages due to the slower development of strength from pozzolanic reactions. The silica fume mixes exhibited comparable strengths to the control. This performance was not as pronounced as typical silica fume usage would warrant and was caused by poor dispersion of silica fume particles during the mixing process and generally low addition rate of 4%. This lower addition rate was to be consistent with the previous project (FDOT BDV31-977-06) which this research builds and expands upon [8]. The 28-day and 56-day strengths for concretes using 4% silica fume replacement of either Type I/II or Type IL cement were approximately 200 psi from each other; therefore, the 28-day and 56-day strengths are not statistically significantly different in either cementitious system.

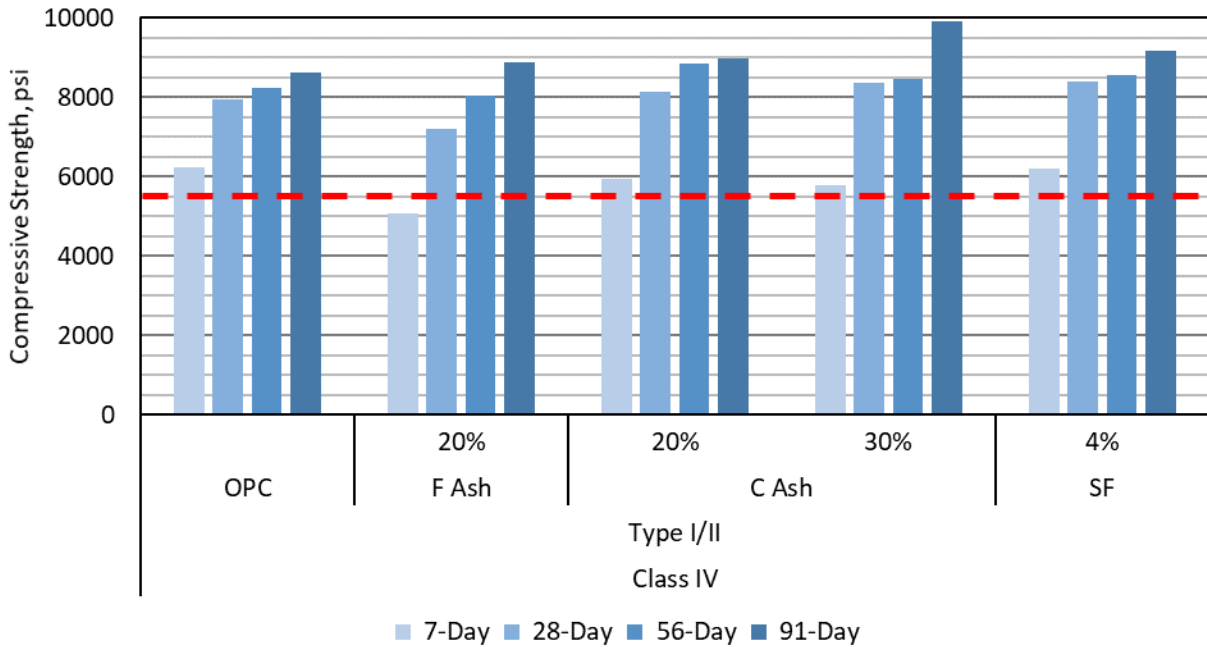


Figure 4-6: Compressive strength of concrete with 20 – 30% F or C ash, or 4% SF as I/II cement replacements.

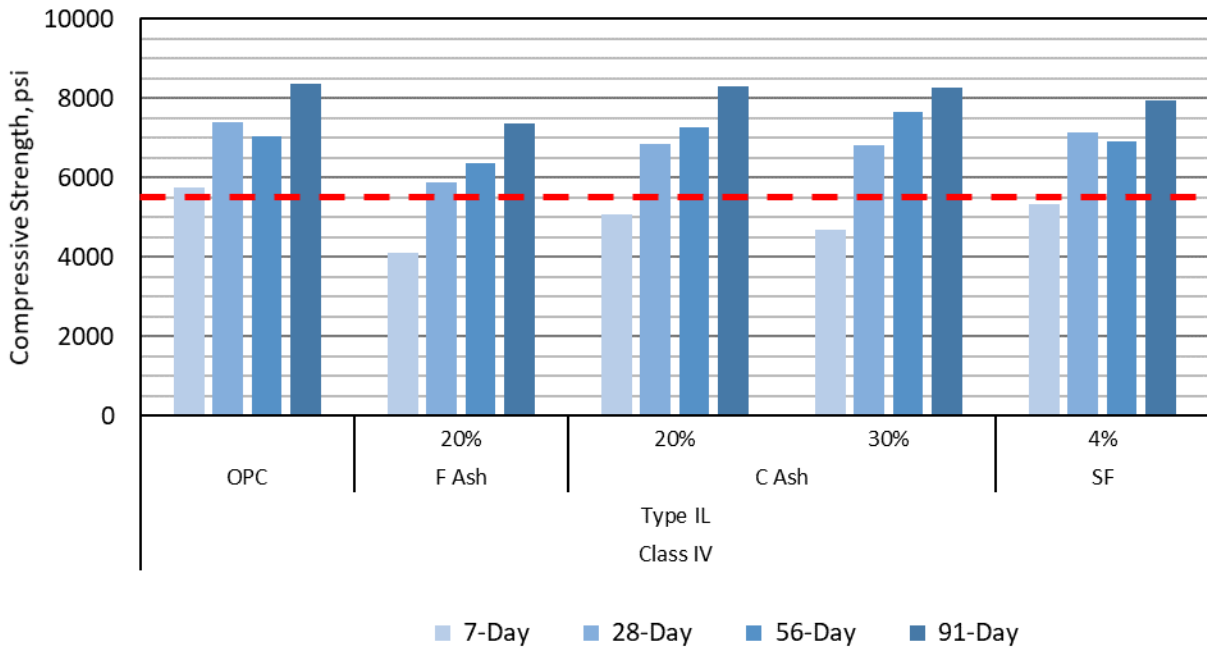


Figure 4-7: Compressive strength of concrete with 20 – 30% F or C ash, or 4% SF as IL cement replacements.

4.4.1.1.4 Ternary Mixes

Compressive strength results of Class IV ternary mixes with Class C fly ash and SCBA are shown in Figure 4-8 and Figure 4-9. The results were influenced by the Class C fly ash due to the high replacement percentage, with slight variations depending on the second SCM being used. Additionally, Class C fly ash is hydraulic and reacts faster than Class F fly ash. However, the mixes that incorporated SCBA-A exhibited higher strengths than the SCBA-B mixes or the 30% Class C fly ash mix without SCBA. Most mixes exhibited strengths that were comparable to the control with the exception of 91-day strengths, which exhibited increasing late-age strengths as seen with binary mixes of Class C fly ash. However, with respect to the Type IL cement mixes, the mixes with SCBA-A exhibited higher 91-day strength than SCBA-B (which was comparable to control). The Class C fly ash and SCBA-A mixes exhibited higher strengths than the control at 91 days. Each of the mixes exceeded the minimum strength (f'_c) per the FDOT Specification at 28 days.

The compressive strengths presented in Figure 4-10 and Figure 4-11 correspond to Class IV concrete ternary mixes that incorporated Class C fly ash with GG, F ash, VR, and SF. The strengths were comparable to the control at each age after 7 days, with the exception of C ash and F ash mixes, which had lower 7-day strengths and higher 91-day strengths. Each of the ternary mixes exceeded the 28-day specified minimum compressive strength (f'_c).

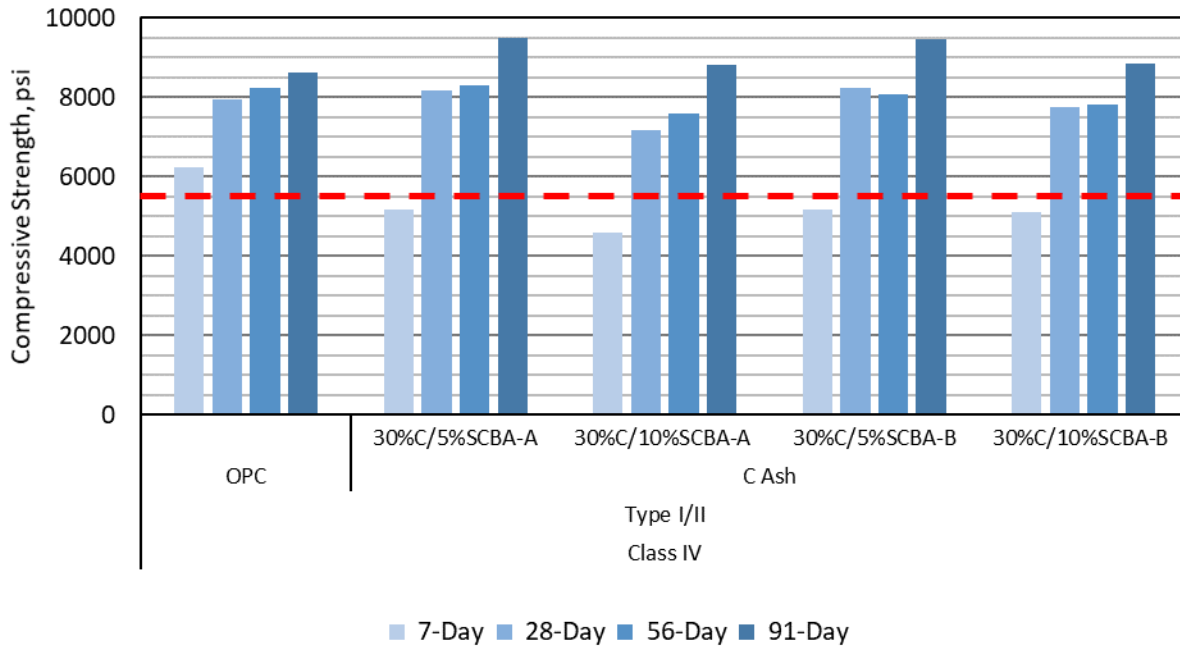


Figure 4-8: Compressive strength of mixes containing 30% C fly ash and 5% – 10% SCBA as Type I/II replacements.

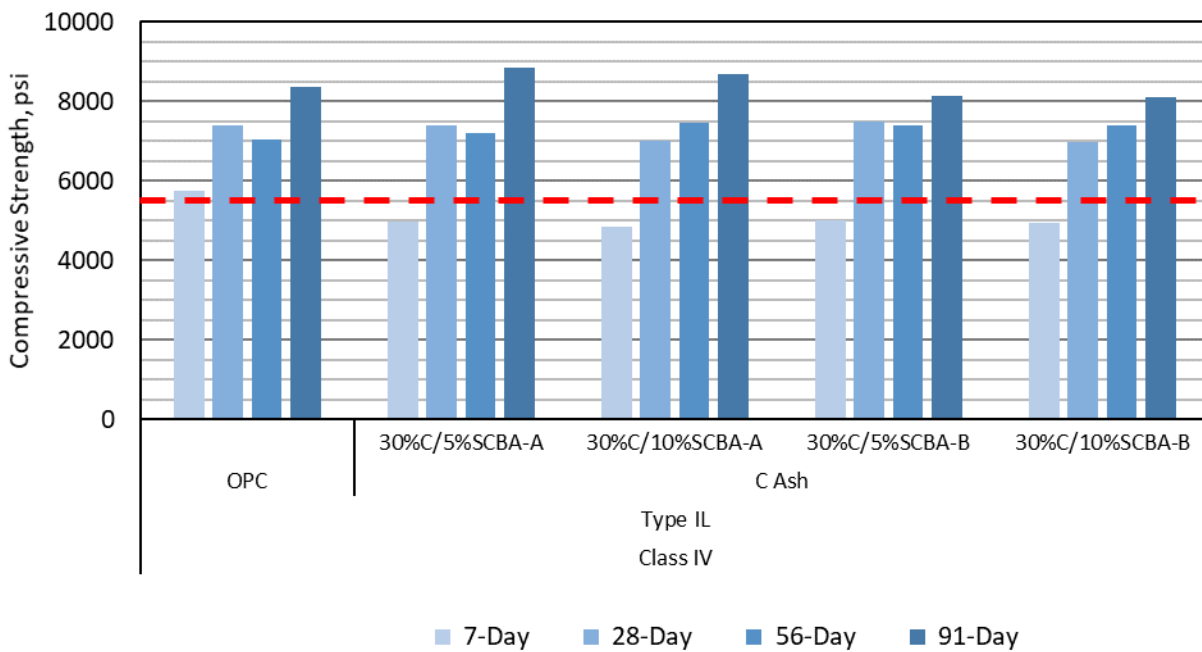


Figure 4-9: Compressive strength of mixes containing 30% C ash with 5% – 10% SCBA as Type IL replacements.

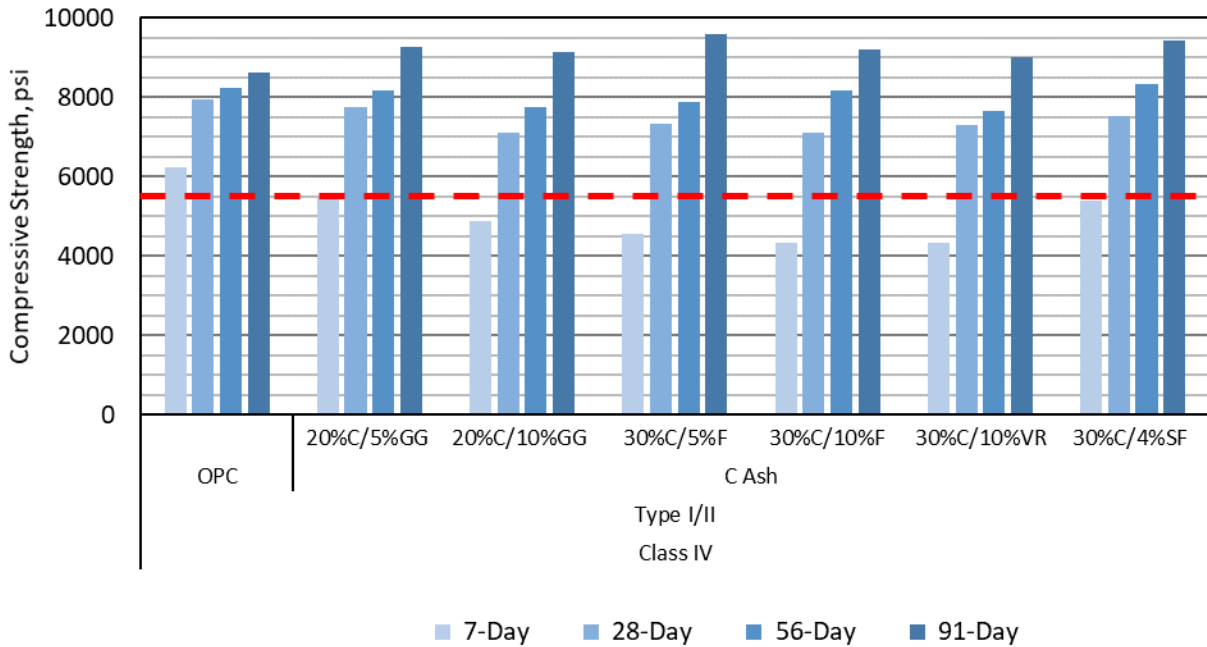


Figure 4-10: Compressive strength of ternary mixes containing 20% or 30% C ash with 5-10% GG, 10% F ash, 10% VR, or 4% SF as I/II cement replacements.

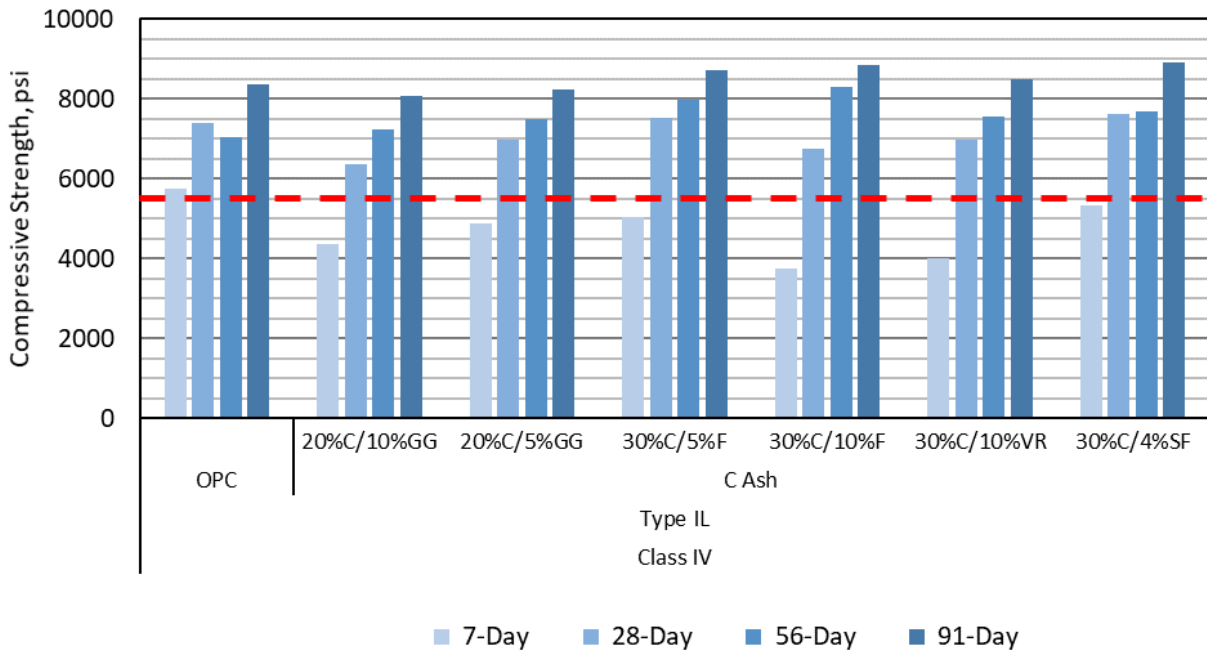


Figure 4-11: Compressive strength of ternary mixes containing 20% C ash and 5% or 10% GG or 30% C ash with 5% – 10% F ash, 10% VR, or 4% SF as IL cement replacements.

Table 4-14 provides a summary of the compressive strength of Class IV concrete using Type I/II cement with various supplementary cementitious material replacements. Table 4-15

provides the compressive strengths normalized to the control at the stated ages for the same mixture designs.

Table 4-14: Summary table of compressive strength results for Class IV concrete mixes utilizing Type I/II cement.

Compressive Strength of Concrete using Type I/II Cement (psi)				
Mix	7 Day	28 Day	56 Day	91 Day
OPC – Type I/II	6240	7930	8250	8620
Class IV Binary Mixes				
20% - GG	5010*	7210*	7120*	8330
30% - GG	4510*	6800*	7320	7900*
40% - GG	2940*	5980*	7090	8050
10% - SCBA-A	6280	8170*	8690	8990
20% - SCBA-A	5200	7090*	7410	7850*
30% - SCBA-A	4360*	5930*	6340*	7260*
10% - SCBA-B	6120	7270	7850	8190
20% - SCBA-B	5380*	6680*	7090*	7430*
30% - SCBA-B	5140*	6710*	6770*	7280*
20% - VR	5030*	6540*	7000*	6970*
4% - SF	6200	8390	8560	9180
20% - C Ash	5950	8140	8850	8990
30% - C Ash	5780	8360	8460	9990
20% - F Ash	5080	7210*	8030	8890
Class IV Ternary Mixes				
20C/5GG	5490*	7740	8170	9270*
20C/10GG	4880*	7120	7740	9130*
30C/5SCBA-A	5170*	8180	8290	9500*
30C/10SCBA-A	4600*	7170*	7590	9020
30C/5SCBA-B	5180*	8230*	8080	9450*
30C/10SCBA-B	5100	7740	7800	8840
30C/10VR	4330*	7290	7660	9010
30C/4SF	5380*	7510	8340	9440*
30C/5F	4540*	7340	7870	9580*
30C/10F	4340	7100*	8180	9210*

Note: Mixes denoted with an asterisk (*) indicate results that are statistically significantly different from control based upon a two-tailed T-test assuming unequal variances, and a 95% confidence interval.

Table 4-15: Summary table of normalized compressive strengths for Class IV concrete mixes utilizing Type I/II cement.

Normalized Compressive Strength of Concrete using Type I/II Cement				
Mix	7 Day	28 Day	56 Day	91 Day
OPC – Type I/II	100%	100%	100%	100%
Class IV Binary Mixes				
20% - GG	80%	91%	86%	97%
30% - GG	72%	86%	89%	92%
40% - GG	47%	75%	86%	93%
10% - SCBA-A	101%	103%	105%	104%
20% - SCBA-A	83%	89%	90%	91%
30% - SCBA-A	70%	75%	77%	84%
10% - SCBA-B	98%	92%	95%	95%
20% - SCBA-B	86%	84%	86%	86%
30% - SCBA-B	82%	85%	82%	84%
20% - VR	81%	82%	85%	81%
4% - SF	99%	106%	104%	106%
20% - C Ash	95%	103%	107%	104%
30% - C Ash	93%	105%	103%	116%
20% - F Ash	81%	91%	97%	103%
Class IV Ternary Mixes				
20C/5GG	88%	98%	99%	108%
20C/10GG	78%	90%	94%	106%
30C/5SCBA-A	83%	103%	100%	110%
30C/10SCBA-A	74%	90%	92%	105%
30C/5SCBA-B	83%	104%	98%	110%
30C/10SCBA-B	82%	98%	95%	103%
30C/10VR	69%	92%	93%	105%
30C/4SF	86%	95%	101%	110%
30C/5F	73%	93%	95%	111%
30C/10F	70%	90%	99 %	107%

Table 4-16 provides a summary of the compressive strength of Class IV concrete using Type II cement with various supplementary cementitious material replacements. Table 4-17 provides the compressive strengths normalized to the control at the stated ages for the same mixture designs.

Table 4-16: Summary table of compressive strength results for Class IV concrete mixes utilizing Type II cement.

Compressive Strength of Concrete using Type II Cement (psi)				
Mix	7 Day	28 Day	56 Day	91 Day
OPC – Type II	5740	7400	7050	8360
Class IV Binary Mixes				
20% - GG	4030*	5930*	6360*	7330*
30% - GG	3400*	5410*	6100*	6970*
40% - GG	3090*	5210*	5940*	7120*
10% - SCBA-A	5620	7040	6870	7460*
20% - SCBA-A	5230	6950*	6880	7440*
30% - SCBA-A	3760*	5560*	5820*	6190*
10% - SCBA-B	5490	6040*	6510	6960*
20% - SCBA-B	5010*	5780*	6070*	6550*
30% - SCBA-B	4630*	5370*	5830*	6500*
20% - VR	4640*	6060*	6110*	6650*
4% - SF	5340	7140*	6910	7930
20% - C Ash	5070	6840*	7270	8300
30% - C Ash	4700*	6830*	7640*	8280
20% - F Ash	4110*	5880*	6370*	7350*
Class IV Ternary Mixes				
20C/5GG	4890	6990*	7500	8230
20C/10GG	4360*	6370*	7230	8060
30C/5SCBA-A	4960	7380	7190	8850
30C/10SCBA-A	4860*	7020	7460	8670
30C/5SCBA-B	5020	7500	7410	8140
30C/10SCBA-B	4930*	6990*	7390	8090
30C/10VR	4000*	6990*	7550	8480
30C/4SF	5340	7620	7670*	8910*
30C/5F	5050	7530	7990	8650
30C/10F	4080	7020	8240*	8880*

Note: Mixes denoted with an asterisk (*) indicate results that are statistically significantly different from control based upon a two-tailed T-test assuming unequal variances, and a 95% confidence interval.

Table 4-17: Summary table of normalized compressive strengths for concrete mixes utilizing Type II cement.

Normalized Compressive Strength of Concrete using Type II Cement				
Mix	7 Day	28 Day	56 Day	91 Day
OPC – Type II	100%	100%	100%	100%
Class IV Binary Mixes				
20% - GG	70%	80%	90%	88%
30% - GG	59%	73%	87%	83%
40% - GG	54%	70%	84%	85%
10% - SCBA-A	98%	95%	97%	89%
20% - SCBA-A	91%	94%	98%	89%
30% - SCBA-A	66%	75%	83%	74%
10% - SCBA-B	96%	82%	92%	83%
20% - SCBA-B	87%	78%	86%	78%
30% - SCBA-B	81%	73%	83%	78%
20% - VR	81%	82%	87%	80%
4% - SF	93%	96%	98%	95%
20% - C Ash	88%	92%	103%	99%
30% - C Ash	82%	92%	108%	99%
20% - F Ash	72%	79%	90%	88%
Class IV Ternary Mixes				
20C/5GG	85%	94%	106%	98%
20C/10GG	76%	86%	103%	96%
30C/5SCBA-A	86%	100%	102%	106%
30C/10SCBA-A	85%	95%	106%	104%
30C/5SCBA-B	87%	101%	105%	97%
30C/10SCBA-B	86%	94%	105%	97%
30C/10VR	70%	94%	107%	101%
30C/4SF	93%	103%	109%	107%
30C/5F	88%	102%	113%	103%
30C/10F	71%	95%	117%	106%

4.4.1.2 Class I Concrete

4.4.1.2.1 Sugarcane Bagasse Ash (SCBA-A and SCBA-B) in Class I Concrete

The compressive strength of Class I concrete mixes with SCBA replacements are shown in Figure 4-12. The Class I concrete mixes incorporating SCBA-A and SCBA-B exhibited the same general behavior as observed in Class IV concrete using I/II cement. Each mix met the 28-day strength requirement of 3,000 psi (most by 7 days) with the majority of the mixes having

compressive strengths exceeding 4,000 psi at 28 days indicating acceptable strength for a Class I Pavement mix design.

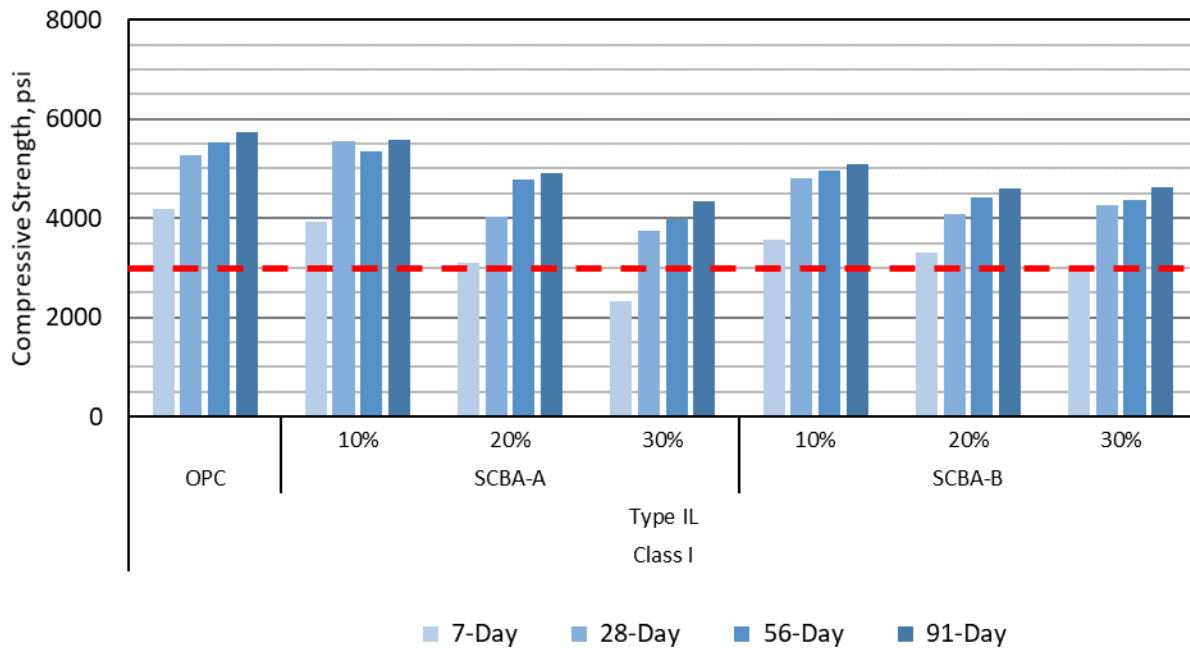


Figure 4-12: Compressive strength of concrete with 10% – 30% SCBA-A or SCBA-B as Type II cement replacements.

4.4.1.2.2 Ground Glass (GG) and Volcanic Rock (VR)

The results for Class I GG and VR concrete mixes using Type II cement are presented in Figure 4-13. As the replacement of ground waste glass increased, the compressive strength decreased for each age tested. Volcanic rock also exhibited consistently lower strengths than the control at each age. However, the mixes in Figure 4-13 exceeded the specified minimum compressive strength (f'_c) of 3,000 psi at 28 days.

Additionally, the 56-day strength of the volcanic rock was lower than the 28-day strength; however, the difference of the strengths is within the precision and bias of the test method. Furthermore, from evaluating the 91-day strength, it is evident that beyond the 28 days of curing, the strength of each mixture ceased to increase substantially, and the volcanic rock did not provide pozzolanic benefit. This is consistent with the results noted in the mortar cube testing.

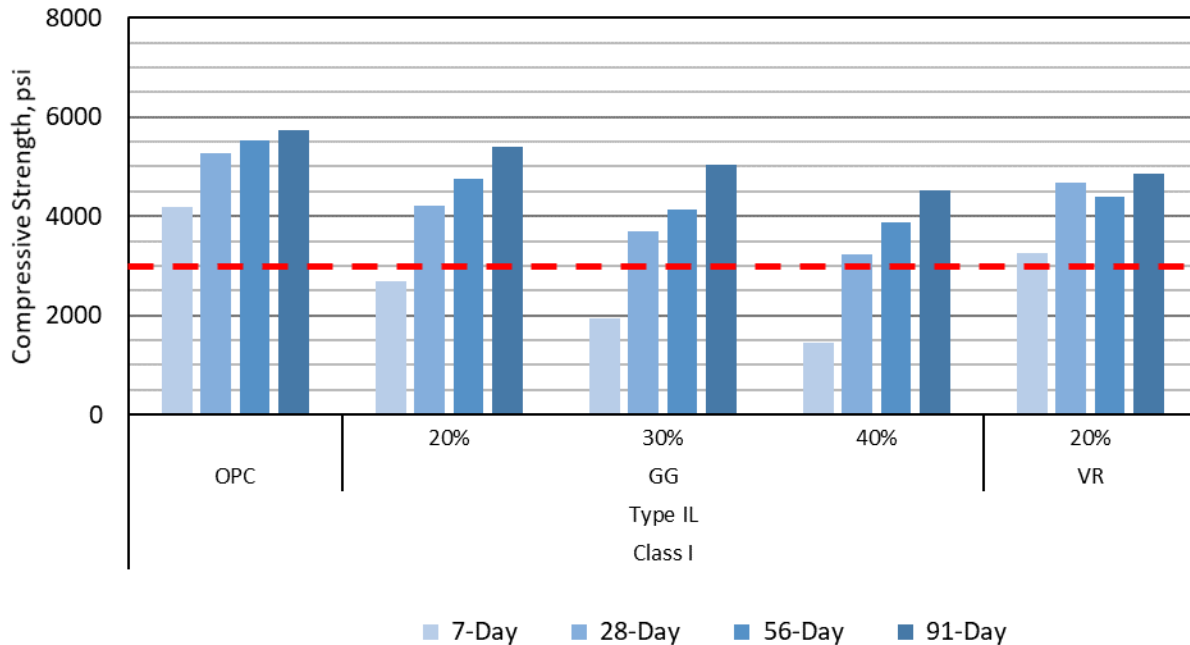


Figure 4-13: Compressive strength of concrete with 20% – 40% GG and 20% VR as IL cement replacements.

4.4.1.2.3 Class F and C Fly Ash (F Ash and C Ash), and Silica Fume (SF)

Figure 4-14 compares Class F fly ash (F ash), Class C fly ash (C ash), and silica fume (SF) replacements to the control in Class I concrete. As expected, the mixes were comparable to the control at most ages, with the C ash mixes having a higher strength than the control at 91 days. The F ash mix was consistently lower than control, but the mixes had a higher strength than the specified minimum compressive strength (f'_c) at 28-days.

The 30% replacement of Class C fly ash was observed to have higher compressive strengths than the 20% Class C fly ash mixes at each testing age beyond 7 days. This result is not anticipated since typically as the amount of an SCM increased, the strength decreased for the 28-day and potentially 56-day strengths due to reduced pozzolanic activity from dilution. However, since the Class C fly ash is a hydraulic material, it will react with water, and this ability to produce strength-bearing phases contributes to its higher rate of strength gain with increasing additions.

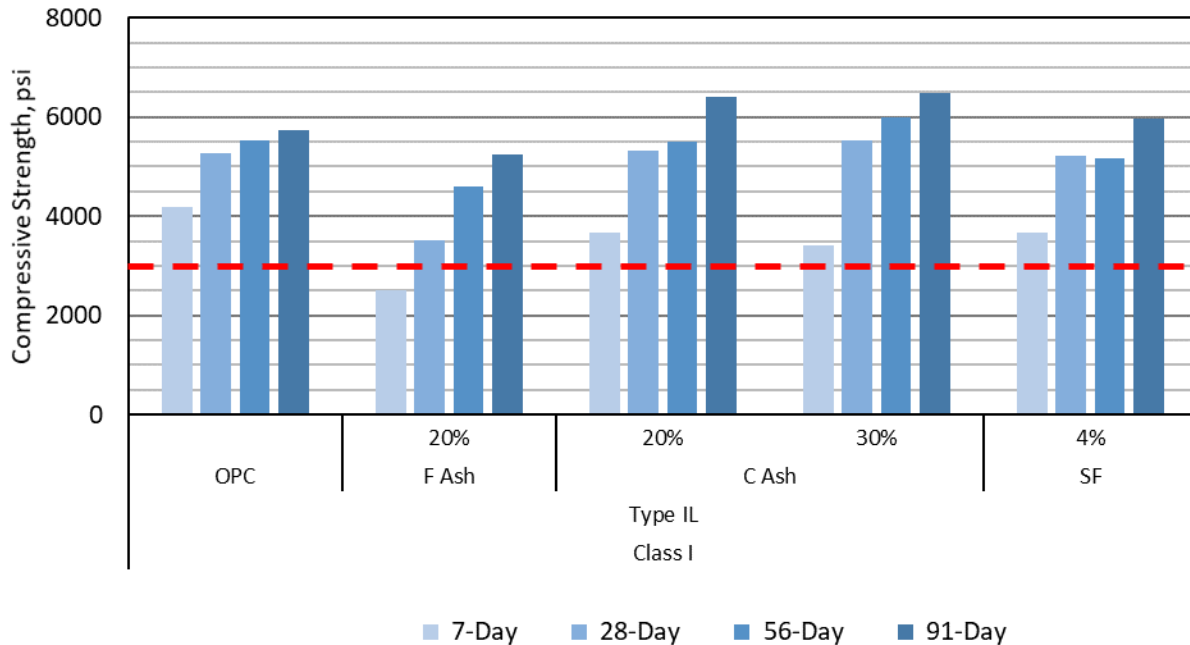


Figure 4-14: Compressive strength of concrete with 20 – 30% F or C ash, or 4% SF as IL cement replacements.

4.4.1.2.4 Ternary Mixes

The Class I ternary mixes using Type IL cement are shown in Figure 4-15 and Figure 4-16. Similar to the Class IV ternary mixes, the strength was most influenced by the C ash. Most mixes had comparable or higher strength than the control at 91 days except for the mix incorporating ground volcanic rock. The 7-day strengths were lower than the control, but at 56 days and beyond, the strengths were comparable or greater than that of the control. The Class I ternary mixes exceeded the specified minimum 28-day compressive strength ($f'c$) of 3,000 psi. Each of the mixes evaluated had compressive strengths well above the minimum by 28 days with most being at least 1,000 psi higher. This indicates that the high replacement of Type IL cement with at least 30% Class C fly ash and 5% or 10% of another alternative supplementary cementitious material would be suitable for a concrete pavement mixture design.

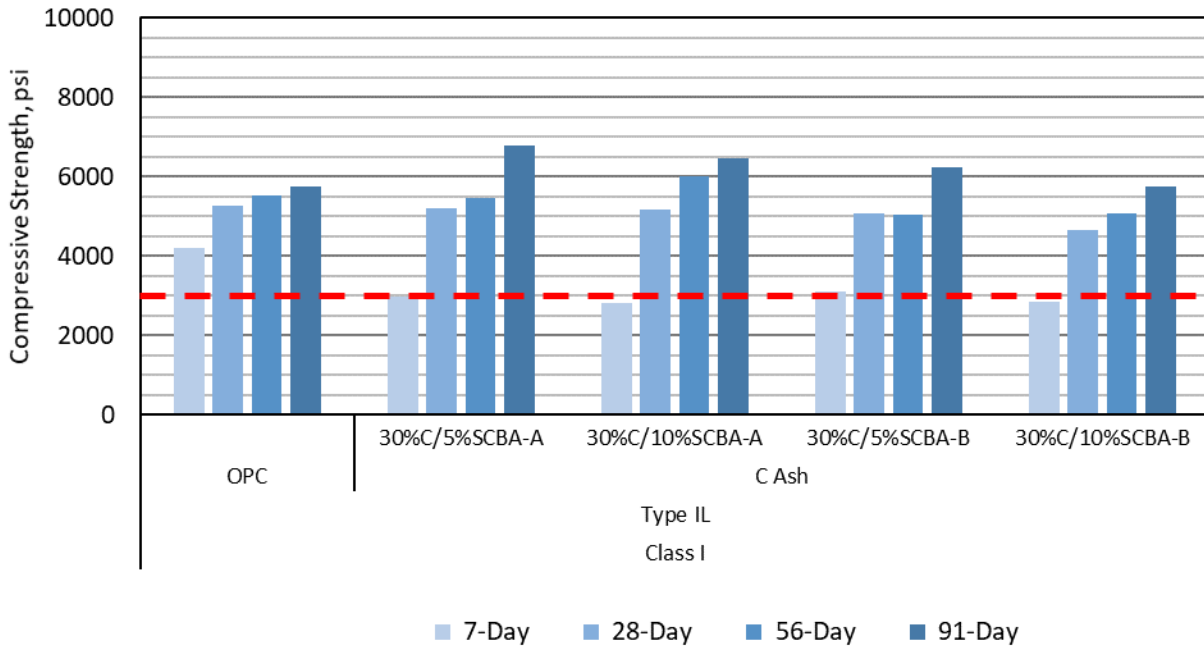


Figure 4-15: Compressive strength of Class I ternary mixes containing 30% C ash with 5% – 10% SCBA-A and SCBA-B as IL cement replacements.

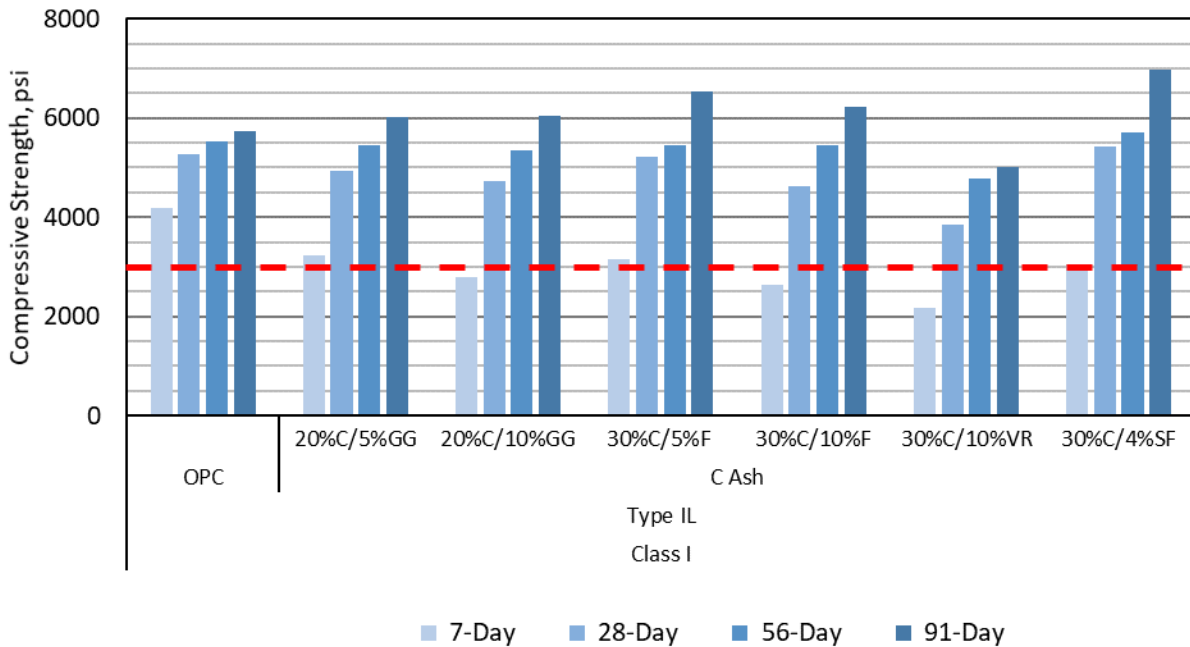


Figure 4-16: Compressive strength of Class I ternary mixes containing 20% C ash and 5% or 10% GG or 30% C ash with 5% – 10% F ash, 10% VR, or 4% SF as IL cement replacements.

Table 4-18 provides a summary of the compressive strength of Class I concrete using Type II cement with various supplementary cementitious material replacements. Table 4-19

provides the compressive strengths normalized to the control at the stated ages for the same mixture designs.

Table 4-18: Summary table of compressive strength results for Class I concrete mixes utilizing Type II cement.

Compressive Strength of Concrete using Type II Cement (psi)				
Mix	7 Day	28 Day	56 Day	91 Day
OPC – Type II	4190	5270	5520	5740
Class I Binary Mixes				
20% - GG	2690*	4200*	4760*	5390*
30% - GG	1940*	3690*	4140*	5030*
40% - GG	1460*	3220*	3880*	4520*
10% - SCBA-A	3930	5550	5360	5570
20% - SCBA-A	3110*	4030*	4770*	4900*
30% - SCBA-A	2320*	3740*	3980*	4340*
10% - SCBA-B	3580	4810*	4950	5090*
20% - SCBA-B	3300*	4080*	4420*	4600*
30% - SCBA-B	3010*	4260*	4380*	4620*
20% - VR	3270*	4680*	4390*	4870*
4% - SF	3670	5210	5180	5960*
20% - C Ash	3670	5330	5510	6400*
30% - C Ash	3420*	5540	5990*	6490*
20% - F Ash	2500*	3690*	4600*	5240*
Class I Ternary Mixes				
20C/5GG	3220*	4930	5440	6010
20C/10GG	2800*	4740	5350	6050
30C/5SCBA-A	2990*	5190	5450	6790
30C/10SCBA-A	2820*	5170	6000	6730*
30C/5SCBA-B	3110*	5060	5530	6240
30C/10SCBA-B	2830*	4640*	5060	5740
30C/10VR	2170*	3840*	4780*	5010*
30C/4SF	3040*	5420	5720	6970*
30C/5F	3160*	5230	5460	6530*
30C/10F	2650*	4620*	5450	6230*

Note: Mixes denoted with an asterisk (*) indicate results that are statistically significantly different from control based upon a two-tailed T-test assuming unequal variances, and a 95% confidence interval.

Table 4-19: Summary table of normalized compressive strengths for Class I concrete mixes utilizing Type IL cement.

Normalized Compressive Strength of Concrete using Type IL Cement				
Mix	7 Day	28 Day	56 Day	91 Day
OPC – Type IL	100%	100%	100%	100%
Class I Binary Mixes				
20% - GG	64%	80%	86%	94%
30% - GG	46%	70%	75%	88%
40% - GG	35%	61%	70%	79%
10% - SCBA-A	94%	105%	97%	97%
20% - SCBA-A	74%	76%	86%	85%
30% - SCBA-A	55%	71%	72%	76%
10% - SCBA-B	85%	91%	90%	89%
20% - SCBA-B	79%	77%	80%	80%
30% - SCBA-B	72%	81%	79%	80%
20% - VR	78%	89%	80%	85%
4% - SF	88%	99%	94%	104%
20% - C Ash	88%	101%	100%	111%
30% - C Ash	82%	105%	109%	113%
20% - F Ash	60%	70%	83%	91%
Class I Ternary Mixes				
20C/5GG	77%	94%	99%	105%
20C/10GG	67%	90%	97%	105%
30C/5SCBA-A	71%	98%	99%	118%
30C/10SCBA-A	67%	98%	109%	117%
30C/5SCBA-B	74%	96%	100%	109%
30C/10SCBA-B	68%	88%	92%	100%
30C/10VR	52%	73%	87%	87%
30C/4SF	73%	103%	104%	121%
30C/5F	75%	99%	99%	114%
30C/10F	63%	88%	99%	109%

4.4.2 Splitting Tensile Strength – ASTM C496

The splitting tensile strengths for the concrete mixes are presented below; they are ordered by concrete class, SCM type, and then cement type. The tables compare SCM type to the respective control for the type of cement used and the class of concrete produced. The strengths are also presented as normalized values to the control. ASTM C496 has a 14% allowable deviation from specimen to specimen to be considered statistically comparable.

4.4.2.1 Class IV Concrete

The results presented in Table 4-20 and Table 4-21 correspond to the splitting tensile strengths of the Class IV concrete mixes using Type I/II cement and the normalized splitting strengths, respectively. The ternary mixes typically exhibited higher strengths than the control (likely due to the C ash producing additional C-S-H during pozzolanic hydration and additional hydraulic activity). It can therefore be concluded that generally, the splitting tensile strength is minimally affected by the addition of the alternative supplementary cementitious materials.

Table 4-20: Splitting tensile strength results for Class IV concrete utilizing Type I/II cement.

Splitting Tensile Strength (psi)		
Mix	28-Day	91-Day
OPC – Type I/II	675	745
Class IV Binary Mixes		
20% - GG	600	725
30% - GG	680	680
40% - GG	650	705
10% - SCBA-A	655	730
20% - SCBA-A	550	690
30% - SCBA-A	610	700
10% - SCBA-B	655	680
20% - SCBA-B	530	625
30% - SCBA-B	520	600
20% - VR	525	555
4% - SF	615	635
20% - C Ash	775	685
30% - C Ash	635	710
20% - F Ash	640	795
Class IV Ternary Mixes		
20C/5GG	695	870
20C/10GG	710	745
30C/5SCBA-A	675	920
30C/10SCBA-A	685	775
30C/5SCBA-B	720	830
30C/10SCBA-B	700	645
30C/10VR	685	735
30C/4SF	665	815
30C/5F	595	685
30C/10F	595	620

Table 4-21: Comparison of splitting tensile strength results normalized to control for Class IV concrete utilizing Type I/II cement.

Normalized Splitting Tensile Strength		
Mix	28-Day	91-Day
OPC – Type I/II	100%	100%
Class IV Binary Mixes		
20% - GG	89%	97%
30% - GG	101%	91%
40% - GG	96%	95%
10% - SCBA-A	97%	98%
20% - SCBA-A	81%	93%
30% - SCBA-A	90%	94%
10% - SCBA-B	97%	91%
20% - SCBA-B	79%	84%
30% - SCBA-B	77%	81%
20% - VR	78%	74%
4% - SF	91%	85%
20% - C Ash	115%	92%
30% - C Ash	94%	95%
20% - F Ash	95%	107%
Class IV Ternary Mixes		
20C/5GG	103%	117%
20C/10GG	105%	100%
30C/5SCBA-A	100%	123%
30C/10SCBA-A	101%	104%
30C/5SCBA-B	107%	111%
30C/10SCBA-B	104%	87%
30C/10VR	101%	99%
30C/4SF	99%	109%
30C/5F	88%	92%
30C/10F	88%	83%

Table 4-22 and Table 4-23 correspond to the splitting tensile strength of the Class IV concrete mixes using Type IL cement and the normalized splitting tensile strengths, respectively. The majority of ternary mixes had comparable strengths to the control. Significant decreases in tensile strength were exhibited in the ground volcanic rock mix, as well as the 20% and 40% ground glass mixes. Based on the results, a 30% replacement of ground glass is close to the optimal replacement with respect to splitting tensile strength. Additionally, there was a slightly lower strength observed in the 30% SCBA-B mix.

Table 4-22: Splitting tensile strength results for Class IV concrete utilizing Type IL cement.

Splitting Tensile Strength (psi)		
Mix	28-Day	91-Day
OPC – Type IL	650	670
Class IV Binary Mixes		
20% - GG	480	555
30% - GG	655	595
40% - GG	520	480
10% - SCBA-A	650	685
20% - SCBA-A	640	670
30% - SCBA-A	585	645
10% - SCBA-B	550	660
20% - SCBA-B	610	715
30% - SCBA-B	550	610
20% - VR	480	550
4% - SF	630	670
20% - C Ash	705	580
30% - C Ash	745	N/A
20% - F Ash	540	680
Class IV Ternary Mixes		
20C/5GG	620	710
20C/10GG	705	665
30C/5SCBA-A	520	590
30C/10SCBA-A	695	750
30C/5SCBA-B	735	695
30C/10SCBA-B	655	705
30C/10VR	575	800
30C/4SF	715	610
30C/5F	715	695
30C/10F	710	660

Table 4-23: Comparison of splitting tensile strength results normalized to control for Class IV concrete utilizing Type IL cement.

Normalized Splitting Tensile Strength		
Mix	28-Day	91-Day
OPC – Type IL	100%	100%
Class IV Binary Mixes		
20% - GG	74%	83%
30% - GG	101%	89%
40% - GG	80%	72%
10% - SCBA-A	100%	102%
20% - SCBA-A	98%	100%
30% - SCBA-A	90%	96%
10% - SCBA-B	85%	99%
20% - SCBA-B	94%	107%
30% - SCBA-B	85%	91%
20% - VR	74%	82%
4% - SF	97%	100%
20% - C Ash	108%	87%
30% - C Ash	115%	NA
20% - F Ash	83%	101%
Class IV Ternary Mixes		
20C/5GG	95%	106%
20C/10GG	108%	99%
30C/5SCBA-A	80%	88%
30C/10SCBA-A	107%	112%
30C/5SCBA-B	113%	104%
30C/10SCBA-B	101%	105%
30C/10VR	88%	119%
30C/4SF	110%	91%
30C/5F	110%	104%
30C/10F	109%	99%

4.4.2.2 Class I Concrete

The splitting tensile strengths of the Class I concrete test specimens incorporating IL cement are generally comparable to the control strength as shown in Table 4-24 and Table 4-25. A similar relationship with the Class IV ternary mixes was observed with a generally comparable or higher tensile strength than the control. The 28-day splitting tensile strengths for most of the SCBA mixes were slightly lower than the control strength, but the 91-day strength was generally comparable.

Table 4-24: Splitting tensile strength results for Class I concrete utilizing Type II cement.

Splitting Tensile Strength (psi)		
Mix	28-Day	91-Day
OPC – Type II	500	565
Class I Binary Mixes		
20% - GG	475	585
30% - GG	485	555
40% - GG	430	535
10% - SCBA-A	530	565
20% - SCBA-A	405	470
30% - SCBA-A	400	490
10% - SCBA-B	420	495
20% - SCBA-B	410	545
30% - SCBA-B	405	520
20% - VR	480	520
4% - SF	540	635
20% - C Ash	530	555
30% - C Ash	540	640
20% - F Ash	500	605
Class I Ternary Mixes		
20C/5GG	460	610
20C/10GG	545	665
30C/5SCBA-A	535	720
30C/10SCBA-A	560	605
30C/5SCBA-B	565	605
30C/10SCBA-B	570	570
30C/10VR	460	720
30C/4SF	605	620
30C/5F	590	690
30C/10F	495	680

Table 4-25: Comparison of splitting tensile strength results normalized to control for Class I concrete utilizing Type IL cement.

Normalized Splitting Tensile Strength		
Mix	28-Day	91 Day
OPC – Type IL	100%	100%
Class I Binary Mixes		
20% - GG	95%	104%
30% - GG	97%	98%
40% - GG	86%	95%
10% - SCBA-A	106%	100%
20% - SCBA-A	81%	83%
30% - SCBA-A	80%	87%
10% - SCBA-B	84%	88%
20% - SCBA-B	82%	96%
30% - SCBA-B	81%	92%
20% - VR	96%	92%
4% - SF	108%	112%
20% - C Ash	106%	98%
30% - C Ash	108%	113%
20% - F Ash	100%	107%
Class I Ternary Mixes		
20C/5GG	92%	108%
20C/10GG	109%	118%
30C/5SCBA-A	107%	127%
30C/10SCBA-A	112%	107%
30C/5SCBA-B	113%	107%
30C/10SCBA-B	114%	101%
30C/10VR	92%	127%
30C/4SF	121%	110%
30C/5F	118%	122%
30C/10F	99%	120%

4.4.3 Flexural Strength – ASTM C78

Flexural strength testing was only performed on Class I concrete pavement specimens. Class I concrete specimens were only produced using IL cement, as this is an extension of project FDOT BDV31-977-06. The results of flexural testing are presented in Table 4-26 and Table 4-27. ASTM C78 has an allowable flexural strength difference of 17.1% between two tests of similar specimens having a flexural strength between 600-800 psi. For specimens with strength greater than 800 psi, the allowable variation is 31.8%. There were no mixes tested that had flexural strengths higher than the control that were statistically significant.

Table 4-26: Summary of flexural strength results for Class I concrete utilizing Type II cement.

Flexural Strength (psi)		
Mix	28-Day	91-Day
OPC – Type II	755	705
Class I Binary Mixes		
20% - GG	665	740
30% - GG	550	710
40% - GG	550	625
10% - SCBA-A	670	695
20% - SCBA-A	685	695
30% - SCBA-A	560	655
10% - SCBA-B	675	660
20% - SCBA-B	610	610
30% - SCBA-B	630	640
20% - VR	640	695
4% - SF	725	755
20% - C Ash	760	825
30% - C Ash	730	860
20% - F Ash	595	725
Class I Ternary Mixes		
20C/5GG	710	880
20C/10GG	740	780
30C/5SCBA-A	725	825
30C/10SCBA-A	690	770
30C/5SCBA-B	690	760
30C/10SCBA-B	715	825
30C/10VR	600	715
30C/4SF	710	825
30C/5F	650	775
30C/10F	655	770

Table 4-27: Summary of normalized flexural strength results for Class I concrete utilizing Type IL cement.

Normalized Flexural Strength		
Mix	28-Day	91-Day
OPC – Type IL	100%	100%
Class I Binary Mixes		
20% - GG	88%	105%
30% - GG	73%	101%
40% - GG	73%	89%
10% - SCBA-A	89%	99%
20% - SCBA-A	91%	99%
30% - SCBA-A	74%	93%
10% - SCBA-B	89%	94%
20% - SCBA-B	81%	87%
30% - SCBA-B	83%	91%
20% - VR	85%	99%
4% - SF	96%	107%
20% - C Ash	101%	117%
30% - C Ash	97%	122%
20% - F Ash	79%	103%
Class I Ternary Mixes		
20C/5GG	94%	125%
20C/10GG	98%	111%
30C/5SCBA-A	96%	117%
30C/10SCBA-A	91%	109%
30C/5SCBA-B	91%	108%
30C/10SCBA-B	95%	117%
30C/10VR	79%	101%
30C/4SF	94%	117%
30C/5F	86%	110%
30C/10F	87%	109%

The flexural strengths of the 30-40% ground glass mixtures were significantly lower than that of the control at 28 days. However, the strength gain at later ages can be observed here in the comparable strength to control at 91 days. The 30% SCBA-A and 20% SCBA-B mixes also had lower strength at earlier ages, but at 91 days, the strengths were comparable.

4.4.4 Modulus of Elasticity – ASTM C469

The modulus of elasticity was determined for the concrete mixtures for both Class I and Class IV concretes with both Type I/II and Type IL cements. The modulus of elasticity was measured at 28 days and 91 days using compression data obtained on the same day. ASTM C469 lists a 5% precision in results from the test, meaning the modulus of elasticity of two identical mixtures should not differ by more than 5%. None of the evaluated mixes exhibited a statistically higher modulus of elasticity than the control.

4.4.4.1 Class IV Concrete

The Class IV mixes with Type I/II cement had relatively consistent results over time. Most of the mixes that exhibited lower MOE values stayed consistent with respect to the control, as seen in Table 4-28, meaning the increase in MOE over time was similar to that of the control. The MOE values for the Class IV mixes with Type IL cement, presented in Table 4-29, were similar to those using Type I/II cement. However, there was slightly more variance from different testing ages than what was observed in the Type I/II mixes.

Table 4-28: Summary of MOE values for Class IV concrete utilizing Type I/II cement.

Mix	Modulus of Elasticity (psi)		Normalized Modulus of Elasticity	
	28 Day	91 Day	28 Day	91 Day
OPC – Type I/II	5,250,000	5,500,000	100%	100%
Class IV Binary Mixes				
20% - GG	5,000,000	5,500,000	95%	100%
30% - GG	5,100,000	5,350,000	97%	97%
40% - GG	5,050,000	5,300,000	96%	96%
10% - SCBA-A	5,950,000	5,350,000	113%	97%
20% - SCBA-A	4,750,000	5,000,000	90%	91%
30% - SCBA-A	4,450,000	4,750,000	85%	86%
10% - SCBA-B	5,150,000	6,050,000	98%	110%
20% - SCBA-B	4,850,000	5,250,000	92%	95%
30% - SCBA-B	4,950,000	5,150,000	94%	94%
20% - VR	4,900,000	5,150,000	93%	94%
4% - SF	5,300,000	5,400,000	101%	98%
20% - C Ash	5,350,000	5,650,000	102%	103%
30% - C Ash	5,250,000	5,700,000	100%	104%
20% - F Ash	5,000,000	5,700,000	95%	104%
Class IV Ternary Mixes				
20C/5GG	5,400,000	5,500,000	103%	100%
20C/10GG	5,200,000	5,500,000	99%	100%
30C/5SCBA-A	5,300,000	5,650,000	101%	103%
30C/10SCBA-A	5,000,000	5,500,000	95%	100%
30C/5SCBA-B	5,200,000	5,550,000	99%	101%
30C/10SCBA-B	5,100,000	5,550,000	97%	101%
30C/10VR	5,250,000	5,650,000	100%	103%
30C/4SF	5,050,000	5,500,000	96%	100%
30C/5F	5,000,000	5,550,000	95%	101%
30C/10F	4,800,000	5,500,000	91%	100%

Table 4-29: Summary of MOE values for Class IV concrete utilizing Type II cement.

Mix	Modulus of Elasticity (psi)		Normalized Modulus of Elasticity	
	28 Day	91 Day	28 Day	91 Day
OPC – Type II	5,300,000	5,350,000	100%	100%
Class IV Binary Mixes				
20% - GG	5,250,000	5,200,000	99%	97%
30% - GG	4,850,000	5,000,000	92%	93%
40% - GG	4,700,000	4,850,000	89%	91%
10% - SCBA-A	4,800,000	5,150,000	91%	96%
20% - SCBA-A	4,650,000	4,850,000	88%	91%
30% - SCBA-A	4,300,000	4,450,000	81%	83%
10% - SCBA-B	5,200,000	5,150,000	98%	96%
20% - SCBA-B	5,000,000	5,150,000	94%	96%
30% - SCBA-B	4,850,000	5,050,000	92%	94%
20% - VR	4,850,000	5,250,000	92%	93%
4% - SF	5,000,000	5,150,000	94%	96%
20% - C Ash	5,050,000	5,400,000	95%	101%
30% - C Ash	5,250,000	5,450,000	99%	102%
20% - F Ash	4,700,000	5,300,000	89%	99%
Class IV Ternary Mixes				
20C/5GG	5,130,000	5,500,000	97%	103%
20C/10GG	5,030,000	5,400,000	95%	101%
30C/5SCBA-A	5,100,000	4,450,000	96%	83%
30C/10SCBA-A	5,100,000	4,550,000	96%	85%
30C/5SCBA-B	5,350,000	5,600,000	101%	105%
30C/10SCBA-B	5,300,000	5,600,000	100%	105%
30C/10VR	5,250,000	5,050,000	99%	94%
30C/4SF	5,150,000	4,550,000	97%	85%
30C/5F	5,250,000	5,600,000	99%	105%
30C/10F	5,200,000	5,750,000	98%	107%

4.4.4.2 Class I Concrete

Unlike the Class IV mixes, the Class I mixes seem to exhibit lower MOE values compared to the control for a majority of the mixes as seen in Table 4-30. This is most likely due to the lower cement content that Class I requires compared to Class IV. However, for 91-day testing, several of the mixes reached comparable MOE values to that of the control, which was expected due to pozzolanic reaction.

Table 4-30: Summary of MOE values for Class I concrete utilizing Type II cement.

Mix	Modulus of Elasticity (psi)		Normalized Modulus of Elasticity	
	28 Day	91 Day	28 Day	91 Day
OPC – Type II	5,250,000	5,100,000	100%	100%
Class I Binary Mixes				
20% - GG	4,750,000	4,950,000	90%	97%
30% - GG	4,300,000	3,650,000	82%	89%
40% - GG	4,200,000	4,600,000	80%	90%
10% - SCBA-A	4,800,000	5,450,000	91%	107%
20% - SCBA-A	4,750,000	5,200,000	90%	102%
30% - SCBA-A	3,750,000	4,150,000	71%	81%
10% - SCBA-B	4,600,000	4,750,000	88%	93%
20% - SCBA-B	4,750,000	5,200,000	84%	90%
30% - SCBA-B	4,300,000	4,650,000	82%	91%
20% - VR	4,650,000	4,800,000	89%	94%
4% - SF	4,750,000	4,950,000	90%	97%
20% - C Ash	4,800,000	5,200,000	91%	102%
30% - C Ash	5,000,000	5,400,000	95%	106%
20% - F Ash	4,340,000	5,000,000	83%	98%
Class I Ternary Mixes				
20C/5GG	4,750,000	5,400,000	90%	106%
20C/10GG	4,600,000	5,250,000	88%	103%
30C/5SCBA-A	4,800,000	5,250,000	91%	103%
30C/10SCBA-A	4,800,000	5,250,000	92%	103%
30C/5SCBA-B	4,800,000	5,250,000	91%	103%
30C/10SCBA-B	4,750,000	5,200,000	90%	102%
30C/10VR	4,300,000	5,000,000	82%	98%
30C/4SF	4,900,000	5,300,000	93%	104%
30C/5F	5,400,000	4,800,000	103%	94%
30C/10F	4,700,000	5,400,000	90%	106%

4.4.5 Coefficient of Thermal Expansion – AASHTO T 336

The concrete coefficient of thermal expansion results are presented in Table 4-31 below. The results were organized using the cement type and the class of concrete that was produced. A higher coefficient of thermal expansion represents a higher amount of length change for the same temperature change. The coefficient of expansion, amongst other design considerations is especially important for pavement applications as it controls how long a slab can be between joint cuts (which directly translates into labor costs). Materials with lower thermal expansion

coefficients can have longer uninterrupted spans without the need for cutting joints to account for slab cracking.

Table 4-31: Summary of the CTE results (reported in % microstrain/°C relative to control) for each class of concrete with each type of cement.

Type I/II Cement - Class IV		Type IL Cement - Class IV		Type IL Cement - Class I	
OPC	100%	OPC	100%	OPC	100%
10 SCBA-A	100%	10 SCBA-A	109%	10 SCBA-A	95%
20 SCBA-A	94%	20 SCBA-A	104%	20 SCBA-A	95%
30 SCBA-A	97%	30 SCBA-A	106%	30 SCBA-A	104%
10 SCBA-B	97%	10 SCBA-B	99%	10 SCBA-B	97%
20 SCBA-B	101%	20 SCBA-B	102%	20 SCBA-B	98%
30 SCBA-B	103%	30 SCBA-B	110%	30 SCBA-B	103%
20 GG	98%	20 GG	98%	20 GG	105%
30 GG	95%	30 GG	105%	30 GG	106%
40 GG	93%	40 GG	105%	40 GG	100%
20 VR	-	20 VR	101%	20 VR	99%
4 SF	100%	4 SF	110%	4 SF	99%
20 C	105%	20 C	110%	20 C	108%
30 C	108%	30 C	106%	30 C	103%
20 F	107%	20 F	112%	20 F	104%
30 C/5 SCBA-A	107%	30 C/5 SCBA-A	110%	30 C/5 SCBA-A	103%
30 C/10 SCBA-A	102%	30 C/10 SCBA-A	109%	30 C/10 SCBA-A	100%
30 C/5 SCBA-B	106%	30 C/5 SCBA-B	113%	30 C/5 SCBA-B	107%
30 C/10 SCBA-B	101%	30 C/10 SCBA-B	115%	30 C/10 SCBA-B	106%
20 C/5 GG	106%	20 C/5 GG	110%	20 C/5 GG	103%
20 C/10 GG	105%	20 C/10 GG	113%	20 C/10 GG	106%
30 C/10 VR	101%	30 C/10 VR	107%	30 C/10 VR	111%
30 C/4 SF	101%	30 C/4 SF	120%	30C /4 SF	96%
30 C/5 F	101%	30 C/5 F	111%	30 C/5 F	107%
30C /10 F	106%	30 C/10 F	126%	30 C/10 F	99%

The general trend observed was that the CTE remained generally comparable and was within approximately 1 micro strain/°C. However, the Class I mixes in general produced lower CTE values than the Class IV mixes due to lower paste contents. Crawford et al. noted that the standard deviation of running CTE was 0.135 micro strain/°C; using ASTM C670 this would mean that the acceptable range of two values would (d2s) would be 0.38 micro strain/°C [194,195].

4.5 LONG-TERM DURABILITY TESTING

4.5.1 Alkali-Silica Reaction – ASTM C1293

Alkali-silica reaction (ASR) is a reaction between the aggregate and the alkalis present in the concrete pore solution; this reaction forms a gel that expands in the presence of water and can lead to cracking in the concrete. Determining the potential for mitigation or exacerbation of ASR can be useful for the recommended use or avoidance of a pozzolan. In this method, concrete specimens are created using reactive aggregate, high alkali cement, and sodium hydroxide solution as mixing water. They are measured and monitored over the course of two years. Specimens are kept over a specified amount of water, sealed inside a container lined with wicking material, and stored in a 38°C environmental chamber. The expansion is compared to the initial measurement and expressed as a percentage. The expansion of the specimen can indicate the potential for ASR. The expansion limits are 0.04% at two years (for mixtures containing SCM and only one year if not; the control was only measured for one year), and if surpassed, indicates that the pozzolan being evaluated is insufficient to suppress ASR. An expansion beyond the threshold limits would result in a recommendation that the material not be used, as it is potentially unsafe with respect to long-term durability.

The alkali-silica reactivity testing method ASTM C1293 differs from the ASTM C1567 alkali-silica reactivity testing method in a few ways. Firstly, ASTM C1293 is performed on concrete rather than mortar; secondly, ASTM C1293 is performed at a reduced temperature of 38°C (in a humid environment) rather than 80°C (submerged), and thirdly, there is not a chemical restriction on the materials used in the method (which is important for evaluating alternative supplementary cementitious materials such as ground waste glass.) There are additional differences between the methods such as duration of test method being 2 years compared to 2 weeks, differences in the scope of the test method, differences in the failure threshold, and gradation or material requirements, amongst others. However, the motivation for this evaluation method was to compare to the accelerated mortar bar method to determine if similar results could be obtained for alternative supplementary cementitious materials without the necessity of evaluating the materials for two years.

The mix design specified by ASTM C1293 was followed with one exception: cementitious content was modified from 922 ± 22 to 710 lb/yd^3 for the purposes of comparing

more closely to concrete created for physical testing. Concrete specimens created for long-term alkali-silica reactivity testing follow the same replacements. However, the Florida sand was replaced with sand from Jobe Materials, El Paso, Texas. Sand from Jobe Materials has been found to be susceptible to alkali-silica reaction in concrete [157,196,197] as well as in mortars, as found in Section 3.2.5.2. A high alkali cement was used, and the total cementitious content was kept constant at 710 lb/yd³ in order to be able to closely compare the mixes used to study alkali-silica reaction (ASR) to the regular Class IV concrete mixes. Sodium hydroxide was added to the mixing water to increase the level of available alkalis in the system as prescribed by ASTM C1293. Table 4-32 provides the concrete mixture proportions used for ASTM C1293 testing, and Table 4-33 summarizes the ASTM C1293 concrete expansions measured for these concretes.

Table 4-32: ASTM C1293 concrete binder proportions (in lb/yd³) using high-alkali Type I/II cement.

Mix	HA Cement	SCBA-A	SCBA-B	GG	F Ash	C Ash	VR	SF	Coarse Agg.	Fine Agg.	Water
76	710	-	-	-	-	-	-	-	1,684	1,083	298
77	568	-	-	142	-	-	-	-	1,684	1,062	298
78	497	-	-	213	-	-	-	-	1,684	1,052	298
79	426	-	-	284	-	-	-	-	1,684	1,042	298
80	568	-	-	-	-	142	-	-	1,684	1,065	298
81	497	-	-	-	-	213	-	-	1,684	1,056	298
82	568	-	-	-	142	-	-	-	1,684	1,047	298
83	682	-	-	-	-	-	-	28	1,684	1,073	298
84	639	-	71	-	-	-	-	-	1,684	1,065	298
85	568	-	142	-	-	-	-	-	1,684	1,046	298
86	497	-	213	-	-	-	-	-	1,684	1,028	298
87	568	-	-	-	-	-	142	-	1,684	1,072	298
88	639	71	-	-	-	-	-	-	1,684	1,069	298
89	568	142	-	-	-	-	-	-	1,684	1,055	298
90	497	213	-	-	-	-	-	-	1,684	1,040	298
91	462	36	-	-	-	213	-	-	1,684	1,049	298
92	426	71	-	-	-	213	-	-	1,684	1,042	298
93	462	-	36	-	-	213	-	-	1,684	1,047	298
94	426	-	71	-	-	213	-	-	1,684	1,038	298
95	533	-	-	36	-	142	-	-	1,684	1,060	298
96	497	-	-	71	-	142	-	-	1,684	1,055	298
97	426	-	-	-	-	213	71	-	1,684	1,050	298
98	462	-	-	-	36	213	-	-	1,684	1,047	298
99	426	-	-	-	71	213	-	-	1,684	1,038	298
100	469	-	-	-	-	213	-	28	1,684	1,046	298

4.5.1.1 Sugarcane Bagasse Ash (SCBA)

Expansion was reduced in the SCBA-A system as replacement increased. The expansion limit of 0.04% was exceeded with replacements of 10 and 20%, but not the mixture containing 30% replacement as shown in Figure 4-17. However, as the final expansion of the 30% SCBA-A mixture was exactly 0.04% expansion, and this is an average of four specimens, two of the specimens did exceed the 0.04% expansion threshold. This performance trend is similar to that of the SCBA-A replacement of Type I/II cement in ASTM C1567 whereby the 10% replacement had little effect on the total expansion and the 30% replacement fared the best; yet did not completely mitigate expansion.

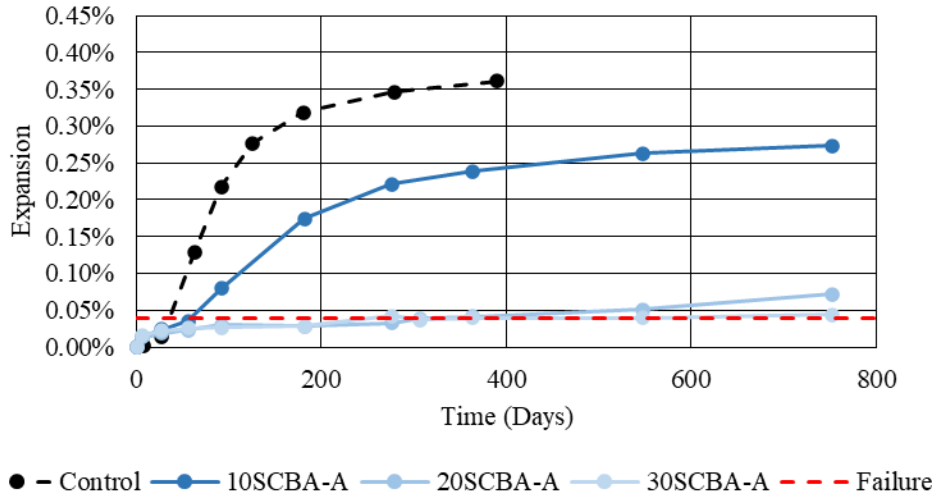


Figure 4-17: Concrete prism test results for mixtures incorporating SCBA-A.

SCBA-B was ineffective at reducing ASR expansion, with 20 and 30% replacements increasing expansion compared to control as shown in Figure 4-18. The differences in performance exhibited by SCBA-A and SCBA-B are most likely due to their respective reactivity due to their crystallinity. Higher reactivity results in a denser microstructure and lower water permeability, thus reducing the potential for ASR gel to expand. The equivalent alkali content in SCBA-B is also higher than SCBA-A with contents of 3.4% and 1.1% respectively. An increase in alkalis is likely to contribute to the production of more gel, increasing the potential for cracking and expansion [73].

In comparison to the ASTM C1567 results, the ASTM C1283 concrete prism results are fairly consistent with the SCBA-B replacements largely having little mitigating potential due to lack of reactivity. Based on the results, it would appear that for SCBA, the ASTM C1567 test gives comparable results to the ASTM C1293 test.

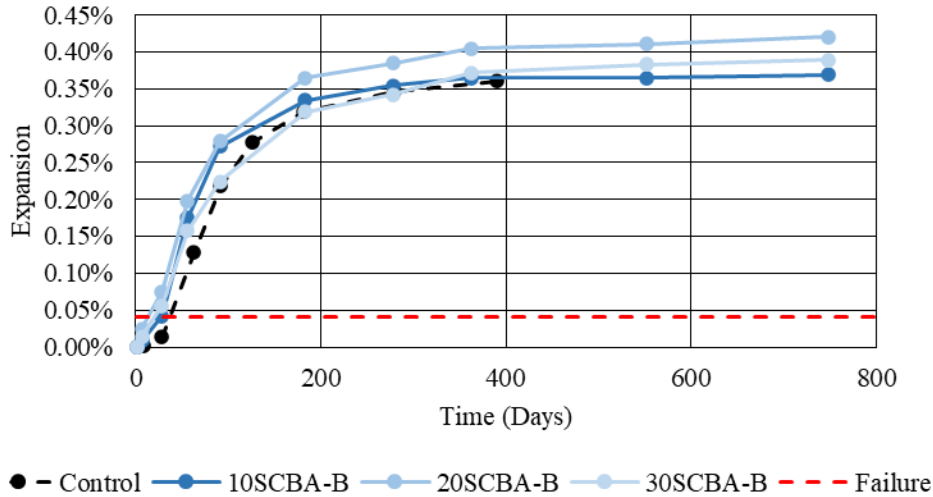


Figure 4-18: Concrete prism test results for mixtures incorporating SCBA-B.

4.5.1.2 Ground Glass (GG)

The ground glass mixtures decreased the expansion caused by ASR as replacements increased. The 40% replacement had similar expansions to Class C fly ash and SF. However, the 0.04% expansion limit was surpassed by each of the ground glass mixtures. Therefore, it can be concluded that GG is effective in mitigating ASR expansion caused by Jobe sand, but it is not effective in suppressing it. This result further reinforces the statement from ASTM C1567 that SCM containing more than 4.0% will produce unrealistically low expansions; and therefore, the accelerated ASR test method is not appropriate for ground glass as a cement replacement if ASR is anticipated.

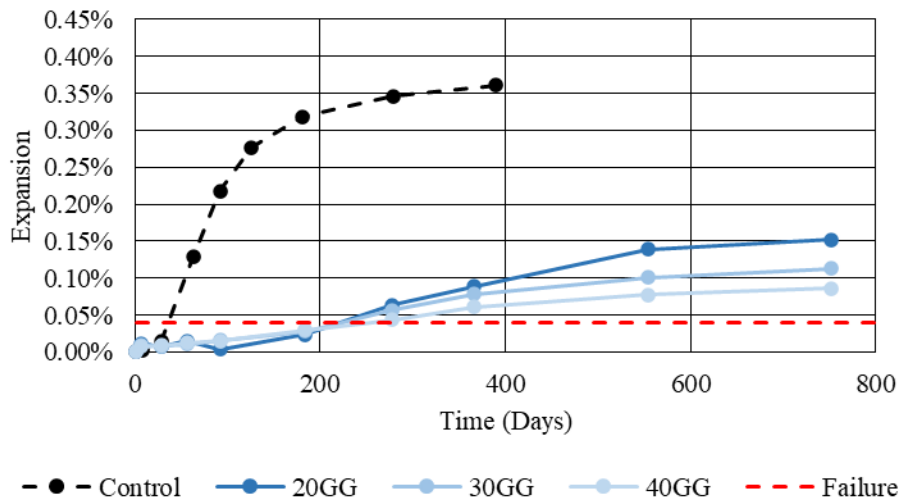


Figure 4-19: Concrete prism test results for mixtures incorporating ground glass.

4.5.1.3 Fly Ash (Class F and Class C)

Class C fly ash surpassed the 0.04% expansion limit at both replacements as shown in Figure 4-20. The 20% and 30% replacements of Class C fly ash had similar results in terms of expansion (0.07% and 0.08%, respectively). The Class F fly ash did not surpass the 0.04% expansion limits having a final expansion of 0.03%. The alumina content in the F ash is slightly higher, which is a contributor to the better performance.

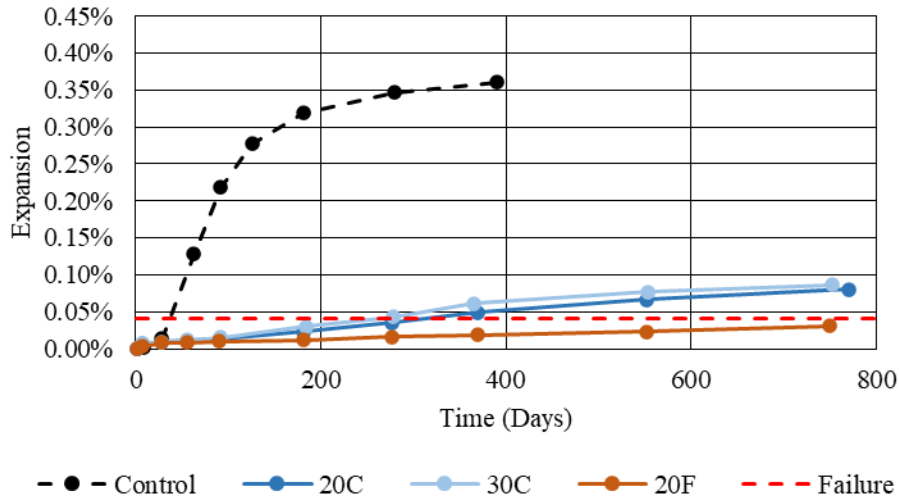


Figure 4-20: Concrete prism test results for mixtures incorporating C ash and F ash.

4.5.1.4 Volcanic Rock (VR) and Silica Fume (SF)

Similar to other evaluation methods, VR performed poorly, surpassing the 0.04% expansion limit within 91 days of testing as shown in Figure 4-21. The expansion was reduced, but this is most likely due the ground volcanic rock acting as a particle filler and not significantly contributing to the pozzolanic reaction. This result is consistent with the ASTM C1567 results, which showed that the volcanic rock mixture expanded beyond the failure threshold at approximately the same rate as the control mixture. The SF mix performed similarly to the C ash with the expansion over time being almost identical. It can be concluded that a 4% replacement of SF can mitigate ASR expansion but cannot suppress it.

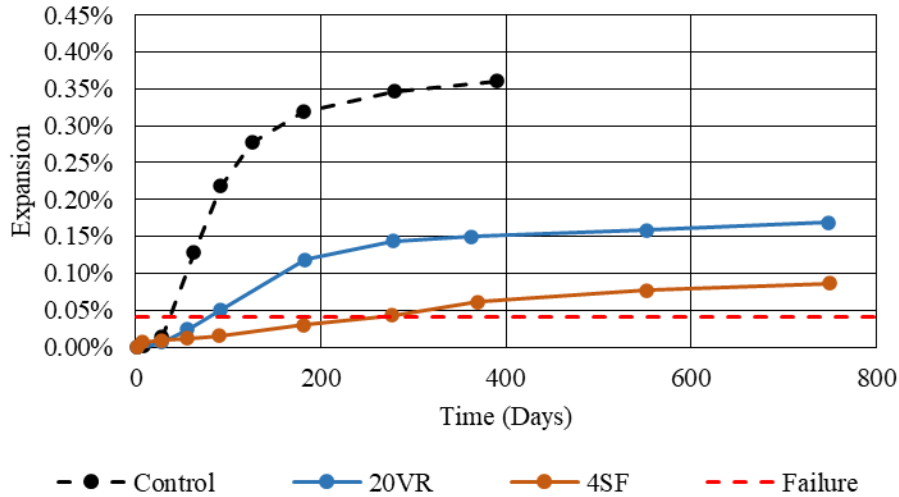


Figure 4-21: Concrete prism test results for mixtures incorporating VR and SF.

4.5.1.5 Ternary Mixtures

The ternary mixtures containing 30% C ash were the best performing mixtures with virtually every mix being below 0.04% expansion at two years of exposure. The ternary mixtures containing 20% C ash were unsuccessful in reducing expansion below 0.04% with a maximum expansion of 0.15% for the 20% C ash and 5% GG mix. It is important to note that even though the ternary blends with 30% C ash were below 0.04% expansion at two years with as little as 4% of another SCM, the 30% C ash binary mix had a two-year expansion of 0.08%. Therefore, while the use of high volumes of C Ash replacement are beneficial, it is not sufficient in a binary mix and must be accompanied by another SCM to perform adequately in ASTM C1293.

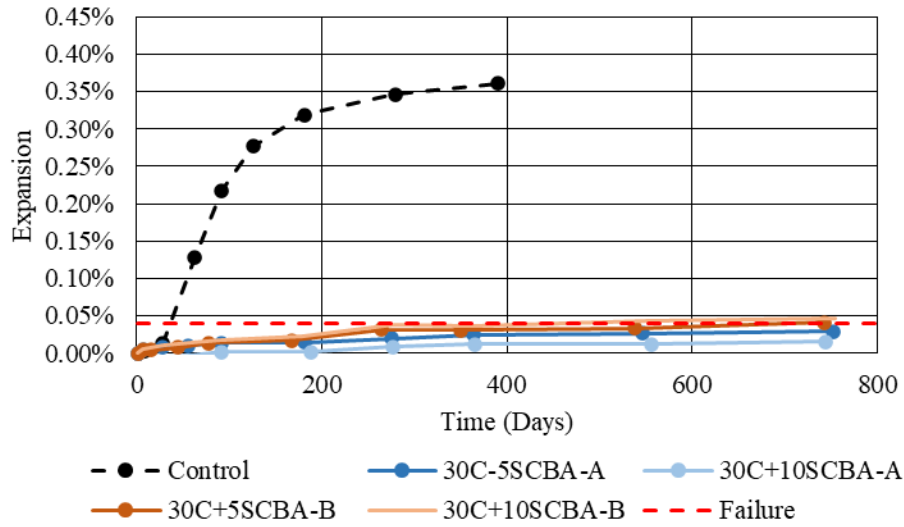


Figure 4-22: Concrete prism test results for ternary mixtures incorporating SCBA.

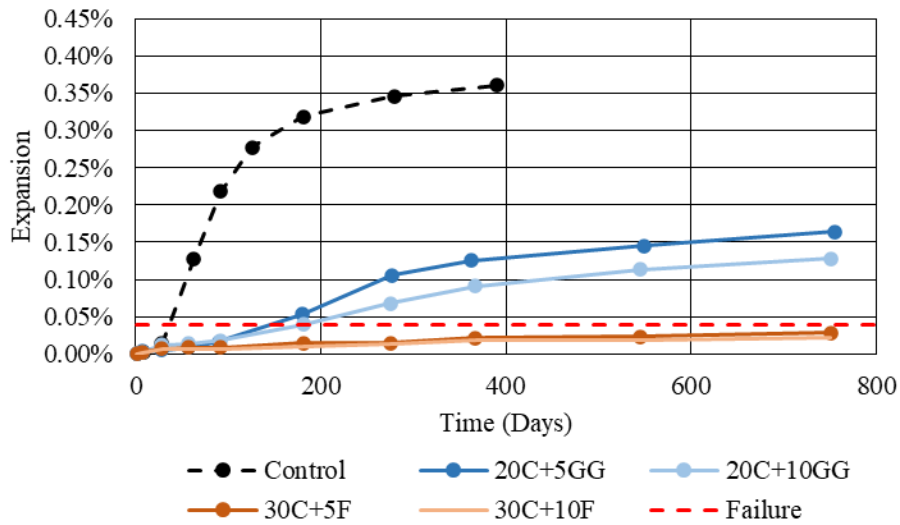


Figure 4-23: Concrete prism test results for ternary mixtures incorporating GG and F ash.

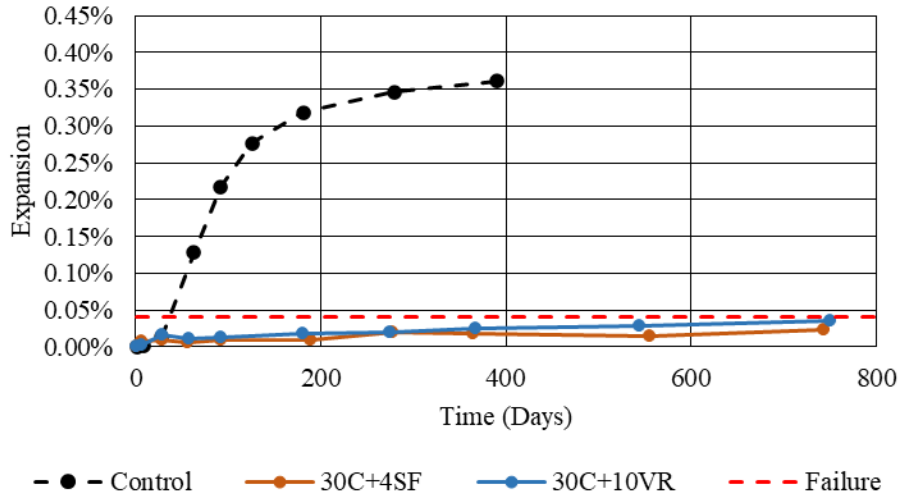


Figure 4-24: Concrete prism test results for ternary mixtures incorporating SF and VR.

A comparison of ASTM C1567 and ASTM C1293 results for alternative SCM is shown in Figure 4-25. The red dotted lines highlight the failure thresholds for both test methods. In general, both test methods provide similar conclusions with regards to the lack of suppression of ASR provided by the SCM tested. The mixtures with expansions lower than the failure limit of ASTM C1567 were only made with ground glass. However, based on the test method, these results are invalid due to the alkali content present in ground glass. The ASTM C1293 results exceed the expansion limits, leading to the conclusion that ground glass mixtures do not suppress ASR expansion caused by Jobe sand.

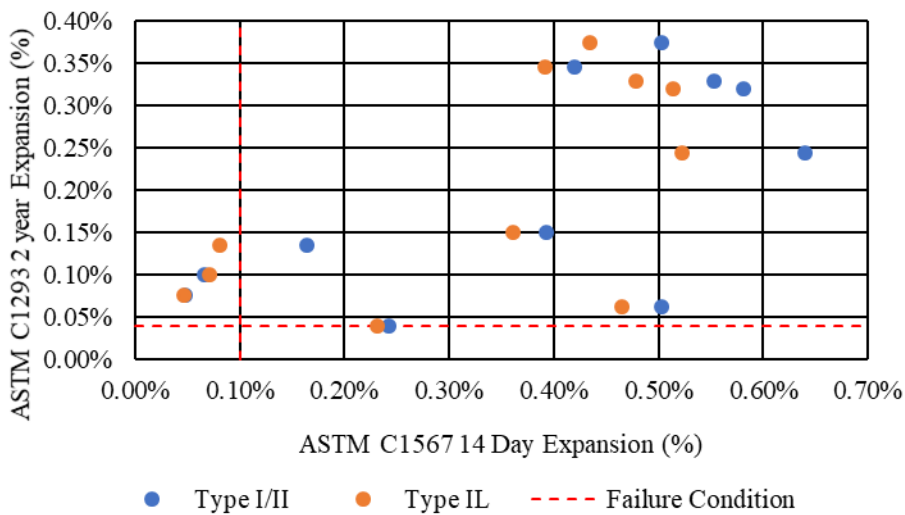


Figure 4-25: Comparison of test results for binary systems utilizing Type I/II and Type IL cements replaced with alternative SCM

Table 4-33: Summary of ASTM C1293 expansion of concrete with SCM.

Mix	1 Year Expansion	2 Year Expansion
OPC	0.36%	NA
Binary Mixes		
10SCBA-A	0.24%	0.27%
20SCBA-A	0.04%	0.07%
30SCBA-A	0.04%	0.04%
10SCBA-B	0.36%	0.37%
20SCBA-B	0.40%	0.42%
30SCBA-B	0.37%	0.39%
20GG	0.09%	0.15%
30GG	0.08%	0.11%
40GG	0.06%	0.09%
20VR	0.15%	0.17%
20C	0.05%	0.08%
30C	0.03%	0.04%
20F	0.02%	0.03%
4SF	0.04%	0.07%
Ternary Mixes		
30C+5SCBA-A	0.02%	0.03%
30C+10SCBA-A	0.01%	0.02%
30C+5SCBA-B	0.03%	0.04%
30C+10SCBA-B	0.04%	0.05%
20C+5GG	0.13%	0.16%
20C+10GG	0.09%	0.13%
30C+10VR	0.02%	0.04%
30C+5F	0.02%	0.03%
30C+10F	0.02%	0.02%
30C+4SF	0.02%	0.02%

4.5.2 Durability Blocks

Concrete durability blocks were cast in conjunction with the ASTM C1293 specimens to provide performance in the field in addition to laboratory testing data. There has been scrutiny over the various testing methods that employ elevated temperature for ASR determination, and the use of larger specimens placed into a field site would provide more realistic data that represents typical Floridian climate. The expansion results from the durability blocks serve only to compare ASTM C1293 results with those in the field. There is no way to control the temperature or humidity in the exposure site and therefore there are no failure criteria associated with durability blocks.

The blocks are cubic specimens measuring 14" on each side and were cast following the procedure developed at the University of Texas as there is not standardized method for site-exposed specimens [198]. Concrete molds were created using phenolic-coated plywood to ease form removal; each form had six locations fabricated into the mold for threaded inserts such that gauge studs could be cast into the specimen on three sides (two gauge studs per side to act as gauge points for a mechanical strain gauge). The gauge studs were 3/8" diameter by 3" long threaded rods that had a fine conical hold machined into the face using a centering drill in a milling machine, and then were inserted nominally 10 inches apart from each other; Figure 4-26.



Figure 4-26: Gauge point created by drilling into threaded rod before embedding into concrete.

The concrete was placed into phenolic plywood forms in three layers and vibrated with an internal vibrator at each layer. Each pair of gauge points was measured three separate times using a mechanical strain gauge with a digital indicator with a 0.0001" precision and averaged to reduce measuring error; Figure 4-27. Prior to each measurement, the gauge points and the comparator points were both wiped clean to remove any debris that would foul the reading. The mechanical strain gauge was then calibrated to a 10" length reference bar shown in Figure 4-28.



Figure 4-27: Measurement of "top" face of block using mechanical strain gauge with digital indicator of 0.0001" precision.



Figure 4-28: Reference bar used to calibrate the comparator before each measurement.

During measurement, pressure was placed as illustrated in Figure 4-29, both perpendicular to the block face along with pressure to extend the comparator in order to consistently measure length change; block sides were oriented in the same direction so that measurement pressure was exerted in the same way for every measurement.



Figure 4-29: Measurement of "right" face of block with applied pressure in the direction of the red arrows.

A concrete block with a thermocouple cast internally was placed on the exposure site in order to provide internal block temperatures rather than ambient temperatures, as seen in Figure 4-30. The temperature of each block was recorded for every measurement as a means to calibrate for fluctuations in measurements due to external temperature. While humidity could not be controlled, blocks were not measured in the 24-hour period following rain.



Figure 4-30: Durability block internal temperature measurement with embedded thermocouple.

The blocks were demolded 24 hours after being cast, measured for initial gauge lengths, and stored in a moist curing room. After 7 days, the blocks were removed from the moist curing room, measured, and stored indoors. After another 7 days, the blocks were measured and placed at the outdoor exposure site. Once at the exposure site, a stainless-steel identification tag was placed onto the finished face (which did not contain gauge studs) as seen in Figure 4-31. The blocks were measured at 1 day, 7 days, 14 days, 21 days, 28 days, 56 days, 12 weeks, and 16 weeks. The blocks were then measured periodically as weather permitted throughout the year.



Figure 4-31: Example block and measurement orientation.

The exposure site had a 4” thick crushed lime rock base and was located at the University of Florida Wertheim College of Engineering’s Powell Family Structures and Materials Laboratory as shown in Figure 4-32.



Figure 4-32: Concrete exposure site at Powell Laboratory, University of Florida

The results presented in the figures below use the “top” measurement data as it was found that the top face experienced the most expansion, resulting in the most conservative measurements. Some trends in the durability block expansions were different from those observed in the ASTM C1293 evaluations though. From ASTM C1293 testing, it was known that F ash mitigated ASR-induced expansion. However, there was an observed increase in expansion of the exposure blocks, similar to that found for the GG mixtures in ASTM C1293 testing. It is possible that the lack of moisture/temperature control and higher surface area of the block led to a higher water transport, causing higher expansion values [199]. The conclusions about SCBA-B that were made with ASTM C1293 results differ in terms of the overall trend. While the main conclusion that SCBA-B has poor reduction in expansion is correct, the 30% replacement did provide a decrease in expansion, which is contrary to what was observed in ASTM C1293. The expansion observed in the SF and VR mixtures are also somewhat different than the ASTM C1293 evaluations. The durability blocks of both mixes have similar expansions, but the ASTM C1293 results show a higher expansion in the VR mixture. While both failed to reduce expansion in ASTM C1293, different expansion rates were observed. The ternary mixture durability block

expansions support the conclusions made in the ASTM C1293 evaluations with similar behaviors.

4.5.2.1 Sugarcane Bagasse Ash

The SCBA-A measurements of the durability blocks follow similar trends as the ASTM C1293 results. A 10% replacement had little effect in reducing the expansion caused by ASR, while the 20 and 30% replacements were much more effective. As of this report, visible cracking had appeared in the 10% replacement, but not in the 20 or 30% replacements. At two years, the expansion of the 30% SCBA-A block was less than 0.04%.

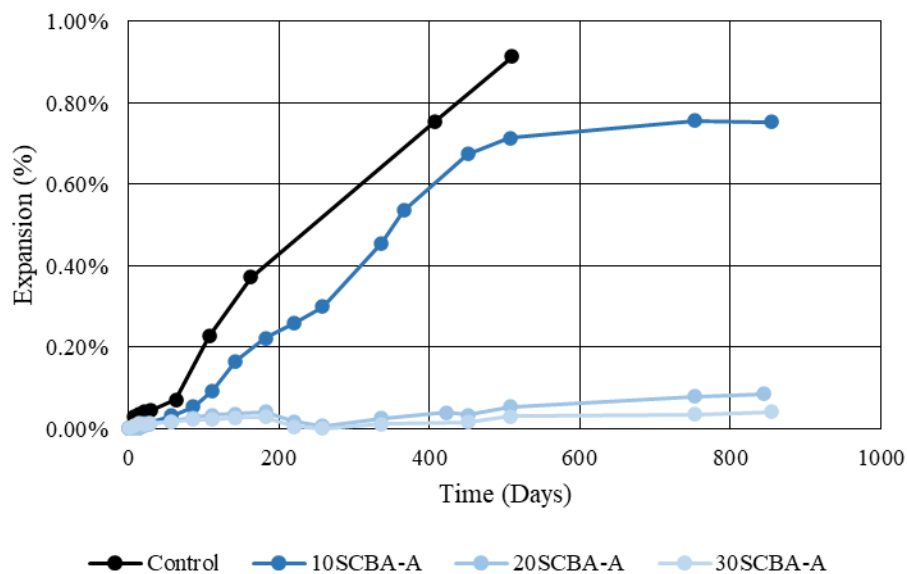


Figure 4-33: Expansion of durability blocks containing high alkali cement, reactive aggregate, and 10% - 30% SCBA-A.

Similar to the trends observed in the ASTM C1293 results, the 20% SCBA-B replacement performed worse than the 10% replacement. However, there was a clear decrease in expansion for the 30% replacement, which was not observed in the ASTM C1293 evaluation but was observed in the ASTM C1567 evaluation. The differences in results show the potential for variability among the ASR evaluation methods.

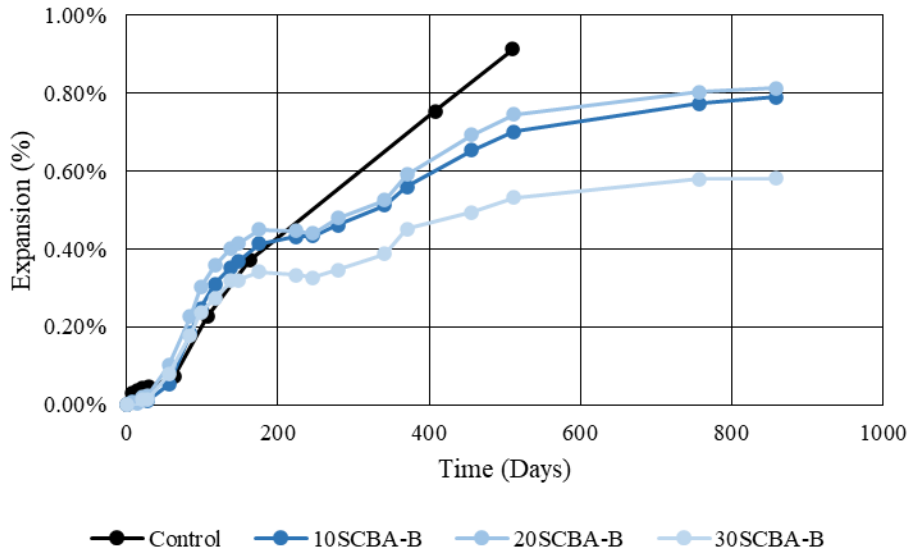


Figure 4-34: Expansion of durability blocks containing high alkali cement, reactive aggregate, and 10% - 30% SCBA-B.

4.5.2.2 Ground Glass

Much like the ASTM C1293 and ASTM C1567 results, the ground glass durability block measurements show a clear reduction in expansion caused by ASR. These results are similar to those seen in the Class F fly ash measurements, with expansion beginning at a similar age and a similar rate. The use of durability block testing may reduce the level of leaching in the system by decreasing the surface area to volume ratio of the specimen; however, with uncontrolled temperatures and humidity, it is not assured. With alkali leaching being a concern, a durability block may be a more reliable way of evaluating the performance.

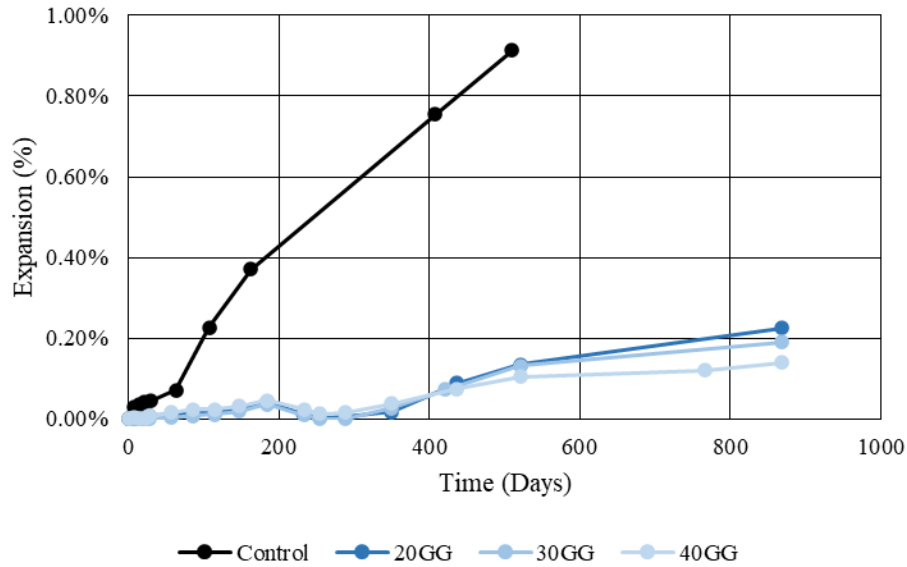


Figure 4-35: Expansion of durability blocks containing high alkali cement, reactive aggregate, and 20% - 40 % ground glass.

4.5.2.3 Fly Ash

Contrary to the results seen in ASTM C1293, the F ash durability block measurements are showing increases in expansion. This is most likely due to changes in humidity and temperature, along with increased exposure to water whenever it rained, resulting in a more extreme evaluation [199]. Additionally, the 20% replacement is too low to suppress the expansion caused by Jobe sand. An increase in replacement would likely reduce the expansion further [200].

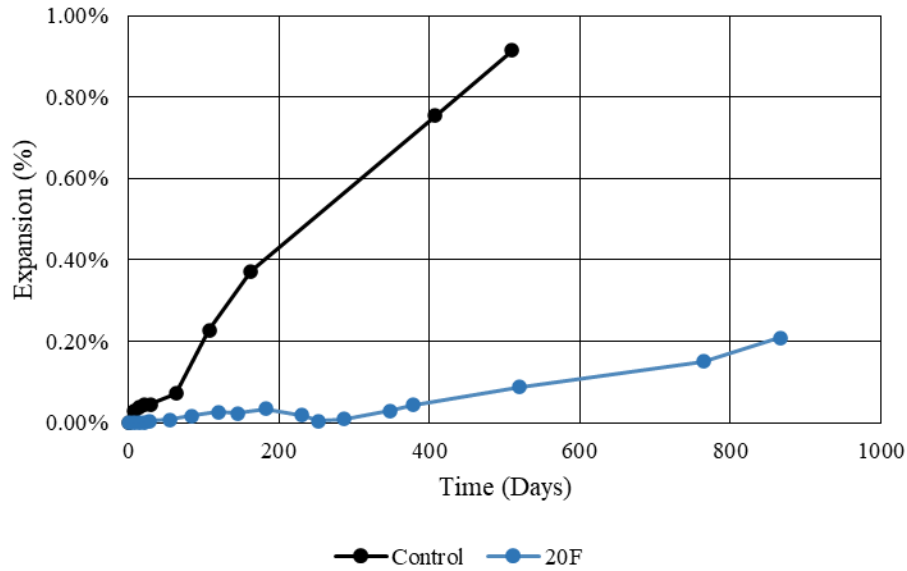


Figure 4-36: Expansion of durability blocks containing high alkali cement, reactive aggregate, and 20% Class F fly ash.

The C ash durability block results are different from the ASTM C1293 results in that a higher replacement of C ash caused a decrease in expansion in the durability blocks. However, there is still observed expansion in the 30% mixture, even though it took longer for the expansion to occur. Previous research has shown that a larger replacement of Class C fly ash is required to completely suppress the expansive nature of the Jobe sand [201,202]. Additionally, the conditions of the field exposure resulted in more expansion when compared to specimens exposed to the conditions of ASTM C1293. Based upon this, the amount of fly ash required to suppress expansion caused by ASR in field conditions is higher than the amount of fly ash for specimens exposed in ASTM C1293.

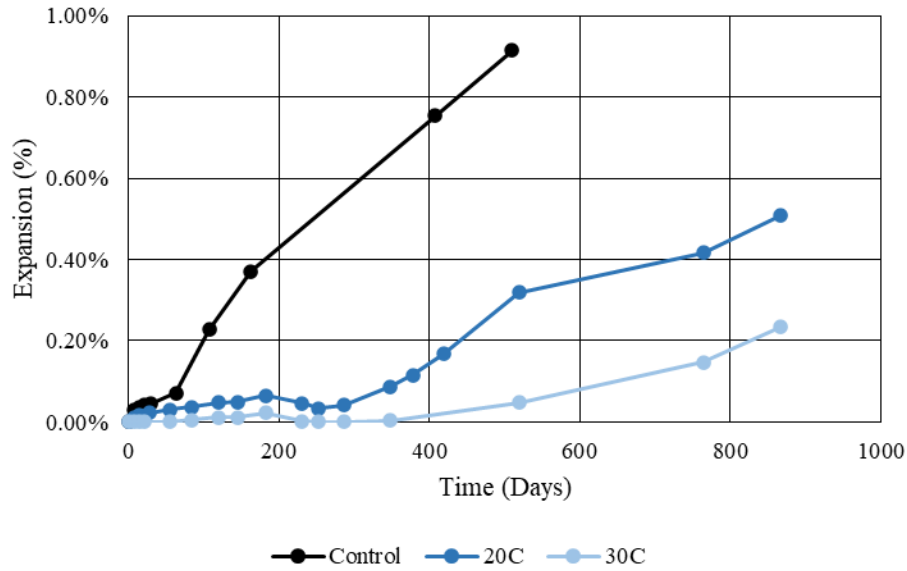


Figure 4-37: Expansion of durability blocks containing high alkali cement, reactive aggregate, and 20% - 30% Class C fly ash.

4.5.2.4 Volcanic Rock

Similar to the evaluation with ASTM C1567 and ASTM C1293 the ground volcanic rock showed very little reaction and had a relatively low mitigation potential with regards to alkali-silica reactivity. The expansion of the durability block for the volcanic rock concrete mixture is presented in Figure 4-38 and shows a nearly identical magnitude of expansion, although the initiation of the expansion is delayed, especially compared to the low replacement sugarcane bagasse ash mixes. This may be due to the reduced alkalis in the system caused by dilution by the presence of the volcanic rock.

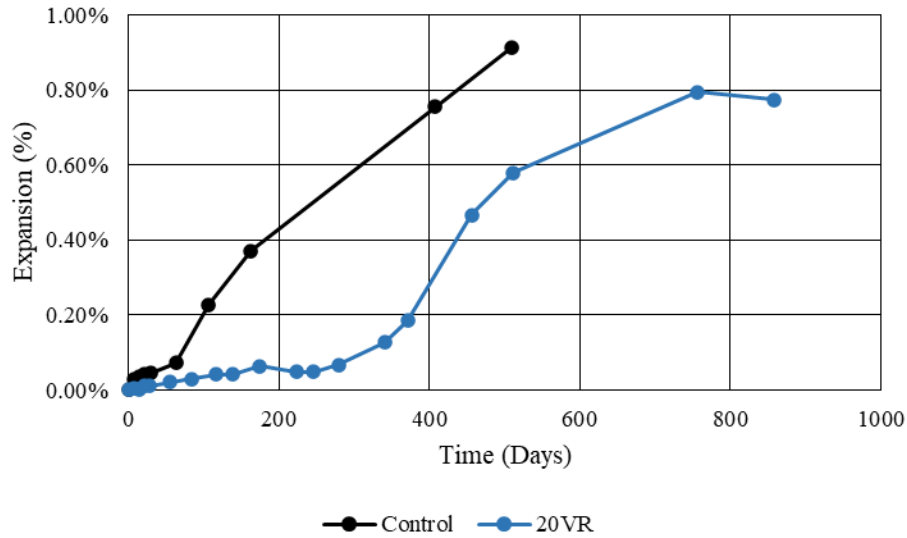


Figure 4-38: Expansion of durability blocks containing high alkali cement, reactive aggregate, and 20% volcanic rock.

4.5.2.5 Silica Fume

A similar conclusion can be formed from the durability block results and the ASTM C1293 results in that a 4% replacement of SF does not suppress ASR; this is confirmed by published research [203,204]. Additionally, the age in which expansion passed the threshold was later than the mixture containing VR. However, the durability block measurements are rather similar between both mixtures.

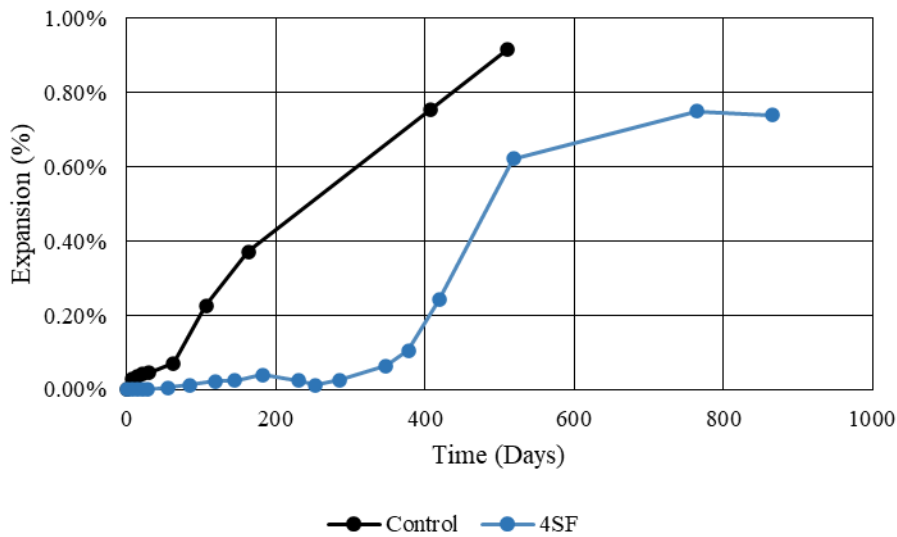


Figure 4-39: Expansion of durability blocks containing high alkali cement, reactive aggregate, and 4% silica fume.

4.5.2.6 Ternary Mixtures

The ternary mixture durability blocks performed similarly to the ASTM C1293 evaluation. The ternary mixtures with SCBA-A outperformed those with SCBA-B. The ASTM C1293 results show that the ternary mixtures with SCBA-B surpassed the expansion limits while the ternary mixtures with SCBA-A did not. The durability block data in Figure 4-40 shows that all four mixes significantly mitigated ASR with results for Class C FA-SCBA-B mixes similar to those for binary 20% Class F fly ash and results for Class C FA-SCBA-A mixes similar to those for binary SCBA-A as shown in Figure 4-36.

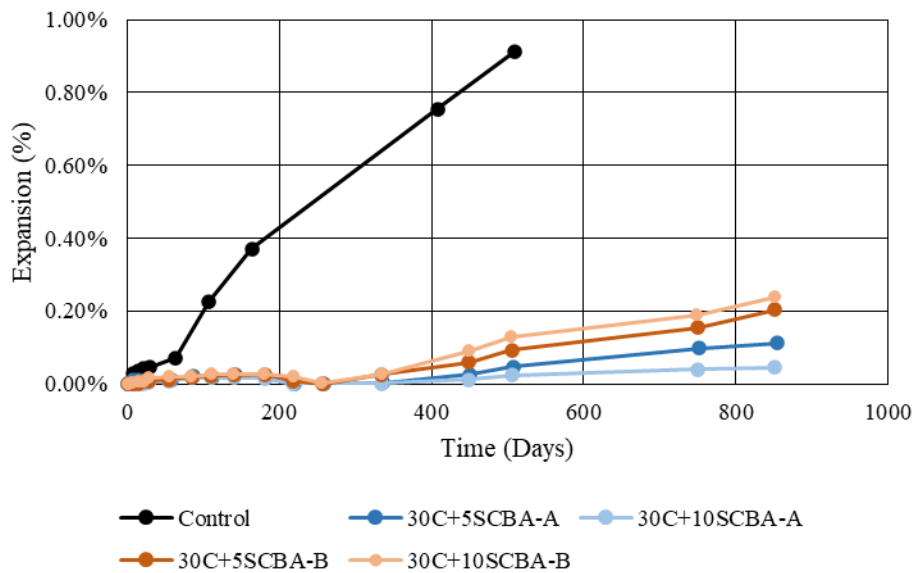


Figure 4-40: Expansion of durability blocks containing high alkali cement, reactive aggregate, and 30% Class C fly ash and 5% or 10% of SCBA-A or SCBA-B.

The ground glass ternary mixture results also align with the ASTM C1293 results. In both evaluation mixes the expansion observed with the ternary blend of 20% Class C fly ash and 5% or 10% ground glass did not indicate sufficient mitigation to cease the expansion caused by ASR. The expansion of the durability blocks for the ground glass ternary blended mixtures are shown in Figure 4-41. There was very little difference between the 5% and 10% ground glass additions with 20% Class C fly ash, although the additional ground glass does appear to marginally reduce ultimate expansion. At two years, the expansion of the 20% Class C fly ash and 10% ground glass mixture had an expansion of approximately 0.27%.

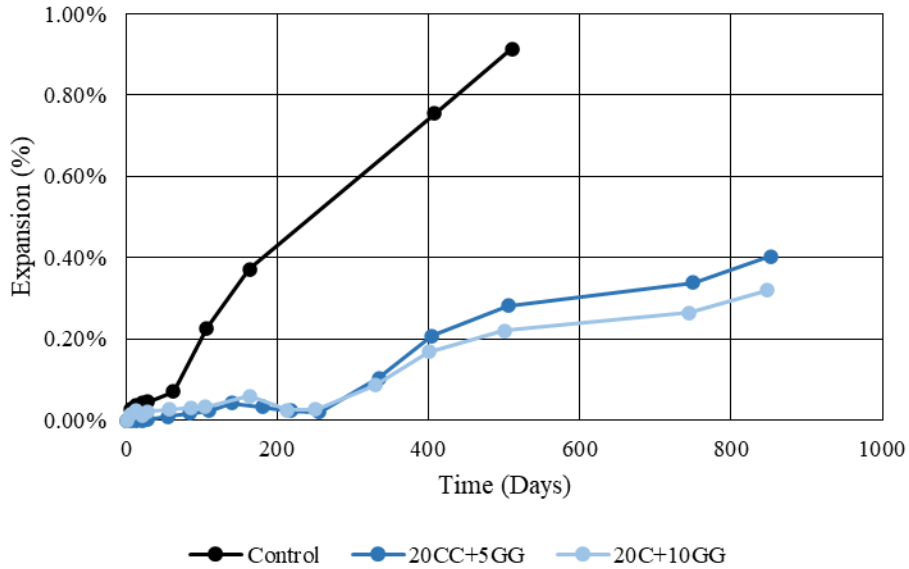


Figure 4-41: Expansion of durability blocks containing high alkali cement, reactive aggregate, and 20% Class C fly ash and 5% or 10% ground glass.

The ternary Class C-Class F fly ash durability block results were consistent with the results from the ASTM C1293 evaluation and showed a lower level of expansion as shown in Figure 4-42. However, the rate of expansion appeared to be increasing, which is indicative of impending expansion. The expansive nature of the alkali-silica reaction is one that is sudden, and mixes can appear to suppress the reaction, only to begin expanding after a long period of time. Further observation will be required to determine efficacy of these ternary blends against ASR.

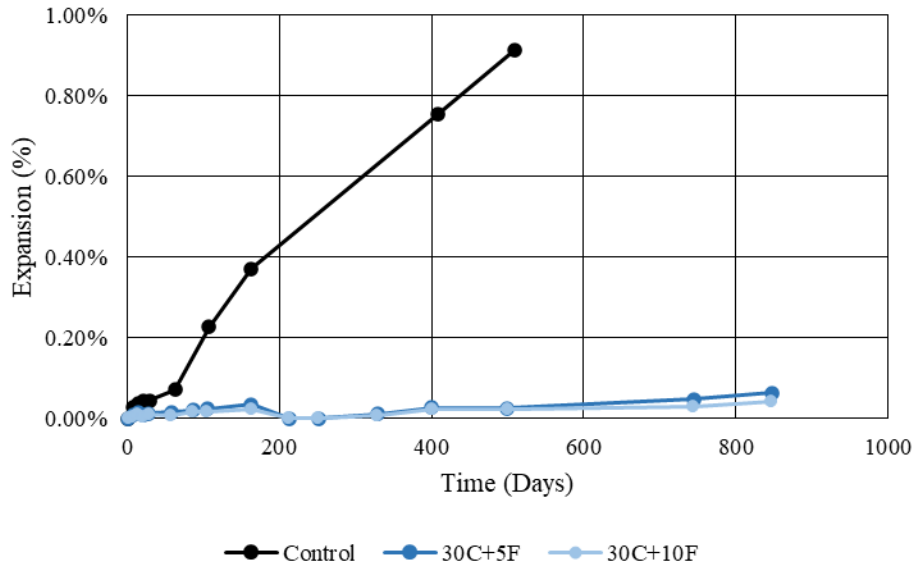


Figure 4-42: Expansion of durability blocks containing high alkali cement, reactive aggregate, and 30% Class C fly ash and 5% or 10% Class F fly ash.

For ternary blended concretes incorporating 30% Class C fly ash and 10% ground volcanic rock, at two years, the expansion was low but was slowly increasing. The conclusion made from ASTM C1293 was that the mixture reduced expansion below the threshold at the two-year mark. The results of the ternary blend of Class C fly ash and silica fume were very much in line with those observed in ASTM C1293.

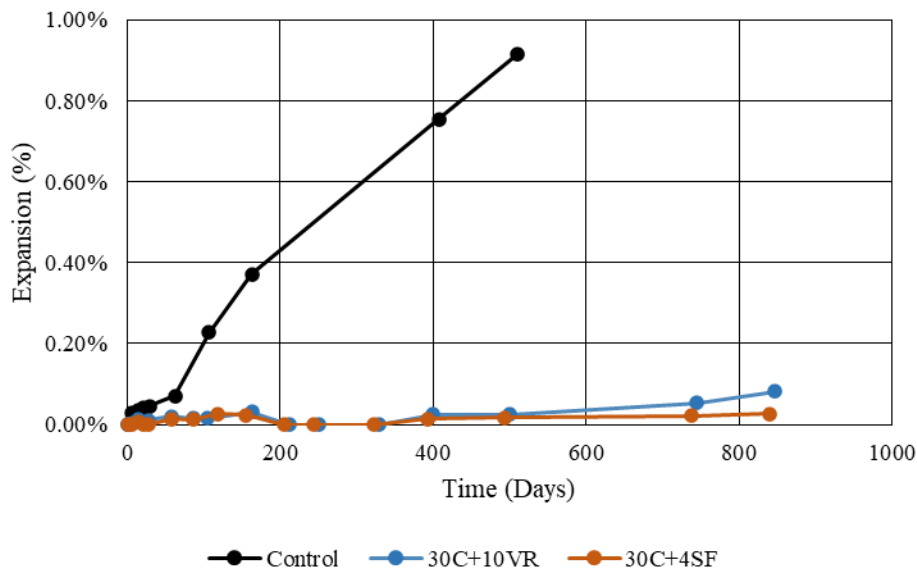


Figure 4-43: Expansion of durability blocks containing high alkali cement, reactive aggregate, and 30% Class C fly ash with 10% volcanic rock or 4% silica fume.

4.5.3 Comparison of ASTM C1293 and Concrete Durability Blocks

The use of the various methods to evaluate alkali-silica reactivity have benefits and drawbacks for each method. Accelerated mortar bar specimens (ASTM C1567) require aggregate to be crushed to a specific gradation and must be kept at very high temperatures, which change hydration characteristics and phase assemblages. However, the accelerated method allows very quick evaluation of materials (two weeks) compared to the other methods, which generally require several months (AASHTO T380) or several years (ASTM C1293). The ASTM C1293 test also requires specific gradations to be used, but only for the coarse aggregate, and uses slightly elevated temperatures (38°C); however, it does require mixes amended with SCM to be evaluated for more than 12 months. Therefore, the conditioned space requirements are very high. Finally, the durability blocks have the drawback of large specimens and require outdoor space and are not controlled, however, they expose specimens to conditions that are more consistent with field exposure than laboratory conditions, which will tend to be harsher due to thermal cycling and exposure to various precipitation events.

Comparing the two-year expansion percentages of ASTM C1293 to the expansion of the durability blocks of the same mixes shows that the expansions of the durability blocks were greater for mixes that expanded beyond the ASTM C1293 0.04% expansion threshold as shown in Figure 4-44. This data shows that mixes that are borderline (0.04% expansion in ASTM C1293) have expansions ranging from 0.04% to 0.15%. This seems to indicate that the durability blocks represent a harsher conditioning exposure with more specimens experiencing expansions beyond 0.04%; this is likely due to the more extreme thermal cycling associated with external placement and storage.

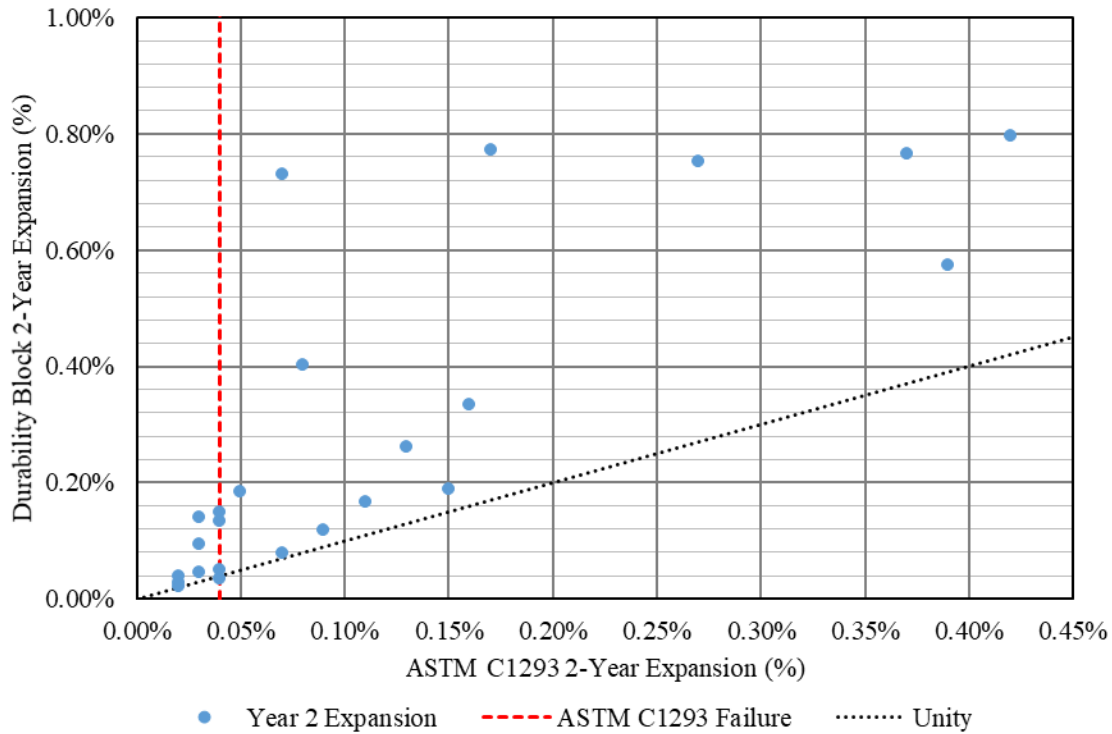


Figure 4-44: Comparison of ASTM C1293 and durability block expansion.






4.5.4 Surface and Bulk Resistivity

The surface resistivity test method involves measuring the electrical surface resistivity along the surface of a 4" x 8" concrete specimen with a 4-pin Wenner probe array [205]. Higher electrical resistivity generally relates to smaller pore diameters, which are related to a reduction in permeability and chloride ion penetration [206,207]. The bulk electrical resistivity of a 4" x 8" concrete sample is measured by placing the specimen between two stainless steel plates that act as electrodes. An AC current is applied to the plates and the resulting voltage is measured. Much like the surface resistivity test, the results indicate the concrete's ability to resist chloride ion penetration. The difference between bulk and surface resistivity is that bulk measures the resistivity of the concrete cylinder as a whole, not just the surface. Bulk resistivity measurements can be compared to the rapid chloride penetration test (RCPT, ASTM C1202) measurements [208]. The advantage of bulk resistivity over RCPT is that the duration of testing is much shorter, while still indicating the potential for chloride penetration resistance.

A summary of the surface and bulk resistivity values along with the corresponding color codes for the AASHTO chloride ion penetrability classification values (see Table 4-34) are

presented in Table 4-35 for Class IV concrete mixtures using Type I/II cement, Table 4-36 for Class IV concrete mixtures using Type IL cement, and Table 4-37 for Class I concrete mixtures using Type IL cement.

Table 4-34: Chloride ion penetrability classification values for surface and bulk resistivity. Adapted from [205,209].

Chloride Ion Penetration	Surface Resistivity Test		Uniaxial (Bulk) Resistivity	
	100-by-200-mm (4-by-8in.) Cylinder (kΩ-cm)		100-by-200-mm (4-by-8in.) Cylinder (kΩ-cm)	
High		<12	<5.2	
Moderate		12-21	5.2-10.4	
Low		21-37	10.4-20.8	
Very Low		37-254	20.8-207	
Negligible		>254	>207	

4.5.4.1 Sugarcane Bagasse Ash

In the case of both Sugarcane Bagasse Ash (SCBA) types, the 7-day surface and bulk resistivities decreased as replacements increased. Typically, this would indicate a progressively less dense microstructure as replacement increased; however, previous research has shown that this is most likely due to the elevated presence of conductive carbon in the concrete [210]. These results contradict previous findings that concluded that surface resistivity increased with increasing replacement [211]. However, the results were based on evaluating the concrete at 28 and 56 days and using a sieving technique that involved the removal of carbon particles. At later ages, the increase in replacement produced a comparable or greater resistivity. It is possible that the pozzolanic reaction negates the effects of the conductive carbon through the production of a more densified concrete structure.

Figure 4-45 through Figure 4-47 show that despite the larger doses of SCBA-A and SCBA-B performing better than the control at 3 years, the improvement is minimal compared to the other alternative supplementary cementitious materials investigated. This is likely due to the elevated amounts of electrically conductive carbon present resulting in skewed electrical testing results [210]. Regardless of the class of concrete or type of cement used, the 30% replacements generally resulted in approximately 50% higher resistance than the control.

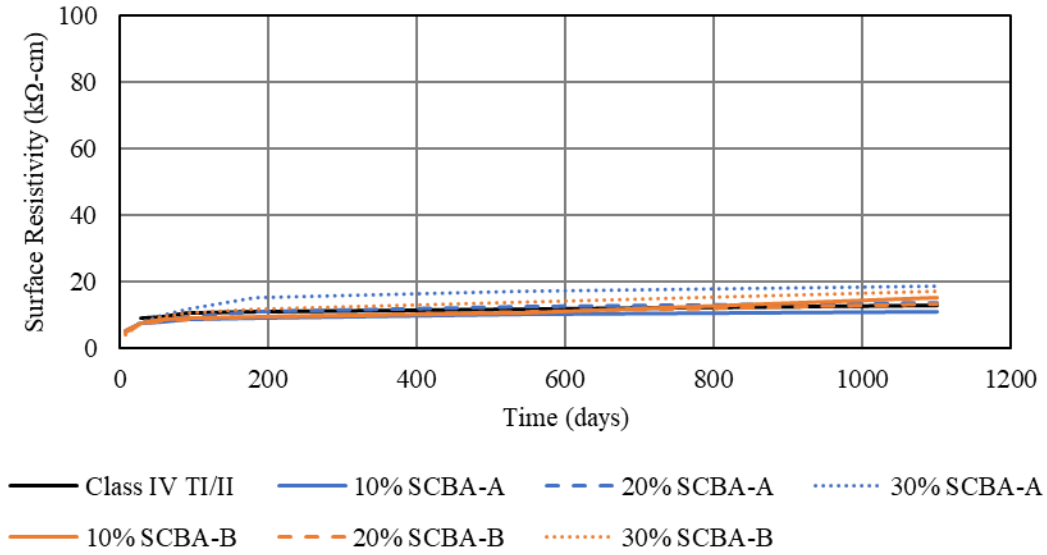


Figure 4-45: Surface resistivity of Class IV concrete with Type I/II cement and SCBA.

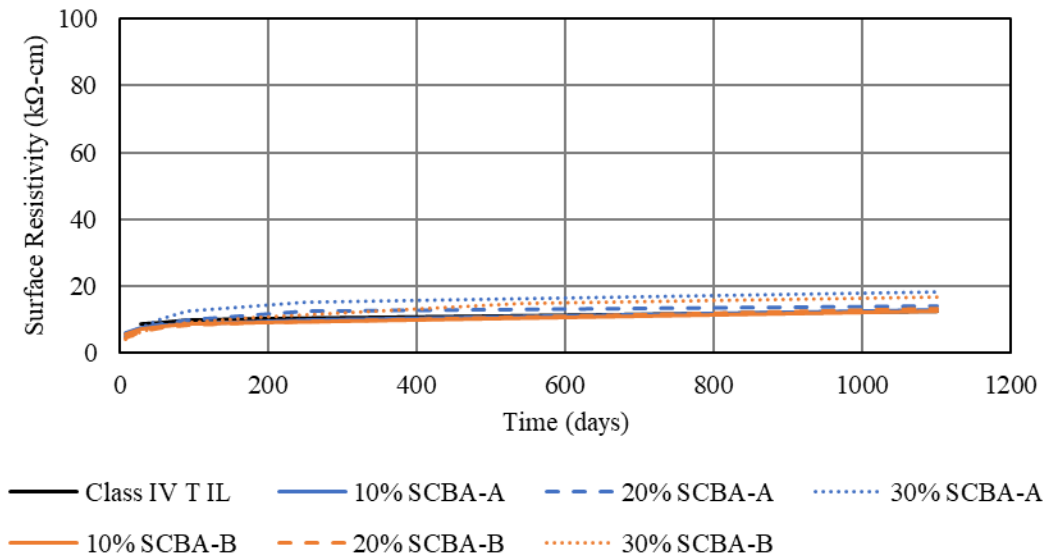


Figure 4-46: Surface resistivity of Class IV concrete with Type IL cement and SCBA.

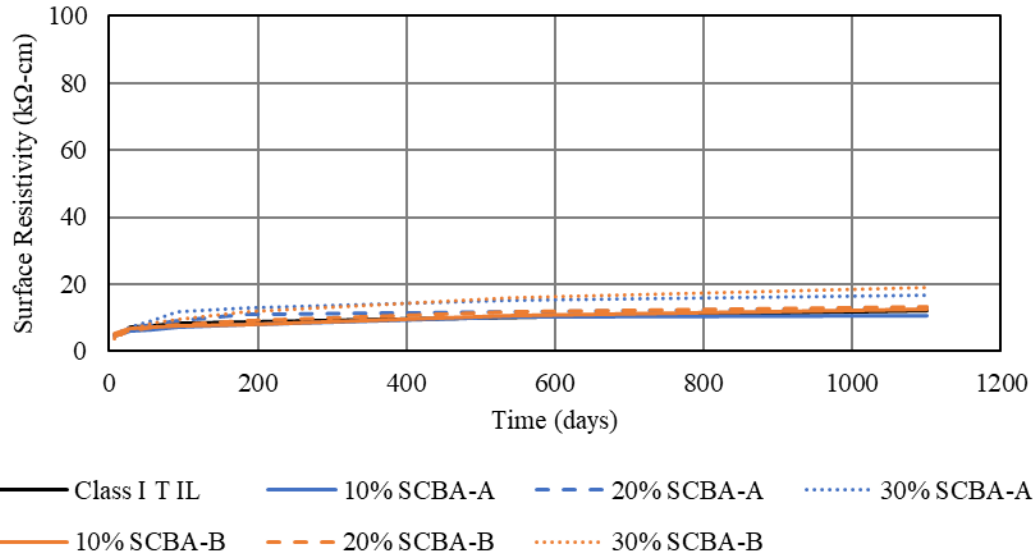


Figure 4-47: Surface resistivity of Class I concrete with Type IL cement and SCBA.

Bulk resistivity values of the sugarcane bagasse ash mixes result in resistance to penetration classifications that are generally higher than the corresponding surface resistivity values. This is similar to previously published work using the same materials which found that electric test methods under-predicted physical performance with respect to chloride penetration resistance [210]. The bulk resistances for the binary sugarcane bagasse ash mixes are presented in Figure 4-48 through Figure 4-50. As anticipated from the surface resistivity testing, the bulk resistivity numbers were moderately higher than the control but did not rise more than approximately 100% higher than control by the end of three years.

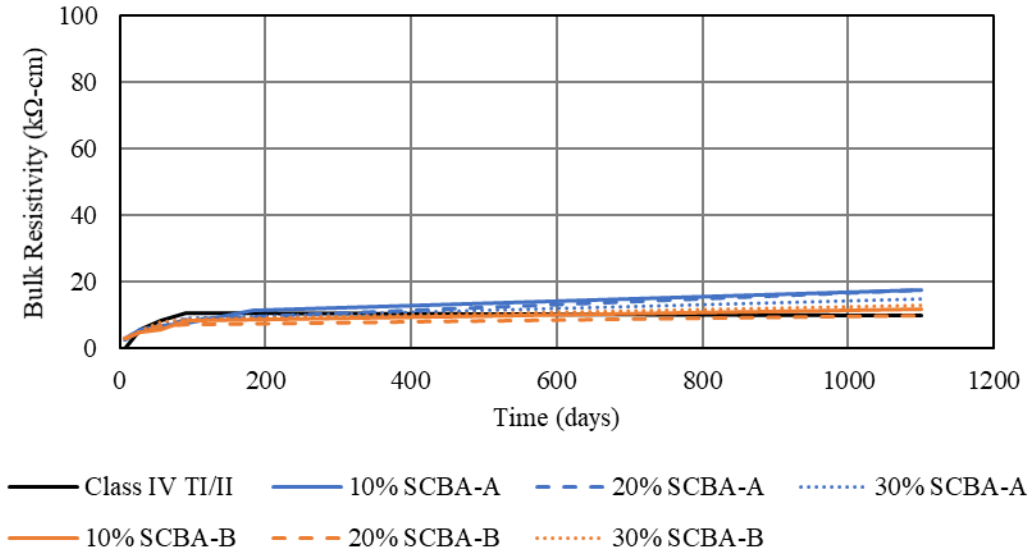


Figure 4-48: Bulk resistivity of Class IV concrete with Type I/II cement and SCBA.

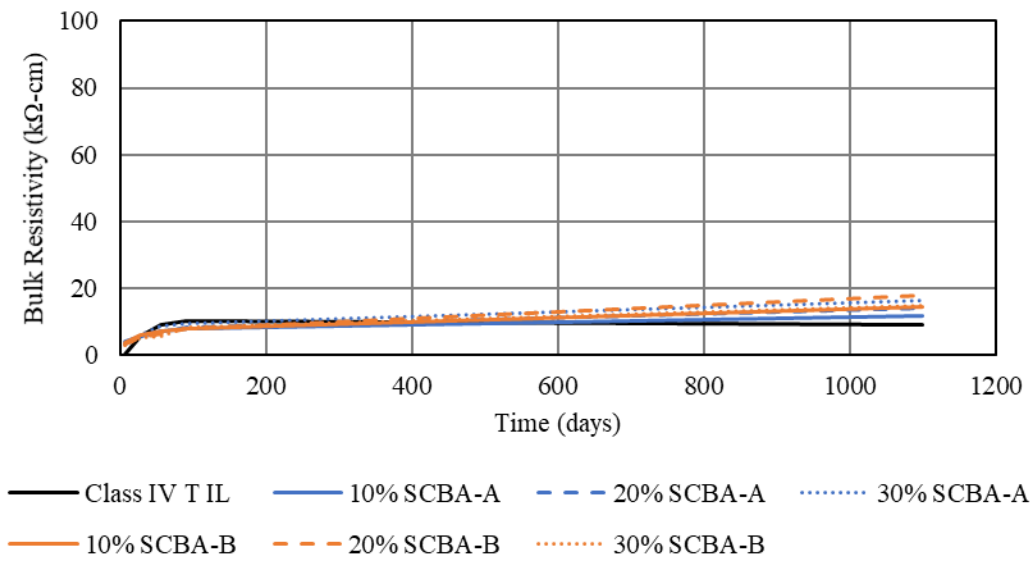


Figure 4-49: Bulk resistivity of Class IV concrete with Type IL cement and SCBA.

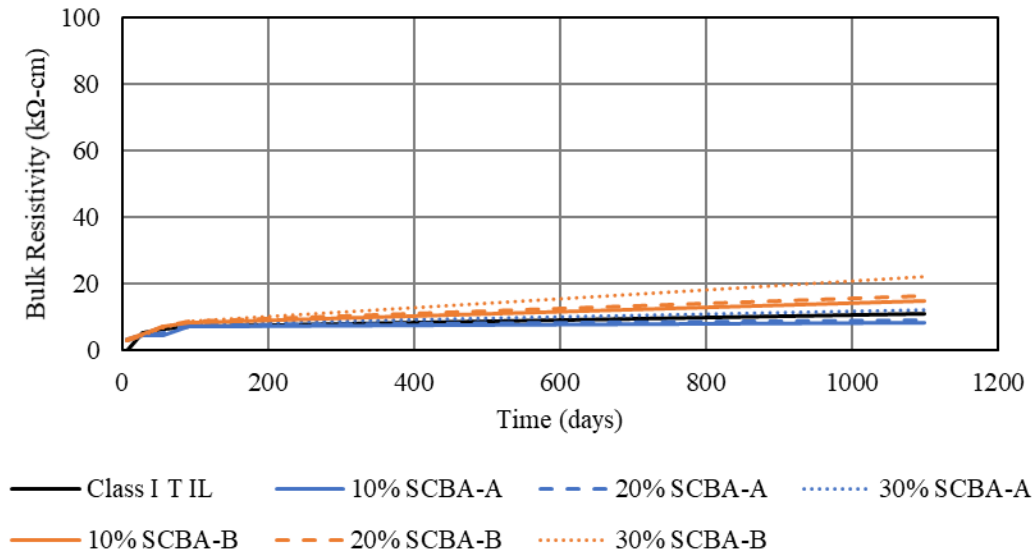


Figure 4-50: Bulk resistivity of Class I concrete with Type IL cement and SCBA.

4.5.4.2 Ground Glass and Fly Ash

The 40% ground glass binary mixtures, regardless of class of concrete or type of cement, provided the highest surface resistivity as seen in Figure 4-51 through Figure 4-53. Generally speaking, the ground glass mixes were classified between “moderate” and “low” penetrability at 28 days. Additionally, each of the ground glass mixtures exhibited an increase in resistivity and a presumed high resistance to chloride attack. These conclusions are congruent with other electrical studies on GG amended concrete [58,212,213]. The conductivity of the pore solution of GG amended concretes has been observed to be higher than that of fly ash and control concretes, mainly due to the elevated presence of alkalis in GG [212,213]. However, the increased pore conductivity is outweighed by the decreased penetrability from the high pozzolanic reactivity of the ground glass, resulting in higher surface and bulk resistivities. As GG replacement increased, pore connectivity was found to increase at early ages and decrease at later ages [213]. It has been reported that the decrease in the early-age electrical conduction is caused by a decrease in pore connectivity due to the presence of unreacted filler, rather than a more densified pore structure, which is the main reason for higher resistivity at later ages [213].

The 20% Class F fly ash mixes performed as expected in each of the cementitious systems. While the 28-day chloride ion penetration was “high”, there was an increase in resistivity caused by the pozzolanic reaction taking place in later ages. The 20% Class C fly ash mixtures had the lowest performance of the fly ash mixtures; these mixes had similar 28-day

performance as the F ash but did not have as much of an increase in resistivity over time as the F ash mixes. The Class C fly ash mixes with 30% replacements exhibited performance that was in between the performance of the 20% Class C fly ash mixtures and the 20% Class F fly ash mixtures. The overall performance of the 30% Class C fly ash mixtures is indicative of a high-quality C ash, which is confirmed by the low alkali content measured in Section 2. Similar results were observed in other publications [214,215]. However, research has shown that concrete amended with C ash may not show improved resistivity values in poor quality C ashes [216].

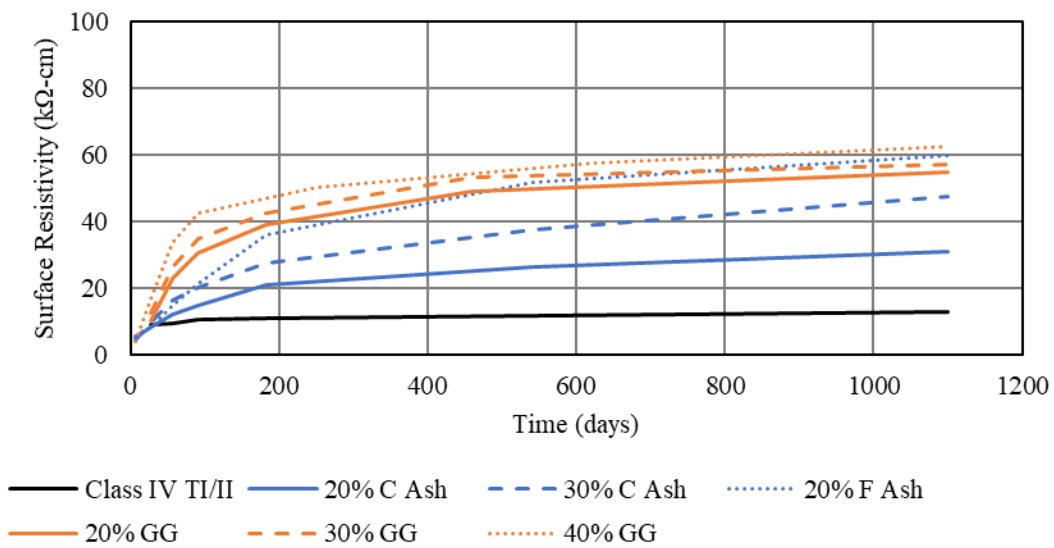


Figure 4-51: Surface resistivity measurements for Class IV concrete with Type I/II cement and Class C fly ash, Class F fly ash, or ground glass replacements.

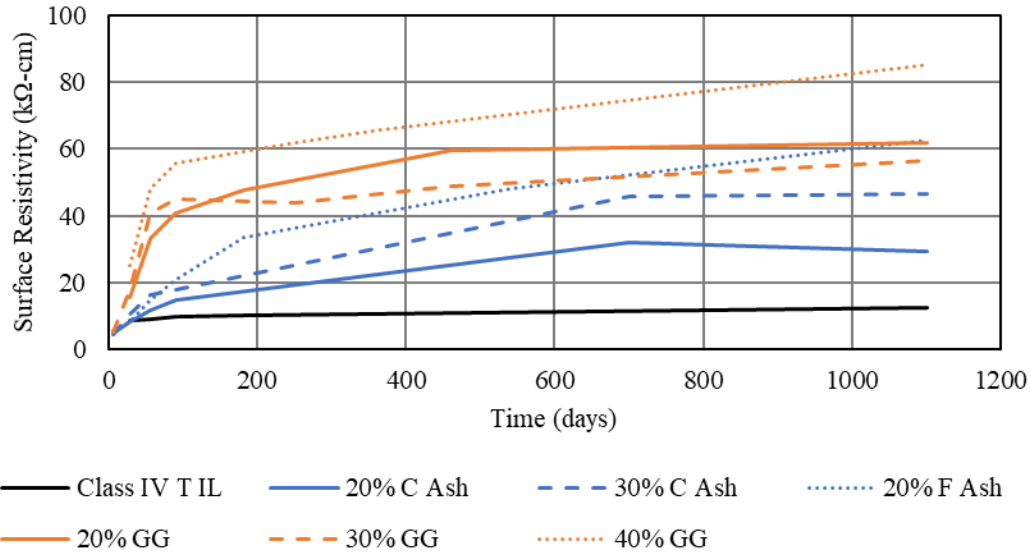


Figure 4-52: Surface resistivity measurements for Class IV concrete with Type IL cement and Class C fly ash, Class F fly ash, or ground glass replacements.

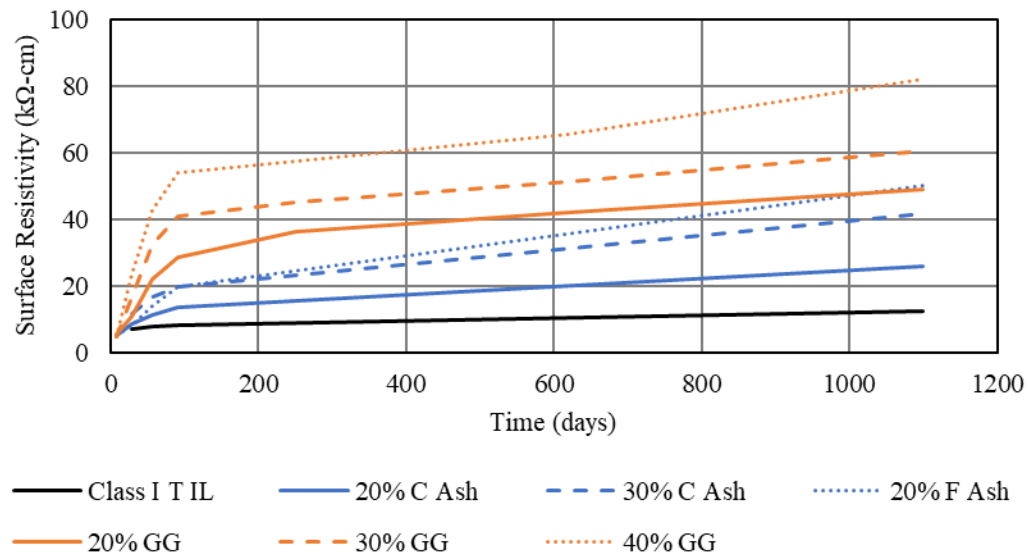


Figure 4-53: Surface resistivity measurements for Class I concrete with Type IL cement and Class C fly ash, Class F fly ash, or ground glass replacements.

The bulk resistivity measurements for the mixes containing binary mixes of Class C fly ash, Class F fly ash, or ground glass are presented in Figure 4-54 through Figure 4-56. Following the trend of the surface resistivity, the 40% ground glass mixtures provided the largest benefit over the control in the majority of mixtures with the 20% Class C fly ash providing the least benefit. However, even the 20% Class C fly ash mixes were approximately 100% more resistive than the control mixes. There are similarities between the F ash and ground glass mixtures in

terms of electrical resistivity, particularly with the same levels of replacement. The GG mixtures had a higher resistivity than the F ash mixtures at early ages, but the resistivity values for GG and F ash are comparable at 3 years. Additionally, the electrical resistivity of the mixtures with ground glass increased as the replacement increased. Similar improvement to resistivity have been observed by other publications [58,212,217].

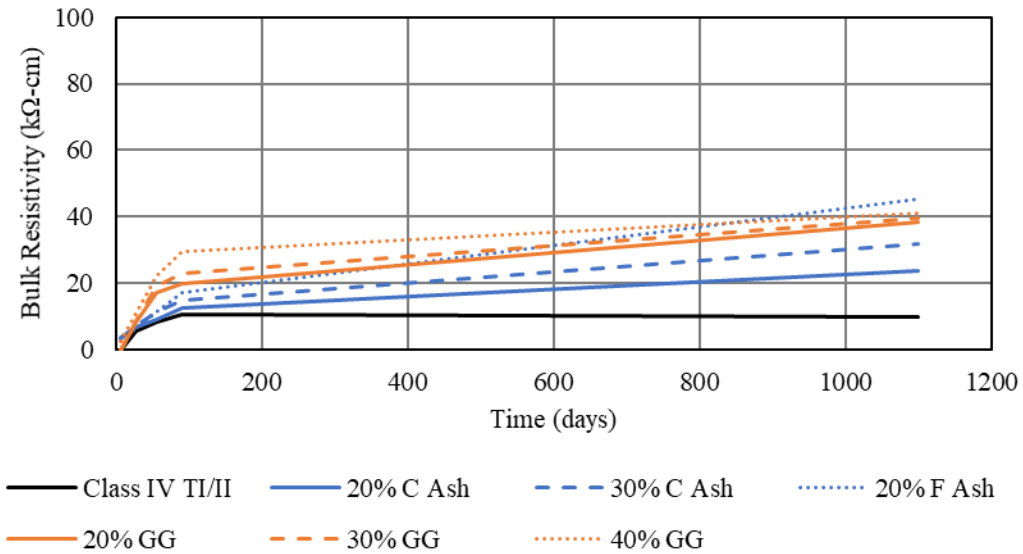


Figure 4-54: Bulk resistivity measurements for Class IV concrete with Type I/II cement and Class C fly ash, Class F fly ash, or ground glass replacements.

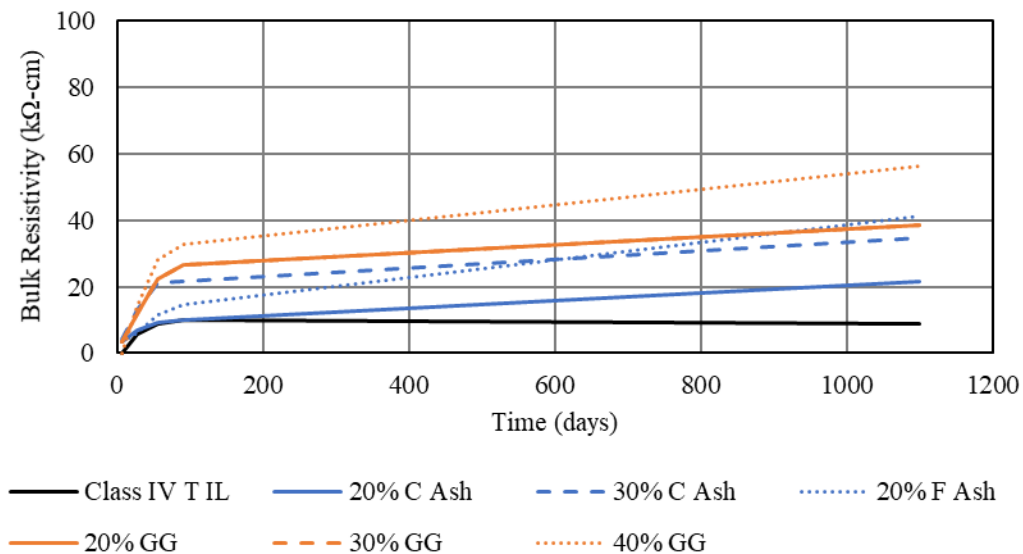


Figure 4-55: Bulk resistivity measurements for Class IV concrete with Type IL cement and Class C fly ash, Class F fly ash, or ground glass replacements.

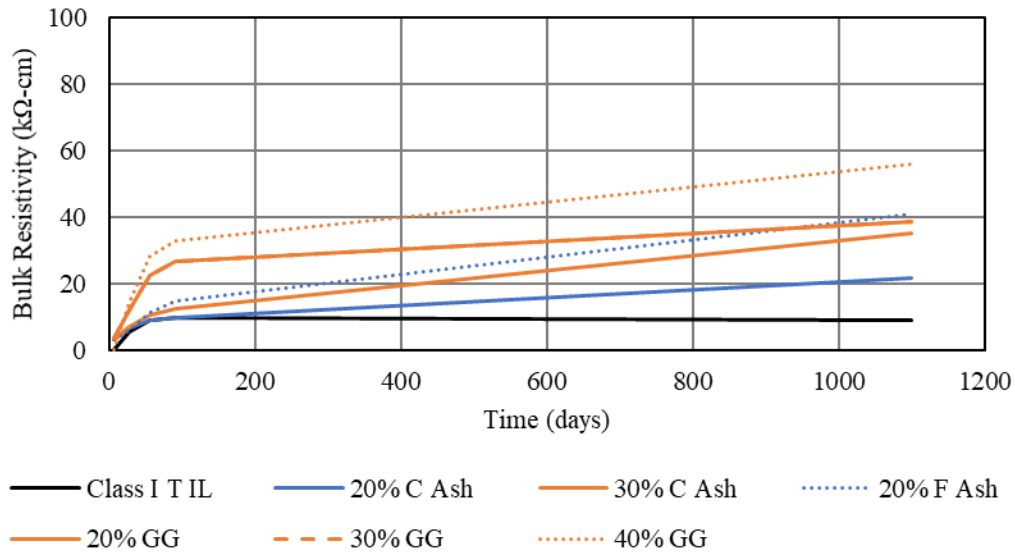


Figure 4-56: Bulk resistivity measurements for Class I concrete with Type IL cement and Class C fly ash, Class F fly ash, or ground glass replacements.

4.5.4.3 Volcanic Rock and Silica Fume

Volcanic Rock (VR) generally exhibited statistically comparable surface resistivity to control. The reduced performance compared to the other materials is consistent with the other evaluation methods noted in this report in that ground volcanic rock lacks reactivity and provides little to no improvement in the performance characteristics of the concrete.

The mixtures incorporating silica fume exhibited an increase in surface resistivity over time and were consistently higher than control, which is consistent with reported literature [218–220]. However, the changes in surface resistivity from day 56 to day 91 were minimal. This is caused by the exhaustion of the reaction between silica fume and the calcium hydroxide produced during hydration [35,210]. The 4% silica fume mixes generally produced surface resistivity values approximately 30-40% higher than the control mixes. While the 28-day classification was “moderate” there was little to no increase in resistivity throughout the three years of measurement. The surface resistivity of the ground volcanic rock and the mixes incorporating silica fume are found in Figure 4-57 through Figure 4-59.

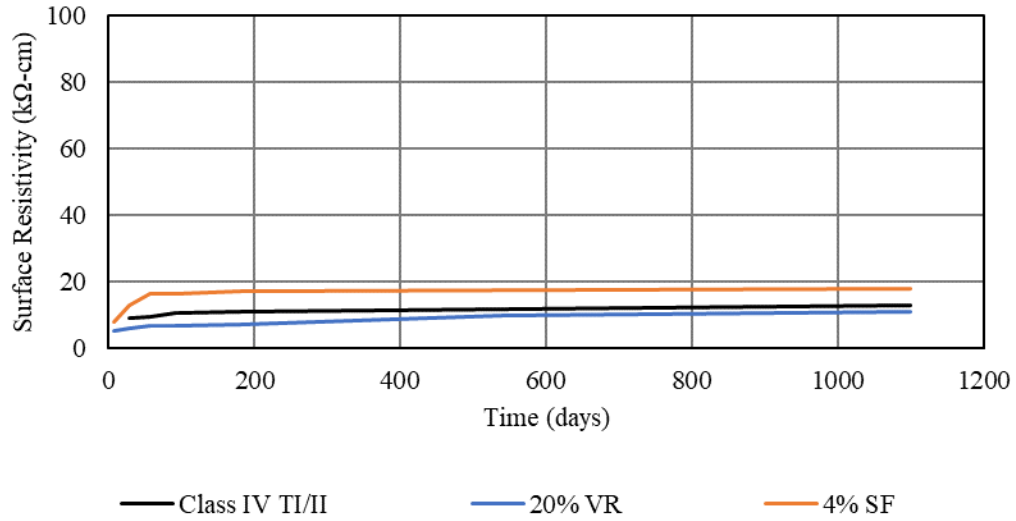


Figure 4-57: Surface resistivity measurements for Class IV concrete with Type I/II cement and volcanic rock or silica fume replacements.

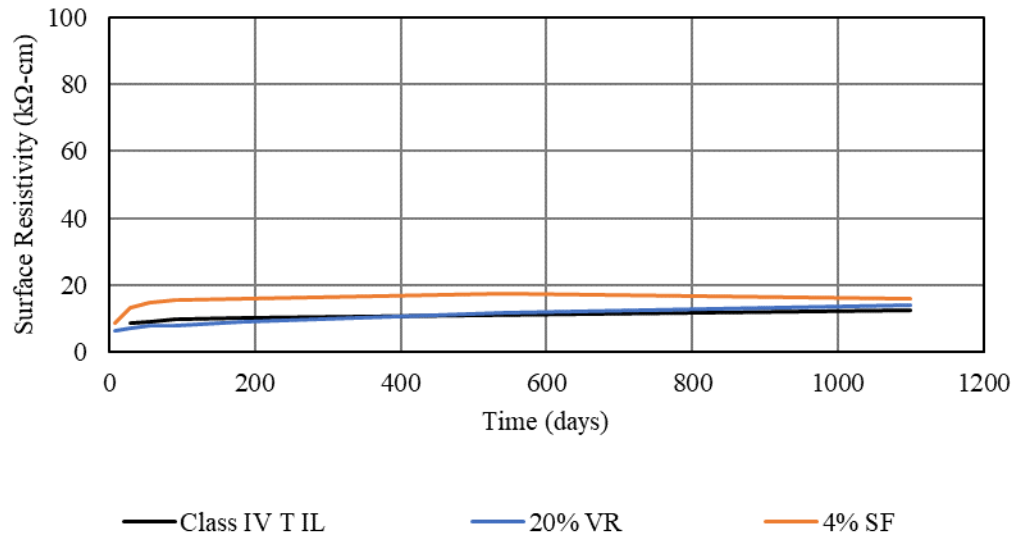


Figure 4-58: Surface resistivity measurements for Class IV concrete with Type IL cement and volcanic rock or silica fume replacements.

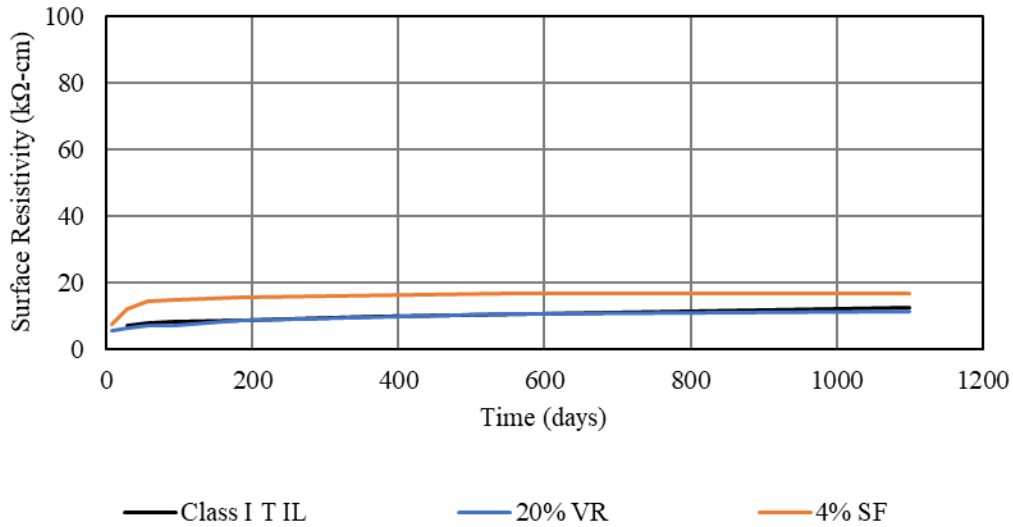


Figure 4-59: Surface resistivity measurements for Class I concrete with Type IL cement and volcanic rock or silica fume replacements.

As anticipated, the binary mixtures of 20% volcanic rock and 4% silica fume, Figure 4-60 through Figure 4-62, did not improve the chloride ion penetration resistance classification as per AASHTO T 358. The 20% volcanic rock mix tended to perform more closely to the control mix with regards to the surface resistivity, the bulk resistivity performed similarly to the silica fume mixture.

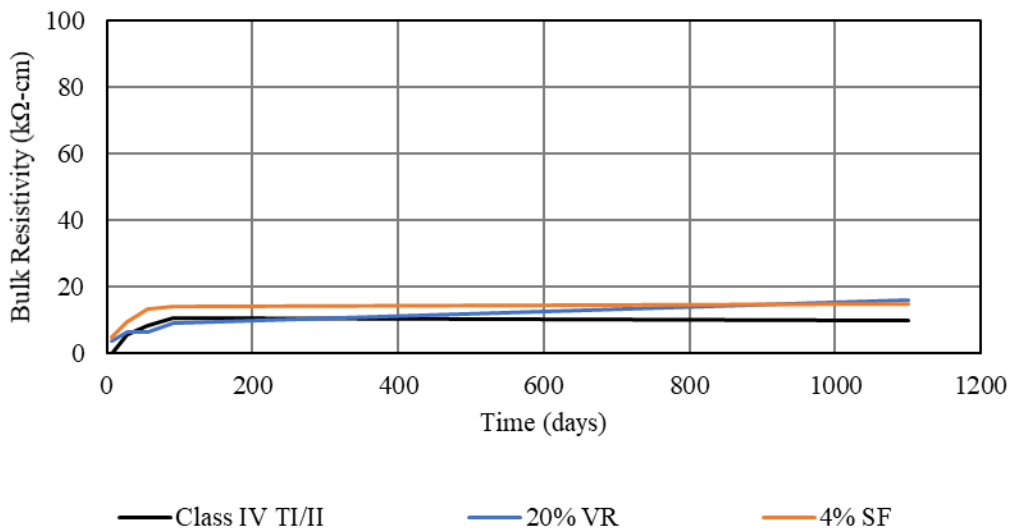


Figure 4-60: Bulk resistivity measurements for Class IV concrete with Type I/II cement and volcanic rock or silica fume replacements.

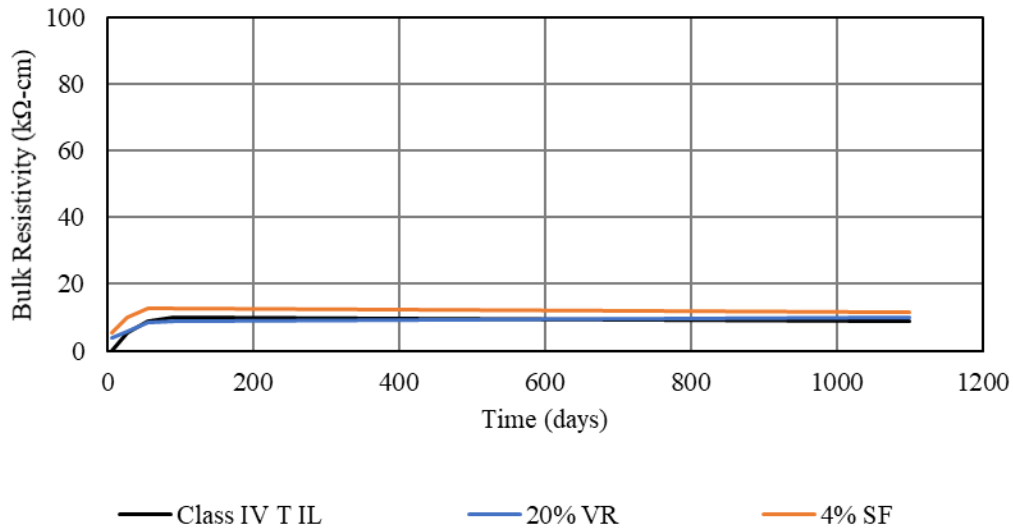


Figure 4-61: Bulk resistivity measurements for Class IV concrete with Type IL cement and volcanic rock or silica fume replacements.

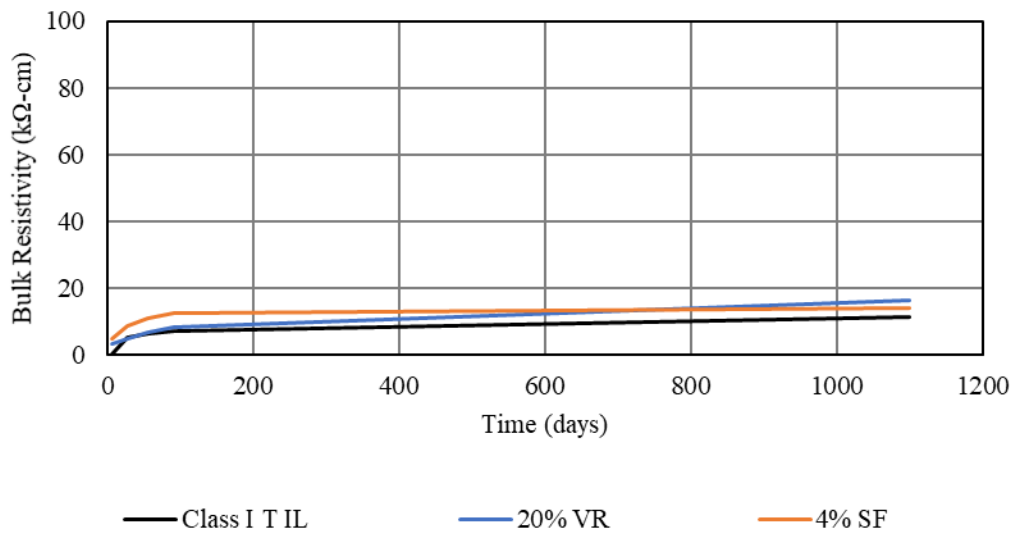


Figure 4-62: Bulk resistivity measurements for Class I concrete with Type IL cement and volcanic rock or silica fume replacements.

4.5.4.4 Ternary Mixtures

Overall, the ternary mixes performed considerably better than the binary mixes with respect to surface resistivity. Additionally, the ternary blends incorporating sugarcane bagasse ash performed similarly in each class of concrete with both cement types. The blends incorporating ground glass also performed similarly to the sugarcane bagasse ash mixes and

would be classified as “high” or “moderate” chloride ion penetrability, depending on the type of concrete, as shown in Figure 4-63 through Figure 4-65.

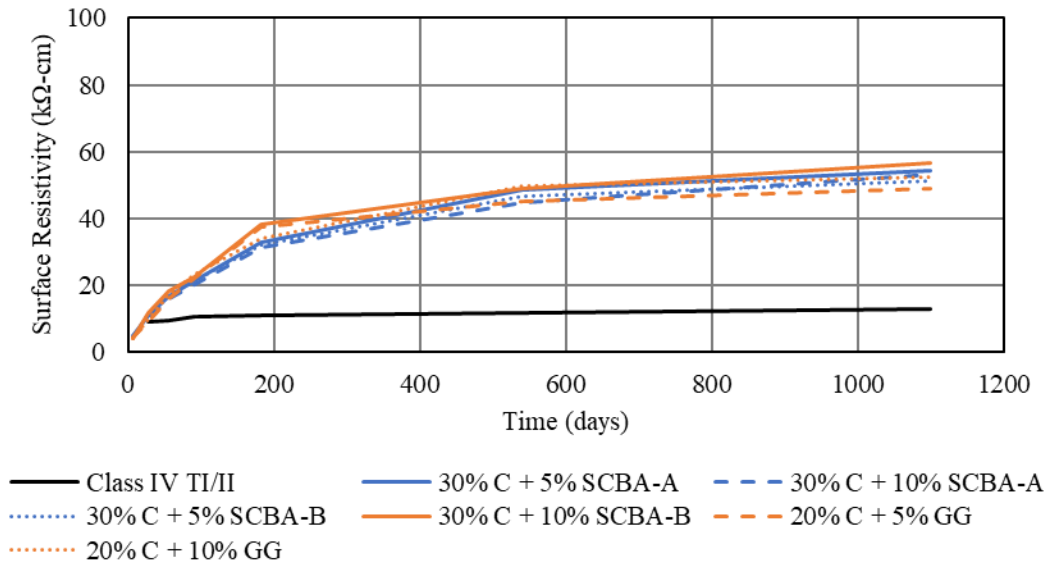


Figure 4-63: Surface resistivity measurements for Class IV concrete ternary blends with Type I/II cement, Class C fly ash, and SCBA-A, SCBA-B, or ground glass replacements.

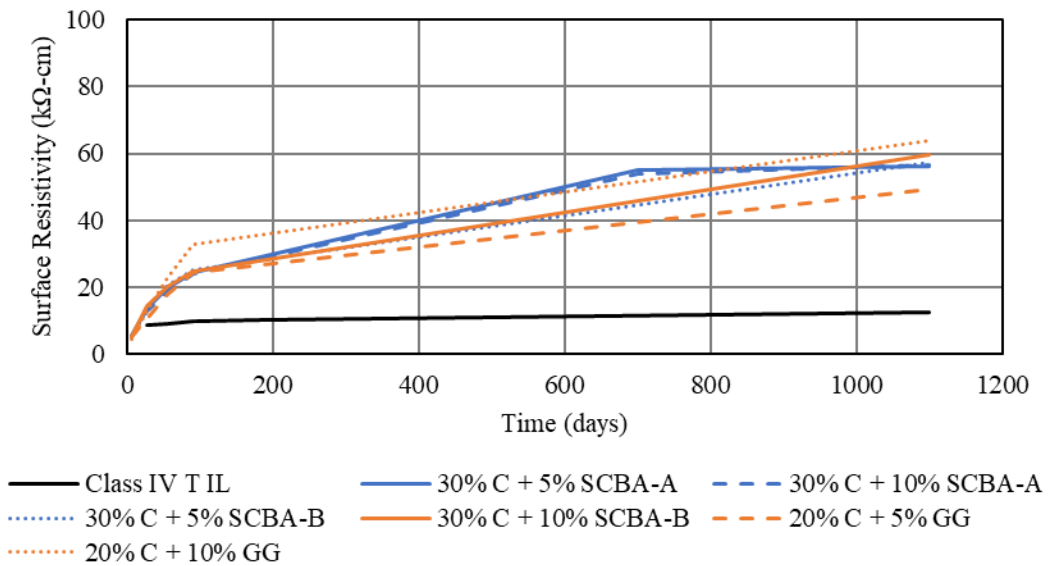


Figure 4-64: Surface resistivity measurements for Class IV concrete ternary blends with Type IL cement, Class C fly ash, and SCBA-A, SCBA-B, or ground glass replacements.

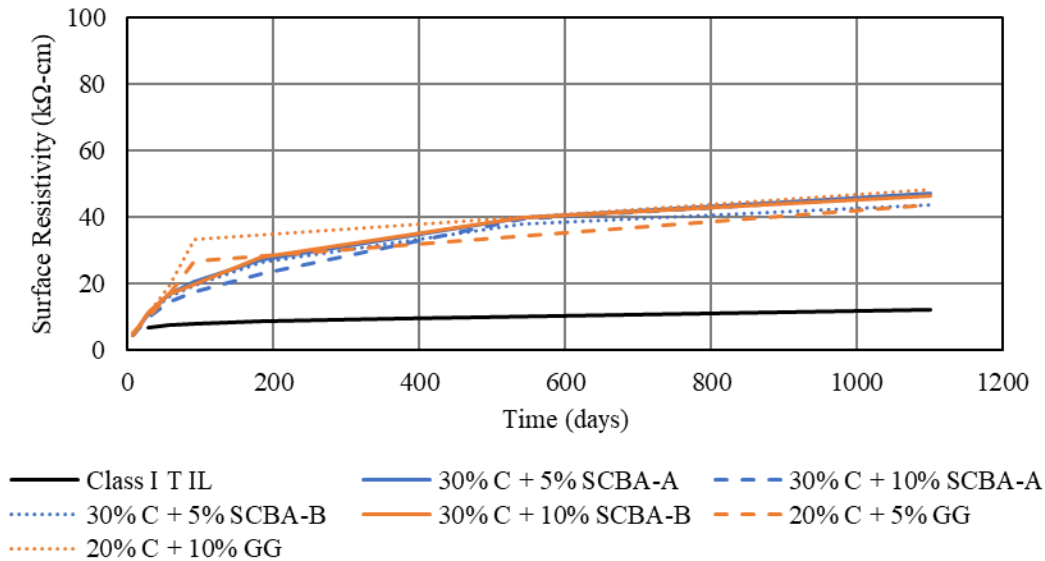


Figure 4-65: Surface resistivity measurements for Class I concrete ternary blends with Type IL cement, Class C fly ash, and SCBA-A, SCBA-B, or ground glass replacements.

The bulk resistivity measurements of the ternary blended concretes were similar to the surface resistivity measurements in that they contributed 200 – 300% additional penetration resistance compared to control at three years as shown in Figure 4-66 through Figure 4-68. The bulk resistivities of all the ternary mixtures increased linearly throughout the test period, whereas the surface resistivities of some of the ternary mixtures tended to increase at a reduced rate toward the end of the test, apparently beginning to level off. Correlations between bulk resistivity measurements and surface resistivity measurements were not consistent. For instance, in Figure 4-66, the 30% C + 5% SCBA-A mixture performed the best, while in Figure 4-68, the 20% C + 10% GG mixture performed best. These differences are distinct in the bulk resistance measurements but are absent in the surface resistivity measurements. Furthermore, each of the bulk resistance charts below has a different mix that performed best, and a different mix (ignoring the control) that performed the worst at three years.

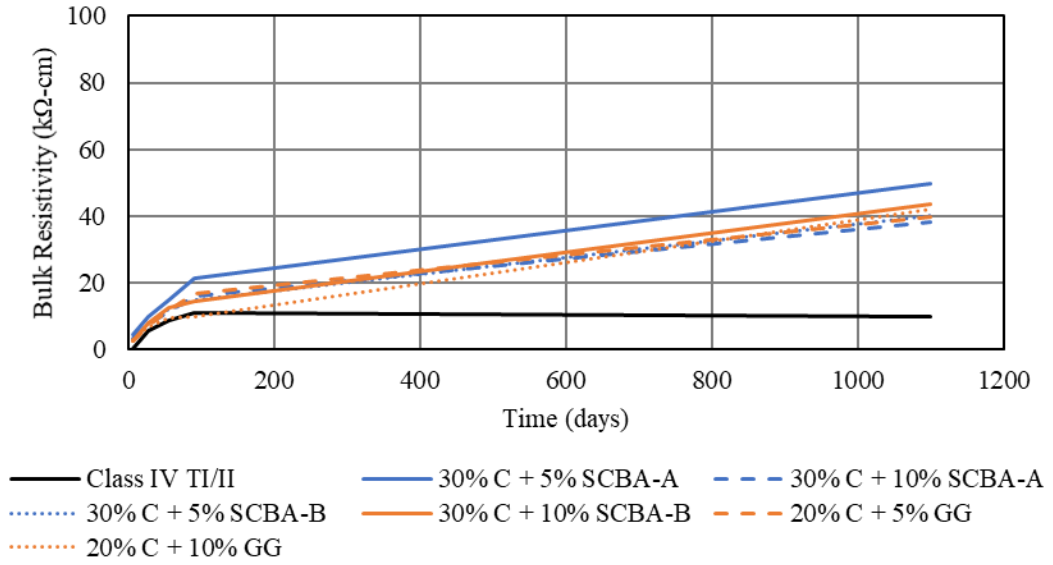


Figure 4-66: Bulk resistivity measurements for Class IV concrete ternary blends with Type I/II cement, Class C fly ash, and SCBA-A, SCBA-B, or ground glass replacements.

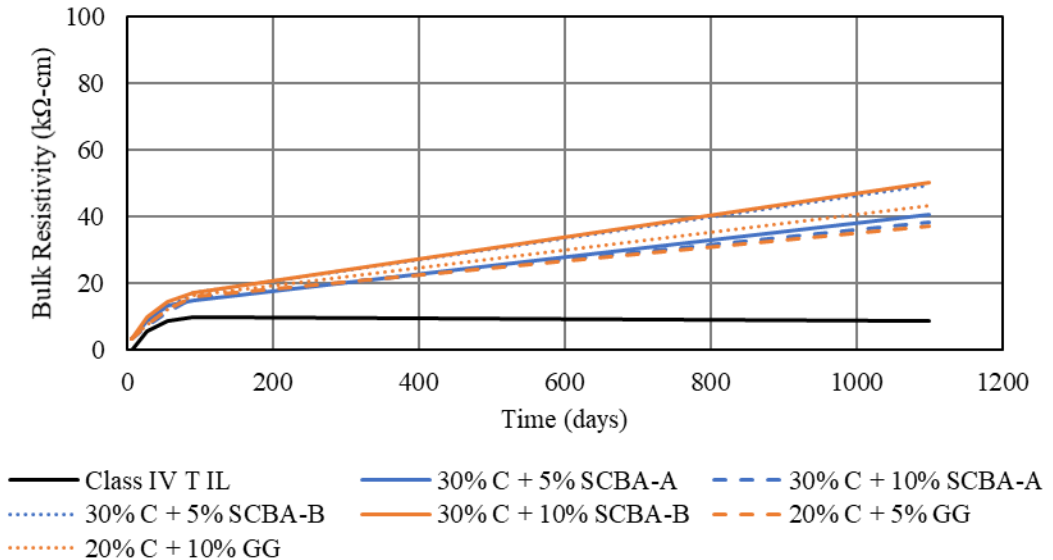


Figure 4-67: Bulk resistivity measurements for Class IV concrete ternary blends with Type IL cement, Class C fly ash, and SCBA-A, SCBA-B, or ground glass replacements.

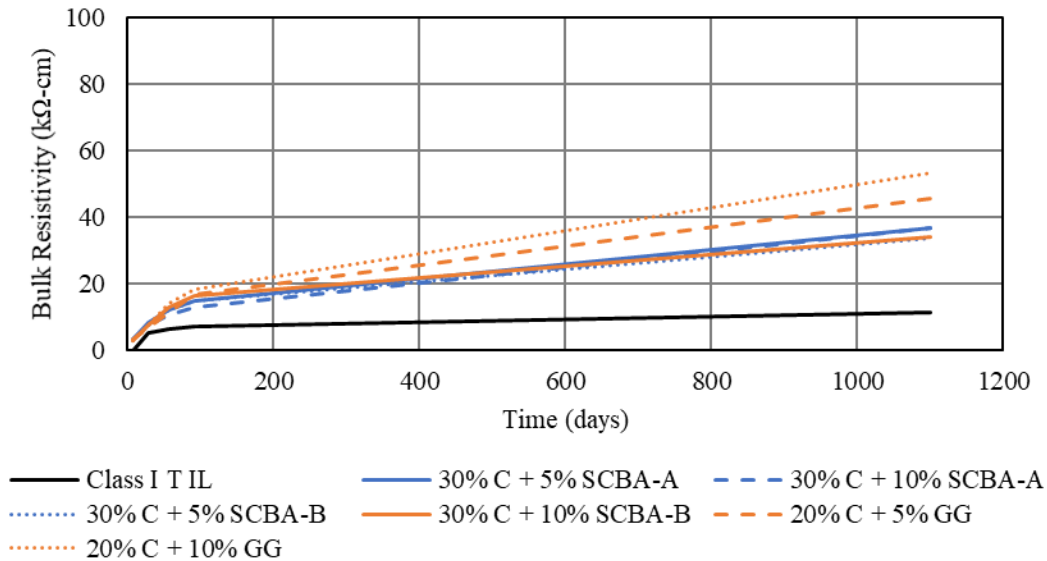


Figure 4-68: Bulk resistivity measurements for Class I concrete ternary blends with Type IL cement, Class C fly ash, and SCBA-A, SCBA-B, or ground glass replacements.

When incorporating ternary blends of Class C fly ash along with 5% or 10% Class F fly ash, there was a stark difference in ultimate surface resistivity at three years which can be seen in Figure 4-69 through Figure 4-71. The marginal increase in Class F fly ash resulted in considerable increases in total surface resistivity amounting to an approximately 20-25% increase in total surface resistance and was statistically better. The performance of ternary blends of 30% Class C fly ash with 4% silica fume fell between the performance of the two ternary blends with Class F fly ash in all three mixtures. Lastly, the ternary blends of the 30% Class C fly ash with 10% volcanic rock performed worse in surface resistivity than the fly ash or silica fume mixes.

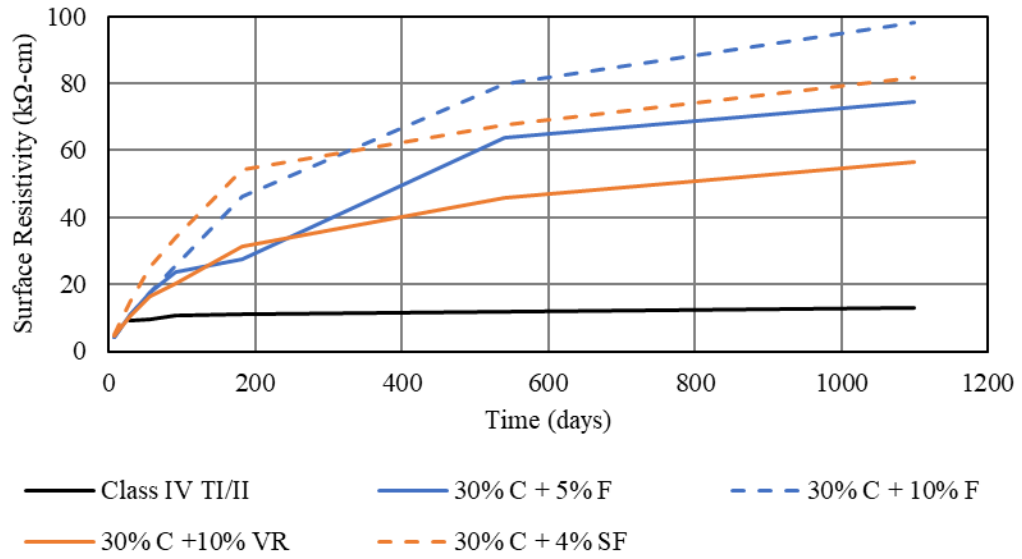


Figure 4-69: Surface resistivity measurements for Class IV concrete ternary blends with Type I/II cement, Class C fly ash, and Class F fly ash, volcanic rock, or silica fume replacements.

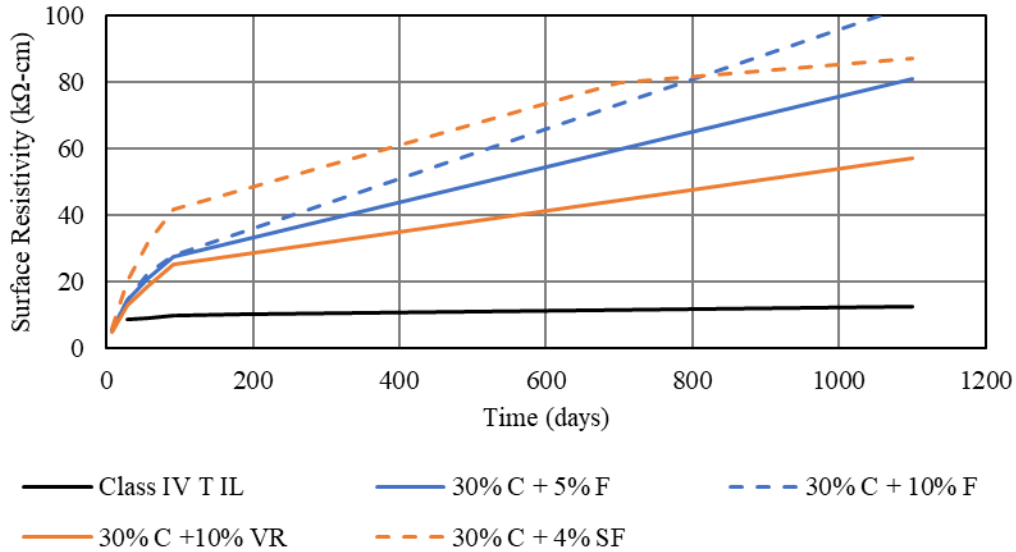


Figure 4-70: Surface resistivity measurements for Class IV concrete ternary blends with Type IL cement, Class C fly ash, and Class F fly ash, volcanic rock, or silica fume replacements.

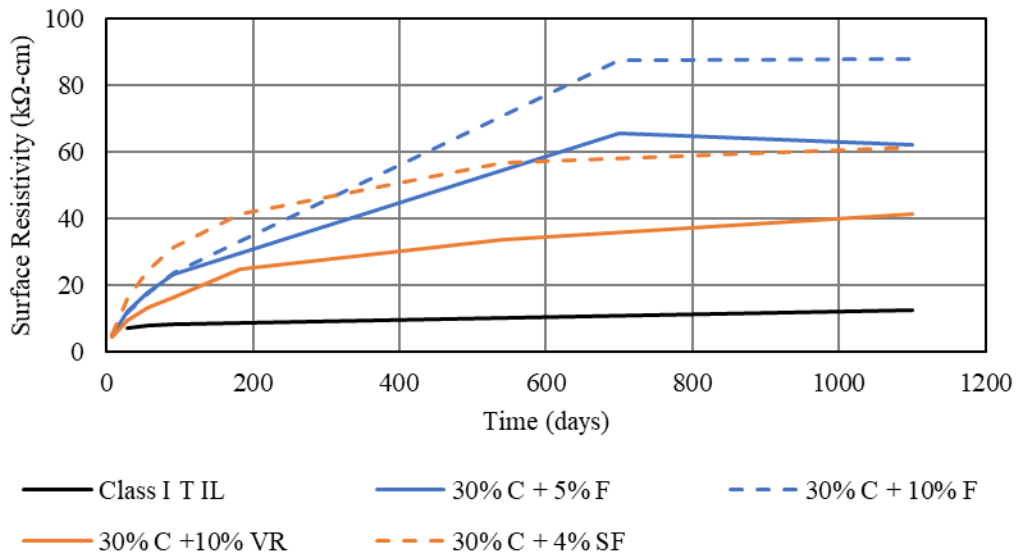


Figure 4-71: Surface resistivity measurements for Class I concrete ternary blends with Type IL cement, Class C fly ash, and Class F fly ash, volcanic rock, or silica fume replacements.

For the majority of the ternary blends below, the mixtures performed in line with what was seen in the surface resistivity measurements; 30% Class C fly ash with either 10% Class F fly ash or 4% silica fume produced in the highest resistance. While this was the same trend seen in Figure 4-72 and Figure 4-74, it was not the case for Figure 4-73 where the 30% C + 5% F ash mixture performed the best with the Class IV Type IL cementitious system. Generally speaking, these mixes performed at least 300% better than the control at three years of age.

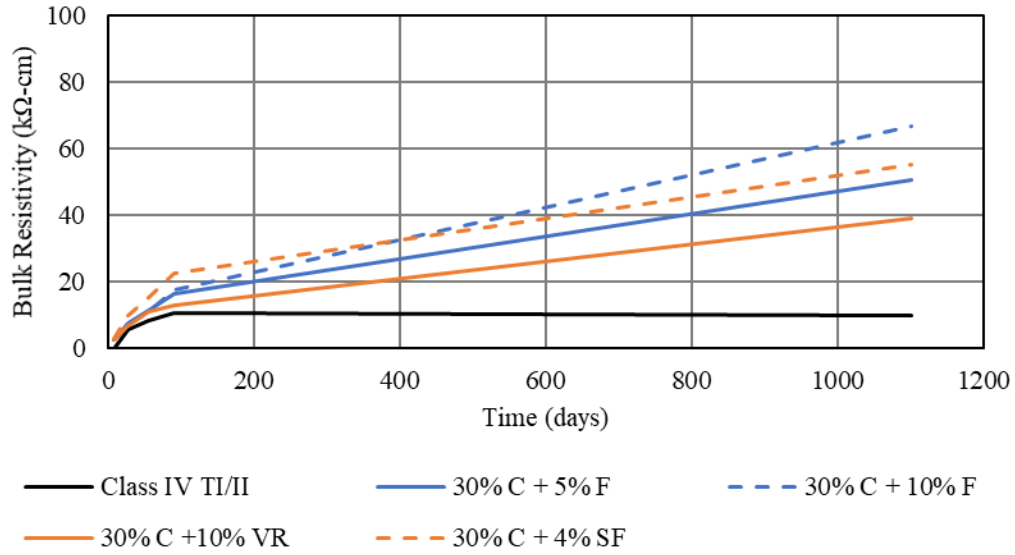


Figure 4-72: Bulk resistivity measurements for Class IV concrete ternary blends with Type I/II cement, Class C fly ash, and Class F fly ash, volcanic rock, or silica fume replacements.

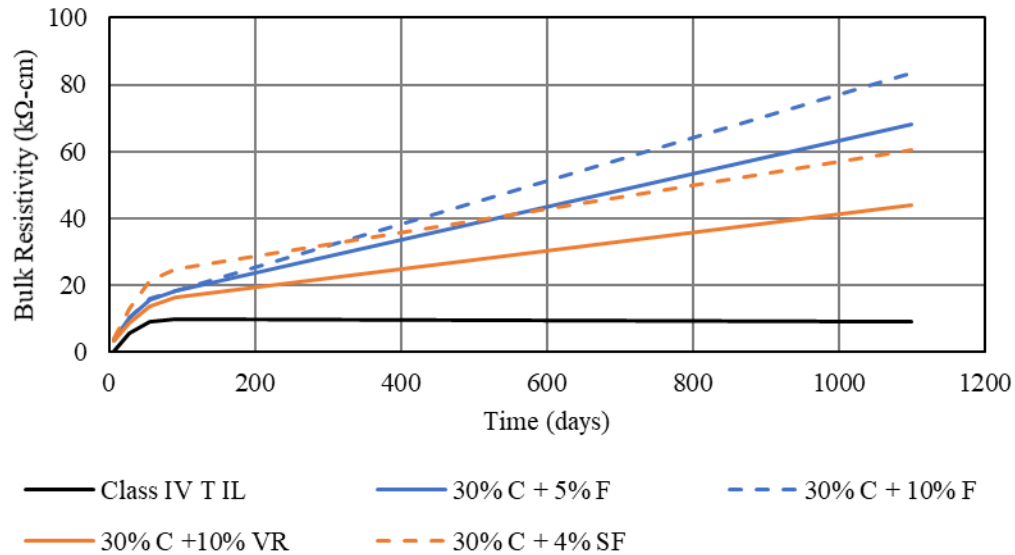


Figure 4-73: Bulk resistivity measurements for Class IV concrete ternary blends with Type II cement, Class C fly ash, and Class F fly ash, volcanic rock, or silica fume replacements.

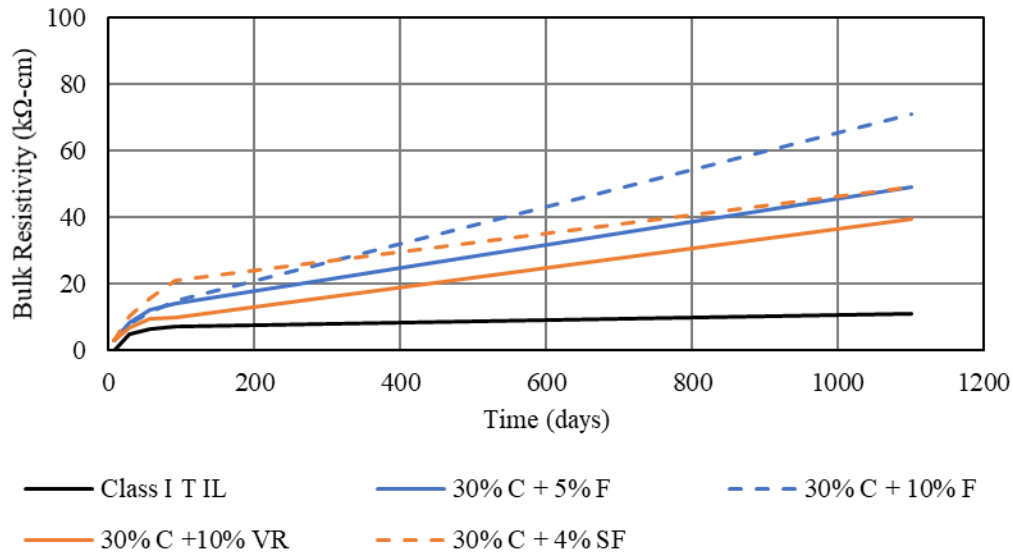


Figure 4-74: Bulk resistivity measurements for Class I concrete ternary blends with Type IL cement, Class C fly ash, and Class F fly ash, volcanic rock, or silica fume replacements.

There were many similarities between Class IV concrete made with Type I/II cement and Class IV concrete made with Type IL cement. Both control mixes were comparable to each other with respect to surface and bulk resistivity. When comparing the results of the cement types, 80% of the mixes had higher surface resistivity when using the Type IL cement compared to the type I/II cement. This is partially attributed to the limestone filler in the Type IL system decreasing the electrical conductivity, this has been reported previous for concretes incorporating GG [213]. Additionally, the Type IL cement is partially composed of calcium carbonate, which promotes the decomposition of ettringite into monosulfate. Instead of monosulfate, calcium mono- or hemi-carboaluminate is formed, which leads to a higher volume of hydration products [133,221]. The increased resistivity was observed during 28-day and 91-day measurements and the difference is more pronounced in 28-day measurements, in part due to the filler having a larger scale effect before the pozzolanic reaction takes place. The bulk resistivity results show a similar behavior to the surface resistivity results.

The trends in Class I concrete using Type IL cement are similar to that of the Class IV concrete using Type IL cement. The control along with most of the other mixtures had lower surface and bulk resistivity than that of the Class IV concrete. This is due to the difference in cementitious or paste content between Class I and Class IV concrete. However, when compared

to the Class IV concrete using Type I/II cement, there are several mixes that have a comparable or higher surface resistivity.

Table 4-35: Surface and bulk resistivity results for Class IV concrete using Type I/II cement.

Mix	Surface Resistivity - Class IV Concrete					Bulk Resistivity - Class IV Concrete				
	7-Day	28-Day	56-Day	91-Day	3-Year	7-Day	28-Day	56-Day	91-Day	3-Year
OPC – Type I/II	-	9.0	9.5	10.6	13.0		5.6	8.5	10.7	9.9
10% - SCBA-A	5.2	7.3	7.9	8.5	11.0	3.0	5.8	6.7	7.8	17.5
20% - SCBA-A	5.2	7.3	8.3	9.2	13.6	2.8	5.4	6.6	8.8	17.5
30% - SCBA-A	4.9	7.7	9.8	11.8	18.7	2.9	5.7	6.9	9.3	15.0
10% - SCBA-B	5.2	7.6	8.5	9.2	15.0	3.0	4.9	5.9	8.6	11.9
20% - SCBA-B	4.7	6.9	8.0	8.7	13.1	3.1	5.0	6.8	7.3	9.9
30% - SCBA-B	4.0	7.3	9.2	10.4	17.0	3.1	5.3	8.1	8.9	13.2
20% - GG	-	10.2	22.8	30.7	54.9		8.2	17.3	19.9	38.4
30% - GG	-	12.7	26.6	34.8	57.1		8.9	19.1	22.9	39.6
40% - GG	4.0	16.6	33.5	42.4	62.4	2.8	11.0	22.1	29.5	41.1
20% - VR	5.3	6.2	6.8	6.8	11.1	3.6	6.3	6.4	9.1	16.0
20% - C Ash	5.2	8.2	12.3	14.9	31.1	3.5	6.7	9.2	12.7	23.9
30% - C Ash	4.6	9.8	16.2	20.1	47.4	3.3	7.2	11.3	15.0	32.0
20% - F Ash	5.5	8.4	14.7	21.3	60.0	3.4	6.3	11.5	17.4	45.5
4% - SF	7.9	13.1	16.4	16.5	16.7	5.0	9.6	13.5	14.3	15.0
Ternary Mixes										
30C + 5SCBA-A	4.9	10.8	16.9	21.4	54.4	4.2	9.6	14.7	21.2	49.5
30C + 10SCBA-A	4.8	10.4	16.0	20.3	53.1	3.3	7.3	11.4	15.7	38.4
30C + 5SCBA-B	4.3	11.4	17.6	21.5	51.4	2.7	7.9	11.9	14.9	40.1
30C + 10SCBA-B	4.1	11.7	18.2	22.4	56.5	2.6	7.9	12.3	14.5	43.7
20C + 5GG	4.4	9.2	16.0	21.9	48.8	2.6	7.1	11.7	16.7	39.6
20C + 10GG	4.0	9.6	17.3	23.4	52.3	2.9	6.6	9.2	9.8	42.2
30C + 5F	4.3	10.7	17.6	23.6	74.3	2.7	7.6	11.3	16.4	50.8
30C + 10F	4.3	10.9	17.8	25.5	98.0	2.7	7.4	11.1	17.6	66.8
30C + 10VR	4.4	10.5	16.5	20.4	56.5	2.7	7.0	11.1	13.2	39.1
30C + 4SF	4.9	14.4	25.2	34.2	81.7	3.1	10.1	15.4	22.8	55.4

Table 4-36: Surface and bulk resistivity results for Class IV concrete using Type II cement.

Mix	Surface Resistivity - Class IV Concrete					Bulk Resistivity - Class IV Concrete				
	7-Day	28-Day	56-Day	91-Day	3-Year	7-Day	28-Day	56-Day	91-Day	3-Year
OPC – Type II	-	8.7	8.9	9.9	12.4	-	5.6	8.9	9.9	8.9
10% - SCBA-A	6.2	7.7	8.5	8.8	13.1	3.8	5.6	7.1	7.9	11.4
20% - SCBA-A	5.5	7.5	8.9	9.8	14.2	3.3	5.6	6.6	8.1	14.0
30% - SCBA-A	5.0	7.6	10.3	12.4	18.4	3.0	5.8	8.4	9.4	16.3
10% - SCBA-B	5.7	7.2	8.1	8.5	12.5	3.6	5.8	6.9	7.9	14.2
20% - SCBA-B	4.6	6.3	7.4	8.2	13.5	3.0	5.1	6.4	7.9	17.8
30% - SCBA-B	4.1	6.3	7.9	9.1	16.7	2.7	4.9	5.4	8.3	14.7
20% - GG	-	15.3	33.2	40.6	61.9	3.6	11.9	22.4	26.7	38.6
30% - GG	5.0	18.0	41.0	45.0	56.5	3.6	11.9	22.4	26.7	38.6
40% - GG	-	25.2	47.9	55.9	85.4	-	14.2	28.2	32.8	56.1
20% - VR	6.2	7.2	7.8	8.0	13.9	3.8	5.8	8.4	8.9	9.9
20% - C Ash	4.7	8.3	11.5	14.7	29.5	3.3	6.9	9.1	9.9	21.6
30% - C Ash	4.5	10.7	16.4	-	46.4	4.1	13.0	21.3	-	34.5
20% - F Ash	5.5	8.4	14.6	20.9	62.5	3.3	6.1	11.4	14.7	41.1
4% - SF	8.6	13.3	14.9	15.3	16.0	5.3	10.2	12.7	12.7	11.4
Ternary Mixes										
30C + 5SCBA-A	5.4	13.5	19.7	24.5	56.3	3.3	8.6	13.5	14.7	40.4
30C + 10SCBA-A	5.3	12.8	18.8	23.9	56.4	3.3	8.6	12.4	15.7	43.4
30C + 5SCBA-B	5.2	13.5	20.4	25.0	57.4	3.3	8.6	12.4	17.3	49.3
30C + 10SCBA-B	5.3	14.4	20.0	24.9	59.6	3.3	9.9	14.5	17.0	50.3
20C + 5GG	5.0	10.6	17.9	24.4	49.1	3.3	7.6	12.2	16.0	37.1
20C + 10GG	4.5	12.7	22.8	32.7	63.7	3.3	7.6	12.2	16.3	43.2
30C + 5F	5.5	14.4	21.1	27.6	81.1	3.6	10.2	15.5	18.3	68.1
30C + 10F	5.2	14.7	22.7	27.8	103	3.3	10.2	16.0	18.3	83.3
30C + 10VR	4.8	12.8	18.7	25.1	57.1	3.0	8.6	13.5	16.3	43.9
30C + 4SF	5.9	20.1	31.8	42.0	87.2	3.8	13.0	21.3	24.6	60.5

Table 4-37: Surface and bulk resistivity results for Class I concrete using Type II cement.

Mix	Surface Resistivity - Class I Concrete					Bulk Resistivity - Class I Concrete				
	7-Day	28-Day	56-Day	91-Day	3-Year	7-Day	28-Day	56-Day	91-Day	3-Year
OPC – Type II	-	7.0	7.7	8.2	12.3	-	5.1	6.4	7.1	11.2
10% - SCBA-A	4.6	5.8	6.4	7.0	10.5	3.2	4.4	4.5	7.0	8.4
20% - SCBA-A	4.9	6.8	7.9	9.1	12.8	3.1	4.6	5.1	7.7	9.1
30% - SCBA-A	4.8	7.2	9.2	11.7	16.8	3.3	4.8	7.1	7.9	12.2
10% - SCBA-B	5.4	6.8	7.1	7.5	12.4	3.4	4.8	7.1	8.4	14.7
20% - SCBA-B	4.4	6.1	7.0	7.9	13.3	2.8	4.5	7.0	8.6	16.5
30% - SCBA-B	3.9	6.2	8.3	9.6	18.9	2.8	4.5	7.0	8.5	22.1
20% - GG	5.5	11.0	22.1	28.5	48.8	3.5	7.7	14.7	20.7	43.9
30% - GG	4.7	16.6	32.3	40.7	60.3	3.1	11.3	21.0	25.9	50.0
40% - GG	4.8	23.5	42.7	53.9	82.0	3.1	15.7	26.8	34.4	63.0
20% - VR	5.3	6.3	6.9	7.2	11.3	3.4	4.8	6.8	8.4	16.3
20% - C Ash	5.2	8.5	11.3	13.6	26.0	3.1	5.6	7.7	10.3	23.6
30% - C Ash	5.1	11.6	16.6	19.9	41.7	3.1	7.2	10.6	12.5	35.3
20% - F Ash	5.1	8.3	14.1	19.9	50.2	3.2	6.9	9.6	13.4	41.7
4% - SF	7.4	12.0	14.2	14.7	16.8	4.9	8.5	11.0	12.6	14.0
Ternary Mixes										
30C + 5SCBA-A	4.8	11.3	17.1	20.5	47.3	3.2	8.3	12.0	14.9	36.8
30C + 10SCBA-A	4.7	9.9	14.6	17.8	46.9	3.2	7.3	10.6	13.0	36.8
30C + 5SCBA-B	4.5	11.0	16.3	19.5	43.8	2.9	7.4	12.3	14.7	33.8
30C + 10SCBA-B	4.4	11.5	16.8	20.1	46.4	2.8	7.6	13.1	16.2	34.0
20C + 5GG	5.3	10.0	16.8	27.0	43.8	3.3	6.7	11.3	16.6	45.5
20C + 10GG	4.8	11.2	19.3	33.6	48.4	3.1	7.5	14.0	18.3	53.3
30C + 5F	4.9	12.1	17.6	23.2	62.1	3.1	8.4	12.2	14.2	49.0
30C + 10F	4.8	11.7	17.3	23.5	87.9	3.0	7.9	11.4	14.9	71.1
30C + 10VR	4.4	9.4	13.3	16.2	41.4	3.0	6.6	9.3	9.8	39.6
30C + 4SF	5.2	16.0	24.5	31.2	61.3	3.1	10.3	15.5	21.2	49.0

5. Summary and Recommendations

Following the extensive investigation into the alternative supplementary cementitious materials combined with two different cement types, there are several key takeaways with respect to each material that are appropriate to summarize. For the Type IL cement, generally speaking, the performance was comparable to Type I/II cement with slight reductions in strength and workability; however, increased durability in alkali-silica reactivity was observed due to formation of carboaluminates and increased particle packing. The largest discrepancy between the two cements was with sulfate resistance; the specific Type IL cement used was considerably more susceptible to sulfate attack than the Type I/II cement. The SCMs, in the proportions used, were generally unable to prevent degradation due to the exposure.

Sugarcane bagasse ash has the potential to improve concrete performance with some drawbacks. The two largest issues being workability concerns (or admixture requirements and potential interactions with air-entraining admixtures), and whether the large amount of unburnt carbon contributes to a high water demand. Incinerating the sugarcane bagasse ash for longer will reduce the carbon but will tend to make a less reactive (and less beneficial) material. The second largest issue is that of qualification: fast and easy electrical methods such as RCPT and surface resistivity will underestimate physical performance of the sugarcane bagasse ash amended concretes. This leaves much slower bulk diffusion testing to evaluate the resistance to penetration (permeability) of deleterious substances, such as chlorides and sulfates, from the surrounding environment.

Ground glass was found to generally provide a benefit in concrete and mortars with respect to workability and durability where potential for alkali-silica reactivity was reduced and resistance to sulfate attack was greatly improved. However, accelerated testing methods for alkali-silica reactivity such as ASTM C1567 will overestimate the ASR mitigation potential of ground glass compared to ASTM C1293 or field-placed specimens, which could lead to premature failure. Ground glass should not be solely relied upon to suppress ASR.

Class C fly ash was shown to provide benefit to concrete in essentially every evaluation with the exception of time of setting. While the Class C fly ash did not sufficiently suppress ASR in field-placed specimens or in ASTM C1293, ternary blended mixes incorporating large volumes of Class C fly ash performed best in both test methods. Similarly, some ternary blends

were able to arrest sulfate expansion for 18 months of exposure. 20% - 30% replacements of Class C fly ash with small replacements of other SCM like Class F fly ash or silica fume did particularly well in most evaluation methods and would provide a means for greatly extending the current supply of Class F fly ash.

The volcanic rock showed very little benefit to use, it did not suppress alkali-silica reactivity (although it was slightly delayed), and it did not appear to mitigate sulfate attack (in Type I/II cementitious systems it performed worse than control). However, it did not appear to be deleterious either, generally it acted more like an inert filler than actively taking part in the hydration of the cement.

While there was no material that provided benefit in every aspect of each evaluation method, GG and SCBA provided benefits in certain tests and would make adequate additions to the FDOT *Standard Specifications for Road and Bridge Construction*. Existing accepted SCM are not expected to be perfect materials for every exposure condition and understanding the shortcomings of each material is essential to proper application, design, and designation into concrete mixes. The research presented herein shows conclusively that these alternative cementitious materials can be used in binary and ternary blended systems to perform comparably or better than some currently accepted concrete mixture designs such as binary mixtures of Class F fly ash. Acceptance of these materials into the Florida DOT specification would ease the burden on the material demand throughout the state and allow for a greater variety of sustainable building materials to be reused to build our roadways.

RECOMMENDATIONS

Based upon the findings from this study, the following recommendations are suggested:

- Make provisions within the FDOT Standard Specification for Road and Bridge Construction Section 929 to make allowances for the use of Class N fly ash that does not meet ASTM C618 with respect to loss on ignition only. This will allow for the use of Sugarcane Bagasse Ash as a pozzolan in concrete.
- Consider making provisions within the FDOT Standard Specification for Road and Bridge Construction Section 929 that allow the use of Class C fly ash in applications that do not require long-term durability testing.
- Make provisions within the FDOT Standard Specification for Road and Bridge Construction Section 929 to allow the use of ground glass. At the time of this report, Section 929-6 was revised to make provisions for the use of ground glass borne from the findings in this research.

- Consider making provisions within the FDOT Standard Specification for Road and Bridge Construction Section 929 that allow the use of ground glass that meets ASTM 1866 [222] in applications that do not require long-term durability testing
- Make provisions within the FDOT Standard Specification for Road and Bridge Construction Section 346 that allow the use of ground glass in ternary systems.

MATERIAL-SPECIFIC RECOMMENDATIONS

Based upon the findings from this study, the following recommendations are suggested if any of the following materials are accepted as a qualified material:

Sugarcane Bagasse Ash

- Material with a chloride content higher than 0.3% should be limited to 10% addition for slightly aggressive environments and should not be used in extremely aggressive environments. For use in non-structural applications, inclusion rate should not be limited.
- Electrical test methods, such as surface resistivity, bulk resistivity, or chloride ion penetrability should not be performed on mixes incorporating sugarcane bagasse ash; conductive carbon within the material will give false measurements.
- Should not be used in a binary mix when resistance to sulfate attack or alkali-silica reactivity is required.

Ground Glass

- The use of accelerated ASR testing methods should not be used with ground glass with an alkali content above 4.0%; this will produce unconservatively low results.
- Inclusions rates for binary mixtures should be limited to no more than 30% to ensure proper strength development.

RECOMMENDATIONS FOR FUTURE STUDY

- The research conducted in this study indicates that alternative pozzolans, including sugarcane bagasse ash, ground glass, and Class C fly ash should be investigated further on a pilot scale for initial validation of use, application, and durability in service in a non-aggressive environment.
- Sugarcane bagasse ash and ground glass should be investigated further to determine threshold values for replacement level, particle size, optimum processing (bagasse ash), and long-term chloride durability (with electrical and physical testing).
- Investigate correction factors for sugarcane bagasse ashes of varying carbon contents to correct electric test methods such as surface resistivity, bulk resistivity, and chloride ion penetrability.

References

- [1] Mindess, S., Young, F., and Darwin, D., 2003, *Concrete*, Prentice-Hall, Inc, Upper Saddle River, NJ.
- [2] AASHTO, 2016, *AASHTO Subcommittee on Materials (SOM) 2016 Fly Ash Task Force Report*, American Association of State Highway and Transportation Officials, Washington, D.C.
- [3] Paris, J. M., Roessler, J. G., Ferraro, C. C., DeFord, H. D., and Townsend, T. G., 2016, “A Review of Waste Products Utilized as Supplements to Portland Cement in Concrete,” *J. Clean. Prod.*, **121**, pp. 1–18.
- [4] Aprianti, E., Shafigh, P., Bahri, S., and Farahani, J. N., 2015, “Supplementary Cementitious Materials Origin from Agricultural Wastes – A Review,” *Constr. Build. Mater.*, **74**, pp. 176–187.
- [5] Aprianti S, E., 2017, “A Huge Number of Artificial Waste Material Can Be Supplementary Cementitious Material (SCM) for Concrete Production – a Review Part II,” *J. Clean. Prod.*, **142**, pp. 4178–4194.
- [6] Fapohunda, C., Akinbile, B., and Shittu, A., 2017, “Structure and Properties of Mortar and Concrete with Rice Husk Ash as Partial Replacement of Ordinary Portland Cement—A Review,” *Int. J. Sustain. Built Environ.*, **6**(2), pp. 675–692.
- [7] Wang, T., Xue, Y., Zhou, M., Lv, Y., Chen, Y., Wu, S., and Hou, H., 2017, “Hydration Kinetics, Freeze-Thaw Resistance, Leaching Behavior of Blended Cement Containing Co-Combustion Ash of Sewage Sludge and Rice Husk,” *Constr. Build. Mater.*, **131**, pp. 361–370.
- [8] Ferraro, C., Paris, J., Townsend, T., and Tia, M., 2016, *Evaluation of Alternative Pozzolanic Materials for Partial Replacement of Portland Cement in Concrete*, BDV31-977–06, Tallahassee, FL.
- [9] Mehta, P. K., and Monteiro, P. J. M., 2014, *Concrete: Microstructure, Properties, and Materials*, McGraw-Hill Education.
- [10] Neville, A., and Brooks, J., 2010, “Concrete Technology. 2nd. Canada,” *Build. Environ.*
- [11] Kosmatka, S., and Wilson, B., 2016, *Design and Control of Concrete Mixtures*, Portland Cement Association, Skokie, IL.
- [12] Gartner, E., Maruyama, I., and Chen, J., 2017, “A New Model for the C-S-H Phase Formed during the Hydration of Portland Cements,” *Cem. Concr. Res.*, **97**, pp. 95–106.
- [13] Scrivener, K. L., Juilland, P., and Monteiro, P. J. M., 2015, “Advances in Understanding Hydration of Portland Cement,” *Cem. Concr. Res.*, **78**, pp. 38–56.

- [14] Bullard, J. W., Jennings, H. M., Livingston, R. A., Nonat, A., Scherer, G. W., Schweitzer, J. S., Scrivener, K. L., and Thomas, J. J., 2011, “Mechanisms of Cement Hydration,” *Cem. Concr. Res.*, **41**(12), pp. 1208–1223.
- [15] Gartner, E., Young, J. F., Damidot, D., and Jawed, I., 2001, “Hydration of Portland Cement,” *Structure and Performance of Cements*, CRC Press.
- [16] Neville, A., 2011, *Properties of Concrete*, Prentice Hall.
- [17] ASTM C150, 2018, “Standard Specification for Portland Cement.”
- [18] Libby, J. R., 2012, *Modern Prestressed Concrete: Design Principles and Construction Methods*, Springer Science & Business Media.
- [19] Ferraro, C., Ishee, C., and Bergin, M., 2010, *Report of Changes to Cement Specifications AASHTO M85 and ASTM C150 Subsequent to Harmonization*, FL/DOT/SMO/10-536). Tallahassee, FL: Florida Department of Transportation.
- [20] ASTM C595, 2018, “Standard Specification for Blended Hydraulic Cements.”
- [21] FDOT, 2020, *Standard Specifications for Road and Bridge Construction*, Florida Department of Transportation, Tallahassee, FL.
- [22] Mehdipour, I., Kumar, A., and Khayat, K. H., 2017, “Rheology, Hydration, and Strength Evolution of Interground Limestone Cement Containing PCE Dispersant and High Volume Supplementary Cementitious Materials,” *Mater. Des.*, **127**, pp. 54–66.
- [23] Arora, A., Vance, K., Sant, G., and Neithalath, N., 2016, “A Methodology to Extract the Component Size Distributions in Interground Composite (Limestone) Cements,” *Constr. Build. Mater.*, **121**, pp. 328–337.
- [24] Misra, A., Ramteke, R., and Bairwa, M. L., 2007, “Study on Strength and Sorptivity Characteristics of Fly Ash Concrete,” *ARPN J. Eng. Appl. Sci.*, **2**(5), pp. 54–59.
- [25] Ramezaniapour, A. M., and Hooton, R. D., 2014, “A Study on Hydration, Compressive Strength, and Porosity of Portland-Limestone Cement Mixes Containing SCMs,” *Cem. Concr. Compos.*, **51**, pp. 1–13.
- [26] Marzouki, A., Lecomte, A., Beddey, A., Diliberto, C., and Ouezdou, M. B., 2013, “The Effects of Grinding on the Properties of Portland-Limestone Cement,” *Constr. Build. Mater.*, **48**, pp. 1145–1155.
- [27] Tsivilis, S., Chaniotakis, E., Kakali, G., and Batis, G., 2002, “An Analysis of the Properties of Portland Limestone Cements and Concrete,” *Cem. Concr. Compos.*, **24**(3–4), pp. 371–378.

- [28] Tsivilis, S., Batis, G., Chaniotakis, E., Grigoriadis, Gr., and Theodossis, D., 2000, “Properties and Behavior of Limestone Cement Concrete and Mortar,” *Cem. Concr. Res.*, **30**(10), pp. 1679–1683.
- [29] Ghrici, M., Kenai, S., and Said-Mansour, M., 2007, “Mechanical Properties and Durability of Mortar and Concrete Containing Natural Pozzolana and Limestone Blended Cements,” *Cem. Concr. Compos.*, **29**(7), pp. 542–549.
- [30] Moon, G. D., Oh, S., Jung, S. H., and Choi, Y. C., 2017, “Effects of the Fineness of Limestone Powder and Cement on the Hydration and Strength Development of PLC Concrete,” *Constr. Build. Mater.*, **135**, pp. 129–136.
- [31] Hawkins, P., Tennis, P. D., and Detwiler, R. J., 1996, *The Use of Limestone in Portland Cement: A State-of-the-Art Review*, Portland Cement Association.
- [32] Thomas, M., 2013, *Supplementary Cementing Materials in Concrete*, CRC press.
- [33] Juenger, M. C. G., and Siddique, R., 2015, “Recent Advances in Understanding the Role of Supplementary Cementitious Materials in Concrete,” *Cem. Concr. Res.*, **78**, pp. 71–80.
- [34] Siddique, R., and Khan, M. I., 2011, *Supplementary Cementing Materials*, Springer.
- [35] Lothenbach, B., Scrivener, K., and Hooton, R. D., 2011, “Supplementary Cementitious Materials,” *Cem. Concr. Res.*, **41**(12), pp. 1244–1256.
- [36] ASTM C618, 2019, *Standard Specification for Coal Fly Ash and Raw or Calcined Natural Pozzolan for Use in Concrete*, ASTM International, West Conshohocken, PA.
- [37] Rashad, A. M., 2015, “An Exploratory Study on High-Volume Fly Ash Concrete Incorporating Silica Fume Subjected to Thermal Loads,” *J. Clean. Prod.*, **87**, pp. 735–744.
- [38] Saha, A. K., 2018, “Effect of Class F Fly Ash on the Durability Properties of Concrete,” *Sustain. Environ. Res.*, **28**(1), pp. 25–31.
- [39] Thomas, M., Fournier, B., Folliard, K. J., and others, 2012, *Selecting Measures to Prevent Deleterious Alkali-Silica Reaction in Concrete: Rationale for the AASHTO PP65 Prescriptive Approach.*, United States. Federal Highway Administration.
- [40] Silica Fume Association, 2005, “Silica Fume User’s Manual.”
- [41] ASTM C1240, 2020, *Standard Specification for Silica Fume Used in Cementitious Mixtures*, ASTM International, West Conshohocken, PA.
- [42] Pandey, A., Soccol, C. R., Nigam, P., and Soccol, V. T., 2000, “Biotechnological Potential of Agro-Industrial Residues. I: Sugarcane Bagasse,” *Bioresour. Technol.*, **74**(1), pp. 69–80.
- [43] Ríos-Parada, V., Jiménez-Quero, V. G., Valdez-Tamez, P. L., and Montes-García, P., 2017, “Characterization and Use of an Untreated Mexican Sugarcane Bagasse Ash as

- Supplementary Material for the Preparation of Ternary Concretes,” *Constr. Build. Mater.*, **157**, pp. 83–95.
- [44] Bahurudeen, A., Marckson, A., Kishore, A., and Santhanam, M., 2014, “Development of Sugarcane Bagasse Ash Based Portland Pozzolana Cement and Evaluation of Compatibility with Superplasticizers,” *Constr. Build. Mater.*, **68**, pp. 465–475.
- [45] Cordeiro, G., Tavares, L., and Toledo Filho, R., 2016, “Improved Pozzolanic Activity of Sugar Cane Bagasse Ash by Selective Grinding and Classification,” *Cem. Concr. Res.*, **89**, pp. 269–275.
- [46] Bahurudeen, A., Kanraj, D., Gokul Dev, V., and Santhanam, M., 2015, “Performance Evaluation of Sugarcane Bagasse Ash Blended Cement in Concrete,” *Cem. Concr. Compos.*, **59**, pp. 77–88.
- [47] Rossignolo, J. A., Rodrigues, M. S., Frias, M., Santos, S. F., and Junior, H. S., 2017, “Improved Interfacial Transition Zone between Aggregate-Cementitious Matrix by Addition Sugarcane Industrial Ash,” *Cem. Concr. Compos.*, **80**, pp. 157–167.
- [48] Patel, J. A., and Raijiwala, D., 2015, “Use of Sugar Cane Bagasse Ash as Partial Replacement of Cement in Concrete - An Experimental Study,” *Glob. J. Res. Eng.*
- [49] Srinivasan, R., and Sathiya, K., 2010, “Experimental Study on Bagasse Ash in Concrete,” *Int. J. Serv. Learn. Eng. Humanit. Eng. Soc. Entrep.*, **5**(2), pp. 60–66.
- [50] Gar, P. S., Suresh, N., and Bindiganavile, V., 2017, “Sugar Cane Bagasse Ash as a Pozzolanic Admixture in Concrete for Resistance to Sustained Elevated Temperatures,” *Constr. Build. Mater.*, **153**, pp. 929–936.
- [51] Kazmi, S. M. S., Munir, M. J., Patnaikuni, I., and Wu, Y.-F., 2017, “Corrigendum to ‘Pozzolanic Reaction of Sugarcane Bagasse Ash and Its Role in Controlling Alkali Silica Reaction’ [*Constr. Build. Mater.* 148 (2017) 231–240],” *Constr. Build. Mater.*, **153**, p. 1010.
- [52] Kazmi, S. M. S., Munir, M. J., Patnaikuni, I., and Wu, Y.-F., 2017, “Pozzolanic Reaction of Sugarcane Bagasse Ash and Its Role in Controlling Alkali Silica Reaction,” *Constr. Build. Mater.*, **148**, pp. 231–240.
- [53] Nassar, R. U. D., and Soroushian, P., 2012, “Strength and Durability of Recycled Aggregate Concrete Containing Milled Glass as Partial Replacement for Cement,” *Constr. Build. Mater.*, **29**, pp. 368–377.
- [54] Idir, R., Cyr, M., and Tagnit-Hamou, A., 2011, “Pozzolanic Properties of Fine and Coarse Color-Mixed Glass Cullet,” *Cem. Concr. Compos.*, **33**(1), pp. 19–29.
- [55] Du, H., and Tan, K. H., 2014, “Effect of Particle Size on Alkali–Silica Reaction in Recycled Glass Mortars,” *Constr. Build. Mater.*, **66**, pp. 275–285.

- [56] Idir, R., Cyr, M., and Tagnit-Hamou, A., 2010, "Use of Fine Glass as ASR Inhibitor in Glass Aggregate Mortars," *Constr. Build. Mater.*, **24**(7), pp. 1309–1312.
- [57] Du, H., and Tan, K. H., 2017, "Properties of High Volume Glass Powder Concrete," *Cem. Concr. Compos.*, **75**, pp. 22–29.
- [58] Carsana, M., Frassoni, M., and Bertolini, L., 2014, "Comparison of Ground Waste Glass with Other Supplementary Cementitious Materials," *Cem. Concr. Compos.*, **45**, pp. 39–45.
- [59] Lee, H., Hanif, A., Usman, M., Sim, J., and Oh, H., 2018, "Performance Evaluation of Concrete Incorporating Glass Powder and Glass Sludge Wastes as Supplementary Cementing Material," *J. Clean. Prod.*, **170**, pp. 683–693.
- [60] Schwarz, N., Cam, H., and Neithalath, N., 2008, "Influence of a Fine Glass Powder on the Durability Characteristics of Concrete and Its Comparison to Fly Ash," *Cem. Concr. Compos.*, **30**(6), pp. 486–496.
- [61] Kamali, M., and Ghahremaninezhad, A., 2016, "An Investigation into the Hydration and Microstructure of Cement Pastes Modified with Glass Powders," *Constr. Build. Mater.*, **112**, pp. 915–924.
- [62] Matos, A. M., and Sousa-Coutinho, J., 2012, "Durability of Mortar Using Waste Glass Powder as Cement Replacement," *Constr. Build. Mater.*, **36**, pp. 205–215.
- [63] Shayan, A., and Xu, A., 2004, "Value-Added Utilisation of Waste Glass in Concrete," *Cem. Concr. Res.*, **34**(1), pp. 81–89.
- [64] Mechti, W., Mnif, T., Chaabouni, M., and Rouis, J., 2014, "Formulation of Blended Cement by the Combination of Two Pozzolans: Calcined Clay and Finely Ground Sand," *Constr. Build. Mater.*, **50**, pp. 609–616.
- [65] Chindapasirt, P., and Rukzon, S., 2015, "Strength and Chloride Resistance of the Blended Portland Cement Mortar Containing Rice Husk Ash and Ground River Sand," *Mater. Struct.*, **48**(11), pp. 3771–3777.
- [66] Alhozaimy, A., Jaafar, M., Al-Negheimish, A., Abdullah, A., Taufiq-Yap, Y., Noorzaie, J., and Alawad, O., 2012, "Properties of High Strength Concrete Using White and Dune Sands under Normal and Autoclaved Curing," *Constr. Build. Mater.*, **27**(1), pp. 218–222.
- [67] Sata, V., Tangpagasit, J., Jaturapitakkul, C., and Chindapasirt, P., 2012, "Effect of W/B Ratios on Pozzolanic Reaction of Biomass Ashes in Portland Cement Matrix," *Cem. Concr. Compos.*, **34**(1), pp. 94–100.
- [68] Ponce, J. M., and Batic, O. R., 2006, "Different Manifestations of the Alkali-Silica Reaction in Concrete According to the Reaction Kinetics of the Reactive Aggregate," *Cem. Concr. Res.*, **36**(6), pp. 1148–1156.

- [69] Yu, Z., Chen, Y., Peng, L., and Wang, W., 2015, “Accelerated Simulation of Chloride Ingress into Concrete under Drying-Wetting Alternation Condition Chloride Environment,” *Constr. Build. Mater.*, **93**, pp. 205–213.
- [70] Erdem, T., Meral, C., Tokyay, M., and Erdogan, T., 2007, “Effect of Ground Perlite Incorporation on the Performance of Blended Cements,” *Proc. Int. Conf Sustain. Constr. Mater. Technol.*, Taylor and Francis, London, ISBN, pp. 978–0.
- [71] ACI Committee 201, 2016, *Guide to Durable Concrete*, American Concrete Institute, Farmington Hills, Michigan.
- [72] Thomas, M. D. A., Fournier, B., and Folliard, K. J., 2013, “Alkali-Aggregate Reactivity (AAR) Facts Book,” (FHWA-HIF-13-019).
- [73] Tora Bueno, E., Paris, J. M., Clavier, K. A., Spreadbury, C., Ferraro, C. C., and Townsend, T. G., 2020, “A Review of Ground Waste Glass as a Supplementary Cementitious Material: A Focus on Alkali-Silica Reaction,” *J. Clean. Prod.*, p. 120180.
- [74] Swamy, R. N., 1991, *The Alkali-Silica Reaction in Concrete*, CRC Press.
- [75] Taylor, H., 2004, *Cement Chemistry*, Thomas Telford Publishing, London.
- [76] ASTM C1295, 2019, *Standard Guide for Petrographic Examination of Aggregates for Concrete*, ASTM International, West Conshohocken, PA.
- [77] ASTM C1293, 2018, *Standard Test Method for Determination of Length Change of Concrete Due to Alkali-Silica Reaction*, ASTM International, West Conshohocken, PA.
- [78] ASTM C1778, 2020, *Standard Guide for Reducing the Risk of Deleterious Alkali-Aggregate Reaction in Concrete*, ASTM International.
- [79] ASTM C227, 2010, “Standard Test Method for Potential Alkali Reactivity of Cement-Aggregate Combinations (Mortar-Bar Method).”
- [80] ASTM C441, 2017, *Standard Test Method for Effectiveness of Pozzolans or Ground Blast-Furnace Slag in Preventing Excessive Expansion of Concrete Due to the Alkali-Silica Reaction*, ASTM International.
- [81] ASTM C1260, 2014, *Standard Test Method for Potential Alkali Reactivity of Aggregates (Mortar-Bar Method)*, ASTM International, 100 Barr Harbor Drive, PO Box C700, West Conshohocken, PA, 19428-2959.
- [82] ASTM C1567, 2013, “Standard Test Method for Determining the Potential Alkali-Silica Reactivity of Combinations of Cementitious Materials and Aggregate (Accelerated Mortar-Bar Method).”

- [83] Lindgård, J., Andiç-Çakır, Ö., Fernandes, I., Rønning, T. F., and Thomas, M. D. A., 2012, “Alkali–Silica Reactions (ASR): Literature Review on Parameters Influencing Laboratory Performance Testing,” *Cem. Concr. Res.*, **42**(2), pp. 223–243.
- [84] Dumitru, I., Song, T., Caprar, V., Brooks, P., and Moss, J., 2010, “Incorporation of Recycled Glass for Durable Concrete,” *2nd International Conference on Sustainable Construction Materials and Technologies*, pp. 28–30.
- [85] Schumacher Kelsea A. and Ideker Jason H., 2015, “New Considerations in Predicting Mitigation of Alkali-Silica Reaction Based on Fly Ash Chemistry,” *J. Mater. Civ. Eng.*, **27**(4), p. 04014144.
- [86] Skalny, J., 2002, “Internal Sulfate Attack - Points of Agreement and Disagreement,” *Proceedings of the International RILEM TC 186-ISA Workshop*, RILEM Publications, Villars, Switzerland, pp. 265–274.
- [87] Haynes, H., and Bassuoni, M., 2011, “Physical Salt Attack on Concrete,” *Concr Int*, **33**, pp. 38–42.
- [88] Menéndez, E., Matschei, T., and Glasser, F. P., 2013, “Sulfate Attack of Concrete,” *Performance of Cement-Based Materials in Aggressive Aqueous Environments*, Springer, pp. 7–74.
- [89] ASTM C1202, 2019, *Standard Test Method for Electrical Indication of Concretes Ability to Resist Chloride Ion Penetration*, ASTM International, West Conshohocken, PA.
- [90] Tosun-Felekoğlu, K., 2012, “The Effect of C3A Content on Sulfate Durability of Portland Limestone Cement Mortars,” *Constr. Build. Mater.*, **36**, pp. 437–447.
- [91] Hossack, A. M., and Thomas, M. D., 2015, “Evaluation of the Effect of Tricalcium Aluminate Content on the Severity of Sulfate Attack in Portland Cement and Portland Limestone Cement Mortars,” *Cem. Concr. Compos.*, **56**, pp. 115–120.
- [92] Hooton, R., Ramezani pour, A., and Schutz, U., 2010, “Decreasing the Clinker Component in Cementing Materials: Performance of Portland-Limestone Cements in Concrete in Combination with Supplementary Cementing Materials,” *2010 Concrete Sustainability Conference, NRMCA*, Arizona State University Tempe, AZ, p. 15.
- [93] Skaropoulou, A., Tsvivilis, S., Kakali, G., Sharp, J., and Swamy, R., 2009, “Thaumasite Form of Sulfate Attack in Limestone Cement Mortars: A Study on Long Term Efficiency of Mineral Admixtures,” *Constr. Build. Mater.*, **23**(6), pp. 2338–2345.
- [94] Ramezani pour, A. M., and Hooton, R. D., 2013, “Sulfate Resistance of Portland-Limestone Cements in Combination with Supplementary Cementitious Materials,” *Mater. Struct.*, **46**(7), pp. 1061–1073.

- [95] Mirvalad, S., and Nokken, M., 2015, “Minimum SCM Requirements in Mixtures Containing Limestone Cement to Control Thaumasite Sulfate Attack,” *Constr. Build. Mater.*, **84**, pp. 19–29.
- [96] Hossack, A. M., and Thomas, M. D., 2015, “The Effect of Temperature on the Rate of Sulfate Attack of Portland Cement Blended Mortars in Na₂SO₄ Solution,” *Cem. Concr. Res.*, **73**, pp. 136–142.
- [97] Ramezani-pour, A. M., and Hooton, R. D., 2013, “Thaumasite Sulfate Attack in Portland and Portland-Limestone Cement Mortars Exposed to Sulfate Solution,” *Constr. Build. Mater.*, **40**, pp. 162–173.
- [98] Joshaghani, A., and Moeini, M. A., 2017, “Evaluating the Effects of Sugar Cane Bagasse Ash (SCBA) and Nanosilica on the Mechanical and Durability Properties of Mortar,” *Constr. Build. Mater.*, **152**, pp. 818–831.
- [99] Li, Y., Hanlon, E., O’Connor, G., Chen, J., and Silveira, M., 2010, “Land Application of Compost and Other Wastes (By-Products) in Florida: Regulations, Characteristics, Benefits, and Concerns,” *HortTechnology*, **20**(1), pp. 41–51.
- [100] FDEP, 2017, *2017 Total Tons of MSW Collected and Recycled By Descending Population*.
- [101] Tucker, E. L., Ferraro, C. C., Laux, S. J., and Townsend, T. G., 2018, “Economic and Life Cycle Assessment of Recycling Municipal Glass as a Pozzolan in Portland Cement Concrete Production,” *Resour. Conserv. Recycl.*, **129**(October 2017), pp. 240–247.
- [102] Bonnaire, J., 2018, “Supply of Material to Florida.”
- [103] Xu, G., and Shi, X., 2018, “Characteristics and Applications of Fly Ash as a Sustainable Construction Material: A State-of-the-Art Review,” *Resour. Conserv. Recycl.*, **136**(August 2017), pp. 95–109.
- [104] Saha, A. K., Khan, M. N. N., Sarker, P. K., Shaikh, F. A., and Pramanik, A., 2018, “The ASR Mechanism of Reactive Aggregates in Concrete and Its Mitigation by Fly Ash: A Critical Review,” *Constr. Build. Mater.*, **171**, pp. 743–758.
- [105] Shehata, M. H., and Thomas, M. D. A., 2002, “Use of Ternary Blends Containing Silica Fume and Fly Ash to Suppress Expansion Due to Alkali-Silica Reaction in Concrete,” *Cem. Concr. Res.*, **32**(3), pp. 341–349.
- [106] Mazarei, V., Trejo, D., Ideker, J. H., and Isgor, O. B., 2017, “Synergistic Effects of ASR and Fly Ash on the Corrosion Characteristics of RC Systems,” *Constr. Build. Mater.*, **153**, pp. 647–655.
- [107] Adams, T. H., 2017, *Coal Ash Recycling Reaches Record 56 Percent Amid Shifting Production and Use Patterns*.

- [108] American Coal Ash Association, 2019, “ACAA 2019 Production and Use Charts” [Online]. Available: <https://www.acaa-usa.org/Portals/9/Files/PDFs/2018-Charts.pdf>. [Accessed: 19-Jan-2021].
- [109] Portland Cement Association, 2018, *Florida Cement Industry*.
- [110] DoD, 2002, “Memorandum Concerning Department of Defense Unified Facilities Criteria.”
- [111] ALDOT, A. D. of T., 2018, *Standard Specifications for Highway Construction*, Alabama Department of Transportation.
- [112] AHTD, 2014, *Standard Specifications for Highway Construction*, Arkansas Highway and Transportation Department.
- [113] Caltrans, 2015, *Standard Specifications*, California State Transportation Agency.
- [114] GDOT, 2013, *Standard Specifications Construction of Transportation Systems*, Georgia Department of Transportation.
- [115] IDOT, 2016, *Standard Specifications for Road and Bridge Construction*, Illinois Department of Transportation.
- [116] LaDOTD, 2016, *Standard Specifications for Roads and Bridges*, Louisiana Department of Transportation and Development.
- [117] MDOT, 2017, *Standard Specifications for Road and Bridge Construction*, Mississippi Department of Transportation.
- [118] NCDOT, 2018, *Standard Specifications for Roads and Structures*, North Carolina Department of Transportation.
- [119] ODOT, 2009, *Standard Specifications*, Oklahoma Department of Transportation.
- [120] SCDOT, 2007, *Standard Specifications for Highway Construction*, South Carolina Department of Transportation.
- [121] TDOT, 2015, *Standard Specifications for Road and Bridge Construction*, Tennessee Department of Transportation.
- [122] TxDOT, 2014, *Standard Specifications for Construction and Maintenance of Highways, Streets, and Bridges*, Texas Department of Transportation.
- [123] VDOT, 2016, *Road and Bridge Specifications*, Virginia Department of Transportation.
- [124] DoD, 2017, “Unified Facilities Guide Specifications.”
- [125] ASTM C1157, 2017, *Standard Performance Specification for Hydraulic Cement*, ASTM International, West Conshohocken, PA.

- [126] Bentz, D., Ardani, A., Barrett, T., Jones, S., Lootens, D., Peltz, M., Sato, T., Stutzman, P., Tanesi, J., and Weiss, W., 2014, “Multi-Scale Investigation of the Performance of Limestone in Concrete,” *Constr. Build. Mater.*, **75**.
- [127] Tanesi, J., and Ardani, A. A., 2013, “Isothermal Calorimetry as a Tool to Evaluate Early-Age Performance of Fly Ash Mixtures,” *Transp. Res. Rec. J. Transp. Res. Board*, **2342**(1), pp. 42–53.
- [128] Chithiraputhiran, S., and Neithalath, N., 2013, “Isothermal Reaction Kinetics and Temperature Dependence of Alkali Activation of Slag, Fly Ash and Their Blends,” *Constr. Build. Mater.*, **45**, pp. 233–242.
- [129] Bentz, D., Ferraris, C., De la Varga, I., Peltz, M., and Winpigler, J., 2010, “Mixture Proportioning Options for Improving High Volume Fly Ash Concretes,” *Int. J. Pavement Res. Technol.*, **33**, pp. 234–240.
- [130] Sandberg, P., 2004, “Optimization of Cement Sulfate Part II: Cement with Admixture,” *Appl. Notes Appl. Notes Thermom.*
- [131] Suraneni, P., and Weiss, J., 2017, “Examining the Pozzolanicity of Supplementary Cementitious Materials Using Isothermal Calorimetry and Thermogravimetric Analysis,” *Cem. Concr. Compos.*, **83**, pp. 273–278.
- [132] Romano, R. C. O., Cincotto, M. A., Pileggi, R. G., Romano, R. C. O., Cincotto, M. A., and Pileggi, R. G., 2018, “Hardening Phenomenon of Portland Cement Suspensions Monitored by Vicat Test, Isothermal Calorimetry and Oscillatory Rheometry,” *Rev. IBRACON Estrut. E Mater.*, **11**(5), pp. 949–959.
- [133] Paris, J. M., and Ferraro, C. C., 2018, “Evaluation of Particle Effects in Portland Cement Systems,” *J. Mater. Civ. Eng.*, **30**(9), p. 04018205.
- [134] Avet, F., Snellings, R., Alujas Diaz, A., Ben Haha, M., and Scrivener, K., 2016, “Development of a New Rapid, Relevant and Reliable (R3) Test Method to Evaluate the Pozzolanic Reactivity of Calcined Kaolinitic Clays,” *Cem. Concr. Res.*, **85**, pp. 1–11.
- [135] Assaad, J. J., Asseily, S. E., and Harb, J., 2010, “Use of Cement Grinding Aids to Optimise Clinker Factor,” *Adv. Cem. Res.*, **22**(1), pp. 29–36.
- [136] Assaad, J. J., and Issa, C. A., 2014, “Effect of Clinker Grinding Aids on Flow of Cement-Based Materials,” *Cem. Concr. Res.*, **63**, pp. 1–11.
- [137] Fuerstenau, D. W., and Sullivan, D. A., 1962, “Size Distributions and Energy Consumption in Wet and Dry Grinding,” p. 6.
- [138] Tabor, D., 1954, “Mohs’s Hardness Scale - A Physical Interpretation,” *Proc. Phys. Soc. Sect. B*, **67**(3), pp. 249–257.

- [139] FM 5-516, 2018, *Florida Method of Test Determining Low-Levels of Chloride in Concrete and Raw Materials*, Florida Department of Transportation, Florida.
- [140] Val, D. V., and Stewart, M. G., 2003, “Life-Cycle Cost Analysis of Reinforced Concrete Structures in Marine Environments,” *Struct. Saf.*, **25**(4), pp. 343–362.
- [141] Kendall, A., Keoleian, G. A., and Helfand, G. E., 2008, “Integrated Life-Cycle Assessment and Life-Cycle Cost Analysis Model for Concrete Bridge Deck Applications,” *J. Infrastruct. Syst.*, **14**(3), pp. 214–222.
- [142] ASTM C1437, 2015, *Standard Test Method for Flow of Hydraulic Cement Mortar*, ASTM International, West Conshohocken, PA.
- [143] ASTM C403, 2017, *Standard Test Method for Time of Setting of Concrete Mixtures by Penetration Resistance*, ASTM International, West Conshohocken, PA.
- [144] ASTM C109, 2020, *Standard Test Method for Compressive Strength of Hydraulic Cement Mortars (Using 2-in. or [50-Mm] Cube Specimens)*, ASTM International, 100 Barr Harbor Drive, PO Box C700, West Conshohocken, PA, 19428-2959.
- [145] ASTM C157/157M, 2008, *Standard Test Method for Length Change of Hardened Hydraulic-Cement Mortar and Concrete*, ASTM International, West Conshohocken, PA.
- [146] ASTM C1012, 2018, *Standard Test Method for Length Change of Hydraulic-Cement Mortars Exposed to a Sulfate Solution*, ASTM International.
- [147] Ataie, F. F., and Riding, K. A., 2013, “Thermochemical Pretreatments for Agricultural Residue Ash Production for Concrete,” *J. Mater. Civ. Eng.*, **25**(11), pp. 1703–1711.
- [148] Aliabdo, A. A., Abd Elmoaty, A. E. M., and Aboshama, A. Y., 2016, “Utilization of Waste Glass Powder in the Production of Cement and Concrete,” *Constr. Build. Mater.*, **124**, pp. 866–877.
- [149] Rashidian-Dezfouli, H., Afshinnia, K., and Rangaraju, P. R., 2018, “Efficiency of Ground Glass Fiber as a Cementitious Material, in Mitigation of Alkali-Silica Reaction of Glass Aggregates in Mortars and Concrete,” *J. Build. Eng.*, **15**, pp. 171–180.
- [150] İnan Sezer, G., 2012, “Compressive Strength and Sulfate Resistance of Limestone and/or Silica Fume Mortars,” *Constr. Build. Mater.*, **26**(1), pp. 613–618.
- [151] Bentz, D. P., Ferraris, C. F., Jones, S. Z., Lootens, D., and Zunino, F., 2017, “Limestone and Silica Powder Replacements for Cement: Early-Age Performance,” *Cem. Concr. Compos.*, **78**, pp. 43–56.
- [152] Huang, L., and Yan, P., 2019, “Effect of Alkali Content in Cement on Its Hydration Kinetics and Mechanical Properties,” *Constr. Build. Mater.*, **228**, p. 116833.

- [153] Holanda, F. do C., Schmidt, H., and Quarcioni, V. A., 2017, “Influence of Phosphorus from Phosphogypsum on the Initial Hydration of Portland Cement in the Presence of Superplasticizers,” *Cem. Concr. Compos.*, **83**, pp. 384–393.
- [154] ASTM C192, 2019, *Practice for Making and Curing Concrete Test Specimens in the Laboratory*, ASTM International, West Conshohocken, PA.
- [155] Bonavetti, V. L., Rahhal, V. F., and Irassar, E. F., 2001, “Studies on the Carboaluminate Formation in Limestone Filler-Blended Cements,” *Cem. Concr. Res.*, **31**(6), pp. 853–859.
- [156] Perotti, R. R., 2016, “Evaluating Free Shrinkage of Concrete Containing Waste Glass as a Partial Cement Replacement,” M.S., Saint Louis University.
- [157] Rajabipour, F., Giannini, E., Dunant, C., Ideker, J. H., and Thomas, M. D. A., 2015, “Alkali-Silica Reaction: Current Understanding of the Reaction Mechanisms and the Knowledge Gaps,” *Cem. Concr. Res.*, **76**, pp. 130–146.
- [158] Taha, B., and Nounu, G., 2008, “Using Lithium Nitrate and Pozzolanic Glass Powder in Concrete as ASR Suppressors,” *Cem. Concr. Compos.*, **30**(6), pp. 497–505.
- [159] Moser, R. D., Jayapalan, A. R., Garas, V. Y., and Kurtis, K. E., 2010, “Assessment of Binary and Ternary Blends of Metakaolin and Class C Fly Ash for Alkali-Silica Reaction Mitigation in Concrete,” *Cem. Concr. Res.*, **40**(12), pp. 1664–1672.
- [160] Hooton, D., Nokken, M., and D. A. Thomas, M., 2007, “Portland-Limestone Cement: State-of-the-Art Report and Gap Analysis For CSA A 3000,” SN3053.
- [161] Panesar, D. K., 2019, “Supplementary Cementing Materials,” *Developments in the Formulation and Reinforcement of Concrete*, S. Mindess, ed.
- [162] D. Breyse, 2010, “Deterioration Processes in Reinforced Concrete: An Overview,” *Non-Destructive Evaluation of Reinforced Concrete Structures: Deterioration Processes and Standard Test Methods*.
- [163] Bonakdar, A., and Mobasher, B., 2010, “Multi-Parameter Study of External Sulfate Attack in Blended Cement Materials,” *Constr. Build. Mater.*, **24**(1), pp. 61–70.
- [164] Orem, W., Gilmour, C., Axelrad, D., Krabbenhoft, D., Scheidt, D., Kalla, P., McCormick, P., Gabriel, M., and Aiken, G., 2011, “Sulfur in the South Florida Ecosystem: Distribution, Sources, Biogeochemistry, Impacts, and Management for Restoration,” *Crit. Rev. Environ. Sci. Technol.*, **41**(sup1), pp. 249–288.
- [165] Diamond, S., 2003, “Thaumasite in Orange County, Southern California: An Inquiry into the Effect of Low Temperature,” *Cem. Concr. Compos.*, **25**(8), pp. 1161–1164.
- [166] Colleparidi, M., 1999, “Thaumasite Formation and Deterioration in Historic Buildings,” *Cem. Concr. Compos.*, **21**(2), pp. 147–154.

- [167] Al-Dulaijan, S. U., Maslehuddin, M., Al-Zahrani, M. M., Sharif, A. M., Shameem, M., and Ibrahim, M., 2003, “Sulfate Resistance of Plain and Blended Cements Exposed to Varying Concentrations of Sodium Sulfate,” *Cem. Concr. Compos.*, **25**(4), pp. 429–437.
- [168] Tang, Z., Li, W., Ke, G., Zhou, J. L., and Tam, V. W. Y., 2019, “Sulfate Attack Resistance of Sustainable Concrete Incorporating Various Industrial Solid Wastes,” *J. Clean. Prod.*, **218**, pp. 810–822.
- [169] Özkan, Ö., and Yüksel, İ., 2008, “Studies on Mortars Containing Waste Bottle Glass and Industrial By-Products,” *Constr. Build. Mater.*, **22**(6), pp. 1288–1298.
- [170] Barrett, T. J., Sun, H., Nantung, T., and Weiss, W. J., 2014, “Performance of Portland Limestone Cements,” *Transp. Res. Rec. J. Transp. Res. Board*, **2441**(1), pp. 112–120.
- [171] Demirhan, S., Turk, K., and Ulugerger, K., 2019, “Fresh and Hardened Properties of Self Consolidating Portland Limestone Cement Mortars: Effect of High Volume Limestone Powder Replaced by Cement,” *Constr. Build. Mater.*, **196**, pp. 115–125.
- [172] Dhir, R. K., Limbachiya, M. C., McCarthy, M. J., and Chaipanich, A., 2007, “Evaluation of Portland Limestone Cements for Use in Concrete Construction,” *Mater. Struct.*, **40**(5), pp. 459–473.
- [173] Lothenbach, B., Le Saout, G., Gallucci, E., and Scrivener, K., 2008, “Influence of Limestone on the Hydration of Portland Cements,” *Cem. Concr. Res.*, **38**(6), pp. 848–860.
- [174] Proske, T., Rezvani, M., Palm, S., Müller, C., and Graubner, C.-A., 2018, “Concretes Made of Efficient Multi-Composite Cements with Slag and Limestone,” *Cem. Concr. Compos.*, **89**, pp. 107–119.
- [175] Proske, T., Hainer, S., Rezvani, M., and Graubner, C.-A., 2013, “Eco-Friendly Concretes with Reduced Water and Cement Contents — Mix Design Principles and Laboratory Tests,” *Cem. Concr. Res.*, **51**, pp. 38–46.
- [176] Ramezani pour, A., and Hooton, R. D., 2014, “Cement & Concrete Composites A Study on Hydration , Compressive Strength , and Porosity of Portland- Limestone Cement Mixes Containing SCMs,” *Cem. Concr. Compos.*, **51**, pp. 1–13.
- [177] Thongsanitgarn, P., Wongkeo, W., Sinthupinyo, S., and Chaipanich, A., 2011, “Effect of Limestone Powders on Compressive Strength and Setting Time of Portland-Limestone Cement Pastes,” *Adv. Mater. Res.*, **343–344**.
- [178] Bentz, D. P., Jones, S. Z., and Lootens, D., 2016, *Minimizing Paste Content in Concrete Using Limestone Powders - Demonstration Mixtures*, NIST TN 1906, National Institute of Standards and Technology.
- [179] Soroka, I., and Setter, N., 1977, “The Effect of Fillers on Strength of Cement Mortars,” *Cem. Concr. Res.*, **7**(4), pp. 449–456.

- [180] Soroka, I., and Stern, N., 1976, “Calcareous Fillers and the Compressive Strength of Portland Cement,” *Cem. Concr. Res.*, **6**(3), p. 10.
- [181] Alexander, K. M., 1972, “The Relationship between Strength and the Composition and Fineness of Cement,” *Cem. Concr. Res.*, **2**(6), pp. 663–680.
- [182] Al-Rawi, R., 1974, “The Effects of Composition and Fineness of Cement in Accelerated Testing of Concrete,” *J. Test. Eval.*, **2**(2), pp. 102–106.
- [183] ASTM C1064/1064M, 2013, *Standard Test Method for Temperature of Freshly Mixed Hydraulic-Cement Concrete*, ASTM International, West Conshohocken, PA.
- [184] Riding, K. A., Poole, J. L., Schindler, A. K., Juenger, M. C. G., and Folliard, K. J., 2008, “Simplified Concrete Resistivity and Rapid Chloride Permeability Test Method,” *Mater. J.*, **105**(4), pp. 390–394.
- [185] Saito, M., Ohta, M., and Ishimori, H., 1994, “Chloride Permeability of Concrete Subjected to Freeze-Thaw Damage,” *Cem. Concr. Compos.*, **16**(4), pp. 233–239.
- [186] ASTM, 2006, *Significance of Tests and Properties of Concrete and Concrete-Making Materials*, ASTM International.
- [187] Ahmad, S., 2003, “Reinforcement Corrosion in Concrete Structures, Its Monitoring and Service Life Prediction—a Review,” *Cem. Concr. Compos.*, **25**(4), pp. 459–471.
- [188] Boğa, A. R., and Topçu, İ. B., 2012, “Influence of Fly Ash on Corrosion Resistance and Chloride Ion Permeability of Concrete,” *Constr. Build. Mater.*, **31**, pp. 258–264.
- [189] Sujjavanich, S., Sida, V., and Suwanvitaya, P., 2005, “Chloride Permeability and Corrosion Risk of High-Volume Fly Ash Concrete with Mid-Range Water Reducer,” *ACI Mater. J. Farmington Hills*, **102**(3), p. 177.
- [190] Kostrzanowska-Siedlarz, A., and Gołaszewski, J., 2015, “Rheological Properties and the Air Content in Fresh Concrete for Self Compacting High Performance Concrete,” *Constr. Build. Mater.*, **94**, pp. 555–564.
- [191] Safiuddin, M., Abdel-Sayed, G., and Hearn, N., 2018, “Effects of Pitch-Based Short Carbon Fibers on the Workability, Unit Weight, and Air Content of Mortar Composite,” *Fibers*, **6**(3), p. 63.
- [192] ASTM C39, 2018, *Standard Test Method for Compressive Strength of Cylindrical Concrete Specimens*, ASTM International, West Conshohocken, PA.
- [193] C511 Committee, 2019, *Standard Specification for Mixing Rooms, Moist Cabinets, Moist Rooms, and Water Storage Tanks Used in the Testing of Hydraulic Cements and Concretes*, ASTM C511, ASTM International, West Conshohocken, PA.

- [194] Crawford, G., Gudimettla, J., and Tanesi, J., 2010, “Interlaboratory Study on Measuring Coefficient of Thermal Expansion of Concrete,” *Transp. Res. Rec. J. Transp. Res. Board*, **2164**, pp. 58–65.
- [195] ASTM C670, 2015, *Standard Practice for Preparing Precision and Bias Statements for Test Methods for Construction Materials*, ASTM International, West Conshohocken, PA.
- [196] Farnam, Y., Geiker, M. R., Bentz, D., and Weiss, J., 2015, “Acoustic Emission Waveform Characterization of Crack Origin and Mode in Fractured and ASR Damaged Concrete,” *Cem. Concr. Compos.*, **60**, pp. 135–145.
- [197] Shehata, M. H., and Thomas, M. D. A., 2010, “The Role of Alkali Content of Portland Cement on the Expansion of Concrete Prisms Containing Reactive Aggregates and Supplementary Cementing Materials,” *Cem. Concr. Res.*, **40**(4), pp. 569–574.
- [198] Folliard, K. J., Barborak, R., Drimalas, T., Du, L., Garber, S., Ideker, J., Ley, T., Williams, S., Juenger, M., Fournier, B., and Thomas, M. D. A., 2006, “Preventing ASR/DEF in New Concrete: Final Report,” p. 266.
- [199] Lindgård, J., Thomas, M. D. A., Sellevold, E. J., Pedersen, B., Andiç-Çakır, Ö., Justnes, H., and Rønning, T. F., 2013, “Alkali–Silica Reaction (ASR)—Performance Testing: Influence of Specimen Pre-Treatment, Exposure Conditions and Prism Size on Alkali Leaching and Prism Expansion,” *Cem. Concr. Res.*, **53**, pp. 68–90.
- [200] Oruji, S., Brake, N. A., Guduru, R. K., Nalluri, L., Günaydın-Şen, Ö., Kharel, K., Rabbanifar, S., Hosseini, S., and Ingram, E., 2019, “Mitigation of ASR Expansion in Concrete Using Ultra-Fine Coal Bottom Ash,” *Constr. Build. Mater.*, **202**, pp. 814–824.
- [201] Saha, A. K., Khan, M. N. N., Sarker, P. K., Shaikh, F. A., and Pramanik, A., 2018, “The ASR Mechanism of Reactive Aggregates in Concrete and Its Mitigation by Fly Ash: A Critical Review,” *Constr. Build. Mater.*, **171**, pp. 743–758.
- [202] Shon, C.-S., Sarkar, S. L., and Zollinger, D. G., 2004, “Testing the Effectiveness of Class C and Class F Fly Ash in Controlling Expansion Due to Alkali-Silica Reaction Using Modified ASTM C 1260 Test Method,” *J. Mater. Civ. Eng.*, **16**(1), pp. 20–27.
- [203] Boddy, A. M., Hooton, R. D., and Thomas, M. D. A., 2003, “The Effect of the Silica Content of Silica Fume on Its Ability to Control Alkali–Silica Reaction,” *Cem. Concr. Res.*, **33**(8), pp. 1263–1268.
- [204] Aquino, W., Lange, D. A., and Olek, J., 2001, “The Influence of Metakaolin and Silica Fume on the Chemistry of Alkali–Silica Reaction Products,” *Cem. Concr. Compos.*, **23**(6), pp. 485–493.
- [205] AASHTO T 358, 2019, *Standard Method of Test for Surface Resistivity Indication of Concrete’s Ability to Resist Chloride Ion Penetration*, American Association of State Highway and Transportation Officials, Washington, DC.

- [206] Kessler, R. J., Powers, R. G., Vivas, E., Paredes, M. A., and Virmani, Y. P., 2008, "Surface Resistivity as an Indicator of Concrete Chloride Penetration Resistance."
- [207] Madani, H., Bagheri, A., Parhizkar, T., and Raisghasemi, A., 2014, "Chloride Penetration and Electrical Resistivity of Concretes Containing Nanosilica Hydrosols with Different Specific Surface Areas," *Cem. Concr. Compos.*, **53**, pp. 18–24.
- [208] Spragg, R., Castro, J., Nantung, T., Paredes, M., and Weiss, J., 2012, "Variability Analysis of the Bulk Resistivity Measured Using Concrete Cylinders," *Var. Anal. Bulk Resist. Meas. Using Concr. Cylind.*
- [209] AASHTO TP 119, 2020, *Standard Method of Test for Electrical Resistivity of a Concrete Cylinder Tested in a Uniaxial Resistance Test*, American Association of State Highway and Transportation Officials, Washington, DC.
- [210] Tibbetts, C. M., Paris, J. M., Ferraro, C. C., Riding, K. A., and Townsend, T. G., 2020, "Relating Water Permeability to Electrical Resistivity and Chloride Penetrability of Concrete Containing Different Supplementary Cementitious Materials," *Cem. Concr. Compos.*, **107**, p. 103491.
- [211] Ashraf, W. B., and Noor, M. A., 2011, "Performance-Evaluation of Concrete Properties for Different Combined Aggregate Gradation Approaches," *Procedia Eng.*, **14**, pp. 2627–2634.
- [212] Jain, J. A., and Neithalath, N., 2010, "Chloride Transport in Fly Ash and Glass Powder Modified Concretes – Influence of Test Methods on Microstructure," *Cem. Concr. Compos.*, **32**(2), pp. 148–156.
- [213] Schwarz, N., DuBois, M., and Neithalath, N., 2007, "Electrical Conductivity Based Characterization of Plain and Coarse Glass Powder Modified Cement Pastes," *Cem. Concr. Compos.*, **29**(9), pp. 656–666.
- [214] Ghosh, P., and Tran, Q., 2015, "Influence of Parameters on Surface Resistivity of Concrete," *Cem. Concr. Compos.*, **62**, pp. 134–145.
- [215] Ardani, A., 2012, "Surface Resistivity Test Evaluation as an Indicator of the Chloride Permeability of Concrete."
- [216] Ghosh, P., and Tran, Q., 2015, "Correlation between Bulk and Surface Resistivity of Concrete," *Int. J. Concr. Struct. Mater.*, **9**(1), pp. 119–132.
- [217] Kasaniya, M., Thomas, M. D. A., and Moffatt, E. G., 2021, "Pozzolanic Reactivity of Natural Pozzolans, Ground Glasses and Coal Bottom Ashes and Implication of Their Incorporation on the Chloride Permeability of Concrete," *Cem. Concr. Res.*, **139**, p. 106259.

- [218] Ghoddousi, P., and Adelzade Saadabadi, L., 2017, “Study on Hydration Products by Electrical Resistivity for Self-Compacting Concrete with Silica Fume and Metakaolin,” *Constr. Build. Mater.*, **154**, pp. 219–228.
- [219] Dotto, J. M. R., Abreu, A. G. de, Dal Molin, D. C. C., and Müller, I. L., 2004, “Influence of Silica Fume Addition on Concretes Physical Properties and on Corrosion Behaviour of Reinforcement Bars,” *Cem. Concr. Compos.*, **26**(1), pp. 31–39.
- [220] Jalal, M., Pouladkhan, A., Norouzi, H., and Choubdar, G., 2012, “Chloride Penetration, Water Absorption and Electrical Resistivity of High Performance Concrete Containing Nano Silica and Silica Fume,” *J. Am. Sci.*
- [221] De Weerd, K., Haha, M. B., Le Saout, G., Kjellsen, K. O., Justnes, H., and Lothenbach, B., 2011, “Hydration Mechanisms of Ternary Portland Cements Containing Limestone Powder and Fly Ash,” *Cem. Concr. Res.*, **41**(3), pp. 279–291.
- [222] ASTM C1866, *Standard Specification for Ground-Glass Pozzolan for Use in Concrete*, ASTM International.

Appendix A – X-Ray Diffractograms

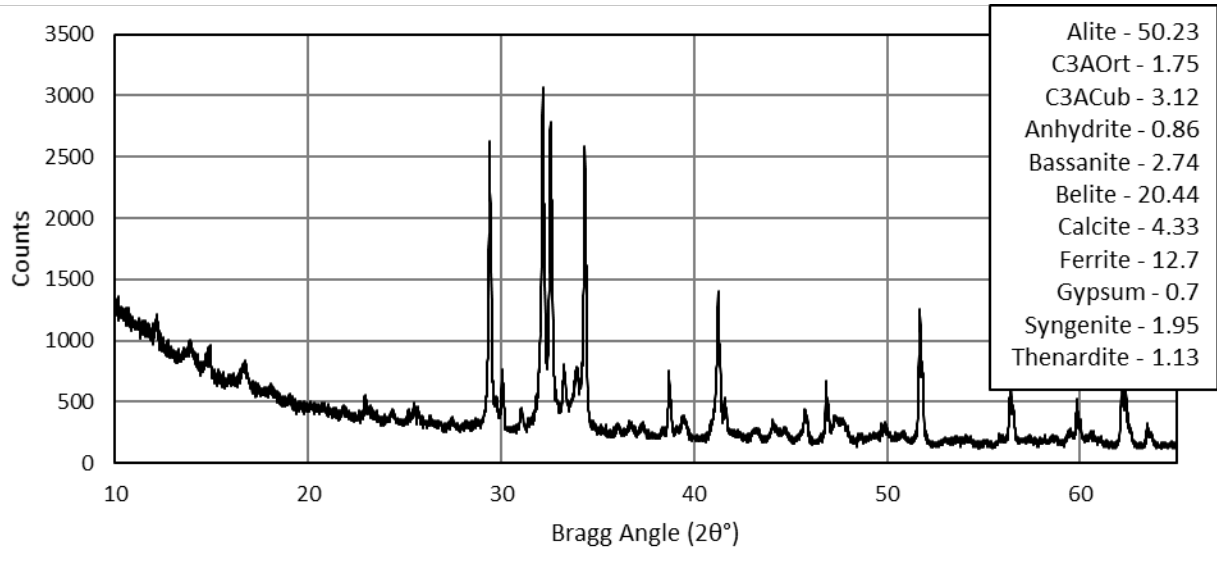


Figure A-1. X-ray diffractogram for Type I/II cement.

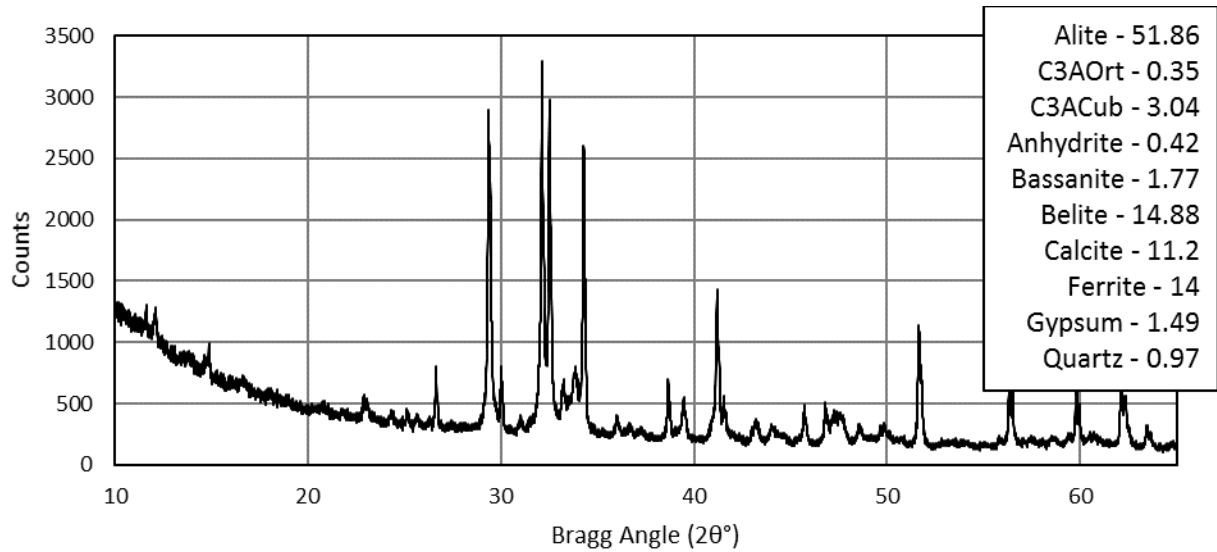


Figure A-2. X-ray diffractogram for Type IL cement.

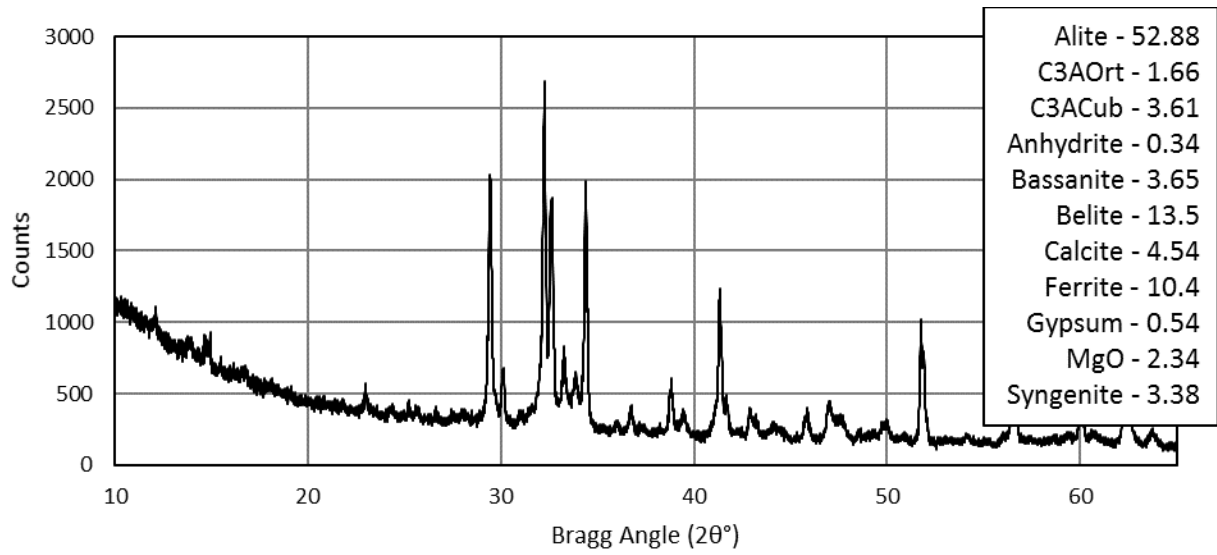


Figure A-3. X-ray diffractogram for high alkali Type I/II portland cement.

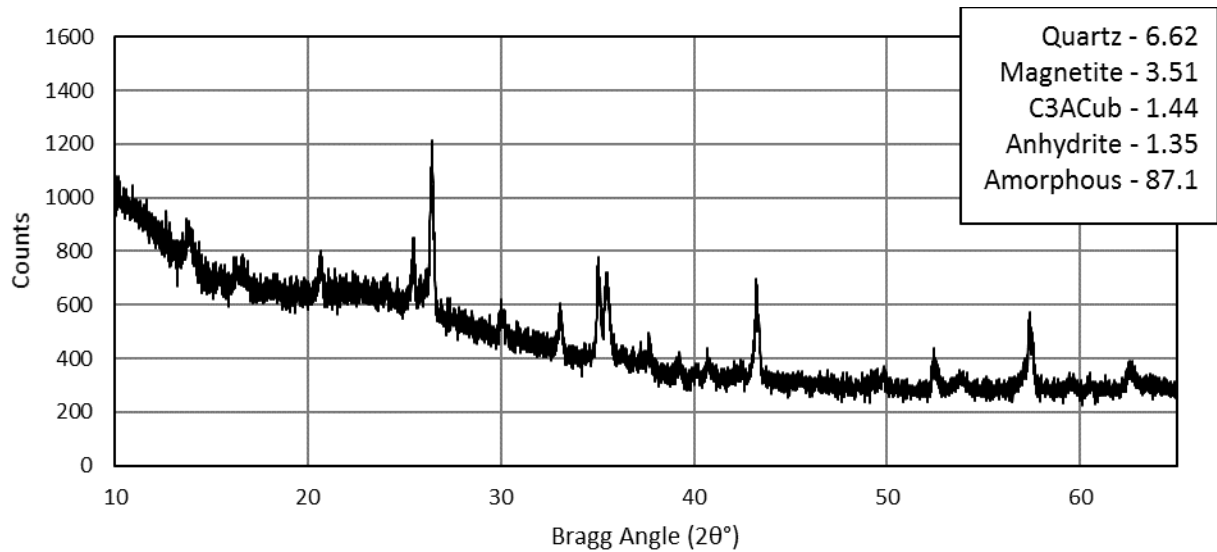


Figure A-4. X-ray diffractogram for Class F fly ash.

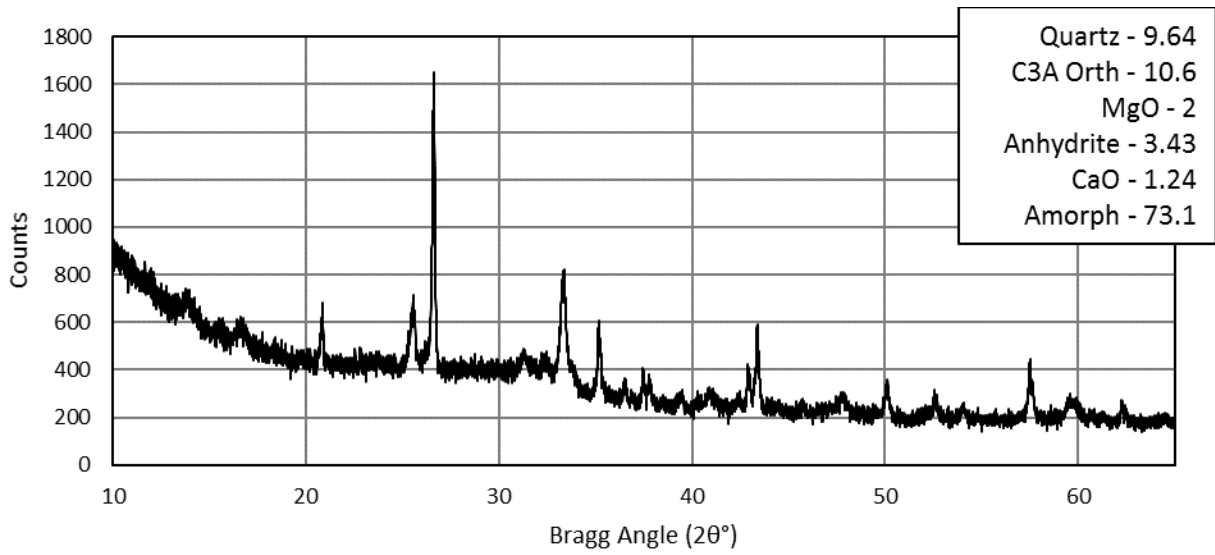


Figure A-5. X-ray diffractogram for Class C fly ash.

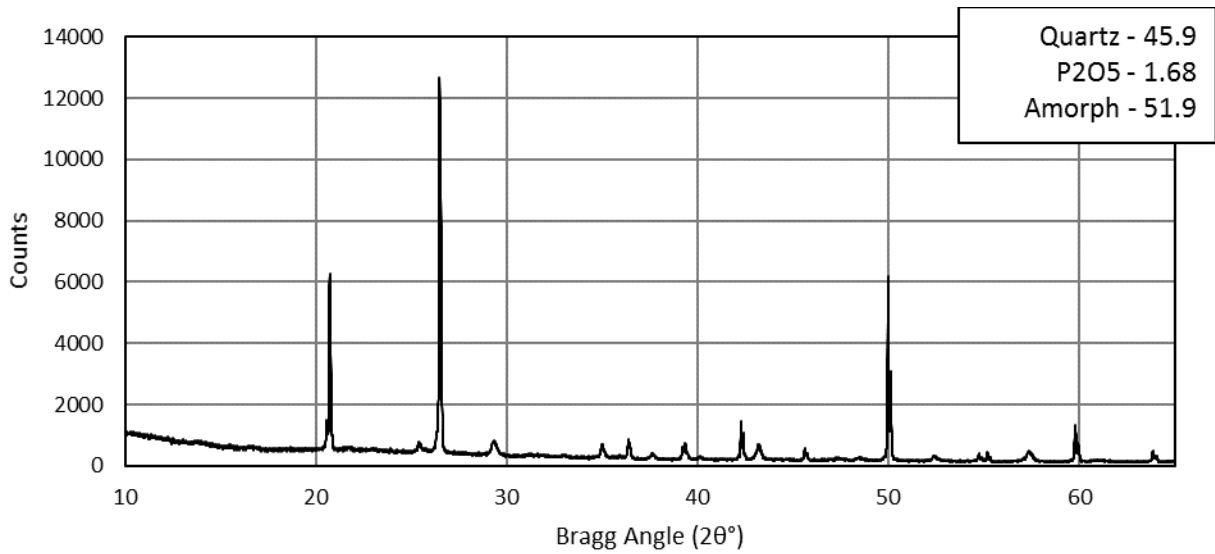


Figure A-6. X-ray diffractogram for SCBA-A.

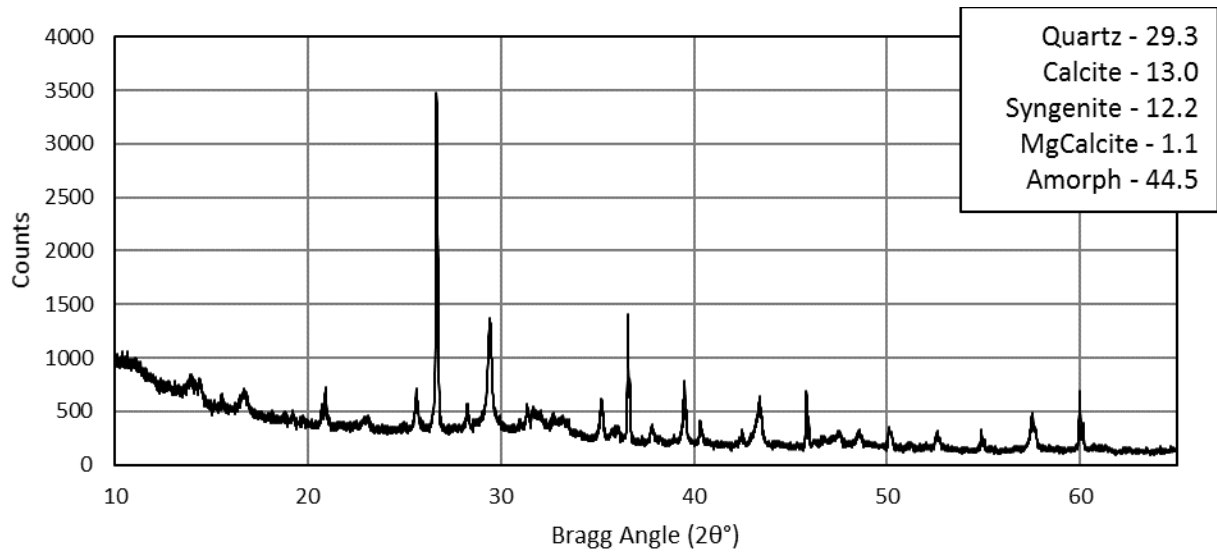


Figure A-7. X-ray diffractogram for SCBA-B.

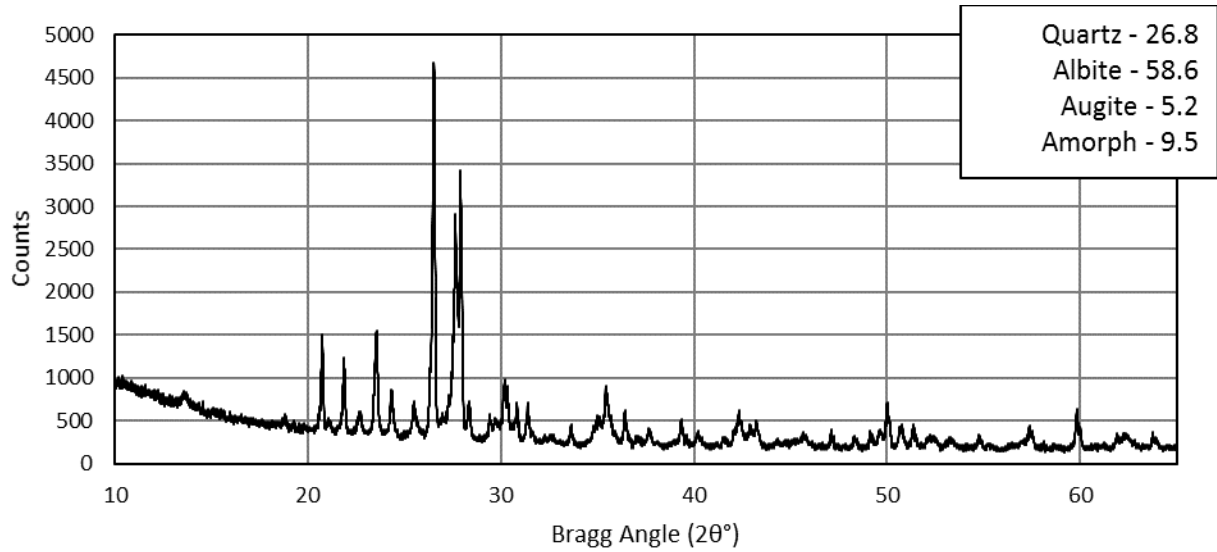


Figure A-8. X-ray diffractogram for VR.